

OZONE IN THE ATMOSPHERIC BOUNDARY LAYER:
TRANSPORT MECHANISMS AND
PREDICTIVE INDICATORS
AT 36°N

By

DAVID JOE WILLIAMS

Bachelor of Arts
The University of Tulsa
Tulsa, Oklahoma
1999

Master of Environmental Science
The University of Oklahoma
Norman, Oklahoma
2001

Master of Science
Oklahoma State University
Stillwater, Oklahoma
2004

Submitted to the Faculty of the
Graduate College of the
Oklahoma State University
in partial fulfillment of
the requirements for
the Degree of
DOCTOR OF PHILOSOPHY
May 2007

COPYRIGHT

By

David Joe Williams

May 2007

OZONE IN THE ATMOSPHERIC BOUNDARY LAYER:
TRANSPORT MECHANISMS AND
PREDICTIVE INDICATORS
AT 36°N

Dissertation Approved:

Dee Ann Sanders, Ph.D.
Dee Ann Sanders, Ph.D., Thesis Advisor

J.D. Carlson, Ph.D.
J.D. Carlson, Ph.D., Committee Member

William Clarkson, Ph.D.
William Clarkson, Ph.D., Committee Member

Greg Wilber, Ph.D.
Greg Wilber, Ph.D., Committee Member

A. Gordon Emslie, Ph.D.
Gordon Emslie, Ph.D., Dean of the Graduate College

“Ye who amid this feverish world would wear
A feverish body free from pain, of cares a mind,
Fly the rank city, shun its turbid air;
Breathe not the chaos of eternal smoke
And volatile corruption.”

--Armstrong

PREFACE

This dissertation is the culmination of a journey that began nearly a decade ago at the University of Tulsa, where I was given the opportunity to participate in research for the very first time. It should come as no surprise that the topic was ground-level ozone. Many years and countless courses have since passed, and I've enjoyed every moment.

Along the way, family, friends, and colleagues have been instrumental in fostering an environment of creativity and learning. In particular, I would like to acknowledge Dr. Bryan Tapp and Dr. Steven Bellovich at the University of Tulsa, as their expertise and enthusiasm encouraged a young scientist to learn more. My numerous requests to them for the customary letters of recommendation that accompany scholarship applications were never refused. Gratitude is also expressed to Dr. Petra Klein at the University of Oklahoma, with whom I continued researching ozone, ultimately providing a basis for my doctoral work.

During my time at Oklahoma State, I've had the distinct pleasure of learning from many talented professors. I wish to especially thank my committee – Dr. J.D. Carlson, Dr. Will Clarkson, Dr. Dee Ann Sanders, and Dr. Greg Wilber. Each one of you were willing to share welcome opinions and advice about a wide range of topics not strictly limited to research, and I found this to be an enjoyable diversion. Dr. Ken Ede, a member of my

master's committee, is of the same caliber. I consider you to be an exceptional group of scholars and friends.

Acknowledgements of the contributions to this project would be incomplete without recognition to the United States Environmental Protection Agency, who deemed this research study worthy of full funding for three years as part of the Greater Research Opportunities Doctoral Research Fellowship. Paperwork is much easier with the assistance of wonderful persons like Stephanie Willett, my EPA project officer. Additional monies were awarded by the Sigma Xi Grants in Aid of Research, the Oklahoma Chapter of the Air and Waste management Association, the Cherokee Nation, and the American Indian Science and Engineering Society. My research would not have been possible without generous support and assistance from Leon Ashford, Kent Stafford, Phil Bowers, and Waymon Brooks at the Oklahoma Department of Environmental Quality, nor would it have been possible without Mike Nichols, a communications specialist for the City of Tulsa. The successful deployment of an ozone sounding was no small feat, either, and I am grateful to Dr. Bill Potter and to Harry Mueller for a successful launch.

Finally and most importantly, I must thank my family. My parents, Thomas and Nedra Williams, have always supported my desire to learn, offering encouragement and financial support. A college education is much easier without the worries of financial constraint, and words cannot express how fortunate I am to have such wonderful parents. Lauren, the last couple of lines are reserved for you, as you are my true love. Your

continual radiance makes everything shine. The ability and dedication that you exhibit in every aspect of your life are at the level that everyone should strive for but few attain, and more so, you are the epitome of kindness and compassion. You always champion my causes, and I thank you for your unconditional love and support.

TABLE OF CONTENTS

Chapter	Page
1. INTRODUCTION.....	1
2. HYPOTHESIS AND RESEARCH OBJECTIVES	5
2.1. Research Hypothesis.....	5
2.2. Statement of Objectives	6
3. OZONE PHOTOCHEMISTRY.....	7
3.1. Atomic Structure of Ozone	8
3.2. The Chapman Cycle and Photochemical Principles	8
3.3. The Leighton Relationship and NO _x Chemistry.....	11
3.4. Hydroxyl Chemistry.....	14
3.5. VOC Influences on the Ozone Cycle.....	19
3.6. The Special Case of Methane	26
3.7. Summary	29
4. AIR POLLUTION METEOROLOGY	30
4.1. Upper-Level Dynamics.....	30
4.1.1. Rossby Wave Formation.....	31
4.1.2. Polar Front Theory and the Polar Jet Stream	35
4.1.3. Baroclinic Wave Formation.....	44
4.2. Boundary-Layer Meteorology	54
4.2.1. Structure and Stability.....	54
4.2.2. Vertical Wind Profile.....	60
4.2.3. Nocturnal Low-Level Jet	64
4.2.4. Meteorological Variables.....	70
4.2.5. Summary	74
5. OZONE AND HUMAN HEALTH	75
5.1. Asthma in Sensitive Populations	76
5.2. Mortality	76

5.3. Pulmonary Responses to Ozone Inhalation	77
6. THE REGULATORY ENVIRONMENT	79
6.1. Federal Regulations	80
6.2. Local Implementation	83
7. RECENT OZONE STUDIES	87
7.1. Boundary-Layer Considerations	87
7.2. Tower Studies	88
7.3. Tropospheric Background Concentrations	92
7.4. Subtropical Anti-Cyclones	96
7.5. Exchange between the Stratosphere and Troposphere	97
7.6. Lightning NO _x Fixation in the Tropics	99
7.7. Hadley Cell Circulation	101
7.8. Frontal Boundaries	103
7.9. Biogenic Ozone Production	104
7.10. Summary	105
8. METHODS AND MATERIALS	107
8.1. Theory of Ozone Measurement	107
8.2. Experimental Measurement	108
8.3. Meteorological Data Sources	111
8.4. Ozonesonde Payload and Launch	113
9. RESULTS AND DISCUSSION	114
9.1. Local-Scale Phenomena	114
9.1.1. Boundary-Layer Ozone Concentrations	115
9.1.2. Dry-Bulb Temperature	122
9.1.3. Water Vapor	126
9.1.4. Air Pressure	132
9.1.5. Wind Speed and Direction	134
9.1.6. Ultraviolet Radiation	145
9.2. Ozonesonde Measurements of Background O ₃	150
9.3. Vertical Transport and the Global Atmospheric Circulation	157
9.4. Horizontal Transport	172
9.4.1. Local Surface Winds	172
9.4.2. Nocturnal Low-Level Jet	178
10. SUMMARY AND CONCLUSIONS	186

10.1. Background Ozone in the Troposphere	186
10.2. Local Meteorological Variables.....	191
10.3. Horizontal Transport.....	195
10.4. Implications Resulting from Climate Change.....	196
10.5. Recommendations for Implementation and Future Study	200
10.6. Concluding Remarks.....	207
 BIBLIOGRAPHY	 212
SELECTED REFERENCES.....	224
 APPENDIX I: METEOROLOGICAL TRENDS	 238
APPENDIX II: OPERATIONAL PHOTOGRAPHS	241
APPENDIX III: NEWS ARTICLES	246
APPENDIX IV: ORIGINAL PUBLICATIONS	249
APPENDIX V: OZONE ANALYZER SPECIFICATIONS	252

LIST OF TABLES

Table	Page
3.1. Reaction rates (k) as a function of ultraviolet wavelength for selected O ₃ and NO _x photochemical processes	18
3.2. Molar yields of H ₂ O ₂ for selected VOCs	23
3.3. Average VOC lifetimes in the presence of OH, NO ₃ , O ₃ , and $h\nu$ (in days)	25
9.1. Percentages of O ₃ exceedances at selected dry-bulb temperatures.....	123
9.2. Frequencies of ground-level wind direction with ground-level ozone \geq 0.08 parts per million	140
9.3. Frequencies of 210-meter wind direction with ground-level ozone \geq 0.08 parts per million	141
9.4. Frequencies of ground-level wind direction with 210-meter ozone \geq 0.08 parts per million	143
9.5. Frequencies of 210-meter wind direction with 210-meter ozone \geq 0.08 parts per million	144
9.6. Nocturnal low-level jet statistics, Haskell, Oklahoma, 01 Jun 2005 – 30 Nov 2005.....	180
9.7. Comparison of nocturnal low-level jet frequency and magnitude at Haskell, Oklahoma between July 2005 and November 2005	180
10.1. Maximum correlations (as R ²) observed between ozone (ground-level, 210 meters) and ground-level meteorological variables.....	192

LIST OF FIGURES

Figure	Page
3.1. Atomic structure of ozone.....	8
3.2. The altitudes and corresponding wavelengths at which photolysis of N ₂ , O, O ₂ , and O ₃ occurs in the atmosphere; O ₃ photolysis occurs in the UV-A, B, and C bands, with most ground-level photochemistry occurring within the A band.....	10
3.3. Diurnal ozone behavior at several metropolitan Tulsa, Oklahoma monitoring sites, 26 July 200; sunrise occurred at 05:26 CST.	13
3.4. NO _x , OH influences on O ₃ cycle.....	15
3.5. The cyclic relationship between NO _x , VOCs (as radicals), and O ₃	19
3.6. O ₃ concentration isopleths as a function of NO _x and VOC concentrations	21
3.7. Possible reaction pathway between NO ₃ and isoprene (C ₅ H ₈).....	24
3.8. The complexity of the O ₃ cycle	28
4.1. Conservation of potential vorticity a) vertically over a mountain, and b) horizontal development of a trough on the lee side of a mountain.....	33
4.2. β-shifts of atmospheric Rossby waves.....	34
4.3. Pascal’s principle of equal pressure exertion on all surfaces of a fluid.....	37
4.4. Hydrostatic forces acting on a fluid.....	38
4.5. Maximum upward and downward motion overlying surface low and high pressure (dashed isobars) in relation to a baroclinic wave (denoted as solid geopotential height lines).....	49
4.6. Stages of cyclogenesis, including A) a disturbance underlying the upper-tropospheric trough; B) amplification of the surface cyclone and overlying	

upper-tropospheric trough; and C) upper-tropospheric closed low in phase with surface cyclone at maximum strength. Upper-tropospheric geopotential height contours are denoted by thick solid lines, while surface geopotential height contours are denoted by thin solid lines. The 1000-500 hPa thickness is represented by dashed lines.....	52
4.7. Atmospheric boundary layer structure.....	55
4.8. RUC analysis of 16:00 CST boundary-layer heights (in kilometers), 15 March 2007	57
4.9. Wind speed as a function of height within the boundary layer.....	61
4.10. Geostrophic flow around a cyclone	62
4.11. Deviation of the actual wind vector from the geostrophic wind vector in the middle portion of the atmospheric boundary layer	64
4.12. Wind angle deflection versus height within the atmospheric boundary layer.....	65
4.13. Vertical wind speed profile indicating nocturnal low-level jet, Tulsa, Oklahoma, 03:00 CST, 8 August 1951	66
4.14. Number of nocturnal low-level jet occurrences meeting or exceeding Criterion 1, January 1959 through December 1960.....	67
4.15. Number of nocturnal low-level jet occurrences meeting or exceeding Criterion 2, January 1959 through December 1960.....	68
4.16. Number of nocturnal low-level jet occurrences meeting or exceeding Criterion 3, January 1959 through December 1960.....	69
4.17. Derivation of time-averaged wind speed from instantaneous wind speed	71
5.1. O ₃ reactions near the surface of the lung	77
6.1. <i>Tulsa World</i> cartoon commentary on local air pollution	79
6.2. Tulsa, Oklahoma Early Action Compact (EAC) boundary	84
6.3. Daily air quality report example	86

7.1.	Physical and photochemical processes acting on O ₃ in the middle troposphere and in the boundary layer.....	88
7.2.	10-day comparison of O ₃ concentrations measured at ground level and at 433 meters in Garner, NC.....	89
7.3.	Vertical O ₃ concentration correlation plots, Garner, NC.....	90
7.4.	Ground-level and 433 meter time-dependent O ₃ concentration correlations, Garner, NC.....	91
7.5.	7-day comparison of O ₃ concentrations measured at ground level in the Oklahoma City metropolitan area and at Buffalo Mountain, a rural elevated site in southeastern Oklahoma.....	92
7.6.	Typical nocturnal O ₃ concentrations in the atmospheric boundary layer and lower troposphere.....	94
7.7.	Tropopause folding and subsequent introduction of O ₃ into the troposphere.....	98
7.8.	Modeled O ₃ concentrations in the middle troposphere resulting from tropopause folding immediately behind a trough and associated cyclone.....	99
7.9.	Cross-section of mean 1980-1989 stratospheric ozone concentrations (Dobson units per km), measured by the Nimbus-7 weather satellite, with arrows indicating the transport of ozone from the equatorial region to the mid-latitudes, consistent with the Brewer-Dobson circulation.....	101
7.10.	Hadley Cell circulation between the tropics and the mid-latitudes	102
8.1.	O ₃ study site locations in metropolitan Tulsa, Oklahoma.....	109
8.2.	TEC Model 49C O ₃ analyzer flow schematic.....	110
9.1.	12-hour daytime correlation between 210-meter and ground-level O ₃ concentrations (08:00 CST – 20:00 CST), 01 June 2005 – 30 November 2005.....	116
9.2.	9-hour daytime correlation between 210-meter and ground-level O ₃ concentrations (08:00 CST – 17:00 CST), 01 June 2005 – 30 November 2005.....	117

9.3.	5-hour morning correlation between 210-meter and ground-level O ₃ concentrations (08:00 CST – 13:00 CST), 01 June 2005 – 30 November 2005.....	118
9.4.	4-hour afternoon correlation between 210-meter and ground-level O ₃ concentrations (13:00 CST – 17:00 CST), 01 June 2005 – 30 November 2005.....	119
9.5.	9-hour daytime correlation between 210-meter and ground-level O ₃ concentrations (08:00 CST – 17:00 CST; 210-meter O ₃ concentrations offset to previous hour ground-level O ₃ concentrations), 01 June 2005 – 30 November 2005.....	120
9.6.	Correlation between nighttime 210-meter and ground-level O ₃ concentrations (20:00 CST – 08:00 CST), 01 June 2005 – 30 November 2005.....	121
9.7.	Correlation between ground-level O ₃ and dry-bulb temperature, 01 June 2005 – 30 November 2005.....	122
9.8.	Correlation between ground-level O ₃ and dry-bulb temperature, 01 June 2005 – 30 September 2005	124
9.9.	Correlation between 210-meter O ₃ and dry-bulb temperature, 01 June 2005 – 30 November 2005.....	125
9.10.	Correlation between ground-level O ₃ and wet-bulb temperature, 01 June 2005 – 30 November 2005.....	126
9.11.	Correlation between 210-meter O ₃ and wet-bulb temperature, 01 June 2005 – 30 November 2005.....	127
9.12.	Correlation between ground-level O ₃ and relative humidity, 01 June 2005 – 30 November 2005.....	129
9.13.	Correlation between ground-level O ₃ and relative humidity, 01 June 2005 – 30 September 2005	130
9.14.	Six-month correlation between 210-meter O ₃ concentration and relative humidity, 01 June 2005 – 30 November 2005.....	131
9.15.	Correlation between ground-level O ₃ and air pressure, 01 June 2005 – 30 November 2005.....	132
9.16.	Correlation between 210-meter O ₃ and ground-level air pressure, 01 June 2005 – 30 November 2005.....	133

9.17.	Correlation between ground-level O ₃ and ground-level wind speed, 01 June 2005 – 30 November 2005	135
9.18.	Correlation between ground-level O ₃ and 210-meter wind speed, 01 June 2005 – 30 November 2005.....	136
9.19.	Correlation between 210-meter O ₃ and ground-level wind speed, 01 June 2005 – 30 November 2005.....	137
9.20.	Correlation between 210-meter O ₃ and 210-meter wind speed, 01 June 2005 – 30 November 2005.....	138
9.21.	Ground-level wind frequency plot, 01 June 2005 – 30 November 2005.....	139
9.22.	210-meter wind frequency plot, 01 June 2005 – 30 November 2005.....	142
9.23.	Correlation between ground-level O ₃ and solar radiation, 01 June 2005 – 30 November 2005.....	146
9.24.	Maximum correlation between ground-level O ₃ and solar radiation (2-hour offset), 01 June 2005 – 30 November 2005.....	147
9.25.	Correlation between 210-meter O ₃ and solar radiation, 01 June 2005 – 30 November 2005.....	148
9.26.	Maximum correlation between 210-meter O ₃ and solar radiation (4-hour offset), 01 June 2005 – 30 November 2005.....	149
9.27.	A) Vertical ozone concentrations measured at 8:00 CST on 08 October 2005 at Tulsa, Oklahoma, and B) Corresponding 6:00 CST atmospheric sounding from Norman, Oklahoma	151
9.28.	300 hPa geopotential height analysis, 6:00 CST, 08 October 2005.....	152
9.29.	A) Polar jet stream; and B) the passage of the polar front, 06 October 2005.....	153
9.30.	A) Ozone maximum in the mid-troposphere at Huntsville, Alabama corresponding to the B) approach of an upper-level trough (300 hPa heights expressed as meters) at 12:00 CST on 08 April 2000	155
9.31.	A) Ozone maximum in the lower troposphere at Huntsville, Alabama corresponding to the B) departure of an upper-level trough (300 hPa heights expressed as meters) at 00:00 CST on 09 April 2000	156
9.32.	210-meter ozone concentrations measured in Tulsa, Oklahoma during the 2005 ozone season	158

9.33.	Upper-air sounding locations in relation to Tulsa, Oklahoma.....	159
9.34.	A) Mean 300 hPa polar jet stream, July 2005, and B) mean 300 hPa polar jet stream, November 2005	160
9.35.	300 hPa geopotential heights observed at 26°N (Brownsville, Texas), 35°N (Norman, Oklahoma), and 46°N (Aberdeen, South Dakota) during the 2005 six-month ozone season	161
9.36.	210-meter ozone concentrations measured in Tulsa, Oklahoma (36°N) compared with 300 hPa geopotential heights measured in Brownsville, Texas (26°N)	162
9.37.	210-meter ozone concentrations measured in Tulsa, Oklahoma (36°N) compared with 300 hPa geopotential heights measured in Norman, Oklahoma (35°N)	163
9.38.	Boundary-layer O ₃ concentrations measured in Tulsa, Oklahoma (36°N) compared with 300 hPa geopotential heights measured in Aberdeen, South Dakota (46°N)	164
9.39.	Correlation (as R ²) based on time shift between 210-meter ozone concentrations measured in Tulsa, Oklahoma and 300 hPa geopotential heights measured in close proximity to the polar jet stream at Aberdeen, South Dakota; Positive shifts correspond to height values that have been advanced in time with respect to ozone, while negative shifts correspond to ozone concentrations that have been advanced in time with respect to geopotential heights	165
9.40.	Boundary-layer ozone concentrations measured in Tulsa, Oklahoma (36°N) compared with 300 hPa geopotential heights measured in Aberdeen, South Dakota (46°N) for the period beginning on 18 July 2005 and ending on 27 July 2005	168
9.41.	300 hPa geopotential height analysis, 18 July 2005	169
9.42.	300 hPa geopotential height analysis, 23 July 2005	170
9.43.	300 hPa geopotential height analysis, 27 July 2005	171
9.44.	Location of Burneyville, Oklahoma in relation to the Dallas – Fort Worth, Texas metropolitan area	173
9.45.	Correlation between ozone concentrations at Burneyville, Oklahoma and Denton, Texas during the 1999 and 2000 O ₃ seasons.....	175

9.46.	Latency between peak ozone concentrations at Burneyville, Oklahoma and Denton, Texas during the 1999 O ₃ season	176
9.47.	Latency between peak ozone concentrations at Burneyville, Oklahoma and Denton, Texas during the 2000 O ₃ season	177
9.48.	Evolution of the nocturnal low-level jet in the Tulsa metropolitan area, 18:00 CST, 02 November 2005 – 06:00 CST, 03 November 2005	183
9.49.	12-hour NOAA HYSPLIT steady-state O ₃ plume simulation with NCEP GDAS meteorological data at 06:00 CST on 03 November 2005 (concentrations reported in µg·m ⁻³).....	184
10.1.	210-meter ozone concentrations superimposed on ground-level ozone concentrations, indicating the homogeneity of the boundary layer during the daytime, when maximum concentrations at the two levels are nearly identical; non-overlapping minimum concentrations are indicative of nocturnal measurements when the boundary layer decouples.....	191
10.2.	Positive and negative radiative forcing of greenhouse gases that contribute to a net warming and cooling of the atmosphere, respectively. “LOSU” refers to the level of scientific understanding.....	199
10.3.	Point forecast matrix issued by the NWS forecast office in Tulsa, Oklahoma on June 7, 2006.....	203

NOMENCLATURE

CAA	Clean Air Act
CFR	U.S. Code of Federal Regulations
CST	Central Standard Time
EAC	Early Action Compact
EPA	United States Environmental Protection Agency
FEV	forced expiratory volume
GFS	Global Forecast System model
INCOG	Indian Nations Council of Governments
MOA	Memorandum of Agreement
NAAQS	National Ambient Air Quality Standard
NAM-WRF	North American Mesoscale, Weather Research and Forecasting model
NOAA	National Oceanic and Atmospheric Administration
ODEQ	Oklahoma Department of Environmental Quality
PEF	peak expiratory flow
ppm	parts per million
R^2	coefficient of determination
RUC	Rapid Update Cycle model
SIP	State Implementation Plan

LIST OF MATHEMATICAL SYMBOLS

a	boundary-layer roughness coefficient
C	boundary-layer integration constant (Ch. 4); Gaussian O ₃ concentration (Ch. 9)
C_D	drag coefficient
c	forward wave speed (Ch. 4); O ₃ concentration (Ch. 8)
e	vapor pressure (Ch. 4); exponential function (Ch. 8)
e_s	saturation vapor pressure
F	force (∇p)
f	Coriolis parameter
g	gravitational acceleration ($-\nabla\Phi$)
H	scale height (Ch. 4); effective stack height (Ch. 9)
H_{NBL}	nocturnal boundary-layer depth
h	height (Ch. 4.1); boundary-layer depth (Ch. 4.2)
$h\nu$	ultraviolet radiation
I	ultraviolet intensity
k	wave number
$k_{OH}^{CH_4}$	CH ₄ reaction rate
k_1	NO ₂ photolysis rate constant
k_2	NO regeneration rate constant

L_v	latent heat of condensation
l	optical path length
m	mass (Ch. 4.1); total wind speed (Ch. 4.2)
P	potential vorticity (Ch. 4.1); power law exponent (Ch 4.2.2); periodicity (Ch. 4.2.3)
p	atmospheric pressure (absolute)
Q	emissions rate
R	specific gas constant for air
Ri	Richardson number
R_v	water vapor gas constant
T	temperature (absolute)
\bar{T}	mean temperature (absolute)
T_d	dew-point temperature
t	time
U_{RL}	residual-layer wind speed
u	zonal wind speed (Ch. 4.1); boundary-layer wind speed (Ch. 4.2, Ch. 9)
u_g	zonal component of geostrophic wind
\bar{u}	average zonal wind speed
V	horizontal velocity
V_g	geostrophic velocity
\mathcal{V}	volume
v	meridional wind speed

v_g	meridional component of geostrophic wind
W	vertical motion ($-\omega$)
w	mixing ratio
w_s	saturated mixing ratio
z	height within boundary layer
Δu	zonal deviation from geostrophic flow ($u - u_g$)
Δv	meridional deviation from geostrophic flow ($v - v_g$)
ΔZ	geopotential thickness
Γ	environmental lapse rate ($\partial T / \partial z$)
Γ_a	adiabatic lapse rate (dry or moist, depending on process)
Γ_d	dry adiabatic lapse rate
Γ_s	moist adiabatic lapse rate
Φ	geopotential
Ω	angular momentum of Earth
α	linear acceleration (Ch. 4); molecular absorption coefficient of O ₃ (Ch. 8)
β	meridional gradient of the Coriolis parameter ($df / d\phi$)
γ	vertical potential temperature gradient ($\partial\theta / \partial z$)
δp	displacement thickness
ζ	relative vorticity
η	absolute vorticity ($f + \zeta$)
θ	potential temperature

θ_M	mixed-layer potential temperature
κ	Poisson's constant
λ	electromagnetic wavelength
ρ	atmospheric density
σ	static stability parameter (Ch. 4); standard deviation (Ch. 9)
σ_y	horizontal dispersion parameter
σ_z	vertical dispersion parameter
τ_{CH_4}	tropospheric lifetime of CH ₄
ϕ	latitude
χ	geopotential tendency ($\partial\Phi/\partial t$)
ω	vertical velocity
∇	gradient (del) operator
∇^2	Laplacian operator

LIST OF CHEMICAL FORMULAS

CH_2O	formaldehyde (also expressed as HCHO)
CH_3	methyl radical
CH_3O	methoxy radical
CH_3O_2	methyl peroxy radical
CH_3COO_2	acetyl peroxy radical
$\text{CH}_3\text{COO}_2\text{NO}_2$	peroxyacetylnitrate (PAN)
CH_3OOH	methyl hydroperoxide
CH_4	methane
CO_2	carbon dioxide
HNO_3	nitric acid
HO_2	hydroperoxy radical
H_2O	water (or water vapor)
H_2O_2	hydrogen peroxide
M	reaction catalyst
NO	nitric oxide
NO_2	nitrogen dioxide
NO_3	nitrate
NO_x	NO + NO_2
N_2	atmospheric nitrogen

N_2O_5	dinitrogen pentoxide
NMVOC	non-methane VOC
O	elemental oxygen
$\text{O}(^1\text{D})$	excited-state “singlet” oxygen
$\text{O}(^3\text{P})$	ground-state “triplet” oxygen
O_2	atmospheric oxygen
O_3	ozone
OH	hydroxyl radical
R	radical
RH	hydrogen radical
RO	alkoxy radical
ROOH	organic peroxide
RO_2	alkyl peroxy radical
VOC	volatile organic compound

1. INTRODUCTION

Life as it exists today would not be possible without ozone. In fact, this essential molecule, comprised solely of three oxygen atoms, forms a protective layer in the stratospheric region of Earth's atmosphere, twenty-five kilometers above our daily activities. Without the ozone layer, energetic shortwave solar radiation would penetrate through the atmosphere to Earth's surface instead of its normal absorption by high altitude ozone as part of the Chapman Cycle, resulting in a marked increase in skin cancer occurrences.

Yet, ozone itself poses a threat to public health. How can this be? While stratospheric ozone shields the lower atmosphere from considerable ultraviolet radiation, tropospheric ozone acts as a strong oxidant, irritating the respiratory systems of anyone or any creature who inhales the invisible gas in an appreciable concentration. Research has linked ozone to the onset of asthma, particularly in children, and additional studies have shown that human mortality increases in conjunction with severe ozone pollution episodes.

Ozone not only threatens the welfare of public health as a short-term respiratory irritant, but it also poses more profound implications to the long-term meteorological climate. As a greenhouse gas, ozone is responsible for as much as one-third of the observed global warming over the past century, as it is an absorber of long-wave radiation emitted by the

Earth. Increases in tropospheric ozone concentrations will enhance long-wave radiation absorption, further increasing global mean surface temperatures. The decline of air quality is another possible ramification of climate change, as predicted global mean temperature increases of 2.0-4.5°C by the end of this century will likely prompt a chain reaction of large-scale meteorological pattern changes, resulting in mid-latitude ozone pollution episodes of increased duration and severity.

The correlation between increasing ground-level ozone concentrations and adverse health effects has prompted three decades of U.S. Environmental Protection Agency regulation and enforcement, beginning with the Clean Air Act of 1970. As a Clean Air Act provision, a National Ambient Air Quality Standard (NAAQS) for ozone was initially established in 1971, eventually becoming the 1-hour standard of 0.12 parts per million. While the 1-hour ozone standard remains valid and enforceable, new regulations from the EPA have established a new 8-hour standard of 0.08 parts per million, and in some states, even this standard has been superseded by more stringent guidelines.

Compliance of state and federal air quality standards requires knowledge of both the source and the fate of lower tropospheric, or atmospheric “boundary-layer” ozone. Many studies examining the meteorological and chemical aspects of ground-level ozone have been published over the last several decades, including a detailed early attempt by Cornelius Fox (1873), but comparatively few have analyzed the impacts that meteorological conditions have on ozone concentrations at altitude within the boundary layer, where more substantive conclusions can be drawn regarding the relative

magnitudes of transport and local photochemical production, which comprise the total ozone concentration.

High ground-level ozone concentrations impose a burden on the quality of life, both directly as a health concern (particularly to the young, the elderly, and persons who spend considerable time outdoors), as well as indirectly through increased health care costs, physical damages to sensitive agricultural crops, and the burdens of air quality compliance to the local, state, and federal economies. This study sought to clarify the relative magnitudes that local photochemical production and distant transport have on ground-level ozone concentrations at 36°N, and the findings indicate that while local meteorology is particularly important for short-term photochemical processes, a significant component of the ground-level ozone concentration is transferred through large-scale subsidence, relying on atmospheric wave propagation. Therefore, conclusions drawn from this six-month vertical profile of boundary-layer ozone are intended for the improvement of short-term ozone forecasting, which can be used in air quality warning issuance and subsequent control strategies, as well as more general outlooks prepared several days in advance, which consider the positions of atmospheric wave ridges and troughs. Additionally, results from this study serve as an outlook of the long-term prospects of ozone pollution, and in particular, the impact that a changing climate may impart upon ground-level ozone concentrations in the mid-latitudes.

When Schönbein discovered ozone in 1839, he named it after the German word “ozein,” literally describing its pungent odor, which can be readily sensed in the vicinity of a

thunderstorm. Although ozone generally isn't in sufficient ambient atmospheric quantity to identify through the sense of smell, it is in concentrations high enough to threaten public welfare, perhaps as a mild irritation to the nose and throat, or perhaps as the trigger for a life-threatening asthma attack. Understanding the dynamics of ozone in the context of large-scale production and transport will improve the forecasting of persistent and dangerous pollution episodes, ensuring that it doesn't become a suffocating blanket in the air that we breathe.

2. HYPOTHESIS AND RESEARCH OBJECTIVES

Ozone in the lower troposphere, or atmospheric “boundary layer,” is a heavily regulated air pollutant, as epidemiologic studies have shown that exposure results in respiratory distress, even at relatively low concentrations. However, the origin and behavior of ground-level ozone is not fully understood, as local photochemical production is complemented by an appreciable background concentration within the greater vertical expanse of the troposphere, well above the adjacent surface of the Earth.

2.1. Research Hypothesis

Therefore, this study hypothesizes that the analysis of ozone concentrations at an elevation of 210 meters within the boundary layer, and subsequent comparison of these concentrations with control values measured at ground level, will offer insight regarding the sources of distantly produced ozone, as well as estimates of magnitude. Furthermore, this study hypothesizes that since meteorological conditions are a dominant factor in the behavior of boundary-layer ozone, conclusions can be drawn regarding the likelihood of significant ozone pollution episodes based on specific meteorological regimes of varying scale.

2.2. Statement of Objectives

Evaluation of the hypotheses proposed in this study will require the fulfillment of the following objectives:

- 1) Estimation of the background ozone concentration specific to the study location.
- 2) Correlation of the behavior of ozone concentrations at 210 meters with the control values measured at ground level.
- 3) Evaluation of the relationships between specific meteorological parameters and ozone concentrations measured at 210 meters and at ground level.
- 4) Identification of transport pathways, based on meteorological conditions, for ozone concentrations not explained by local photochemical production.

Execution of the aforementioned objectives will result in a more detailed profile of ozone origin and behavior at the study location, providing decision-making support for ozone forecasting as well as abatement and control strategies. Additionally, improved insight into the large-scale meteorological processes influencing the tropospheric background ozone concentration and subsequent relationship to ground-level ozone will also be achieved, including the possible implications arising from climate change.

3. OZONE PHOTOCHEMISTRY

The existence of ozone in Earth's atmosphere is nothing new. In fact, photochemical reactions in ancient times spurred the production of significant concentrations of ozone, shielding the lower atmosphere from solar radiation as long as 700 million years ago (Graedel and Crutzen, 1993). While these reactions largely transpired in the stratosphere, trace amounts of ozone in the troposphere must also have been present, as nitric oxide, a precursor gas, was undoubtedly generated in sufficient concentrations by soil bacteria as well as by lightning. Yet, background concentrations of ozone in the troposphere are increasing (Lin et al., 2000). Ozone photochemistry has grown more complex, as various industrial sources not only produce nitric oxide, but also emit enormous quantities of a host of organic compounds with the potential to contribute to additional ozone production. While stratospheric ozone chemistry remains relatively simple (although the use of haloalkanes as propellants has altered these processes as well), tropospheric ozone chemistry involves many cycles and sub-cycles, as man-made organics trigger ozone formation and destruction in a multitude of ways. Nonetheless, consideration of these photochemical processes is vital to understanding the mechanisms of ozone formation.

3.1. Atomic Structure of Ozone

Ozone (O_3), the tri-atomic form of molecular oxygen, is a secondary pollutant formed from a series of complex photochemical reactions. Structurally, it is characterized by a molecular weight of 48, a molecular bond length of 1.278 Å, and an inter-bond angle of 116.8° (Figure 3.1) (Wells, 1986).

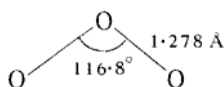


FIGURE 3.1: Atomic structure of ozone (Wells, 1986)

The single O-O bond has a dissociation energy of approximately 105 kJ·mol⁻¹ (Brasseur et al., 1999; Warneck, 2000). Based on the energies associated with the electromagnetic spectrum, this corresponds to a dissociation wavelength limit of 1.19 μm, although the process is much more effective at higher energies (shorter wavelengths) (Warneck, 2000).

3.2. The Chapman Cycle and Photochemical Principles

The most basic production of ozone involves the photolysis of diatomic oxygen (O_2), leaving a free oxygen atom to combine with additional O_2 . In fact, this reaction is responsible for the ozone layer, a protective barrier to ultraviolet radiation within the stratosphere (Graedel and Crutzen, 1993):



Reactions 3.1 – 3.2 were first proposed by Sydney Chapman in 1930, and are therefore referred to as the Chapman cycle, along with his proposed reactions for O₃ destruction (Taylor, 2005):



When the photolysis of any compound includes the production of atomic oxygen (O), one of two states will be observed: the “excited” state O(¹D) or the “ground” state O(³P) (an additional excited state atom, O(¹S), only occurs at altitudes greater than 80 km) (Warneck, 2000). The primary difference between the two is the wavelength (λ) involved in the photo-dissociation of the parent compound (Dessler, 2000). Generally, O(¹D) is the only species generated when λ is less than 0.300 μm, while O(³P) is the only species generated at λ > 0.325 μm (Figure 3.2) (Seinfeld, 1986; Dessler, 2000). Both species are possible at the interim wavelengths of 0.300-0.325 μm. Therefore, the basic reaction of O₃ production in the Chapman cycle (Reaction 3.1) only involves O(¹D), excited-state oxygen, as the λ required for this reaction is less than 0.242 μm, where solar energy in excess of 492 kJ·mol⁻¹ is high enough to dissociate diatomic oxygen (Graedel and Crutzen, 1993; Dessler, 2000; Warneck, 2000). Ultraviolet radiation of such short wavelength is absorbed in the stratosphere, never reaching the lower atmosphere (Taylor,

2005). Consequently, Chapman's mechanism of O₃ production is confined to the stratospheric ozone layer, and is not involved in tropospheric ozone chemistry.

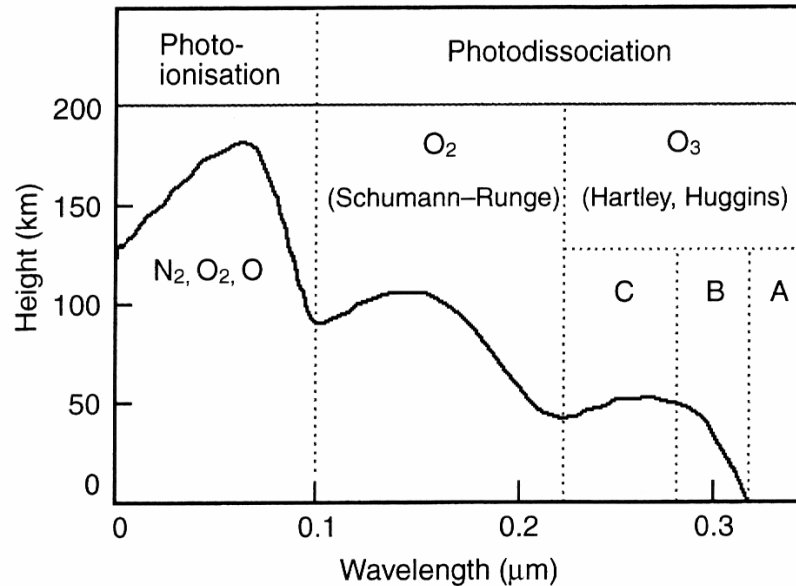


FIGURE 3.2: The altitudes and corresponding wavelengths at which photolysis of N₂, O₂, and O₃ occurs in the atmosphere; O₃ photolysis occurs in the UV-A, B, and C bands, with most ground-level photochemistry occurring within the A band (Taylor, 2005)

Instead, photochemistry in the lower troposphere occurs at λ greater than 0.290 μm , with the majority of ultraviolet radiation confined to λ greater than 0.320 μm (Taylor, 2005). These wavelengths can be classified as UV-A and UV-B, which range from 0.320-0.400 μm and 0.280-0.320 μm , respectively (Taylor, 2005). While all of the UV-A energy reaches the lower troposphere, only a fraction of UV-B does. Most radiation with wavelengths shorter than 0.290 μm is absorbed by O₂ and O₃ at higher altitudes, never reaching the surface of the Earth (Seinfeld, 1975). These shorter, harmful wavelengths

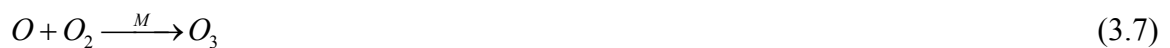
(0.200-0.280 μm), classified as UV-C, are those absorbed by stratospheric ozone, thus protecting the lower atmosphere from highly energetic radiation that poses a health threat to biological entities (Taylor, 2005).

3.3. The Leighton Relationship and NO_x Chemistry

Ozone chemistry in the lower troposphere is largely governed by a catalytic cycle of nitrogen oxide compounds (nitric oxide (NO) and nitrogen dioxide (NO_2), collectively referred to as NO_x). The connection between NO_x and O_3 was first proposed by Philip Leighton, who suggested a cyclic process of ozone creation and destruction (Leighton, 1961):



In Leighton's catalytic cycle, O_3 production is strongly diurnal, as it requires NO_2 photolysis. Conversion from NO_2 to O_3 actually requires a nearly-instantaneous second reaction, a modification of Chapman's equation (Reaction 3.2), that allows either $\text{O}({}^1\text{D})$ or $\text{O}({}^3\text{P})$ to combine with O_2 in the production of O_3 , as both are present in the lower troposphere:



The three fundamental equations of Leighton's relationship are sometimes referred to as the photostationary-state relationship, as the steady-state assumptions result in an equilibrium between NO, NO₂, and O₃ (Finlayson-Pitts and Pitts, 2000; Glickman, 2000). Therefore, when NO and NO₂ are the sole constituents in the diurnal O₃ cycle (i.e. a "clean" atmosphere), the relationship between steady-state O₃ concentrations and corresponding NO and NO₂ concentrations can be described as follows (Leighton, 1961; Seinfeld, 1986; NRC, 1991; Finlayson-Pitts and Pitts, 2000):

$$[O_3] = \frac{k_1[NO_2]}{k_2[NO]} \quad (3.8)$$

Rate constant k_1 is specific to the photolysis of NO₂, (Equation 3.5), while k_2 is defined as the reaction rate constant of NO₂ regeneration (Equation 3.6). While k_1 is dependent on solar intensity, k_2 has been experimentally measured as $1.8 \times 10^{-14} \text{ cm}^3 \cdot \text{molecule}^{-1} \cdot \text{s}^{-1}$ at 298 K (25°C) (Seinfeld, 1986; Warneck, 2000). The National Research Council reports that when NO and NO₂ are available in a ratio of 1:1 at a temperature of 25°C, the corresponding background O₃ concentration is 0.020 ppm, corresponding to a value of $0.009 \text{ cm}^3 \cdot \text{molecule}^{-1} \cdot \text{s}^{-1}$ for k_1 (1991). NO_x reactions are rapid, as NO₂ has an average half life of 100 seconds in the clear, calm atmosphere (Cox, 1988).

Concentrations of NO_x and O₃ are not at equilibrium in the lower atmosphere, however. Emissions from a multitude of natural and anthropogenic sources contribute to ozone process chemistry, and the reactions described in Equations 3.5 – 3.7 cannot be used as a sole explanation for tropospheric ozone chemistry. Even so, Leighton's relationship does

explain the strongly diurnal behavior of ground-level ozone. When photochemical reactions cease in the absence of sunlight, surface deposition of ozone at velocities as high as $1 \text{ cm}\cdot\text{s}^{-1}$ quickly deplete near-surface O_3 concentrations since no additional production occurs during the overnight hours (Brasseur et al., 1999). Therefore, ground-level ozone concentrations minimize at or shortly after sunrise when the solar altitude is insufficient for highly energetic radiation to reach Earth's surface. As a result of surface depositional processes, ozone concentrations at ground-level commonly approach zero during the early morning hours (Figure 3.3).

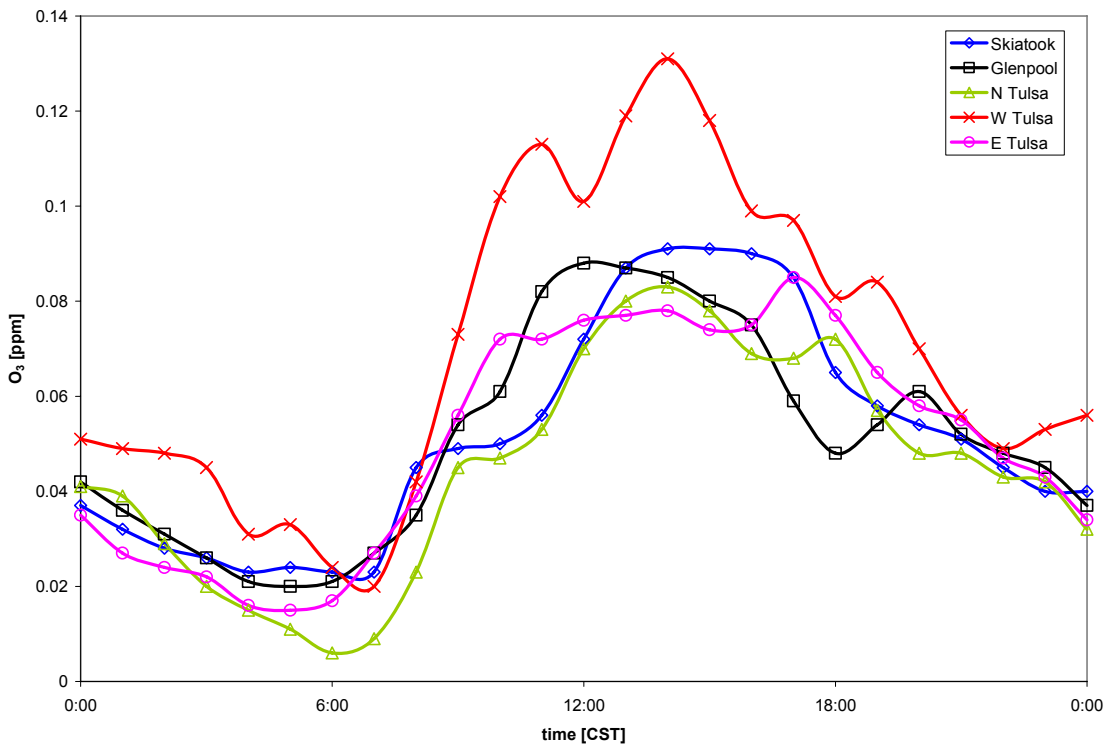


FIGURE 3.3: Diurnal ozone behavior at several metropolitan Tulsa, Oklahoma monitoring sites, 26 July 2001; sunrise occurred at 05:26 CST.

When additional gases of biogenic and anthropogenic origin interfere with the ozone cycle, they do not act in the direct production or conversion of ozone, but instead serve as indirect catalysts that alter the relative concentrations of NO_x through secondary reactions, driving the entire cycle away from steady-state equilibrium. These reactions must occur. Otherwise, no change in the day to day concentration of O_3 would be detectable. The most important secondary ozone reactions involve the hydroxyl radical and a host of volatile organic compounds, and each includes a number of chemical pathways.

3.4. Hydroxyl Chemistry

The rate of ozone formation proceeds as a function of NO_x availability. As demonstrated in Reaction 3.6, NO directly reduces O_3 to NO_2 and O_2 , yielding a net loss of ozone. However, when NO is in the presence of VOCs, the net result is O_3 production as NO reacts with HO_2 to produce additional NO_2 , the ozone precursor gas (Crutzen, 1988).

Thus, NO_2 concentrations in the troposphere are critical to the ozone budget, as it directly controls the rates of O_3 production and destruction, respectively. Without an appreciable reservoir of NO_2 , ozone formation is highly restricted. A NO_2 -limited environment is dependant on the availability of the hydroxyl (OH) radical, the most significant oxidant in the troposphere, which reacts with NO_2 to ultimately form nitric acid, a major ozone sink (Figure 3.4) (Crowley and Carl, 1997).

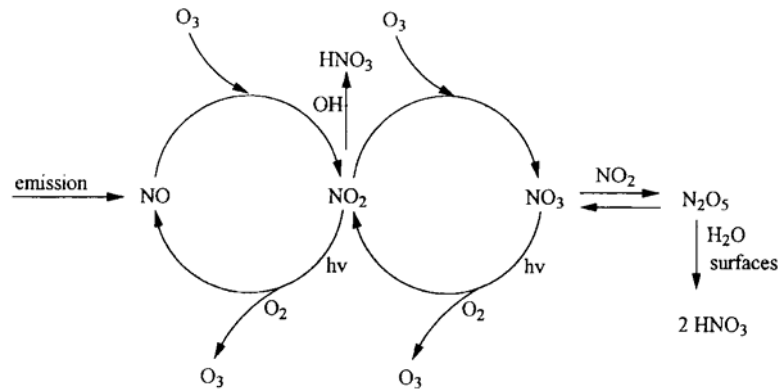


FIGURE 3.4: NO_x, OH influences on O₃ cycle (Atkinson, 2000)

Production of OH requires the presence of O(¹D) (Finlayson-Pitts and Pitts, 1997). Excited state oxygen is much more reactive than O(³P), as it contains 270 kJ·mol⁻¹ more energy than ground-state oxygen (Brasseur et al., 1999). Thus, O(¹D) readily combines with water vapor in the generation of the hydroxyl (OH) radical (Andreae and Crutzen, 1997; Crowley and Carl, 1997; Abram et al., 2000; Folkins and Chatfield, 2000; Lelieveld et al., 2002):



This reaction is the primary source of tropospheric OH, and it acts as an O₃ sink, as O(¹D) doesn't contribute to the direct reformation of O₃, unlike the O(³P) reaction sequence (Folkins and Chatfield, 2000). Reaction times are rapid, as evidenced by measurements taken during a 1999 solar eclipse in England, where OH concentrations minimized nearly instantaneously with a momentary loss of solar radiation (Abram et al., 2000).

Since ultraviolet wavelengths required for $O(^1D)$ production are typically absorbed above ground level, O_3 photolysis in the troposphere yields only 3% of free oxygen as $O(^1D)$, while $O(^3P)$ accounts for the remaining 97% (Lelieveld et al., 2002). Even though $O(^1D)$ is relatively rare at ground level, the lack of water vapor in the upper troposphere confines the reaction to the lower atmosphere (Folkins and Chatfield, 2000).

Experimental evidence confirms the significant role that $O(^1D)$ plays in the NO_2 budget of the lower atmosphere. Hydroxyl radical concentrations are strongly diurnal, and since ultraviolet radiation is required for O_3 photolysis, OH concentrations tend to peak during the daytime hours, concurrent with the theoretical yield of $O(^1D)$ from photolysis (Brown et al., 2004). Subsequently, OH reacts with NO_2 to form HNO_3 , resulting in lower O_3 concentrations. Brown et al. (2004) found OH to be the primary mechanism for daytime NO_2 -limitation, and furthermore determined HNO_3 to be the largest sink of NO_2 within the lower atmosphere:



In addition to the direct conversion of NO_2 to HNO_3 , the nitrate radical (NO_3) is also an important compound in NO_2 -limiting chemistry. NO_3 is primarily a product of the reaction between ozone and nitrous oxide (Gould, 1972; Seinfeld, 1986; Atkinson, 2000):



During the daytime, NO_3 dissociates rapidly (on the order of 5 seconds), and its photo-reactivity occurs over a much larger spectrum than the observed absorption wavelengths for ozone, including those commonly observed in the lower atmosphere (NRC, 1991; Atkinson, 2000; Brimblecombe, 2000):



Approximately 90% of photo-dissociated NO_3 is converted to NO_2 and O, while the remainder reverts to NO (Atkinson, 2000). NO_3 can also combine with free hydrogen radicals to produce nitric acid, another NO_x sink (Le Bras, 1997). According to Andreae and Crutzen (1997), NO_3 is responsible for a significant portion of the global HNO_3 budget:



In the absence of ultraviolet radiation, NO_3 behaves quite differently. In fact, NO_3 dominates the nocturnal chemistry of the lower troposphere, as OH is strongly diurnal (Finlayson-Pitts and Pitts, 1997). Without OH actively removing NO_2 from the ozone cycle, NO_3 performs the same function, generating dinitrogen pentoxide (N_2O_5), a major NO_x sink (Jacob, 2000):



Hydrolysis of N_2O_5 subsequently yields HNO_3 , which is removed from the O_3 cycle through wet and dry depositional processes (Mentel et al., 1999; Brown et al., 2004):



Dinitrogen pentoxide can also revert to NO_3 and NO_2 , but only in a warm lower troposphere, as the reaction is thermal (Jacob, 1998):



Reaction 3.17 requires temperatures in the lower atmosphere in excess of 280 K (7°C) (Jacob, 1998). Otherwise, it will not proceed, and N_2O_5 hydrolysis will dominate. A summarization of the NO_3 photolysis rate constants, as well as constants for the primary lower tropospheric O_3 and NO_x photochemical reactions proposed by Chapman and Leighton, is presented in Table 3.1.

TABLE 3.1: Reaction rates (k) as a function of ultraviolet wavelength for selected O_3 and NO_x photochemical processes (Brasseur et al., 1999)

Reaction	λ (μm)	k (s^{-1})
$O_3 + h\nu \rightarrow O(^1D) + O_2$	< 0.310	1×10^{-5}
$NO_2 + h\nu \rightarrow NO + O(^3P)$	0.250-0.400	8×10^{-3}
$NO_3 + h\nu \rightarrow NO_2 + O(^3P)$	0.400-0.625	2×10^{-1}
$NO_3 + h\nu \rightarrow NO + O_2$	0.585-0.625	2×10^{-2}

3.5. VOC Influences on the Ozone Cycle

While it is true that O_3 production and depletion in the presence of NO_x are the reactions that predominantly drive the surface ozone cycle, many VOC reactions contribute to the cyclic O_3 process as well (Figure 3.5). Otherwise, local ozone concentrations would exhibit no variability, but instead would behave according to Leighton's steady-state equilibrium. However, net ozone production occurs, as organic compounds convert additional amounts of NO to NO_2 (Leighton, 1961).

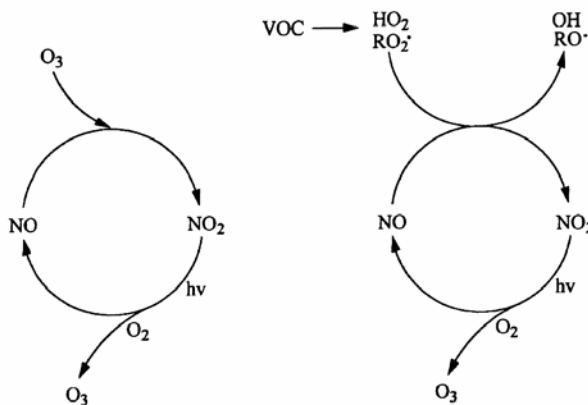


FIGURE 3.5: The cyclic relationship between NO_x , VOCs (as radicals), and O_3 (Atkinson, 2000)

VOCs lead to O_3 formation through intermediate alkoxy radicals (RO), alkyl peroxy radicals (RO_2), and hydroperoxy radicals (HO_2). Alkyl peroxy radicals react with NO to produce NO_2 , which is then available for O_3 production (Seinfeld, 1986; Atkinson, 2000; Finlayson-Pitts and Pitts, 2000; Jacob, 2000):



Net alkyl peroxy radical generation is a precursor of the efficiency of ozone production from VOC contribution. Instantaneous RO_2 concentration is a function of VOC concentration, OH concentration, and the rate of photolysis (Cox, 1988):

$$\frac{d[RO_2]}{dt} = \sum_{VOC} k_{OH}[OH][VOC] + \sum_{VOC} J[VOC] \quad (3.19)$$

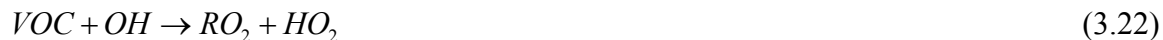
According to Jacob (2000), the simplest role that HO_x plays in the production of NO_2 is the reaction of OH with carbon monoxide (CO):



Once the hydroperoxy radical is available for chemical reaction, it reacts with NO in the production of NO_2 (Seinfeld, 1986; NRC, 1991; Jacob, 1998; Atkinson, 2000; Finlayson-Pitts and Pitts, 2000; Jacob, 2000):



Additional HO_2 is generated by VOC reactions with OH, which also produce RO_2 (Jacob, 1998; Atkinson, 2000; Jacob, 2000):



Formaldehyde (CH_2O), an intermediate VOC compound, also acts in the net production of HO_2 , as it photo-dissociates in the presence of ultraviolet radiation (Jacob, 1998; Jacob, 2000):



As demonstrated in Reactions 3.19 – 3.23, VOCs undoubtedly contribute to net NO_2 production, and therefore net O_3 production, in a cyclic nature, as the generation of RO_2 and HO_2 results in additive NO_2 reactions. Figure 3.6 expresses O_3 concentrations (in parts per million) as a function of NO_x and VOC concentrations.

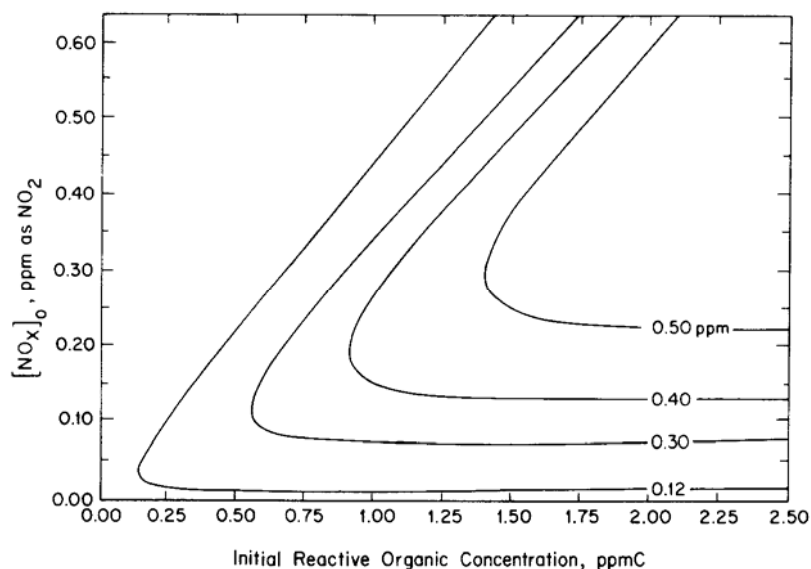
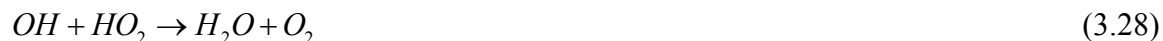


FIGURE 3.6: O_3 concentration isopleths as a function of NO_x and VOC concentrations (Seinfeld, 1986)

Even though the primary O₃ loss mechanism is through rapid reaction with NO, depletion also progresses through reactions with OH and HO₂ (Jacob, 1998; Atkinson, 2000; Jacob, 2000):



Loss of HO₂ from the so-called “HO_x cycle,” and therefore loss from the ozone cycle, proceeds through the following reactions (Seinfeld, 1986; NRC, 1991; Jacob, 1998; Atkinson, 2000; Jacob, 2000):



Generation of hydrogen peroxide (H₂O₂) in Reaction 3.26 is significant in part because it is also a strong oxidant, and has been shown to contribute to plant damage and forest decline (Becker et al., 1990; Brimblecombe, 2000). The relative yields of H₂O₂ as a function of VOC concentration are expressed in Table 3.2 with no water vapor concentration, and with a water vapor partial pressure of 1.3 hPa (1.3 millibars).

TABLE 3.2: Molar yields of H₂O₂ for selected VOCs (Becker et al., 1990)

VOC	%H ₂ O ₂ (no H ₂ O)	%H ₂ O ₂ (1.3 hPa H ₂ O)
Isoprene	0.04	0.10
β-Pinene	0.04	0.15
α-Pinene	0.10	0.50
Δ ₃ -Carene	0.13	0.60
<i>d</i> -Limonene	0.30	1.80
<i>trans</i> -Butene	0.06	0.50
Isobutene	0.04	0.37

Consideration of the role that VOCs play in the larger schemes of NO_x and O₃ chemistry would not be complete without mention of peroxyacetylnitrate (CH₃COO₂NO₂). Abbreviated as PAN, CH₃COO₂NO₂ is generated by the reaction of VOCs with NO₂ through the intermediate acetylperoxy radical (CH₃COO₂) (Lesclaux et al., 1997; Jacob, 2000):



This reaction is efficient in removing NO₂ from the ozone cycle in VOC-polluted areas. However, PAN itself cycles back to NO₂, particularly at high temperatures. Where temperatures exceed 295 K (22°C), Reaction 3.29 reverses (Jacob, 2000):



pathway involving the conversion of NO_3 to RO_2 , and subsequently the net production of OH and NO_2 , has been suggested by Le Bras et al. (1997):



A summary of average tropospheric lifetimes of selected VOCs in the presence of OH , NO_3 , O_3 , and ultraviolet radiation is given in Table 3.3.

TABLE 3.3: Average VOC lifetimes in the presence of OH , NO_3 , O_3 , and $h\nu$ (in days)

(Adapted from NRC, 1991)

VOC	OH	NO_3	O_3	$h\nu$
Methane	4.38×10^3	$> 4.38 \times 10^4$	$> 1.64 \times 10^6$	-
Ethane	6.00×10^1	$> 4.38 \times 10^4$	$> 1.64 \times 10^6$	-
Propane	1.30×10^1	$> 9.13 \times 10^2$	$> 1.64 \times 10^6$	-
<i>n</i> -Butane	6.10×10^0	$> 9.13 \times 10^2$	$> 1.64 \times 10^6$	-
<i>n</i> -Octane	1.80×10^0	2.60×10^2	$> 1.64 \times 10^6$	-
Ethene	1.80×10^0	2.25×10^2	9.70×10^0	-
Propene	2.90×10^{-1}	4.90×10^0	1.50×10^0	-
Isoprene	7.50×10^{-2}	3.47×10^{-2}	1.20×10^0	-
α -Pinene	3.40×10^0	3.47×10^{-3}	1.00×10^0	-
Acetylene	1.90×10^1	$> 9.13 \times 10^2$	2.12×10^3	-

Formaldehyde	1.60×10^0	2.81×10^4	$> 1.64 \times 10^3$	-
Acetaldehyde	1.00×10^0	1.70×10^1	$> 1.64 \times 10^3$	1.67×10^{-1}
Acetone	6.80×10^1	-	$> 1.64 \times 10^3$	1.50×10^1
Methyl ethyl ketone	1.34×10^1	-	$> 1.64 \times 10^3$	-
Methylglyoxal	1.08×10^1	-	$> 1.64 \times 10^3$	8.33×10^{-2}
Methanol	1.70×10^1	$> 7.70 \times 10^1$	-	-
Ethanol	4.70×10^1	$> 5.10 \times 10^1$	-	-
Methyl <i>t</i> -butyl ether	5.50×10^0	-	-	-
Benzene	1.25×10^1	$> 2.19 \times 10^3$	$> 1.64 \times 10^3$	-
Toluene	2.60×10^0	6.94×10^2	$> 1.64 \times 10^3$	-
<i>m</i> -Xylene	3.25×10^{-1}	2.00×10^2	$> 1.64 \times 10^3$	-

3.6. The Special Case of Methane

Methane (CH₄) is an organic greenhouse gas that is abundant in the lower atmosphere. In addition to anthropogenic sources, it is produced naturally in large quantities by anaerobic bacteria that occupy lake sediments, wetland soils, and even the digestive tracts of cattle and termites (Warneck, 2000). Therefore, CH₄ represents a special case of VOC/NO_x chemistry, as it not only is a normal component of the Earth's atmosphere, but it also is structurally simple, thus providing a novel example of the VOC chemical pathway.

The tropospheric lifetime of CH₄ is defined as follows (NRC, 1991):

$$\tau_{CH_4} = \frac{1}{k_{OH}^{CH_4} [OH]} \quad (3.36)$$

Calculation of the kinetic constant required for Equation 3.36 represents the reaction rate between CH₄ and OH. Since CH₄ has a much longer lifetime than OH, reactions involving CH₄ will progress and contribute to net changes in O₃ concentrations (NRC, 1991). According to Warneck (2000), τ equals 8.3 years.

The influence that methane has on ozone concentrations varies depending on the presence of NO. When NO is available for reaction, the net result is the production of ozone, as highlighted by Reactions 3.37 – 3.40 (Cox, 1988):



This sequence continues with Reaction 3.21, followed by Reactions 3.5 and 3.7. When balanced, the final yield is two O₃ molecules for each CH₄ molecule (Cox, 1988). Crutzen (1988) has determined that one CH₄ molecule ultimately produces 3.7 O₃ molecules when NO is included in the reaction sequence. Conversely, when NO is unavailable, one CH₄ molecule results in a net loss of 1.7 O₃ molecules (Crutzen, 1988). Methane reaction in the absence of NO proceeds in the following manner (Cox, 1988; Brasseur et al., 1999):





As a distinction between CH₄ and less common VOCs, some authors refer to the latter as non-methane VOCs, or NMVOCs. A simplified schematic of the complete ozone cycle, with contributions from VOCs (including CH₄), OH, and NO_x is presented in Figure 3.8.

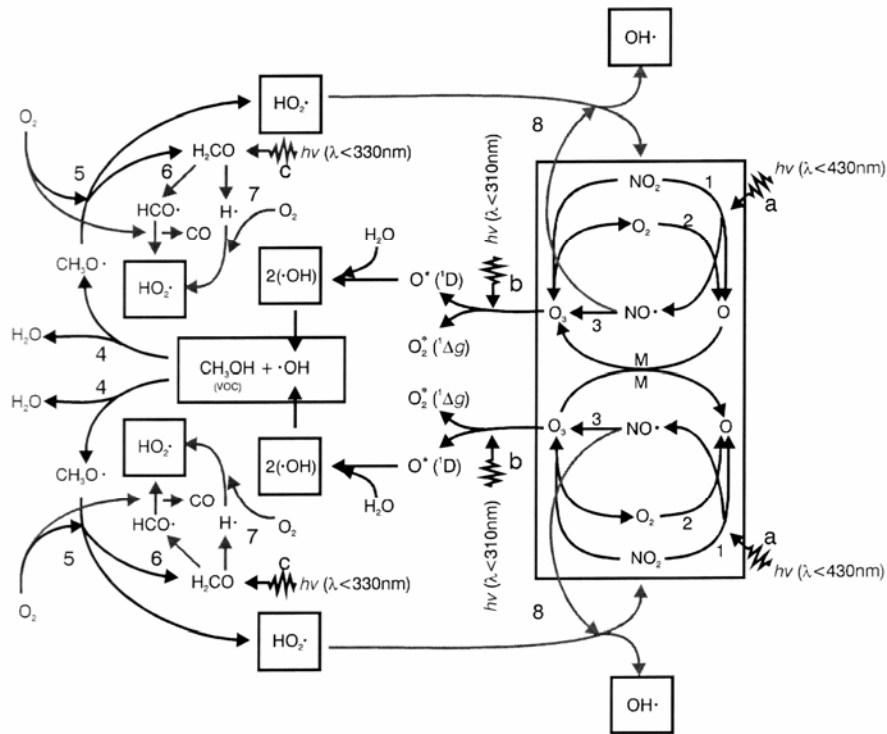


FIGURE 3.8: The complexity of the O₃ cycle (Mudway and Kelly, 2000)

3.7. Summary

In summary, the chemistry involving ozone and all associated compounds is quite complex, and furthermore, many of the secondary and tertiary reactions involving VOCs are not fully understood. The Leighton relationship provides a basis for the consideration of photochemical ozone production, as it is undoubtedly driven by the catalytic NO_x cycle. However, significant consideration must also be given to the interaction of OH with NO_x , as hydroxyl is the primary tropospheric oxidant, and even though it has a very short residence time, it nonetheless drives many NO_x production and destruction reactions. Finally, VOCs present exceptional difficulty when considering ozone chemistry, as the various organic compounds emitted by human sources (in addition to many natural sources) can be structurally complex, leading to numerous additional reactions that influence ozone concentrations.

4. AIR POLLUTION METEOROLOGY

The generation, transport, and fate of tropospheric ozone as an air pollutant are largely governed by meteorological processes of varying scale. When discussing the size and scope of meteorological systems, they are generally divided into the following categories: micro-scale (< 2 km), meso-scale (2-2000 km), and synoptic-scale (> 2000 km) (Glickman, 2000). Ozone is influenced by local, short-term fluctuations of environmental variables, including dry-bulb temperature, wind speed, and boundary-layer thickness, as well as by large-scale events of long duration, including the location and magnitude of the polar jet stream. Therefore, it is appropriate to discuss ozone in a global context of upper-level atmospheric dynamics and in a local context of boundary-layer characteristics.

4.1. Upper-Level Dynamics

Dynamic motion in Earth's atmosphere drives the phenomenon known as "weather." Without the continuous movement of air resulting from Earth's rotation as well as the permanent thermal contrast between the polar region and the equator, the atmosphere would be devoid of waves that bring changing conditions with them. However, the atmosphere is in motion, and within it are waves of varying magnitude and duration that are not only responsible for weather, but also impact the large-scale behavior of

tropospheric ozone. These systems, from synoptic-scale Rossby waves to meso-scale baroclinic waves, are the primary mechanisms in the distribution of ozone in the mid-latitudes. Therefore, a more complete understanding of dynamic wave motion in the atmosphere is an important consideration of ozone formation and transport.

4.1.1. Rossby Wave Formation

At any given time, the circulation of the upper troposphere is characterized by a series of slow-moving, large-amplitude waves. These large-scale disturbances, also known as planetary waves, were first theorized in 1939 by Carl-Gustav Rossby, thus carrying his name (Hess, 1979).

In the broadest sense, Rossby waves originate from the variation of the Coriolis force with latitude. Indeed, the Coriolis force is dynamic, equaling zero at the equator and increasing with latitude, maximizing at the poles. This effect can easily be calculated from the Coriolis force equation, since Earth's angular momentum (Ω) can be considered as a constant $7.292 \times 10^{-5} \text{ rad}\cdot\text{s}^{-1}$, leaving latitude (ϕ) as the only variable (Hess, 1979; Fleagle and Businger, 1980):

$$f = 2\Omega \sin \phi \tag{4.1}$$

Thus, at a latitude of 0° , f equals zero, while at a latitude of 90° , f equals $14.6 \times 10^{-5} \text{ rad}\cdot\text{s}^{-1}$, twice Earth's angular momentum.

Vorticity is defined as the “curl” of a fluid per unit area, and the Coriolis force is nothing more than vorticity measured at any fixed point on Earth’s surface, thus accounting for “planetary” vorticity exerted by the movement of fluid in a rotating system (Glickman, 2000). Relative vorticity (ζ), or vorticity neglecting the effects of the Coriolis force, can be expressed in Cartesian coordinates as the difference between the displacement of the zonal and meridional components of flow (Cushman-Roisin, 1994):

$$\zeta = \frac{\partial v}{\partial x} - \frac{\partial u}{\partial y} \quad (4.2)$$

Absolute vorticity (η) is therefore the sum of relative vorticity and planetary vorticity (Cushman-Roisin, 1994):

$$\eta = \zeta + f \quad (4.3)$$

Finally, potential vorticity (P) defines absolute vorticity as a function of a characteristic pressure thickness, δp :

$$P = \frac{\eta}{|\delta p|} \quad (4.4)$$

Any large decrease in δp (i.e. flow over tall mountain ranges) will result in an increase in η , as P is conserved (Cushman-Roisin, 1994). This relationship is commonly expressed

as the Ertel vorticity theorem, and is valid for frictionless, adiabatic flows (Carlson, 1998).

The conservation of potential vorticity therefore explains why Rossby waves form in the first place. In the Northern Hemisphere, a decrease in δp in westerly flow increases cyclonic vorticity, which deflects the flow toward the equator (Fleagle and Businger, 1980). At some point in time after the flow has deflected, δp no longer decreases, and the flow curves toward the north, with increasing f (Figure 4.1) (Fleagle and Businger, 1980). Again, potential vorticity is conserved, and does so through a decrease in relative vorticity, which is characteristically anti-cyclonic.

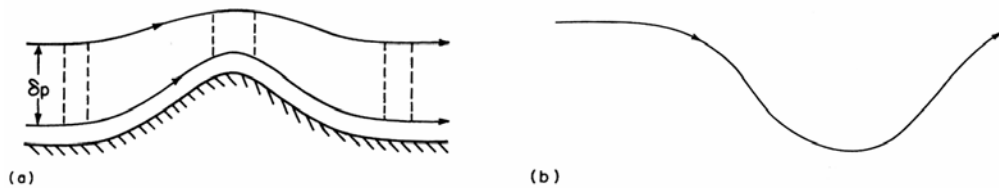


FIGURE 4.1: Conservation of potential vorticity a) vertically over a mountain, and b) horizontal development of a trough on the lee side of a mountain (Fleagle and Businger, 1980)

Perturbations within the upper-tropospheric flow lead to a series of cyclonically/anti-cyclonically paired Rossby waves. These large-scale waves are also referred to as the β -effect, as β is simply defined as the change in the Coriolis force with latitude (Holton, 1992):

$$\beta = \frac{df}{dy} \tag{4.5}$$

In the Northern Hemisphere, any flow disturbance prompting a right (equatorward) deflection constitutes a positive (+) β shift, and will subsequently be followed by a negative (-) β shift toward the pole (Holton, 1992; Carlson, 1998). Thus, the flow of the middle and upper troposphere is characterized by a sinusoidal wave about the original flow equilibrium position that completely encircles the globe (Figure 4.2).

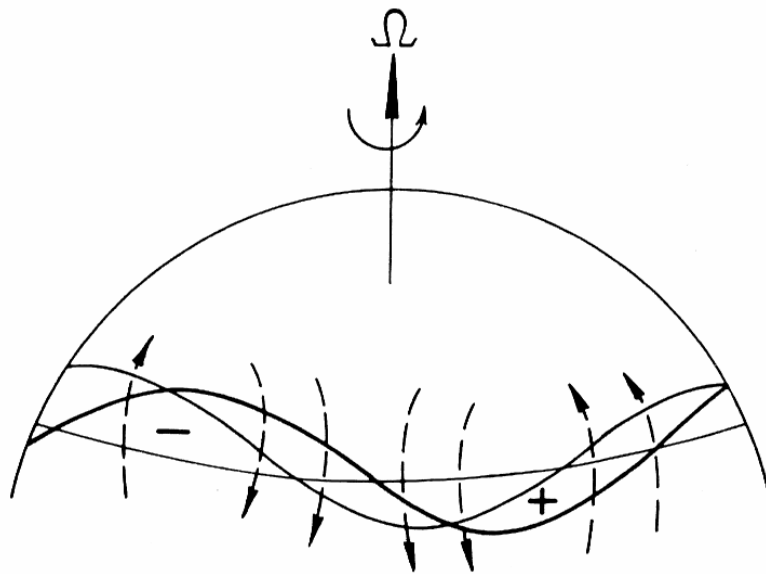


FIGURE 4.2: β -shifts of atmospheric Rossby waves (Holton, 1992)

According to Carlson (1998), the average number of waves in the Northern Hemisphere is seven, although some may be of shorter wavelength than Rossby waves. Palmén and Newton (1969) indicate that four or five concurrent Rossby waves are most common in the planetary circulation.

The propagation of Rossby waves is very slow when compared with upper-level wind speeds. In fact, they often appear to be stationary. While short waves progress at average speeds of 10-20 m·s⁻¹, Rossby waves generally move at speeds less than 8 m·s⁻¹ (Palmén and Newton, 1969). Seasonality also affects Rossby wave propagation, as they travel, on average, 2° of longitude per day during spring, versus 0.8° of longitude per day during the autumn months (Reiter, 1963).

Rossby wave speed can be calculated from the frequency equation, which relates the forward wave speed to the zonal (westerly) flow speed (\bar{u}), β , and the wave number (k) (Fleagle and Businger, 1980):

$$c = \bar{u} - \frac{\beta}{k^2} \tag{4.6}$$

4.1.2. Polar Front Theory and the Polar Jet

Rossby waves propagate within the polar jet stream, a discontinuous ribbon of strong wind speeds in the upper reaches of the troposphere at the middle and high latitudes. The polar jet stream originates from the baroclinicity, or stratification, between the ever-present cold polar air mass and warm subtropical air mass (Reiter, 1963; Palmén and Newton, 1969). This boundary, where stratification results from the difference in density between these air masses of contrasting temperature, is commonly referred to as the polar front (Reiter, 1963).

The polar front is notable in part because it extends from the tropopause downward to Earth's surface. According to Djurić (1994), the shape of the polar front is a function of vertical motion, frontogenesis, and frontolysis. Although it is dynamically connected to the polar jet, the polar front at ground level can sometimes stray several hundred miles from the polar jet, particularly when cold air flows southward as a gravity current when forcing along the polar jet is weak (Djurić, 1994).

In order for the density stratification along the polar front to result in the development of the polar jet stream, two conditions must occur (Reiter, 1963):

1. motion arising from a pressure gradient force in the meridional temperature contrast along the polar front; and
2. angular momentum from a rotating Earth

Pressure forces along the vertical axis of the atmosphere are governed by hydrostatic processes, where the pressure exerted by the weight of overlying atmosphere is balanced by gravity. When a fluid is at rest, no internal shear forces are acting upon it. Therefore, according to Pascal's principle, pressure is acting equally in all directions on the fluid (Figure 4.3) (Michelson, 1970).

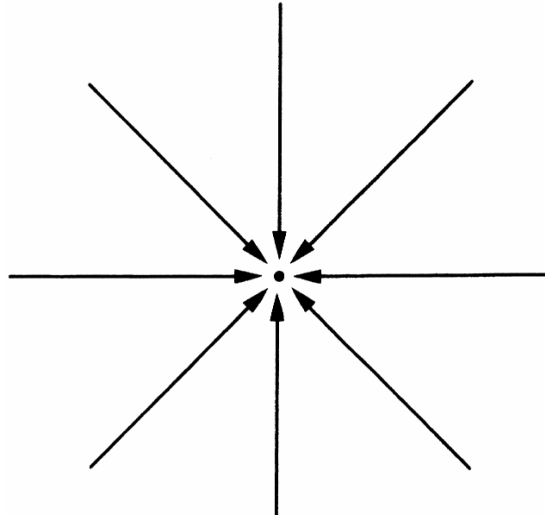


FIGURE 4.3: Pascal's principle of equal pressure exertion on all surfaces of a fluid (Evet and Liu, 1987)

In terms of a three-dimensional coordinate system,

$$p = p_x = p_y = p_z \quad (4.7)$$

This relationship is the basis of the hydrostatic equation. Consider the three-dimensional pressure field acting on a hydrostatic fluid in Figure 4.4:

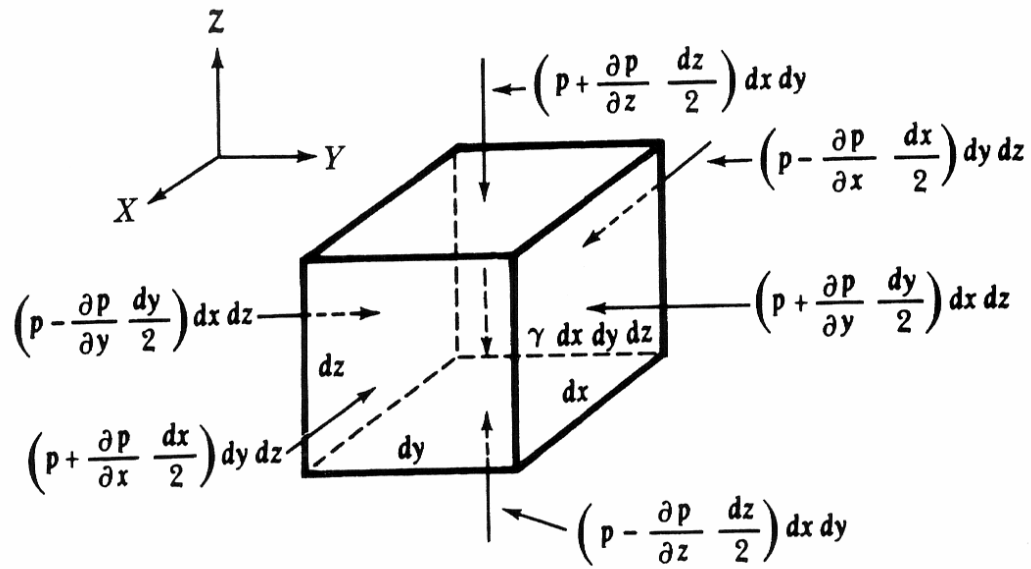


FIGURE 4.4: Hydrostatic forces acting on a fluid (Pefley and Murray, 1966)

Mathematically, the pressure field can be expressed as:

$$dp = \frac{\partial p}{\partial x} dx + \frac{\partial p}{\partial y} dy + \frac{\partial p}{\partial z} dz \quad (4.8)$$

The pressure field equation is a gradient equation, indicating the change in pressure with respect to each axis. For the sake of simplicity, the gradient can be replaced with the del operator, which is appropriate for a collection of partial differential equations, as it is defined as:

$$\nabla = i \frac{\partial}{\partial x} + j \frac{\partial}{\partial y} + k \frac{\partial}{\partial z} \quad (4.9)$$

By substituting, the pressure field of the hydrostatic fluid becomes ∇p . Newton's 2nd Law of Motion states that force is equal to the acceleration of mass (Pefley and Murray, 1966)

$$F = m\alpha \tag{4.10}$$

Since pressure is acting on the hydrostatic fluid in all three directions, then force can be re-defined as the pressure gradient (Pefley and Murray, 1966):

$$F = \nabla p \tag{4.11}$$

The mass of a fluid can be defined as $\rho \, dx \, dy \, dz$, and since the z -axis is aligned with the axis of gravitational acceleration toward Earth's center, it satisfies the required acceleration term (Pefley and Murray, 1966). Thus, in its fundamental form, the hydrostatic equation can be expressed as the following partial differential equation (Feynman, 1971):

$$\nabla p = -\rho \nabla \Phi \tag{4.12}$$

However, the fundamental form of the hydrostatic equation has no solution, as the variation of ρ prevents static equilibrium (Feynman, 1971). If ρ is treated as a constant, however, then the equation can be solved (Michelson, 1970):

$$p + \rho\Phi = \text{const.} \quad (4.13)$$

The hydrostatic relationship can then be applied to the equations of motion in relation to a hydrostatic fluid (Pefley and Murray, 1966):

$$dp = -\rho g_x dx - \rho g_y dy - \rho g_z dz \quad (4.14)$$

The vector of gravitational acceleration was purposely chosen as the alignment of the z -axis. Since g is not acting in the x - or y -planes, the equations of motion in these axes simplify to zero (Prandtl and Tietjens, 1957; Michelson, 1970):

$$\frac{\partial p}{\partial x} = -\rho g_x = 0 \quad (4.15)$$

$$\frac{\partial p}{\partial y} = -\rho g_y = 0 \quad (4.16)$$

Alignment of the z -axis yields the following relationship, where pressure forces are counteracted by gravitational forces (Prandtl and Tietjens, 1957; Michelson, 1970):

$$\frac{\partial p}{\partial z} = -\rho g_z \quad (4.17)$$

Integration of the preceding equation results in the algebraic form of the *hydrostatic equation* (Hess, 1979):

$$\int_0^p dp = -\rho g \int_0^h dz \rightarrow p = -\rho gh \quad (4.18)$$

Along the horizontal axes, however, pressure is not balanced by gravity, but instead is balanced by the Coriolis effect. Consider the horizontal component equations of motion, accounting for the Coriolis force (f) (Hess, 1979; Fleagle and Businger, 1980):

$$-f_v = -\frac{1}{\rho} \frac{\partial p}{\partial x} \quad (4.19)$$

$$f_u = -\frac{1}{\rho} \frac{\partial p}{\partial y} \quad (4.20)$$

These equations constitute the geostrophic balance, which is the horizontal equivalent of the hydrostatic balance (Glickman, 2000). Instead of the gravity force that was noted in the vertical (z) direction, however, note the Coriolis terms f_v and f_u , expressed in component directions.

Since air is compressible, the variable density behavior of the atmosphere must also be considered when describing the balance of forces. The density of a gas varies as a

function of pressure and temperature, and can be stated as the equation of state, or *ideal gas equation* (Pefley and Murray, 1966):

$$pV = mRT \quad (4.21)$$

Density is defined as mass per unit volume, and the ideal gas equation can therefore be re-written as follows:

$$p = \rho RT \quad (4.22)$$

As a combination of the hydrostatic equation and the equation of state, geostrophic balance can be expressed in terms of the x , y , and z axes (Hess, 1979; Fleagle and Businger, 1980; Holton, 1992; Carlson, 1998; Andrews, 2004):

$$\frac{f_v}{T} = -R \frac{\partial \ln p}{\partial x} \quad (4.23)$$

$$\frac{f_u}{T} = R \frac{\partial \ln p}{\partial y} \quad (4.24)$$

$$\frac{g}{T} = -R \frac{\partial \ln p}{\partial z} \quad (4.25)$$

Through cross-differentiation, the following equations can be derived (Hess, 1979; Fleagle and Businger, 1980; Holton, 1992; Carlson, 1998; Andrews, 2004):

$$\frac{\partial u}{\partial p} = \frac{R}{f p} \left(\frac{\partial T}{\partial y} \right) \quad (4.26)$$

$$\frac{\partial v}{\partial p} = -\frac{R}{f p} \left(\frac{\partial T}{\partial x} \right) \quad (4.27)$$

Equations 4.26 – 4.27 are more commonly referred to as the *thermal wind equations*, and they mathematically explain the development of the polar jet stream, expressing the component equations of motion in terms of pressure and the Coriolis force in the x and y directions (Reiter, 1963).

In the atmosphere, heights are commonly defined in terms of a constant pressure, or “isobaric” surface. By considering heights in an isobaric manner, the pressure ridges and troughs located within the polar jet stream that constitute slowly propagating Rossby waves can be readily identified. The standard convention for expressing vertical distances in the atmosphere is not the geometric, or actual height, but instead is geopotential height, a closely related term. If the ideal gas equation is substituted into the hydrostatic equation, it can be expressed as (Hess, 1979):

$$\frac{dp}{p} = -\frac{g}{RT} dz \quad (4.28)$$

The term gdz can be redefined as a thickness term (ΔZ), and when Equation 4.28 is integrated, the geopotential thickness, a measure of specific energy between any two pressure layers, can be calculated (Hess, 1979):

$$\Delta Z = \frac{R}{g} \int_{p_2}^{p_1} T d \ln p \quad (4.29)$$

If the temperature (T) is defined as a mean temperature of the thickness in question, then the geopotential thickness can be restated in the following terms (Holton, 1992):

$$Z = -H \ln \left(\frac{p}{p_0} \right) \quad (4.30)$$

In this form, $H = \overline{RT} / g$, and the initial pressure has been redefined as the surface pressure (p_0) so that the geopotential thickness becomes the geopotential height (Z) (Holton, 1992). Geopotential height is preferred to geometric height in part because the simplification eliminates the necessity for an air density term, and because the two values are nearly identical throughout the troposphere (Andrews, 2004).

4.1.3. Baroclinic Wave Development

In contrast to the large-scale, nearly stationary movement of planetary Rossby waves, baroclinic, or “short” waves are of much smaller wavelength and propagate rapidly along the polar jet stream. Baroclinic waves develop in regions of strong temperature contrast,

or baroclinicity, within the polar jet. As a consequence, pronounced wind shear develops along the periphery of the jet, and baroclinic disturbances amplify into synoptic scale waves. These waves generally propagate at speeds of $10\text{-}20\text{ m}\cdot\text{s}^{-1}$, thus rotating through slow-moving Rossby waves, which propagate at speeds less than $8\text{ m}\cdot\text{s}^{-1}$ (Palmén and Newton, 1969).

Once a baroclinic wave develops, thermal advection acts as a positive feedback loop in strengthening it. Cold air advects equatorward on the west side of the wave axis, while warm air advects poleward on the eastern flank of the axis, creating the characteristic sinusoidal trough-ridge structure of the baroclinic disturbance (Palmén and Newton, 1969; Carlson, 1998). In order to transfer potential energy to wave development and amplification, it is necessary for the baroclinic trough to tilt into the polar jet stream with height (Palmén and Newton, 1969; Holton, 1992).

Baroclinic troughs are synonymous with rising motion in the troposphere, which plays a pivotal role in the vertical distribution of air pollutants. Specifically, the flow of air through a baroclinic trough imparts positive vorticity, as described by the *vorticity equation* (Holton, 1992; Djurić, 1994; Carlson, 1998):

$$\frac{\partial \zeta}{\partial t} + V \cdot \nabla (\zeta + f) = 0 \tag{4.31}$$

When a baroclinic wave is embedded within the polar jet stream, flow tends to accelerate in the bottom of the trough when compared with poleward locations along the wave axis

(Holton, 1992; Djurić, 1994). This differential zone of velocity results in a counter-clockwise spin of the flow, or positive curvature vorticity. From the vorticity equation, several assumptions can be made regarding the behavior of planetary and relative (curvature) vorticity, which in turn yields the *quasi-geostrophic equation* (Holton, 1992):

$$\frac{\partial \zeta_g}{\partial t} = -V_g \cdot \nabla(\zeta_g + f) + f_0 \frac{\partial \omega}{\partial p} \quad (4.32)$$

Geopotential tendency, or the change in geopotential energy (whose gradient is defined as acceleration due to gravity, or $\nabla \Phi = -g$), is defined as $\chi = \partial \Phi / \partial t$ (Holton, 1992).

The quasi-geostrophic equation can subsequently be re-written as follows (Holton, 1992):

$$-V_g \cdot \nabla(\zeta_g + f) = -V_g \cdot \nabla \zeta_g - \beta v_g \quad (4.33)$$

A combination of the modified quasi-geostrophic equation and the thermodynamic energy equation therefore constitutes the *geopotential tendency equation* (Holton, 1992):

$$\left[\nabla^2 + \frac{\partial}{\partial p} \left(\frac{f_0^2}{\sigma} \frac{\partial}{\partial p} \right) \right] \chi = -f_0 V_g \cdot \nabla \left(\frac{1}{f_0} \nabla^2 \Phi + f \right) - \frac{\partial}{\partial p} \left[-\frac{f_0^2}{\sigma} V_g \cdot \nabla \left(-\frac{\partial \Phi}{\partial p} \right) \right] \quad (4.34)$$

This equation expresses the behavior of vorticity within baroclinic waves, and in particular, why rising motions are associated with troughs and sinking motions with

ridges, respectively. The first primary term on the right hand side of the geopotential tendency equation is the vorticity advection term (Holton, 1992):

$$-f_0 V_g \cdot \nabla \left(\frac{1}{f_0} \nabla^2 \Phi + f \right) \quad (4.35)$$

Along the trough and ridge axes of the baroclinic wave, the potential vorticity advection term goes to 0. Therefore, $\partial\Phi/\partial t$ (expressed as χ) is approximated by differential temperature advection, the third term in the geopotential tendency equation (Holton, 1992):

$$-\frac{\partial}{\partial p} \left[-\frac{f_0^2}{\sigma} V_g \cdot \nabla \left(-\frac{\partial\Phi}{\partial p} \right) \right] \quad (4.36)$$

Since baroclinic troughs and ridges are tilted into the flow of the polar jet stream, the upper-tropospheric trough overlies cold air advection, and conversely, the upper-tropospheric ridge overlies warm air advection (Palmén and Newton, 1969; Holton, 1992). The geostrophic wind (V_g) is positive in the case of warm air advection, and the entire term is therefore negative. Thus positive vorticity advection occurs ahead of a baroclinic trough, as $-\partial\Phi/\partial t$ is proportional to temperature, and in this case, $\partial\Phi/\partial t < 0$ (Holton, 1992; Carlson, 1998). When cold air advection is occurring, V_g is negative, and $\partial\Phi/\partial t > 0$, signifying negative vorticity advection as the ridge axis approaches (Holton, 1992; Carlson, 1998).

The vertical motion associated with baroclinic waves is perhaps more completely understood by re-defining quasi-geostrophic flow in terms of vertical velocity (ω) instead of χ . In this case, a diagnostic formula known as the *omega equation* is derived (Holton, 1992; Djurić, 1994; Carlson, 1998):

$$\left(\nabla^2 + \frac{f_0^2}{\sigma} \frac{\partial^2}{\partial p^2} \right) \omega = \frac{f_0}{\sigma} \frac{\partial}{\partial p} \left[V_g \cdot \nabla \left(\frac{1}{f_0} \nabla^2 \Phi + f \right) \right] + \frac{1}{\sigma} \nabla^2 \left[V_g \cdot \nabla \left(-\frac{\partial \Phi}{\partial p} \right) \right] \quad (4.37)$$

In this form, the term on the left side of the equation is proportional to $-\omega$ (Holton, 1992). The positive direction of ω is set so that downward velocity is positive, and the direction of upward vertical motion, defined as W , can therefore be expressed as $-\omega$. Thus, the strongest upward vertical motion in the vicinity of a baroclinic wave ($+W$) occurs in advance of the upper-tropospheric trough in the region of warm air advection, and the strongest downward vertical motion ($-W$) occurs in advance of the upper-tropospheric ridge in the region of cold air advection (Holton, 1992). Again, these systems are tilted into the upper-level flow, and $+W$ therefore directly overlies the accompanying center of surface low pressure, while $-W$ directly overlies the center of surface high pressure (Figure 4.5) (Holton, 1992).

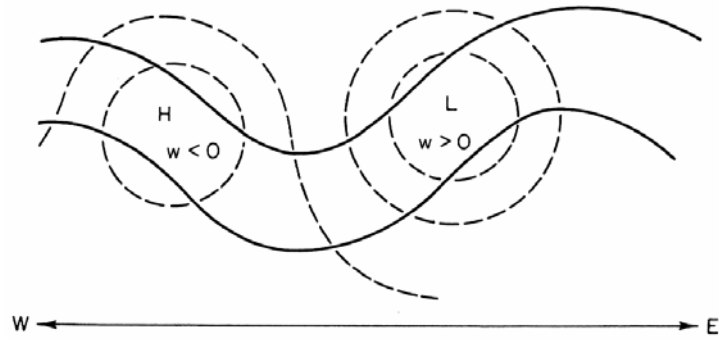


FIGURE 4.5: Maximum upward and downward motion overlying surface low and high pressure (dashed isobars) in relation to a baroclinic wave (denoted as solid geopotential height lines) (Holton, 1992)

The formation processes of waves in the zonal flow of the polar jet stream can continue in the presence of significant baroclinic instability, leading to wave amplification, and in some cases, cyclone formation. According to Palmén and Newton (1969), baroclinic wave amplification is constrained by the following factors:

1. A minimum wavelength is required for amplification.
2. A wavelength range between 2500 and 5000 km is favored for amplification.
3. Intensification is proportional to baroclinicity.

In order for cyclogenesis to proceed, the baroclinic wave requires an underlying surface boundary, such as a front or trough. Thus, meridional mountain ranges within the zonal flow of the polar jet are often the focus for cyclone development, and this phenomenon is

commonly witnessed on the eastern side of the Rocky Mountains, where lee troughs form (Carlson, 1998). Baroclinic zones along fronts and coastlines also promote cyclogenesis (Carlson, 1998).

Flow exiting a baroclinic trough tends to be diffluent, and this characteristic leads to the development of a center of low pressure in the lower atmosphere. Since mass diverges in the upper troposphere ahead of a trough, the principle of conservation of mass dictates that mass compensation, or convergence, must occur in the lower troposphere (Palmén and Newton, 1969; Carlson, 1998). The principle of conservation of mass is mathematically expressed by the continuity equation (a derivation of Reynolds transport theorem), and when combined with the hydrostatic equation, the relationship between mass and pressure can be stated as the *pressure tendency equation* (Palmén and Newton, 1969):

$$\left(\frac{\partial p}{\partial t}\right)_0 = -g \int_0^\infty \rho \nabla_h \cdot V dz - g \int_0^\infty V \cdot \nabla_h \rho dz \quad (4.38)$$

From this equation, mass divergence in the upper troposphere must result in decreasing pressure in the underlying column, as mass is transported upward to compensate for the divergence ahead of the trough. As positive vorticity advects through the base of the trough, this motion is imparted to the convergent flow in the lower troposphere, and a cyclonic circulation subsequently develops (Holton, 1992). If mass divergence at the top of the column exceeds mass convergence below, then the cyclone strengthens (Palmén and Newton, 1969). Due to the aforementioned westward tilt of the baroclinic trough, the

cyclonic circulation in the lower troposphere will develop ahead of the trough axis in the region of divergence.

Thermal advection, or the introduction of warm air ahead of the cyclone and cold air trailing the cyclone, serves as a positive feedback loop as baroclinic instability increases, therefore increasing upper-tropospheric divergence ahead of the wave (Palmén and Newton, 1969). The increased exodus of mass at this level amplifies the surface cyclone, and the process continues. As increasing positive vorticity advects through the strengthening baroclinic trough, the cyclonically rotating motion translates to the pressure field, and a closed contour low within the base of the trough may subsequently develop if the process continues long enough (Figure 4.6) (Palmén and Newton, 1969).

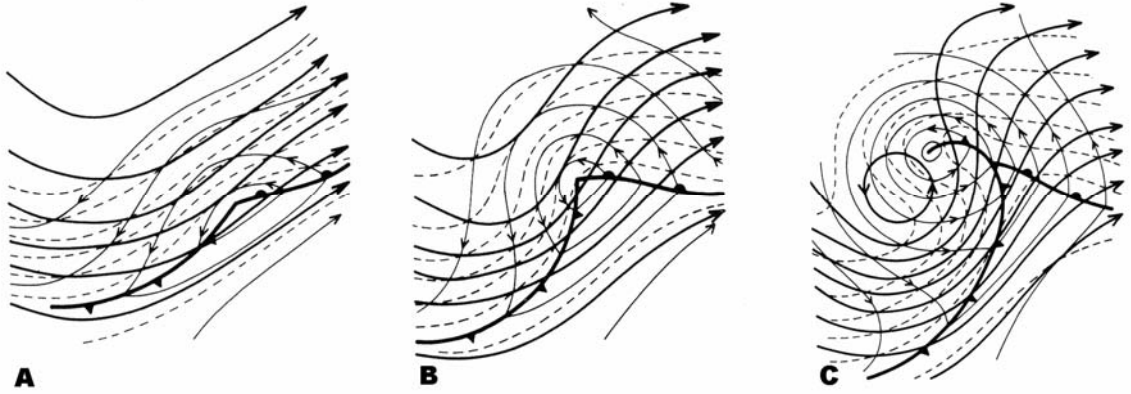


FIGURE 4.6: Stages of cyclogenesis, including **A)** a disturbance underlying the upper-tropospheric trough; **B)** amplification of the surface cyclone and overlying upper-tropospheric trough; and **C)** upper-tropospheric closed low in phase with surface cyclone at maximum strength. Upper-tropospheric geopotential height contours are denoted by thick solid lines, while surface geopotential height contours are denoted by thin solid lines. The 1000-500 hPa thickness is represented by dashed lines (Palmén and Newton, 1969)

Baroclinic wave amplification and cyclogenesis cannot continue infinitely, however, as the positive feedback loop reaches a point when thermal advection no longer increases. The limitation of baroclinic amplification can be examined through the *thermal advection equation* (Palmén and Newton, 1969):

$$\frac{\partial \bar{T}}{\partial t} = -V_0 \nabla \bar{T} + \overline{\omega(\Gamma_a - \Gamma)} \quad (4.39)$$

Normally, the temperature advection term $-V_0 \nabla \bar{T}$ is larger than the static stability term $\overline{\omega(\Gamma_a - \Gamma)}$ (Palmén and Newton, 1969). At some point during wave amplification, however, increasing vertical motion (ω) in response to increasing upper tropospheric mass divergence increases sufficiently that stability offsets horizontal temperature advection, and local temperature change goes to 0. Otherwise, cyclones would infinitely strengthen.

Instead, cyclones associated with baroclinic waves reach maximum intensity and begin to weaken, as the upper tropospheric trough begins to negatively tilt in the presence of strong positive vorticity advection followed by increasing cold air advection behind the trough (Palmén and Newton, 1969; Carlson, 1998). This tilt brings the closed upper tropospheric low into phase with the cyclone, effectively eliminating the overlying mass divergence and weakening the cyclone in a process referred to as cyclolysis (Glickman, 2000). Net increases in mass resulting from the continued convergence in the lower troposphere “fill” the cyclone, and pressure subsequently rises.

4.2. Boundary-Layer Meteorology

The Earth's atmosphere is comprised of many layers – each with distinct physical and chemical properties. Of particular interest when considering near-surface photochemical processes is the atmospheric boundary layer. The boundary layer varies in size and structure on horizontal, vertical, and temporal scales. In general, however, the processes that govern the characteristics of the boundary layer remain constant regardless of location.

4.2.1. Structure and Stability

Boundary-layer processes arise when laminar flow encounters friction, thereby generating a component of drag. Within the atmospheric boundary layer, turbulence is a function of two processes: differential surface heating and mechanical resistance (Seaman, 2000). In the presence of sunlight, terrains of varying elevation and composition heat at different rates. As a function of the ideal gas equation, air density is inversely proportional to ambient temperature (Equation 4.22). Therefore, when parcels of air are differentially heated, they will ascend or descend at rates based on their densities relative to one another.

In addition to turbulence generated by unequal surface heating, the frictional forces within the boundary layer also result from mechanical resistance. When fluids flow over surfaces that vary with respect to elevation and composition, resistive forces of varying

magnitudes are generated. Air that flows through the boundary layer as wind encounters complex terrain, vegetation, and man-made structures. All contribute to the frictional forces that are present in the boundary layer.

The combination of differential surface heating and mechanical resistance within the boundary layer results in thermodynamic and dynamic instability, and turbulent wind motion near the Earth's surface ensues (Shaw et al., 2004). As parcels churn within the boundary layer, they effectively mix the entire depth in which they are acting. This process is commonly known as the development of the mixed layer. This layer, also referred to as the convective mixed layer if convective turbulence is dominant, is diurnally driven, and is capped by a temperature inversion and entrainment zone (EZ) (Figure 4.7) (Stull, 1988).

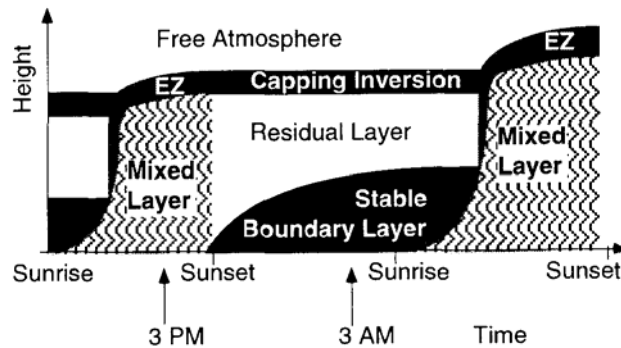


FIGURE 4.7: Atmospheric boundary layer structure (Stull, 2000)

After sunrise, the mixed layer initiates as a shallow layer with the onset of mixing. As convective and mechanical processes increase, the depth of the mixed layer responds by increasing to uniform depth, encompassing much of the total depth of the boundary layer.

Finally, as turbulent processes subside with sunset and the subsequent loss of differential surface heating, the mixed layer dissipates (Stull, 1988). Convective cells within the boundary layer, also known as eddies, may occupy a cross-sectional width of 1 kilometer and last as long as 30 minutes (Seaman, 2000).

Evolution of the depth of the convective boundary layer cannot be easily determined in a mathematical sense, as no simple model can exactly reproduce the multitude of variable processes that govern the full development of the mixed layer (Arya, 2001). However, this thickness can be estimated by a variety of integral models, including the *thermodynamic method of mixed-layer growth* (Arya, 2001):

$$\frac{\partial h}{\partial t} = \frac{1}{\gamma} \frac{\partial \theta_M}{\partial t} \quad (4.40)$$

In Equation 4.40, $\partial h/\partial t$ represents the variable height of the boundary layer, while $\partial \theta/\partial t$ is the change in mixed-layer potential temperature. The symbol γ is used as a proxy for the potential temperature evolution above the boundary layer. Following simplification, the thermodynamic estimation of convective boundary-layer depth can be explicitly computed (Arya, 2001):

$$h(t) = \left[h_0^2 + \frac{2(1+C)}{\gamma} \int_0^t (\overline{\omega\theta})_0 dt \right]^{1/2} \quad (4.41)$$

This form of the thermodynamic growth equation considers the initial boundary-layer depth (h_0), an integration constant (C), and $(\overline{\omega\theta})_0 / \gamma$, the surface heat flux (measured as $\text{W}\cdot\text{m}^{-2}$). Although Equation 4.41 represents a simplified approximation of the depth of the convective boundary layer, it nonetheless requires a rigorous calculation. Therefore, less intensive approximations of boundary-layer depth can be obtained from the analysis of skew-T thermodynamic soundings, vertical reflectivity from wind profilers, and short-term meteorological model outputs, including the Rapid Update Cycle (RUC) (Figure 4.8).

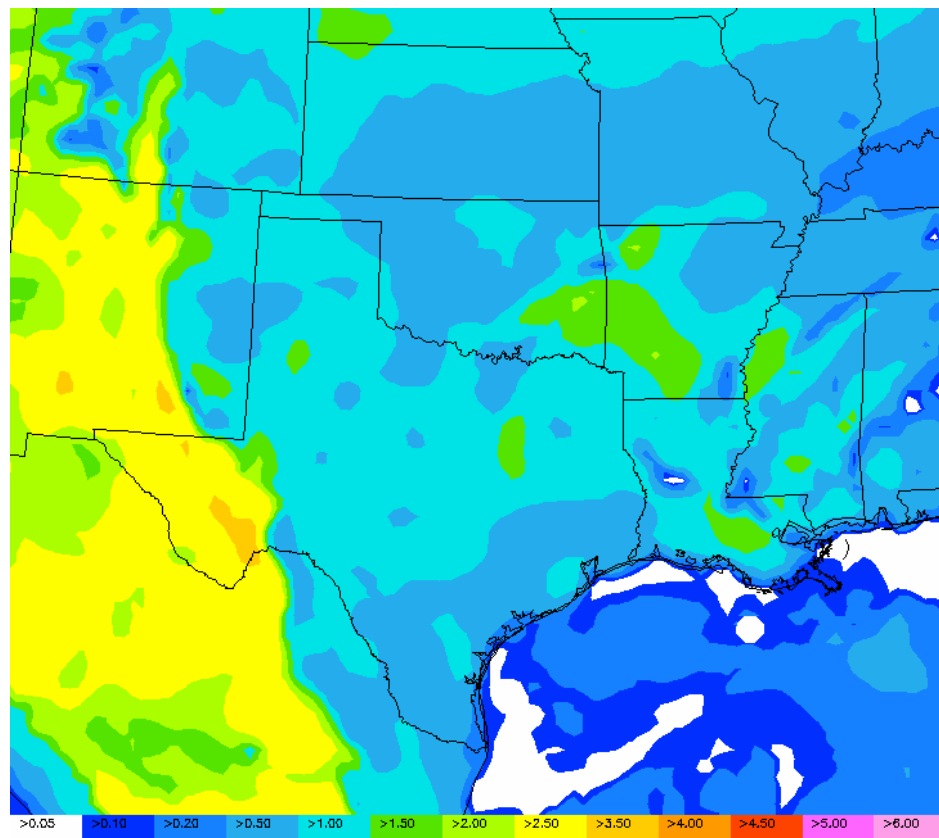


FIGURE 4.8: RUC analysis of 16:00 CST boundary-layer heights (in kilometers), 15 March 2007 (NOAA)

When mixing processes within the boundary layer cease with the loss of daytime heating, the mixed layer transforms into two distinct layers: the nocturnal boundary layer and the residual layer. The nocturnal boundary layer encompasses the lowest few hundred meters of the atmosphere, and is categorically stable since the air temperature increases with height. According to Garratt (1994), the typical depth of the nocturnal boundary layer under calm, clear skies is 100 meters. The minimum depth of the nocturnal boundary layer can be expressed as follows (Stull, 2000):

$$H_{NBL} \approx aU_{RL}^{3/4}\sqrt{t} \quad (4.42)$$

Minimum nocturnal boundary-layer height, H_{NBL} , is a product of a (expressed in $\text{m}^{1/4}\cdot\text{s}^{1/4}$ and estimated as 0.15 for flat terrain), residual-layer wind speed U_{RL} ($\text{m}\cdot\text{s}^{-1}$), and length of time (in seconds) following boundary-layer decoupling. The actual height of the nocturnal boundary layer may be as many as 5 times the value determined in this equation. Even so, it can be seen that with a low residual-layer wind speed (common during the broad regimes of anti-cyclonic subsidence during the summer months), the minimum height of the nocturnal boundary layer will be in close proximity to ground level.

The residual layer, which overlies the nocturnal boundary layer, is classified as statically neutral (Stull, 1988). The temperature within the residual layer is constant with height. Characteristics from recent mixing within the mixed layer continue within the residual layer. Interaction between the residual layer and nocturnal boundary layer is minimized

due to the inverted temperature profile near ground level. Since temperature increases with height in the nocturnal boundary layer, differences in air densities promote stratification between the two layers. The residual layer is effectively decoupled from the nocturnal boundary layer and the Earth's surface, and therefore acts as a potential reservoir for air pollutants that were mixed into the boundary layer during the previous day.

Vertical temperature profiles of the atmospheric boundary layer dictate the degree of stability present adjacent to ground level, thus providing a measure of buoyancy. Within the troposphere, the dry adiabatic lapse rate, or rate at which the temperature of a parcel of air decreases with height in the absence of heat exchange, is defined as follows (Arya, 2001):

$$\Gamma_d = -\frac{\partial T}{\partial z} \quad (4.43)$$

This value is assumed to be $-0.0098 \text{ K}\cdot\text{m}^{-1}$. When a parcel is lifted through a dry adiabatic process, the cooling experienced with increasing elevation results from a decrease in pressure, which is proportional to temperature in the ideal gas equation.

When air is saturated, the lapse rate differs from that of dry adiabatic processes, as latent heat is released with condensation. Again assuming no transfer of heat between the lifted parcel of air and the surrounding atmosphere, the moist adiabatic lapse rate (Γ_s) is lower than the dry adiabatic rate as a result of the latent heat of condensation. The moist

adiabatic lapse rate is a temperature-dependant variable, ranging from $-0.0036 \text{ K}\cdot\text{m}^{-1}$ at 303 K to $-0.0069 \text{ K}\cdot\text{m}^{-1}$ at 273 K.

Actual lapse rates within the atmospheric boundary layer, when compared with the dry and moist adiabatic rates, provide a measure of stability. If the actual lapse rate is greater than the dry adiabatic lapse rate, then the boundary layer is unstable, and air will buoyantly rise and turbulently mix (Hess, 1979). Conversely, the boundary layer is stable when the actual lapse rate is exceeded by the moist adiabatic lapse rate (Hess, 1979). When this condition is present, air parcels are negatively buoyant, thus limiting mixing within a given layer. Nocturnal temperatures in the lower boundary layer often increase with height as an inversion, therefore leading to a very stable lower region that decouples from the middle and upper boundary layer. If a parcel is within a stable environment through a short depth, but will become unstable if lifted above the stable layer, then it is conditionally unstable (Hess, 1979).

4.2.2. Vertical Wind Profile

The magnitude of wind velocities in the atmospheric boundary layer vary as a function of height. During the daytime when significant mixing is present, wind velocities within the boundary layer increase with height, roughly in an exponential fashion. Frictional forces at the surface retard the flow of air, while flow at the top of the boundary layer is nearly laminar (in the case of a fully developed boundary layer). Thus, winds within the boundary layer can be described by the following power law relationship:

$$u = u_0 \left(\frac{z}{z_0} \right)^P \quad (4.44)$$

Wind velocity (u) at height z is calculated by considering known wind velocity (u_0) at known height (z_0) in relation to exponent P , which is a stability variable that ranges between 0 and 1. The greatest variation in boundary-layer wind velocities occurs very close to the Earth's surface (Figure 4.9).

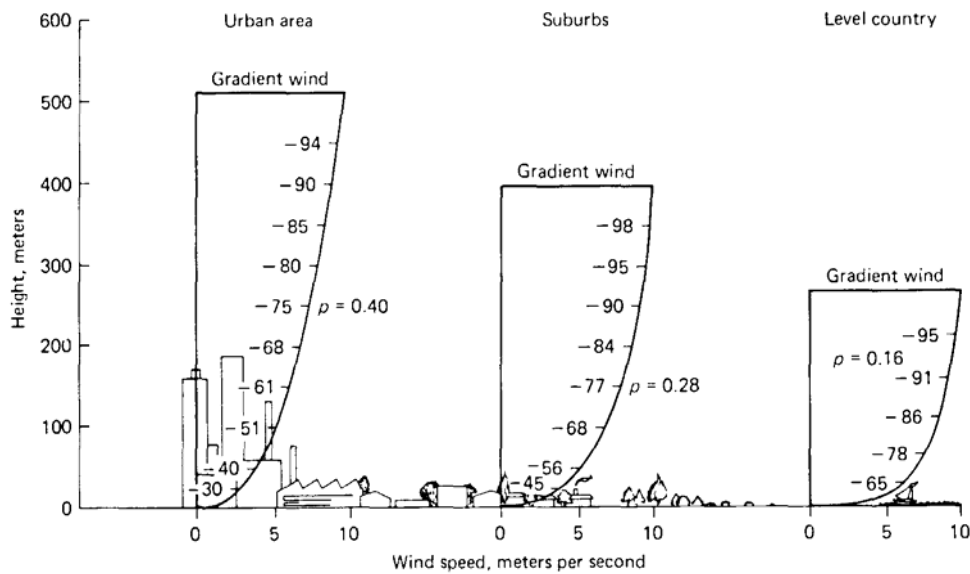


FIGURE 4.9: Wind speed as a function of height within the boundary layer (Wark et al., 1998)

In the free troposphere, large-scale circulations are geostrophic, as the Coriolis force and the pressure gradient force are in balance (Michelson, 1970). Likewise, winds in the upper reaches of the atmospheric boundary layer are approximately geostrophic as well, due to the small magnitude of frictional forces when compared with the lower and middle

portions of the boundary layer. As a result, wind vectors around a cyclone (or anti-cyclone) are tangential to the isobars, or lines of equal pressure (Figure 4.10).

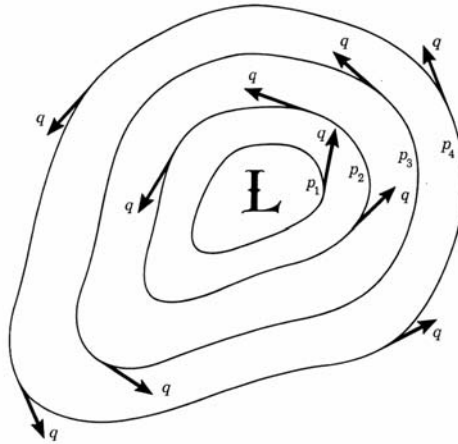


FIGURE 4.10: Geostrophic flow around a cyclone (Michelson, 1970)

Unlike geostrophic winds aloft, however, boundary layer winds are slowed by surface frictional forces, thus deviating from geostrophic balance (Arya, 2001). Frictional forces ultimately slow the attendant flow, and are therefore classified as subgeostrophic (Glickman, 2000). Boundary-layer deviation from geostrophic flow can be expressed as follows (Glickman, 2000):

$$\Delta v = \frac{C_D m u}{fz} \tag{4.45}$$

$$\Delta u = \frac{C_D m v}{fz} \tag{4.46}$$

In Equations 4.45 and 4.46, Δv and Δu are Cartesian components of boundary-layer winds, where Δv is the difference between the actual wind component v and the geostrophic wind component v_g , Δu is the difference between the actual wind component u and the geostrophic wind component u_g , C_D is the coefficient of drag, m is the total wind speed, f is the Coriolis parameter, and z is the depth of the boundary layer.

Since frictional forces within the boundary layer result in an imbalance between the pressure gradient force and the Coriolis force, subgeostrophic wind vectors are not tangential to isobars near ground level. Instead, boundary-layer winds tend to cross isobars, ranging from a very subtle angle of intersection over nearly smooth surface to pronounced angles over rough terrain (Figure 4.11). Water surfaces produce a deviation of approximately 10° , while the deviation from geostrophic flow may be as large as 35° in urban and forested areas (Arya, 2001). In narrow zones of baroclinicity, the angle of deviation can be as high as 70° (Arya, 2001). When flow is counter-clockwise around a cyclone, these subgeostrophic winds are directed toward the center of low pressure, and when an anti-cyclone is present, the flow is directed away from the center of high pressure (Michelson, 1970).

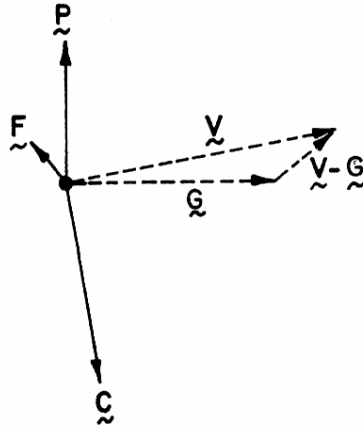


FIGURE 4.11: Deviation of the actual wind vector from the geostrophic wind vector in the middle portion of the atmospheric boundary layer (Arya, 2001)

4.2.3. Nocturnal Low-Level Jet

With the loss of solar heating and decoupling of the nocturnal boundary layer from the residual layer, the frictional forces that affect local winds near the surface during the daytime decrease. In response to the decrease in surface drag, winds immediately above the surface accelerate to compensate for the absence of retarding frictional forces (Fast and McCorcle, 1990; Arya, 1999). The resultant nocturnal wind maximum, commonly referred to as the nocturnal low-level jet, accelerates beyond the geostrophic wind speed, and is subsequently classified as supergeostrophic. The periodicity of the low-level jet is dependent on the Coriolis force (Bonner, 1968; Fast and McCorcle, 1990):

$$P = \frac{2\pi}{f} = \frac{\pi}{\Omega \sin \phi} \quad (4.47)$$

The Coriolis parameter (f) deflects flow to the right in the Northern Hemisphere as a result of the Earth's rotation, and is a function of latitude. Subsequently, the pressure gradient responsible for the development of the nocturnal low-level jet rotates clockwise (Fast and McCorcle, 1990). Winds within the lowest part of the boundary layer exhibit the most significant deflection (Figure 4.12) (Sutton, 1953).

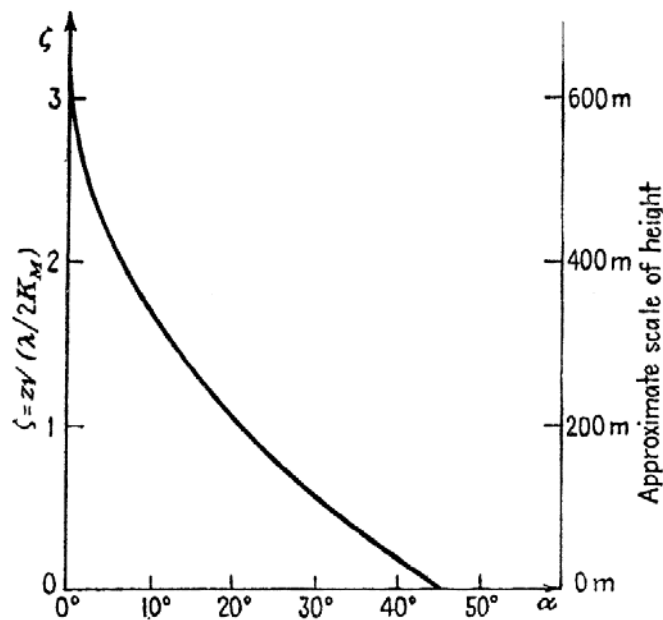


FIGURE 4.12: Wind angle deflection versus height within the atmospheric boundary layer (Sutton, 1953)

The nose of the nocturnal low-level jet coincides with the top of the nocturnal temperature inversion within the atmospheric boundary layer (Figure 4.13) (Blackadar, 1957). Winds within the low-level jet can achieve speeds as high as 30 m s^{-1} in the upper reaches of the nocturnal boundary layer, which is usually within the lowest 300 meters of the atmosphere (Stull, 1988). Wind speed maxima in nocturnal low-level jets commonly

approach $20 \text{ m}\cdot\text{s}^{-1}$ (Fast and McCorcle, 1990). Bonner found that most low-level jets occur between 1 km and 1.5 km above ground level (1968). However, fluctuations in the strength and the height of the nocturnal low-level jet are common on short temporal scales (Blackadar, 1957). Shear forces generated underneath the low-level jet influence the turbulence of the nocturnal boundary layer, thus determining the degree of nocturnal mixing (Banta et al., 2003).

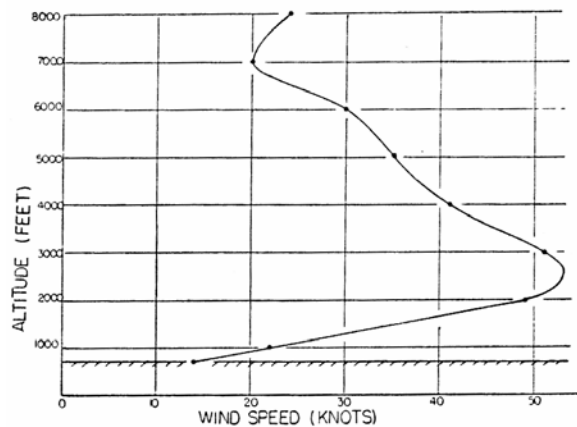


FIGURE 4.13: Vertical wind speed profile indicating nocturnal low-level jet, Tulsa, Oklahoma, 03:00 CST, 8 August 1951 (Blackadar, 1957)

Using a two-year upper-air data set, Bonner developed a set of criteria necessary for the consideration of the presence or absence of nocturnal supergeostrophic winds near the surface (1968). Each class corresponds to an increasing minimum wind speed requirement. Studies indicated that the nocturnal low-level jet is most prevalent in the south-central United States (Bonner, 1968):

- **CLASS 1:** Winds at the height of maximum wind speeds must equal or exceed $12 \text{ m}\cdot\text{s}^{-1}$. Winds must decrease by $6 \text{ m}\cdot\text{s}^{-1}$ to the next highest minimum or to a height of 3 km, whichever is lowest.

As Figure 4.14 indicates, the most prevalent occurrence of this category of nocturnal low-level jet was observed across south-central Kansas and western Oklahoma, where over 400 distinct jets were measured during the two-year study.

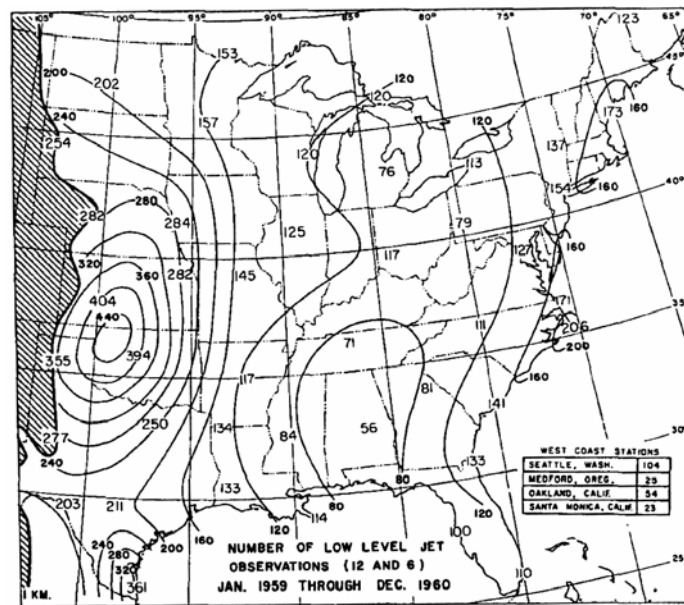


FIGURE 4.14: Number of nocturnal low-level jet occurrences meeting or exceeding Class 1, January 1959 through December 1960 (Bonner, 1968)

- **CLASS 2:** Winds at the height of maximum wind speeds must equal or exceed $16 \text{ m}\cdot\text{s}^{-1}$. Winds must decrease by $8 \text{ m}\cdot\text{s}^{-1}$ to the next highest minimum or to a height of 3 km, whichever is lowest.

Again, the most prevalent region of nocturnal low-level jets as set forth by Bonner's criteria was across south-central Kansas and western Oklahoma, which by far experienced more instances of the low-level jet than any other location (Figure 4.15).

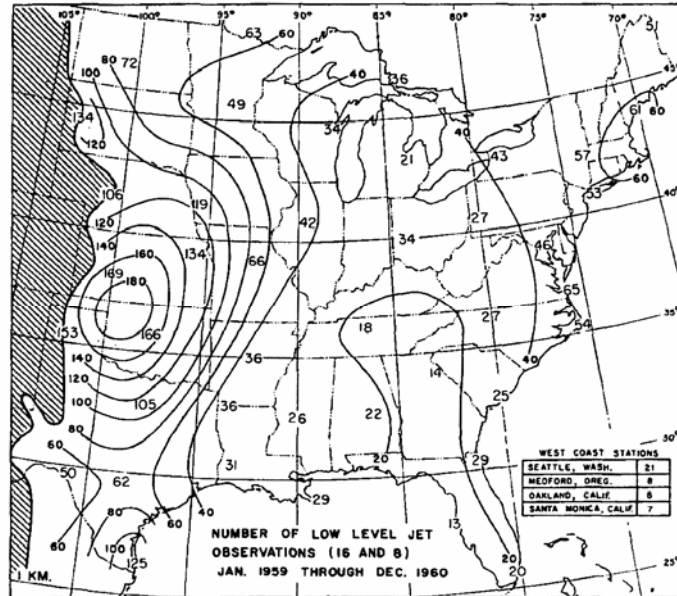


FIGURE 4.15: Number of nocturnal low-level jet occurrences meeting or exceeding Class 2, January 1959 through December 1960 (Bonner, 1968)

- **CLASS 3:** Winds at the height of maximum wind speeds must equal or exceed $20 \text{ m}\cdot\text{s}^{-1}$. Winds must decrease by $10 \text{ m}\cdot\text{s}^{-1}$ to the next highest minimum or to a height of 3 km, whichever is lowest.

As Figure 4.16 indicates, the most frequent occurrence of the nocturnal low-level jet, even at the highest categorical wind speeds was found to exist across south-central Kansas and western Oklahoma. This finding has been supported in a recent study by Whiteman et al. (1997).

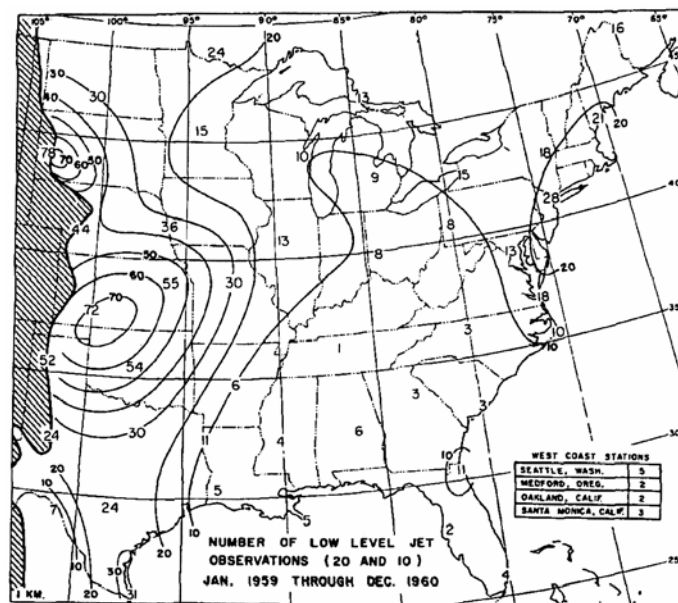


FIGURE 4.16: Number of nocturnal low-level jet occurrences meeting or exceeding Class 3, January 1959 through December 1960 (Bonner, 1968)

While it is inaccurate to describe the low-level jet as an ever-present phenomenon, it is common in this region, where it has been reported in upper-air soundings 30% of the time (Stull, 1988). Additional buoyancy forces related to the general decrease in slope east of

the Rocky Mountains have been attributed to the frequency and magnitude of the nocturnal low-level jet in this region (Fast and McCorcle, 1990).

4.2.4. Meteorological Variables

In addition to wind speed and direction, meteorological parameters commonly measured within the boundary layer include temperature, dew point, relative humidity, and pressure. At National Oceanic and Atmospheric Administration (NOAA) meteorological observation installations, wind speed and direction is measured at 10 meters (33 feet), while other variables are measured at a height of 1.5 meters (5 feet) (NOAA, 1998). Oklahoma Mesonet stations measure dry-bulb temperature, dew-point temperature, relative humidity, and solar radiation at a height of 1.5 meters (5 feet) above the ground, which is in the surface layer of the atmospheric boundary layer. Likewise, air pressure is measured in the surface layer at a height of 0.75 meters (2.5 feet). Winds are measured at a height of 10 meters (33 feet), which is in the mixed layer or nocturnal boundary layer, depending on the time of day (Brock et al., 1995; McPherson et al., 2007). Even though these variables are reported as a time-averaged value ranging from minutes to hours, they tend to fluctuate in a nearly instantaneous manner (Figure 4.17).

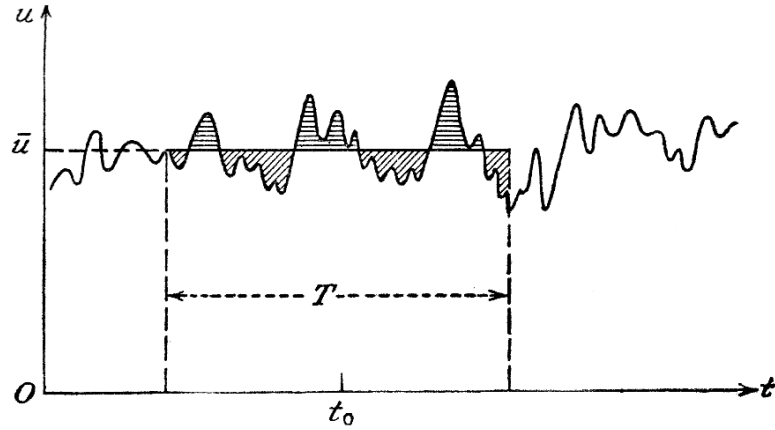


FIGURE 4.17: Derivation of time-averaged wind speed from instantaneous wind speed (Sutton, 1953)

Air temperatures that are commonly measured with mercury thermometers are more formally known as dry-bulb temperatures. In contrast, wet-bulb temperatures account for cooling processes associated with evaporation (Doswell et al., 1991). Wet-bulb temperatures are determined by moistening a wick placed around the bulb of a mercury thermometer and subsequently moving it rapidly with circular motion until all water on the wick has evaporated. A wet-bulb thermometer is referred to as a sling psychrometer.

Potential temperature (θ) is defined as the temperature of an unsaturated parcel of dry air if it has been adiabatically transported from its environmental conditions (T, p) to the standard pressure height (p_0) of 100 kPa (Glickman, 2000). *Poisson's formula* is used to estimate θ (Hess, 1979; Doswell et al., 1991; Glickman, 2000):

$$\theta = T \left(\frac{p_0}{p} \right)^\kappa \tag{4.48}$$

Poisson's constant (κ), equivalent to R_d/c_p , equals 0.286 for dry air (Hess, 1979).

The change in potential temperature with height ($\partial\theta/\partial z$) can be used to estimate the stability of the boundary layer (Banta et al., 2003). Quantification of nocturnal boundary layer stability and depth can be determined by calculating the Richardson number (Berman et al., 1999; Glickman, 2000; Arya, 2001; Banta et al., 2003):

$$Ri = g \frac{\partial\theta}{\partial z} \left| \frac{\partial u}{\partial z} \right|^{-2} \quad (4.49)$$

In addition to the change in potential temperature with height ($\partial\theta/\partial z$), the acceleration of gravity (g) and vertical wind shear ($\partial u/\partial z$) are required for Richardson number calculation. The critical Richardson number is generally assumed to be 0.25. Below this value, conditions are turbulent (Glickman, 2000).

Saturation vapor pressure (e_s) is inversely proportional to temperature, and can be calculated from a variation of the ideal gas equation (Equation 4.22) known as the *Clausius-Clapeyron equation*, where e_0 is a constant 0.611 kPa, L_v/R_v is a constant 5,423 K, and T_0 is a constant 273 K (Hess, 1979; Stull, 2000):

$$e_s = e_0 \cdot \exp \left[\frac{L_v}{R_v} \cdot \left(\frac{1}{T_0} - \frac{1}{T} \right) \right] \quad (4.50)$$

Water vapor content of the lower atmosphere can be directly or indirectly calculated from the vapor pressure derived in Equation 4.50. A common thermodynamic expression of water vapor is the mixing ratio, which is the mass of water vapor to the mass of saturated air (Stull, 2000). Mixing ratios are approximated by calculating specific humidity (Glickman, 2000):

$$w = \frac{0.622e}{p - e} \quad (4.51)$$

Air pressure is represented by the symbol p in Equation 4.51, and the vapor pressure of water is represented by the symbol e . The numerical value $0.622 \text{ g}\cdot\text{g}^{-1}$ is the ratio ε of the gas constant of dry air (R_d) to the gas constant of water vapor (R_v) (Stull, 2000).

Humidity can also be expressed on a relative basis known as relative humidity (RH%). Relative humidity is a percentage ratio of the actual water vapor concentration to the saturation water vapor concentration at a given temperature and pressure (Stull, 2000). Therefore,

$$RH(\%) = \frac{w}{w_s} \cdot 100 \quad (4.52)$$

A common but more complex expression of water vapor concentration is the dew-point temperature, defined as the temperature at which saturation will occur (Stull, 2000):

$$T_d = \left[\frac{1}{T_0} - \frac{R_v}{L_v} \cdot \ln \left(\frac{e}{e_0} \right) \right]^{-1} \quad (4.53)$$

Equation 4.53 simplifies when T_0 , R_v/L_v , and e_0 are considered as constants, leaving actual vapor pressure as the only variable. Dew-point temperature (T_d) is expressed in degrees K.

4.2.5. Summary

Ground-level ozone is highly influenced by meteorological conditions in the boundary layer (Hidy, 2000). In fact, relative concentrations of O_3 are likely more dependent upon meteorological conditions than any other factor. Local photochemical production, an important O_3 formation process, requires sunlight, high temperatures, and weak winds (Zhang et al., 1998). If ozone isn't solely locally produced, then two additional sources must be considered: 1) regional horizontal transport from other source areas; and 2) transport from the free troposphere and adjacent lower stratosphere. Thus, as with local photochemical production, the transport of O_3 also depends largely on meteorological processes, and these processes range from local, short-term events to long-term planetary-scale circulations.

5. OZONE AND HUMAN HEALTH

Ozone is classified as a health-related air pollutant because of its ability to cause respiratory distress. In fact, the EPA (2004) lists the following consequences of ozone inhalation, even at low to moderate concentrations:

- acute respiratory distress
- asthma onset
- temporary lung capacity decreases of 15% - 20% in healthy adults
- inflammation of lung tissue
- increase in emergency room visits and hospital admissions
- decrease in immune system function

The basis for the health-related concerns surrounding ground-level ozone is scientific research, and many studies affirm the information provided by the EPA. In Ohio, Jaffe et al. (2003) calculated a 5% increase in the number of emergency room visits for every 0.01 ppm increase in the 8-hour average O₃ concentration. Wilson et al. (2005) found a correlation between increased ozone and emergency room visits in New England. Lung impairment has been shown to occur at ozone concentrations as low as 0.02 ppm (NRC, 1977).

5.1. Asthma in Sensitive Populations

Asthma is known to result from exposure to ozone pollution (Desqueyroux et al., 2002). Jaffe et al. (2003) and Wilson et al. (2005) noted increases in asthma-related hospital visits with corresponding increases in ground-level O₃ concentrations. According to Lu and Wang (2004), asthma attacks and respiratory infections are more common as O₃ increases. Particularly susceptible are children and the elderly (Wilson et al., 2005). Children who are active in outdoor sports in high O₃ concentration areas are over three times more likely to develop asthma (McConnell et al., 2002). Furthermore, the asthma risk increases with the intensity of the sport and with the number of sports in which children participate (McConnell et al., 2002). Active adults are at risk as well. A study by Selwyn et al. (1983) in Houston, Texas found that runners experienced decreased lung function in the presence of high ozone concentration.

5.2. Mortality

In severe episodes, ozone exposure can be fatal. Mortality is difficult to assess, however, as high ozone concentrations often accompany heat waves, which also statistically increase the probability of death (NRC, 1977). When ground-level O₃ concentrations rose as high as 0.226 ppm in August 2003 in the United Kingdom, 600 deaths were directly attributable to the ozone concentration (Stedman, 2004). In Mexico City, O'Neill et al. (2004) found a positive correlation between O₃ concentration and mortality, where a 0.65% increase in deaths was noted for every 0.01 ppm increase in ozone.

Mortality was higher among the elderly, with a 1.39% increase per 0.01 ppm increase in ozone concentration (O'Neill et al., 2004).

5.3. Pulmonary Responses to Ozone Inhalation

Ozone is much too reactive to reach the surface of the human lung (Mudway and Kelly, 2000). Instead, O_3 reacts in the nasal passages and upper respiratory system (Mudway and Kelly, 2000). At low concentrations, O_3 is neutralized through reaction with uric acid, and doesn't pose a significant risk to the pulmonary system (Mudway and Kelly, 2000). However, eye, nose, and throat irritation is common with exposure to low levels of O_3 (Lu et al., 2004). In fact, Desqueyroux et al. (2002) noted an increase in health-related effects with only modest increases in ozone. At higher concentrations, O_3 overwhelms the neutralization capacity of uric acid in the nasal passages, and secondary oxidation products from reactions with proteins and lipids irritate the lung surface (Figure 5.1) (Mudway and Kelly, 2000).

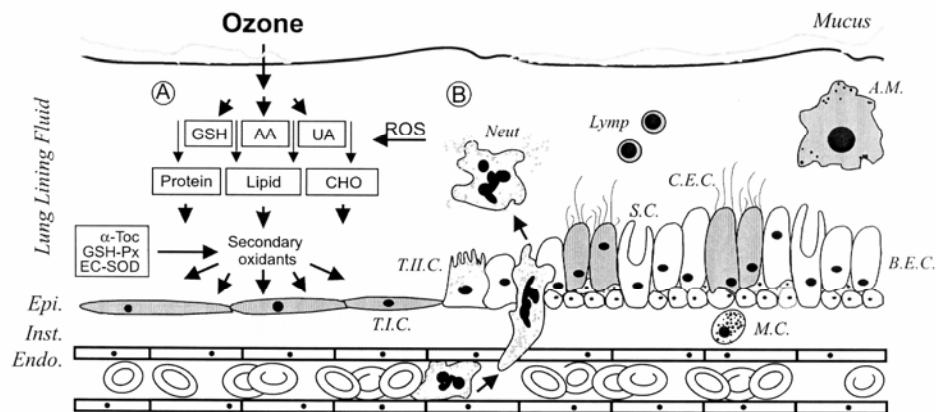


FIGURE 5.1: O_3 reactions near the surface of the lung (Mudway and Kelly, 2000)

Mudway and Kelly (2000) determined that lung function becomes impaired at a threshold of 0.07 ppm. High O₃ concentrations have been associated with decreases in forced expiratory volume (FEV) and peak expiratory flow (PEF) in the human lung (Desqueyroux et al., 2002). According to McDonnell et al. (1983), a 2.6% decrease in FEV was experimentally observed at an ozone concentration of 0.011 ppm, and at 0.043 ppm, an FEV decrease of 24% was observed.

6. THE REGULATORY ENVIRONMENT

The increasing tide of ground-level ozone has generated much policy debate within the United States government, and implications of recurrent ozone episodes place a financial and regulatory strain on metropolitan areas throughout the country. As evidenced by a recent cartoon in the *Tulsa World* (Simpson, 2005), local populations feel the pressure of maintaining ozone compliance and avoiding strain on the local economy:

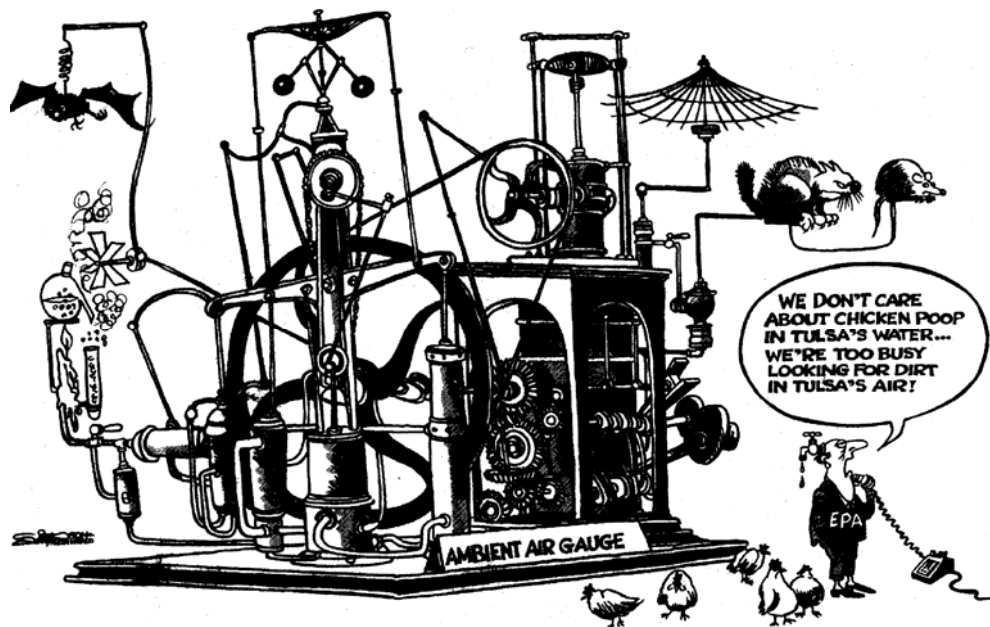


FIGURE 6.1: *Tulsa World* cartoon commentary on local air pollution (Simpson, 2005)

6.1. Federal Regulations

Ozone, defined as a criteria air pollutant in the Clean Air Act (CAA), is subject to regulation in accordance with the National Ambient Air Quality Standards (NAAQS) (EPA, 2005). The O₃ NAAQS, established on 30 April 1971 in Sec. 109 of the CAA, was originally set as a 1-hour standard of 0.08 ppm (EPA, 2005). The 1-hour standard was subsequently increased to 0.12 ppm on 08 February 1979 (EPA, 2005). Penalties for non-attainment listed in 40 CFR 51.900 include the implementation of reasonably available control technologies, vehicle inspection and maintenance programs, vapor recovery systems at fueling stations, transportation control measures, and increased air quality monitoring (EPA, 2006). The O₃ NAAQS definition was again revised on 18 July 1997, with the current 1-hour standard as follows in Section 40 of the Code of Federal Regulations (EPA, 2006):

§50.9 National 1-hour primary and secondary ambient air quality standards for ozone.

- (a) The level of the national 1-hour primary and secondary ambient air quality standards for ozone measured by a reference method based on appendix D to this part and designated in accordance with part 53 of this chapter, is 0.12 parts per million (235 $\mu\text{g}\cdot\text{m}^{-3}$). The standard is attained when the expected number of days per calendar year with maximum hourly average

concentrations above 0.12 parts per million ($235 \mu\text{g}\cdot\text{m}^{-3}$) is equal to or less than 1, as determined by appendix H to this part.

- (b) The 1-hour standards set forth in this section will remain applicable to all areas notwithstanding the promulgation of 8-hour ozone standards under §50.10. The 1-hour NAAQS set forth in paragraph (a) of this section will no longer apply to an area one year after the effective date of the designation of that area for the 8-hour ozone NAAQS pursuant to section 107 of the Clean Air Act. Area designations and classifications with respect to the 1-hour standards are codified in 40 CFR part 81.

- (c) EPA's authority under paragraph (b) of this section to determine that the 1-hour standard no longer applies to an area based on a determination that the area has attained the 1-hour standard is stayed until such time as EPA issues a final rule revising or reinstating such authority and considers and addresses in such rulemaking any comments concerning (1) which, if any, implementation activities for a revised ozone standard (including but not limited to designation and classification of areas) would need to occur before EPA would determine that the 1-hour ozone standard no longer applies to an area, and (2) the effect of revising the ozone NAAQS on the existing 1-hour ozone designations.

In addition, the 1997 O₃ NAAQS Review defined a new 8-hour standard, which accompanies the 1-hour standard in 40 CFR (EPA, 2006):

§50.10 National 8-hour primary and secondary ambient air quality standards for ozone.

- (a) The level of the national 8-hour primary and secondary ambient air quality standards for ozone measured by a reference method based on appendix D to this part and designated in accordance with part 53 of this chapter, is 0.08 parts per million (ppm), daily maximum 8-hour average.
- (b) The 8-hour primary and secondary ozone ambient air quality standards are met at an ambient air quality monitoring site when the average of the annual fourth-highest daily maximum 8-hour average ozone concentration is less than or equal to 0.08 ppm, as determined in accordance with appendix I to this part.

Nearly 50 metropolitan areas in the U.S. are in violation of the 0.12 ppm 1-hour EPA O₃ standard (Rohli et al., 2004). However, the EPA is in the process of adopting the 8-hour ozone standard, thereby phasing out the 1-hour standard. According to 40 CFR 50.9(b), “...the 1-hour NAAQS set forth in paragraph (a) of this section will no longer apply to an area one year after the effective date of the designation of that area for the 8-hour ozone NAAQS pursuant to section 107 of the Clean Air Act...” (EPA, 2006). If a metropolitan

statistical area is designated as not meeting the 8-hour standard, then measures must be taken in order to achieve compliance. Following legal challenges, the EPA is in the process of revising the 1997 O₃ NAAQS Review and proposed 8-hour standard, which is scheduled to become final on 19 December 2007 (EPA, 2005; EPA Review, 2006). As of 2005, all locations in Oklahoma were in attainment with the outgoing 1-hour and new 8-hour O₃ standards (ODEQ, 2005).

6.2. Local Implementation

As a preventative measure to comply with the pending 8-hour O₃ standard and avoid non-attainment, many municipalities have adopted early action compacts (EACs) that voluntarily implement air quality control measures. Local governmental agencies in the Tulsa, Oklahoma metropolitan area collectively share planning responsibilities as the Indian Nations Council of Governments (INCOG). On 31 December 2002, INCOG and the Oklahoma Department of Environmental Quality (ODEQ) entered into a Memorandum of Agreement (MOA) in order to formulate and implement a Clean Air Action Plan (CAAP) "...that will reduce ground-level ozone concentrations in the Tulsa Transportation Management Area to comply with the 8-hour ozone standard by December 31, 2007, and maintain the standard beyond that date..." (INCOG, 2002). The EAC, which was accepted by the EPA, was based on an initial agreement between EPA Region IV and the Texas Commission on Environmental Quality (INCOG, 2002). Tulsa area governments and ODEQ had previously entered into an O₃ Flex Agreement with the

EPA in an attempt to reduce precursor emissions that contribute to the 1-hour O₃ NAAQS (Figure 6.2) (INCOG, 2002).

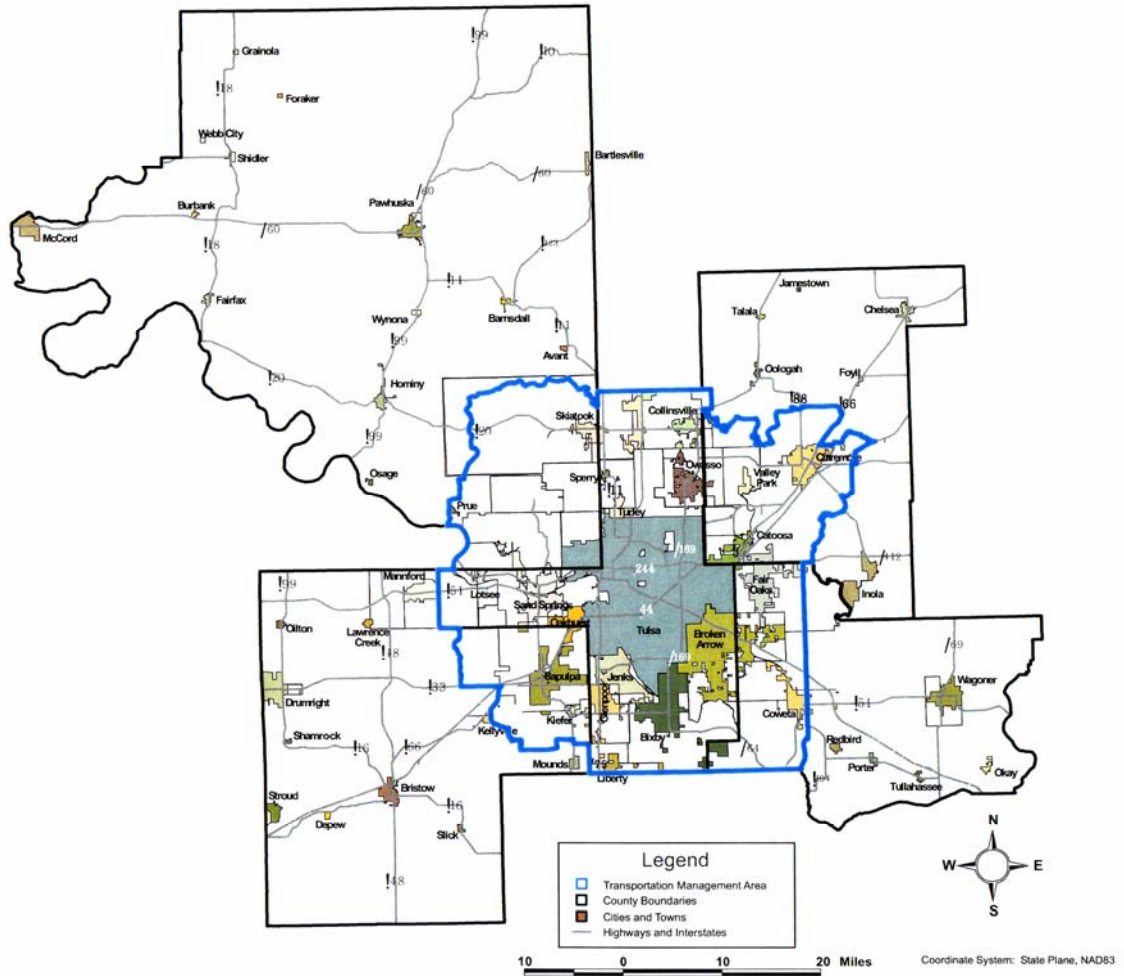


FIGURE 6.2: Tulsa, Oklahoma Early Action Compact (EAC) boundary (INCOG, 2002)

The primary goals of the Tulsa EAC protocol include an accelerated reduction time frame through emissions reduction strategies, increased local control of emissions reduction strategies, and deferral of possible non-attainment designation, provided that EAC protocol milestones are achieved (INCOG, 2002). The Tulsa EAC has been incorporated into the state implementation plan (SIP), which is legally binding (INCOG, 2002). The

final draft of the SIP was submitted to the EPA in December 2004 (ODEQ, 2004). State Implementation Plans are required as described in 40 CFR 51.104 (EPA, 2006).

Of the 29 urban areas that have entered into EACs with the EPA, 15 are currently in attainment of the 8-hour O₃ standard, including the Tulsa metropolitan area. The EAC program requires each participating metropolitan area to issue a report on milestones at regular intervals. Reduction strategies in Tulsa have focused on the transportation sector, and the 31 December 2005 Tulsa EAC progress report indicates a projected 5.23% weekday reduction of NO_x and a 0.05% weekday reduction of VOCs as a result of traffic modifications (ODEQ, 2005).

Provisions of the rules and regulations accompanying the 8-hour ozone standard require air pollution notification to the general public. In the Dallas-Fort Worth, Texas metropolitan area, where O₃ compliance has not been achieved, an air pollution advisory system has been implemented (Stuckey and Sattler, 2003). In 2005, Congress mandated daily air quality forecast issuance by the National Weather Service in large metropolitan areas (Banta et al., 2003). Currently, daily air quality statements are only issued for Oklahoma City within the State of Oklahoma (Figure 6.3).

663
AEUS74 KOUN 281419
AQIOUN
OKZ025-281600-

AIR QUALITY INDEX STATEMENT
OKLAHOMA DEPARTMENT OF ENVIRONMENTAL QUALITY
RELAYED BY THE NATIONAL WEATHER SERVICE NORMAN OK
820 AM CST TUE MAR 28 2006

THE FOLLOWING STATEMENT WAS ISSUED BY THE OKLAHOMA DEPARTMENT OF
ENVIRONMENTAL QUALITY.

THIS MORNING AT 8 AM...THE AIR POLLUTION STANDARD INDEX FOR OKLAHOMA
CITY WAS 38... WITH THE AIR QUALITY RATED GOOD. THE PRIMARY
POLLUTANT WAS OZONE.

FOR FURTHER INFORMATION, TELEPHONE THE OKLAHOMA DEPARTMENT OF
ENVIRONMENTAL QUALITY AT 405-702-4100.

WHEN THE AIR POLLUTION STANDARD INDEX IS LESS THAN 100, NO
PRECAUTIONS ARE NECESSARY.

FIGURE 6.3: Daily air quality report example (NWS Norman, 2006)

Although the program was initiated in 1991, 11 years before the adoption of the EAC, the Indian Nations Council of Governments maintains a comprehensive ozone mitigation and notification program known as “Ozone Alert” (INCOG, 2006). The Ozone Alert program continues as a provision of the EAC, which requires public awareness and involvement (INCOG, 2002). Through coordination with ODEQ, ozone alerts are issued through local media outlets on days that are likely to experience high O₃ concentrations.

As of March 2007, the Tulsa metropolitan area was in compliance with the 8-hour O₃ NAAQS. However, continued implementation of the EAC protocol and SIP were underway in order to fulfill the obligation that the local and state governments have to the EPA and to maintain NAAQS compliance.

7. RECENT OZONE STUDIES

Although ground-level ozone has been well studied over the past three decades, many research projects have focused on the local, diurnal photochemical production of O₃ and precursor compounds, largely ignoring the roles that boundary-layer meteorology and subsequent transport pathways play in the relative changes in ozone concentrations. However, it has been suggested that meteorology is the governing factor in the net change of ground-level ozone concentration (Solomon et al., 2000). Several recent experiments have focused on the relationship between the atmospheric boundary layer and tropospheric ozone.

7.1. Boundary-Layer Considerations

Findings from recent studies indicate that ozone concentrations in the lower atmosphere are driven by the characteristic daily development and dissipation of the atmospheric boundary layer. When the depth of the boundary layer increases during the mid-morning hours, O₃ suspended aloft mixes downward to the Earth's surface (Chan et al., 1998; Zhang et al., 1998; Zhang and Rao, 1999; Aneja et al., 2000; Baumann et al., 2000; Lin et al., 2004; Steinbacher et al., 2004). Conversely, it has also been noted that vigorous boundary-layer mixing not only contributes to the downward transport of O₃, but also upward transport, or "venting," from the boundary layer into the troposphere (Monks,

2000; Seaman, 2000). Bithell et al. (2000) concluded that polluted boundary layer air results in significant tropospheric O_3 production once it is vented by convection. Plaza et al. (1997) found that surface ozone plumes in the Spanish capital city of Madrid extended to heights of 1000 meters to 1200 meters above the surface. According to Banta et al. (2005), increased boundary-layer depth reduces overall O_3 concentration as a result of dilution from the increased mixing volume. Ozone within the free troposphere behaves differently than O_3 in close proximity to the ground surface. O_3 aloft is not subject to surface depositional processes, and thus remains higher (Aneja et al., 2000). Consequently, the lifetimes of O_3 and precursor molecules are much longer above the boundary layer (Figure 7.1) (Ridley et al., 2004).

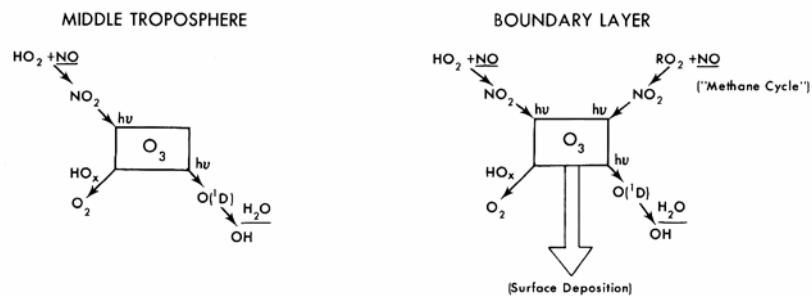


FIGURE 7.1: Physical and photochemical processes acting on O_3 in the middle troposphere and in the boundary layer (Levy, 1984)

7.2. Tower Studies

A select number of recent research projects have implemented tower studies – data acquisition originating from platforms on buildings, broadcast towers, mountains, and other vertical structures within the boundary layer. At Frohnau Tower in Berlin,

Germany (324 meters), O₃ concentrations differed from O₃ measurements at the surface and appeared to have a distinct origin (Rappenglück et al., 2004). According to Aneja et al. (2000), increasing O₃ concentrations with height, recorded at an elevation of 433 meters in North Carolina, signaled the presence of regional transport (Figure 7.2).

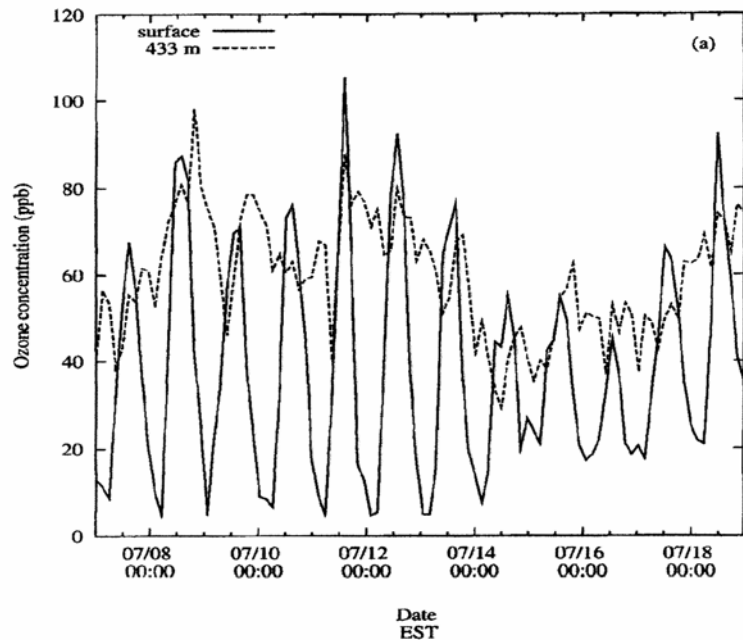


FIGURE 7.2: 10-day comparison of O₃ concentrations measured at ground level and at 433 meters in Garner, North Carolina (Zhang and Rao, 1999)

During the summer months of 1993 through 1995, data were collected continuously from the transmission tower in North Carolina at three elevations: ground level, 250 meters, and 433 meters (Aneja et al., 2000). Linear regression performed on the data set revealed that a distinct correlation axis existed when ground-level O₃ data were compared with concentrations measured at height within the boundary layer, but significant interference was also present at low O₃ concentrations, and the overall correlation was therefore low.

However, when the 250 meter and 433 meter datasets were compared with one another, the low-level interference was eliminated, and correlation therefore increased significantly (Figure 7.3) (Aneja et al., 2000).

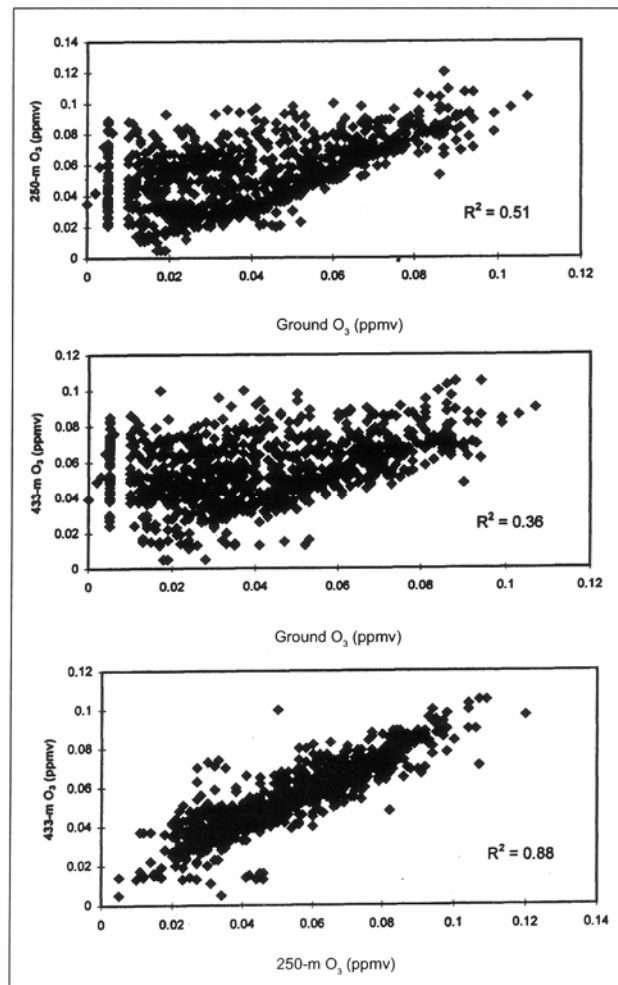


FIGURE 7.3: Vertical O₃ concentration correlation plots, Garner, North Carolina (Aneja et al., 2000)

The ground-level and 433 meter O₃ concentration data were also considered as time-dependent correlations. Kim et al. (2002) found that the strongest concentration

correlations between the two heights occurred during the mid to late afternoon hours, when boundary-layer mixing reached its peak intensity (Figure 7.4).

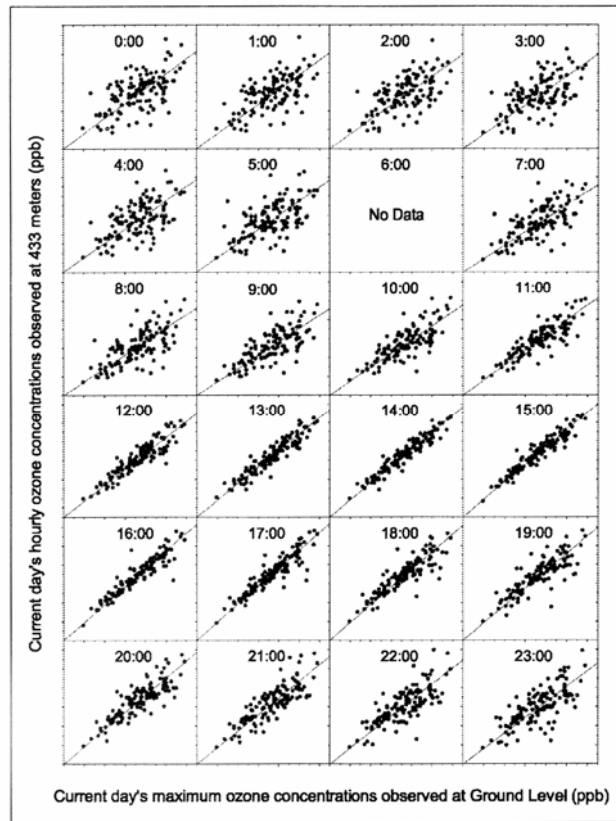


FIGURE 7.4: Ground-level and 433 meter time-dependent O₃ concentration correlations, Garner, North Carolina (Kim et al., 2002)

A previous tower study in southeastern Oklahoma found that ozone behavior aloft was similar to findings of other tower studies, with higher O₃ concentrations prevalent immediately above the low-level temperature inversion within the nocturnal boundary layer (Figure 7.5) (Kastner-Klein et al., 2002). During the 1997 Southern California Ozone Study (SCOS-97), O₃ was measured on both sides of the low-level nocturnal

temperature inversion, with higher concentrations present immediately above the inverted layer (Rosenthal et al., 2003).

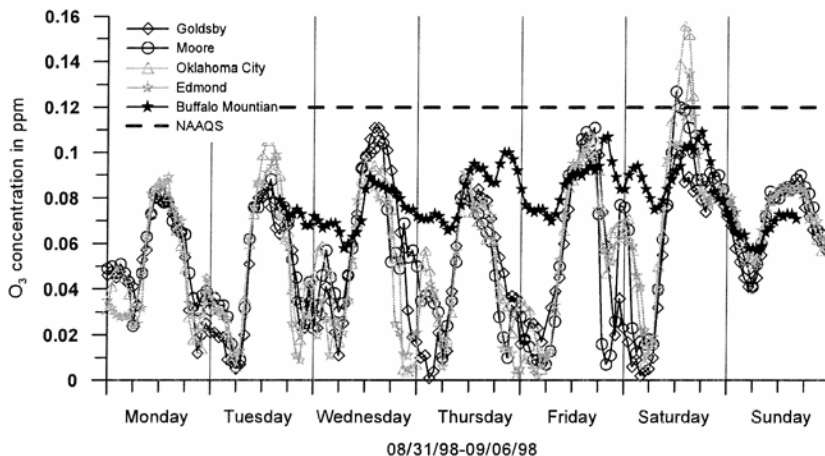


FIGURE 7.5: 7-day comparison of O₃ concentrations measured at ground level in the Oklahoma City metropolitan area and at Buffalo Mountain, a rural elevated site in southeastern Oklahoma (Kastner-Klein et al., 2002)

7.3. Tropospheric Background Concentrations

Background ozone concentrations can be directly measured within the middle part of the atmospheric boundary layer since O₃ at these elevations is not subject to the same degree of depositional processes that occur at Earth's surface. Reports of background concentrations vary, but all values given in recent literature are relatively high. In the 1995 North American Research Strategy for Tropospheric Ozone (NARSTO) campaign, Zhang et al. (1998) examined the presence of an O₃ reservoir along the Atlantic Coast of the United States, where background concentrations varied between 0.08 and 0.1 ppm. Liu et al. (2004) measured background O₃ concentrations between 0.078 and 0.086 ppm

in a layer between 600 meters and 900 meters above ground level in Taiwan. Mudway and Kelly (2000) reported that the background O₃ concentration in London, United Kingdom ranges between 0.02 and 0.04 ppm. In Madrid, Spain, the nocturnal (background) O₃ concentration varied between 0.06 and 0.080 ppm in recent experimental measurements (Plaza et al., 1997). Likewise, background concentrations in the eastern Atlantic were similar to those in southwestern Europe, with measured values between 0.05 and 0.070 ppm (Gangoiti et al., 2001). Ozone is not limited to populated, industrialized areas. Concentrations as high as 0.04 ppm have been measured north of the Arctic Circle in Greenland during the winter months (Heidam et al., 2004). Figure 7.6 illustrates an example of the nocturnal O₃ concentrations vertically through the boundary layer in Nashville, Tennessee.

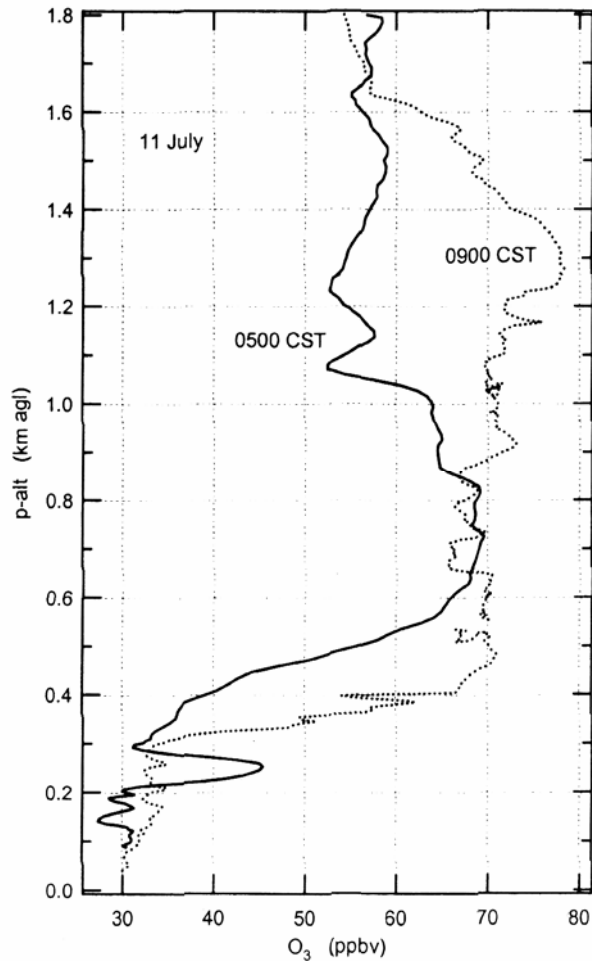


FIGURE 7.6: Typical nocturnal O_3 concentrations in the atmospheric boundary layer and lower troposphere (Baumann et al., 2000)

Rodríguez et al. (2004) concluded that high O_3 concentrations within the nocturnal boundary layer are an indicator of regional transport processes, and thus not of local origin. Pochanart et al. (2004) arrived at a similar conclusion, stating that background O_3 concentrations do not originate from local, short-term surface photochemistry, but instead are indicative of tropospheric ozone. Ozone resulting from local, short-term photochemistry combines with background O_3 , contributing to the overall ozone concentration in a particular location at any given time (Pont and Fontan, 2001). Ridley

et al. (2004) recorded ozone concentrations within the troposphere as high as 0.125 ppm with aircraft instrumentation. With data from the 433-meter tower study in North Carolina, Zhang and Rao (1999) estimated that 50% of the total measured ozone concentration resulted from entrainment, or transport, while the other 50% was due to local photochemistry. On the other hand, Lin et al. (2004) estimated that 40% of total ozone was due to transport, 40% was due to short-term local photochemistry, and 20% was due to residual local photochemistry. Ground-level ozone in New England is also thought to be of remote origin, with baseline concentrations representative of transport (Angevine et al., 2004). European researchers have reported concurring opinions. Fenger (1999) described European ozone as a propagating mobile plume, while Rappenglück et al. (2004) noted that ozone-rich air masses in Germany are likely transported from remote regions.

The origins of background ozone are not fully understood, but certain processes are likely contributors. Of particular interest in the lower atmosphere is the nocturnal low-level jet. Low-level jets have been linked to the horizontal transport of pollutant plumes, including ozone. Steinbacher et al. (2004) measured O₃ concentrations on the Swiss Plateau in central Europe. They found that ozone was transported by a föehn, or nocturnal low-level jet, through the Alps, thus contributing to increases in O₃ concentrations at elevation within the boundary layer (Steinbacher et al., 2004). Zhang et al. (1998) also noted the presence of a nocturnal low-level jet and its possible contribution to ozone transport in the eastern U.S. Carlson et al. (1992) demonstrated the effectiveness of transport within

the low-level jet by constructing trajectories for insect movement through the central United States.

7.4. Subtropical Anti-Cyclones

Synoptic-scale meteorological features that have been linked to episodes of high ozone concentrations include high-pressure systems. High-pressure systems are synonymous with large-scale subsidence through the troposphere, and also coincide with stagnant conditions at Earth's surface. High concentrations of O₃ have been associated with high-pressure systems and attendant subsidence, particularly when the anti-cyclonic circulation surrounding the center of high pressure is weak (Hidy, 2000). Attention has been given to high ozone concentration episodes in southwestern Europe, including Spain and the Canary Islands, which is often under the influence of the semi-permanent Azores High (Plaza et al., 1997; Gangoiti et al., 2001; Millán et al., 2002; Rodríguez et al., 2004). The causal connection linking high-pressure systems to increases in ozone concentrations is also a key finding in studies conducted in eastern Asia. Chan et al. (1998), Wang et al. (1998), and So and Wang (2003) all noted that ozone episodes in Hong Kong were concurrent with high-pressure systems. Common high-pressure systems influencing China include the continental Asian High and the equatorial Australian High (Chan et al., 1998). Lin et al. (2004) published similar conclusions regarding synoptic influences on ozone in Taiwan. Further north, ozone episodes in Seoul, Korea are coupled with the presence of the North Pacific High (Ghim et al., 2001). The connection between high-pressure and high O₃ concentrations is not limited to countries abroad. Within the United

States, a study in Nashville, Tennessee found that high pressure aloft and subsequent stagnation of the boundary layer increases the likelihood of high levels of ground-level ozone (Baumann et al., 2000). Boucouvala and Bornstein (2003) determined that similar synoptic-pressure regimes contribute to an ozone increase on the Pacific Coast of the United States, where the Pacific High tends to dominate. The presence of the Pacific High, a broad, anti-cyclonic circulation, promotes stagnation within the boundary layer in the Los Angeles metropolitan area (Boucouvala and Bornstein, 2003). The Pacific High is marked by strong subsidence through the troposphere (Rosenthal et al., 2003). In the south-central United States, Rohli et al. (2004) discussed the possible contribution of O₃ in Louisiana through horizontal advection around the Bermuda High from sources in southeastern Texas. As the Bermuda High shifts eastward, lower concentrations of ozone appear to enter the region from the Gulf of Mexico (Rohli et al., 2004). Mid-Atlantic air pollution episodes also intensify from synoptic anti-cyclonic circulations, as O₃ rich air propagates into the Baltimore-Washington, D.C. corridor under the influence of high pressure (Blumenthal et al., 1998; Zhang et al., 1998).

7.5. Exchange between the Stratosphere and Troposphere

Cyclonic systems also influence ozone concentrations within the troposphere. According to Kim et al. (2002), high concentrations of O₃ in Korea have been recorded in the presence of a cut-off low – a cyclonic circulation detached from the mean mid-level flow. A similar synoptic pattern, marked by a cut-off low-pressure system, resulted in increased ozone concentrations in the Pyrenees Mountains of Spain (Tulet et al., 2002). Rodríguez

et al. (2004) observed high O₃ concentrations on the western sides of upper-level cyclones in the North Atlantic, and they speculate that stratospheric ozone is entering the troposphere through tropopause folds in these regions as a function of stratospheric-tropospheric exchange (Figure 7.7).

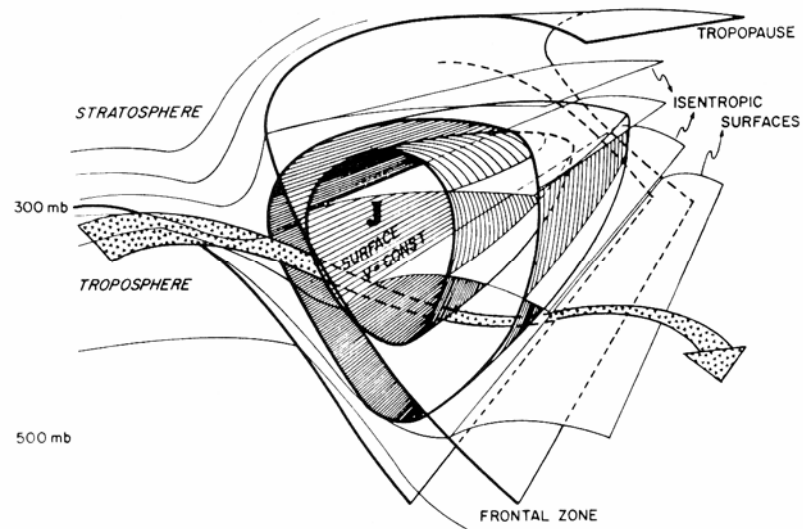


FIGURE 7.7: Tropopause folding and subsequent introduction of O₃ into the troposphere (Reiter, 1978)

In fact, stratospheric-tropospheric exchange is a mechanism that potentially contributes significant ozone concentrations to the troposphere (Chan et al., 1998; Bithell et al., 2000). When a strong, detached low-pressure system is present in the middle atmosphere, the height of the troposphere, or tropopause, descends behind the center of the cyclonic circulation (Tulet et al., 2002). In this scenario, exchange between the stratosphere and troposphere occurs as the tropopause folds underneath the upper-level cyclone or an attendant upper-level trough (Figure 7.8) (Kim et al., 2002; Rao et al.,

2004). These meteorological features are commonly in close proximity to the upper-level jet stream (Rao et al., 2004).

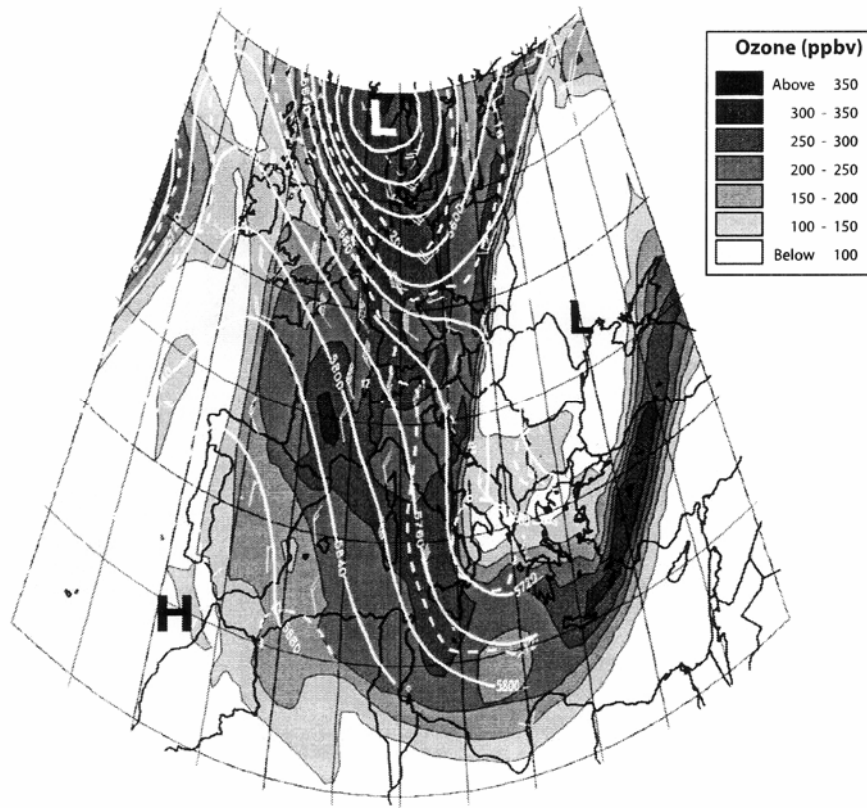


FIGURE 7.8: Modeled O₃ concentrations in the middle troposphere resulting from tropopause folding immediately behind a trough and associated cyclone (Dufour et al., 2005)

7.6. Lightning NO_x Fixation in the Tropics

A major source for ozone involved in stratospheric-tropospheric exchange is the equatorial region, where numerous thunderstorms and subsequent lightning discharges occur with regularity (Egorova et al., 1999; Beirle et al., 2004). According to Rao et al.

(2004), the tropical stratosphere is the primary global O₃ reservoir. Lightning fixes atmospheric nitrogen, in turn generating O₃ (Cooray and Rahman, 2005). Return strokes (also known as cloud-to-ground flashes, or CGs) are responsible for the production of primary NO_x gases (Cooray and Rahman, 2005). Lightning and NO₂ are strongly correlated (Beirle et al., 2004). Positive streamers are most efficient in terms of gas production, with an overall O₃ efficiency of 2-3 x 10¹⁷ molecules·J⁻¹ (Cooray and Rahman, 2005).

Once ozone is generated in tropical thunderstorms, transport to the mid-latitudes occurs as a function of the Brewer-Dobson circulation, a large-scale stratospheric system resulting from Rossby wave motion (Figure 7.9) (Andrews, 2000; Grewe et al., 2002; Rao et al., 2004). At low latitudes, large concentrations of O₃ and NO_x rise into the equatorial stratosphere in the ascending limb of the circulation, followed by horizontal transfer toward the poles. At the middle and high latitudes, momentum decreases sufficiently for descent, and ozone subsides into the upper troposphere (Holton, 1995; Andrews, 2000). While strongest during the winter months in the Northern Hemisphere, the Brewer-Dobson circulation nonetheless continues throughout the year (Holton, 1995).

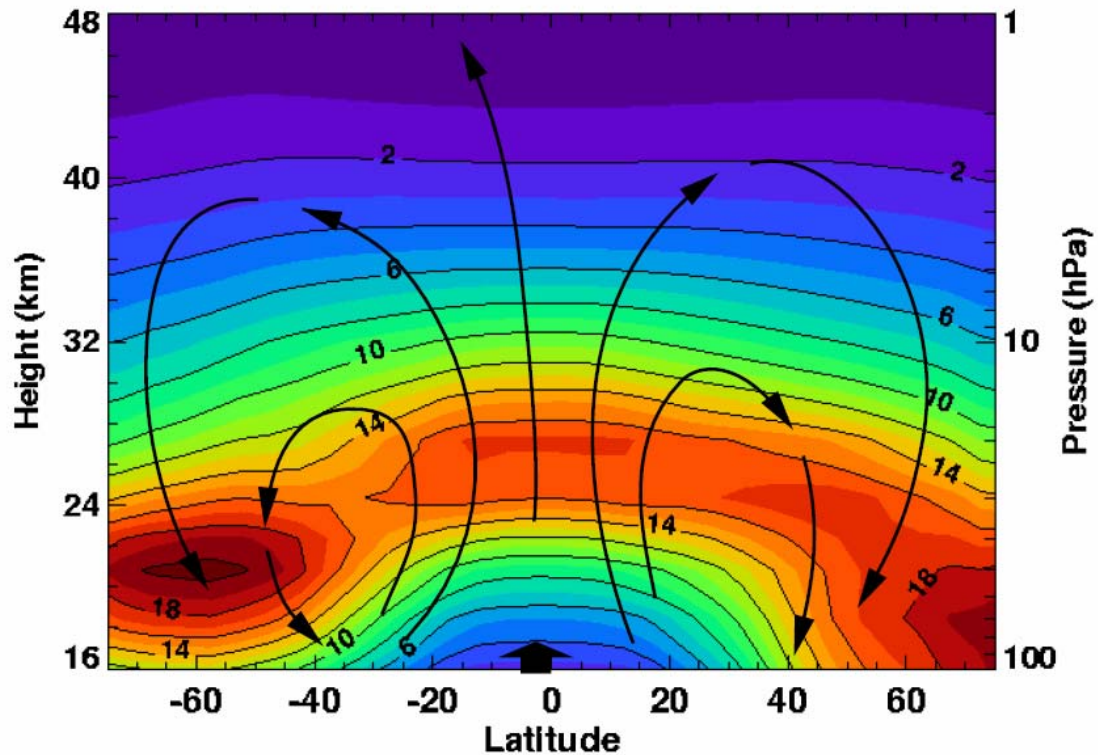


FIGURE 7.9: Cross-section of mean 1980-1989 stratospheric ozone concentrations (Dobson units per km), measured by the Nimbus-7 weather satellite, with arrows indicating the transport of ozone from the equatorial region to the mid-latitudes, consistent with the Brewer-Dobson circulation (NASA, 2000)

7.7. Hadley Cell Circulation

Ozone in the upper reaches of the mid-latitude troposphere is influenced by another large-scale circulation known as the Hadley cell. Driven by warm, moist convection in the tropics, the Hadley cell also ascends at the equator, although it is confined to the troposphere (Figure 7.10) (Palmén and Newton, 1969). Descent occurs in the sub-

tropics, where subsidence drives the development of the large, semi-permanent anti-cyclones associated with ozone pollution episodes at ground level (Djurić, 1994). In addition to the subsidence of ozone introduced through stratospheric-tropospheric exchange, secondary ozone production in the tropical upper troposphere is possibly transferred to the mid-latitudes through the direct mechanisms of this circulation (Grewe et al., 2004). As a result of the Hadley cell and its relationship with the Brewer-Dobson circulation and stratospheric-tropospheric exchange, ozone concentrations within the troposphere are normally quite high, and Grewe et al. (2001) quantified the mid-tropospheric O₃ mixing ratio as 0.075 ppm (by volume).

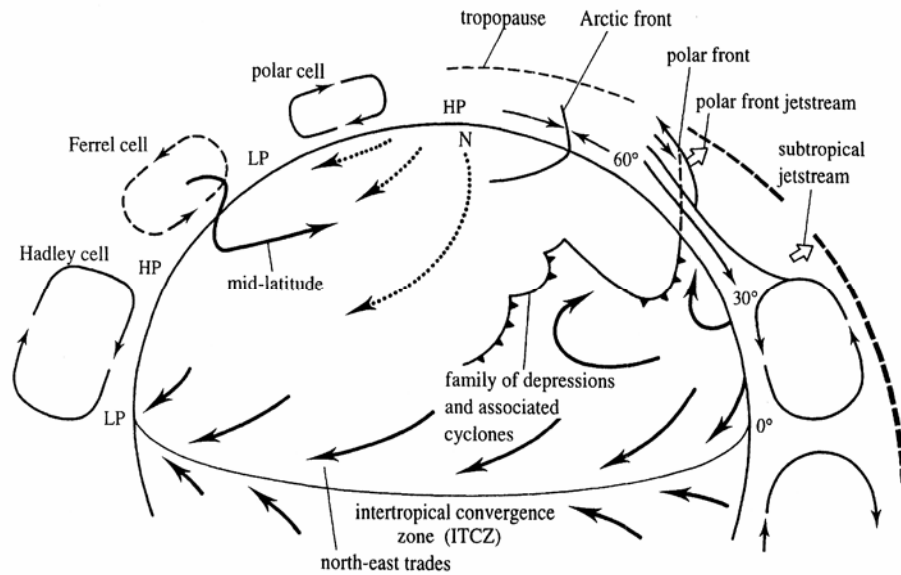


FIGURE 7.10: Hadley Cell circulation between the tropics and the mid-latitudes (Brimblecombe, 1996)

7.8. Frontal Boundaries

Aside from large-scale meteorological features of the middle and upper atmosphere, O₃ is also influenced by smaller-scale meteorological processes, including frontal boundaries. When particularly weak boundaries are present and associated weak, shifting surface winds prevail, ozone re-circulates over an area, increasing total concentration. Re-circulation is particularly problematic in coastal and near-coastal areas where sea breezes result in multiple daily passages of weak boundaries. Wang et al. (1998) reported on the variability of O₃ in Hong Kong as a result of sea-breeze meteorology, and Banta et al. (2005) described re-circulating ozone over the Houston, Texas metropolitan area as a “pollutant wall.” A similar effect is observed in the event of a weak boundary passage far inland, well beyond the range of the sea breeze. Surface winds converge along troughs and frontal boundaries, contributing to a zone of higher pollutant concentration (Gaza, 1998). Weak boundaries tend to be shallow, and O₃ trapping ensues as a result of the frontal structure (Gaza, 1998). Previous research has shown that troughs slowly moving across the Tulsa, Oklahoma metropolitan area result in higher O₃ concentrations along and immediately ahead of the boundary as air pollutants are accumulated through trapping (Williams, 2001). In areas where the predominant terrain is not flat, mountains and valleys amplify the impact that ozone has on local air pollution. Convergent surface winds on the lee side of the Appalachian Mountains in the eastern U.S. have been observed to increase ozone concentrations in a manner similar to trapping along a trough or frontal boundary, leading to multi-day episodes (Zhang et al., 1998). In Mexico City,

where air quality is continually poor, pollutants including O₃ are trapped within the deep valley in which the city is located (Hidy, 2000; O'Neill et al., 2004).

7.9. Biogenic Ozone Production

Sources of tropospheric ozone are thought to originate largely from anthropogenic activities and lightning. However, natural sources independent of atmospheric electrical processes contribute to ground-level ozone as well. Soils have been identified as potential sources of ozone, where NO_x is abundant (Trainer et al., 2000). Pasqualini et al. (2003) established phenols in forested areas as an indicator of ozone production from natural sources. Cultivated fields and forests generate precursor VOC compounds (Pison and Menut, 2004). Solomon et al. (2000) identified isoprene from deciduous vegetation and terpenes from conifers as the predominant biogenic VOCs responsible for O₃ production. Isoprene concentrations in forested areas have been characterized as significant in the O₃ cycle (Trainer et al., 2000). However, contradictory research regarding the contribution of biogenic O₃ sources has been offered in recent literature. According to Yang et al. (2004), uptake through trees in Beijing appeared to reduce urban air pollutants. A national park study in the U.S. indicated the suppression of O₃ formation in high isoprene environments (Kang et al., 2004).

7.10. Summary

Recent research clearly indicates that ozone in the free troposphere is present in appreciable concentrations, ranging from 0.02 to 0.1 ppm, depending on the literature source (Zhang et al., 1998; Mudway and Kelly, 2000). Several studies have confirmed that the background ozone concentration accounts for a significant portion of the daily ground-level ozone maximum, as the development of the atmospheric boundary layer enhances mixing and transports ozone to the surface (Chan et al., 1998; Zhang et al., 1998; Zhang and Rao, 1999; Aneja et al., 2000; Baumann et al., 2000; Lin et al., 2004; Steinbacher et al., 2004). Tower studies, which vertically profile ozone through the depth of the atmospheric boundary layer, have shown that mixing is most effective during the afternoon hours, when a high degree of correlation exists between O₃ at ground-level and aloft (Aneja et al., 2000; Kim et al., 2002).

The mechanisms of background ozone transport in the troposphere are not fully understood, but the nocturnal low-level jet is thought to play a role (Zhang et al., 1998; Steinbacher et al., 2004). Likewise, high O₃ concentrations are known to accompany subtropical anti-cyclones (Plaza et al., 1997; Blumenthal et al., 1998; Chan et al., 1998; Zhang et al., 1998; Baumann et al., 2000; Hidy, 2000; Gangoiti et al., 2001; Ghim et al., 2001; Millán et al., 2002; Boucouvala and Bornstein, 2003; Rosenthal et al., 2003; So and Wang, 2003; Lin et al., 2004; Rodríguez et al., 2004; Rohli et al., 2004). This relationship may occur as a result of ozone exchange between the stratosphere and troposphere in the vicinity of the polar jet stream (Chan et al., 1998; Bithell et al., 2000;

Kim et al., 2002; Tulet et al., 2002; Rao et al., 2004), while some studies suggest that high ozone concentrations coinciding with subtropical anti-cyclones may instead result from the Hadley Cell circulation, which transports air from the tropics, a major ozone source due to frequent lightning, to the sub-tropics, where the transported air sinks and promotes stagnant meteorological conditions (Grewe et al., 2004).

8. METHODS AND MATERIALS

Analysis of ozone formation and transport during the period spanning 01 June – 30 November 2005 required a multi-step data-gathering approach. First, ozone was experimentally measured at 210 meters, and paired measurements were taken at ground level as control data. Second, several meteorological parameters were gathered from external sources and paired with the ground-level and 210-meter ozone concentrations in order to draw conclusions regarding the dependence on meteorology for local photochemical formation as well as long-distance transport, thus incorporating meso-scale and synoptic-scale meteorological processes. Finally, a vertical profile of ozone was measured with a high-altitude balloon payload, or sounding, providing additional insight into the behavior of background ozone concentrations. All data sets were then analyzed with computer-assisted methods for comparison.

8.1. Theory of Ozone Measurement

Ozone can be experimentally measured according to the principle of the Beer-Lambert absorption law:

$$\frac{I}{I_0} = e^{-\alpha c l} \tag{8.1}$$

Transmittance, expressed as I/I_0 , is the ratio of UV intensity of light through ambient air containing ozone to the UV intensity of light through reference (zero concentration) air (TEC, 2004). This ratio is an exponential function of α , the molecular absorption coefficient of O₃ at a wavelength of 0.254 μm ; the O₃ concentration (c) expressed in atm; and the optical path length (l), measured in centimeters.

8.2. Experimental Measurement

Data were collected every five minutes between 00:00 CST on 01 June 2005 and 00:00 CST on 01 December 2005 at two sites in Tulsa (Figure 8.1):

1. Ground level, ODEQ Site 1127, 36th St. North and Peoria Avenue
2. 210 meters, City of Tulsa communications facility, roof of Bank of Oklahoma Tower, 1st St. and Cincinnati Avenue

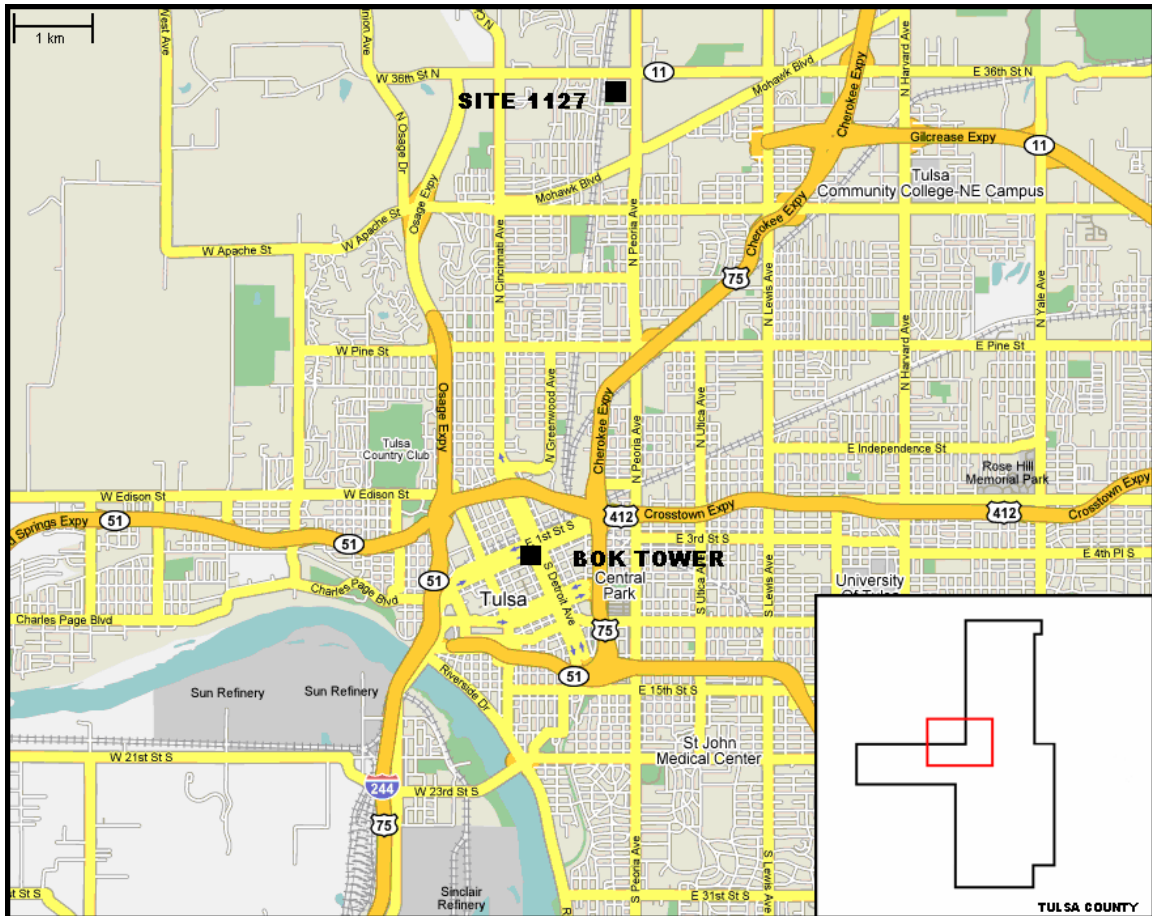


FIGURE 8.1: O₃ study site locations in metropolitan Tulsa, Oklahoma

Ozone measured at ground level was used as control data for the 210-meter concentrations measured at the Bank of Oklahoma Tower. The physical distance between the two sites was approximately 5 km.

Ambient air analysis was performed at each site with the Thermo Electron Corporation Model 49C UV Photometric Analyzer (Figure 8.2). Two Model 49C analyzers were donated by the ODEQ to the Oklahoma State University School of Civil and Environmental Engineering for the purpose of the study. Beer-Lambert constants specific to the Model 49C analyzer are $\alpha = 308 \text{ cm}^{-1}$ and $l = 38 \text{ cm}$. Calibration of the

Model 49C at the Bank of Oklahoma Tower was performed with an O₃ generator prior to the beginning of the study in May 2005, during a routine maintenance visit in August 2005, and following the termination of the study in December 2005. All maintenance and routine ambient air monitoring was conducted in accordance with 40 CFR 50, and therefore meets EPA requirements for O₃ data certification. Ozone measuring equipment at Site 1127 was maintained by the ODEQ during the course of the study, and also adheres to 40 CFR 50. Data collected at the Bank of Oklahoma Tower was retrieved remotely through a telephone connection and *TEI for Windows* software. Electricity, telephone connection, and space at the Bank of Oklahoma Tower site were provided by the City of Tulsa. Data from Site 1127 were retrieved monthly from the ODEQ.

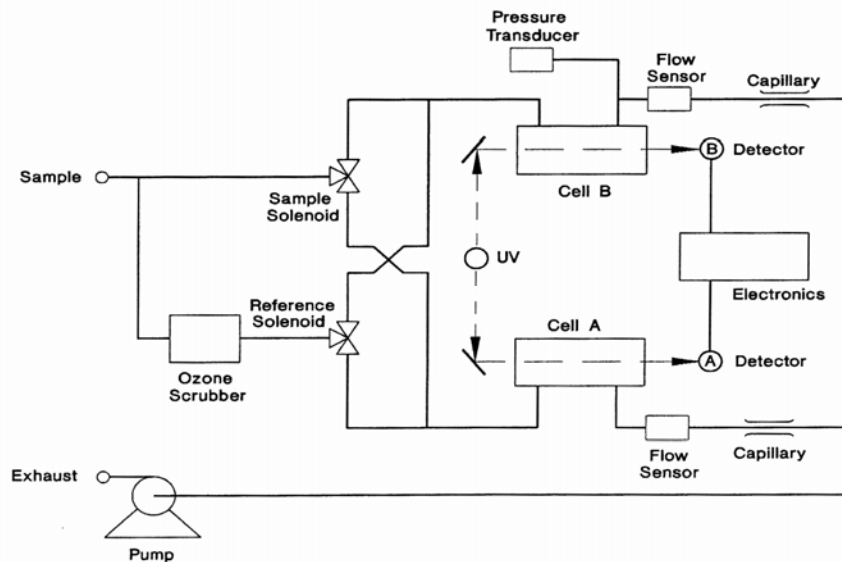


FIGURE 8.2: TEC Model 49C O₃ analyzer flow schematic (TEC, 2004)

Following collection of the ground-level and 210-meter O₃ data, the 5-minute concentrations were re-averaged and converted to an interval of one hour. In addition to

the EPA designation of 1-hour averages in 40 CFR 50.9, many meteorological variables are reported in this interval as well, making it convenient for data analysis. Ozone concentrations measured at both sites were also converted to 24-hour averages for comparison with meteorological sounding data.

8.3. Meteorological Data Sources

In addition to the ozone measurements that were recorded, several meteorological data sets were analyzed as well, including the following:

- Five-minute meteorological data recorded at Skiatook, Oklahoma, approximately 20 km north of the Bank of Oklahoma Tower (data accessed from the Oklahoma Mesonet (<http://www.mesonet.ou.edu/>), converted to 1-hour averages for comparison with O₃).
- Hourly surface meteorological data recorded at the Tulsa International Airport Aviation Weather Observing System (AWOS), approximately 8 km east of the Bank of Oklahoma Tower (data accessed from NOAA National Climatic Data Center (<http://www.ncdc.noaa.gov/>)).
- Hourly 210-meter wind speed and direction were recorded on the roof of the Bank of Oklahoma Tower in conjunction with the 210-meter ozone experiment. Wind speed and direction were measured with a Davis Instruments Weather

Wizard III meteorological station. Data were saved to a Davis Instruments WeatherLink logger and retrieved and analyzed with an accompanying software program.

- Hourly vertical wind profiler data recorded at Haskell, Oklahoma (HKL02), approximately 40 km southeast of the Bank of Oklahoma Tower (data accessed from the NOAA Earth System Research Laboratory, Global Systems Division (<http://profiler.noaa.gov/>)).
- Daily upper-air meteorological sounding data recorded at Brownsville, Texas (KBRO), Norman, Oklahoma (KOUN), and Aberdeen, South Dakota (KABR) (data accessed from NOAA Earth System Research Laboratory, Global Systems Division (<http://raob.fsl.noaa.gov/>)).
- Composite National Centers for Environmental Prediction (NCEP)/National Center for Atmospheric Research (NCAR) upper-air meteorological re-analysis graphics (data accessed from NOAA Earth System Research Laboratory, Physical Sciences Division (<http://www.cdc.noaa.gov/>)).

Surface and upper-air meteorological data were analyzed as paired data with ozone in *Microsoft Excel* and graphically with *RAOB* and *Digital Atmosphere*, two commercially available meteorological software packages.

8.4 Ozonesonde Payload and Launch

A vertical profile of ozone was constructed on 08 October 2005 using a 2B Technologies Model 202 Ozone Monitor attached as a payload to a Scientific Sales, Inc. 600-gram meteorological balloon. The theory of operation of the Model 202 is similar to that of the Model 49C. The molecular absorption coefficient remains constant at 308 cm^{-1} , and the optical path length is shorter (15 cm) (2B Tech., 2001). Launch of the ozonesonde occurred at 08:00 CST at rural site 20 km north of downtown Tulsa, and the total flight time was approximately two hours. Ozone was measured in 10 second increments from ground level to a maximum altitude of 29,000 meters, and data were saved internally. The ozonesonde was tracked with global positioning and radio transmitting and receiving equipment, and once the payload was retrieved, data were downloaded from the Model 202.

9. RESULTS AND DISCUSSION

Measurements taken during the course of this research study centered on ozone behavior in the atmospheric boundary layer, and subsequently, a data set of 4,392 hourly O₃ averages was acquired from the ground-level and 210-meter monitoring sites. Additionally, several ground-level meteorological data sets were obtained, allowing for comparison with the ground-level and 210-meter ozone concentrations. The combination of these locally measured parameters allowed for detailed analysis of the dependence of local photochemical ozone production on meteorological variables, including air temperature, relative humidity, wind speed, and solar radiation. As a result of 210-meter O₃ concentration trends, however, insight regarding the behavior of tropospheric ozone in relation to large-scale, dynamic meteorological process was also gained. Therefore, the results of this research have been subdivided into two components: short-term, local-scale photochemical production and longer-term, distant-origin ozone that propagates in concert with the global atmospheric circulation.

9.1. Local-Scale Phenomena

When assessing the magnitude of local photochemical ozone production, it was appropriate to begin with a comparison between ground-level and 210-meter O₃ in an effort to gauge whether or not ozone measured vertically within the atmospheric

boundary layer behaves as a heterogeneous, layered system or as a well-mixed, homogeneous system. The construction of a vertical ozone profile revealed a time-dependant relationship between the two levels in which both types of systems were observed, yielding important clues regarding the role that the structure of the boundary layer plays in the evolution of the diurnal ozone profile at ground level. Furthermore, the consideration of local meteorological variables allowed for assessment of the conditions in which high ground-level ozone concentrations are favored.

9.1.1. Boundary-Layer Ozone Correlations

Over the course of the 6-month research period, ground-level and 210-meter ozone concentrations for the 12-hour daytime interval beginning at 08:00 CST and ending at 20:00 CST were correlated, as this increment approximated the hours of sunlight during the summer months. A linear response was observed, and the coefficient of determination (R^2) equaled 0.6089 (Figure 9.1). Ozone homogeneity between the two heights generally began within two hours of sunrise, when the structure of the atmospheric boundary layer transitioned from a decoupled low-level stable nocturnal boundary layer and overlying residual layer to a coupled, convectively driven mixed layer in the lower atmosphere.

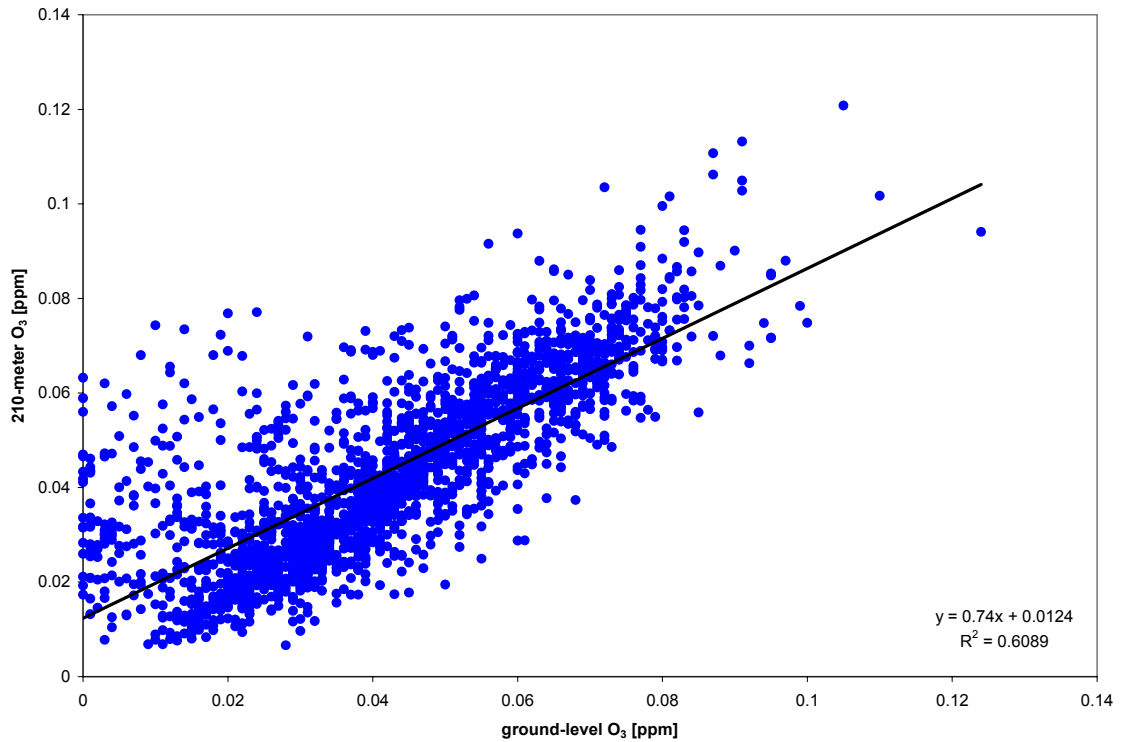


FIGURE 9.1: 12-hour daytime correlation between 210-meter and ground-level O₃ concentrations (08:00 CST – 20:00 CST), 01 June 2005 – 30 November 2005

It was clear, however, that substantial deviation from the linear correlation was present at lower ozone concentrations in the 12-hour daytime data. This interference was attributable to poor correlation at the beginning and end of the 12-hour daytime period, when O₃ concentrations tend to be vertically heterogeneous as a result of decreased boundary layer mixing. The correlation between ground-level and 210-meter O₃ improved with reduction of the daytime interval from 12 hours to 9 hours, beginning at 08:00 CST and ending at 17:00 CST (Figure 9.2). Within this period, R² increased to 0.7919.

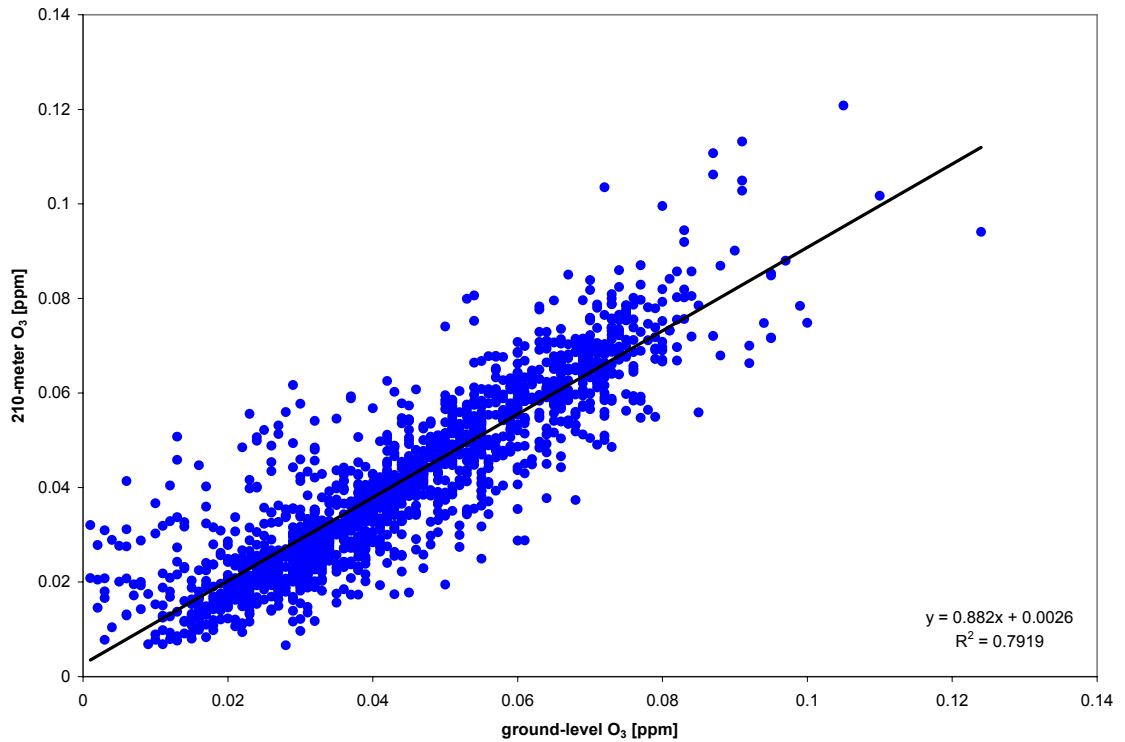


FIGURE 9.2: 9-hour daytime correlation between 210-meter and ground-level O₃ concentrations (08:00 CST – 17:00 CST), 01 June 2005 – 30 November 2005

Additional refinement of the daytime ozone interval into morning and afternoon components improved the correlation between ground-level and 210-meter ozone. Concentrations during the 5-hour morning and early afternoon period, beginning at 08:00 CST and ending at 13:00 CST, remained strongly correlated, but with an R^2 of 0.7253, the correlation was weaker than that of the 9-hour daytime period (Figure 9.3). Interference at low ozone concentrations was slightly more prominent, resulting from the temporal variability of boundary-layer coupling and onset of convective mixing.

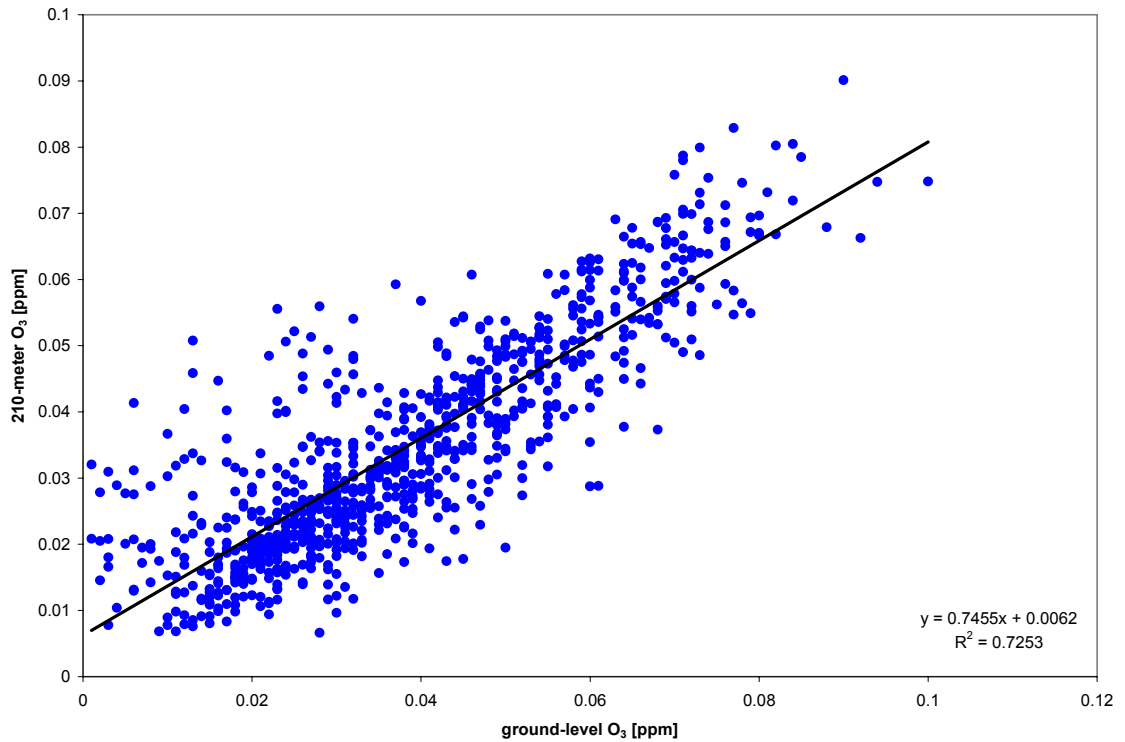


FIGURE 9.3: 5-hour morning correlation between 210-meter and ground-level O₃ concentrations (08:00 CST – 13:00 CST), 01 June 2005 – 30 November 2005

The afternoon period, a 4-hour interval beginning at 13:00 CST and ending at 17:00 CST, provided the highest overall O₃ concentration correlation for the daytime hours (Figure 9.4). Interference at low ozone concentrations, present in the morning concentration correlation data, was noticeably absent. The coefficient of determination consequently increased to 0.8372. Strong correlation in the afternoon data coincided with vigorous convective mixing in the atmospheric boundary layer, which was most pronounced during the afternoon hours when maximum surface heating was realized. During this interval, O₃ concentrations were nearly homogenous through the vertical extent of the boundary layer.

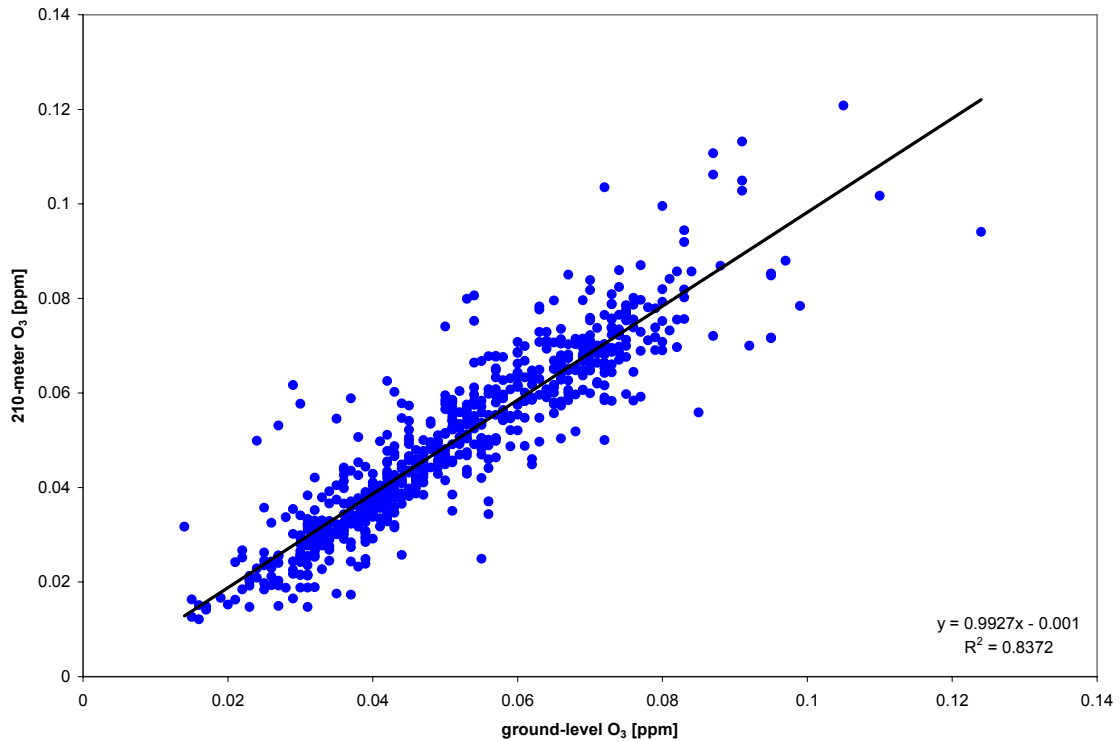


FIGURE 9.4: 4-hour afternoon correlation between 210-meter and ground-level O₃ concentrations (13:00 CST – 17:00 CST), 01 June 2005 – 30 November 2005

Latency is another consideration when measuring vertical ozone concentrations in the boundary layer. Previous research has indicated that convective eddies occur on the order of 30 minutes (Seaman, 2000). Therefore, any ozone resulting from local, surface-based sources during daytime photochemical processes will require additional time to mix from ground level to 210 meters. In an effort to account for convective mixing between the two heights, the 9-hour daytime O₃ correlation data were offset by one hour, with the 210-meter ozone data shifted to match ground-level data from the previous hour. This technique yielded the strongest correlation between ground-level and 210-meter concentrations, with an R² equal to 0.8781 (Figure 9.5).

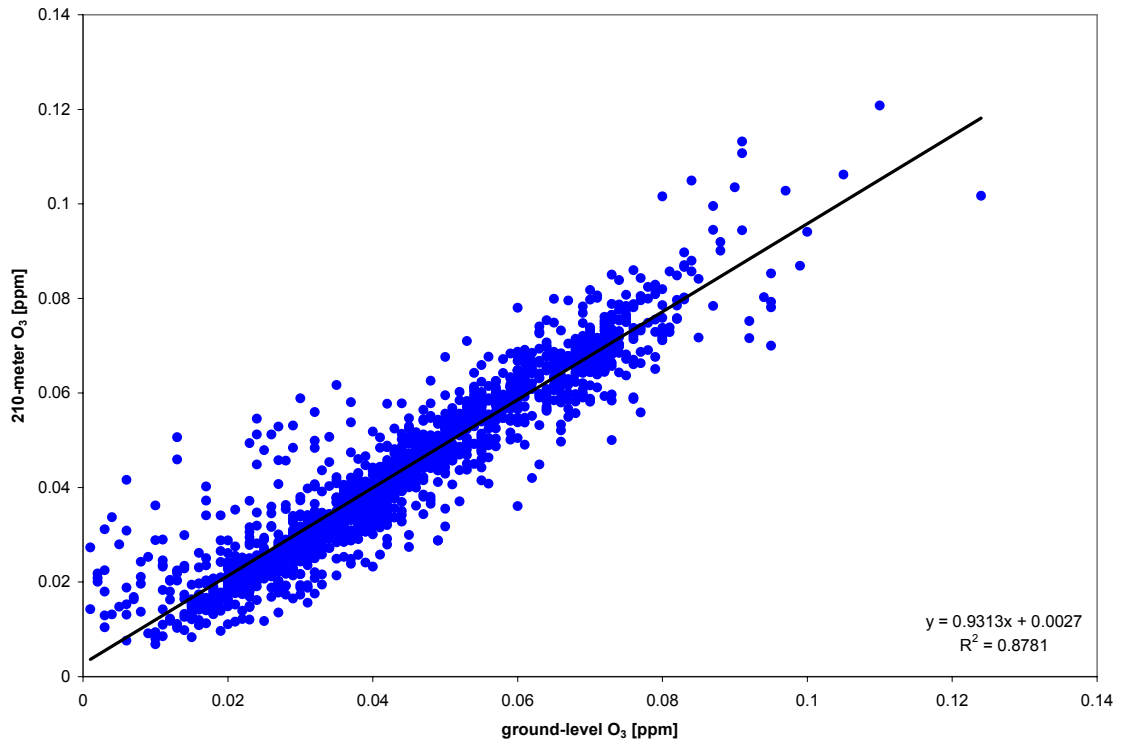


FIGURE 9.5: 9-hour daytime correlation between 210-meter and ground-level O₃ concentrations (08:00 CST – 17:00 CST; 210-meter O₃ concentrations offset to previous hour ground-level O₃ concentrations), 01 June 2005 – 30 November 2005

While ozone concentrations exhibited strong vertical correlation during the daytime, the opposite was true at night. Once surface heating was lost, radiational cooling prompted the decoupling of the atmospheric boundary layer into the stable nocturnal boundary layer and the elevated residual layer from the previous day's convective mixing. Vertical ozone concentrations within the boundary layer dissociated as well, effectively resulting in two independent reservoirs. Ozone concentrations at ground level decreased in response to the cessation of photochemistry and continuance of depositional processes within the nocturnal boundary layer. Depositional processes were much less effective

within the residual layer, and ozone concentrations at 210 meters consequently remained high. Therefore, nocturnal ozone concentrations showed no discernable correlation between ground level and 210 meters. For the 12-hour nighttime period beginning at 20:00 CST and ending at 08:00 CST, R^2 equaled 0.0045 (Figure 9.6).

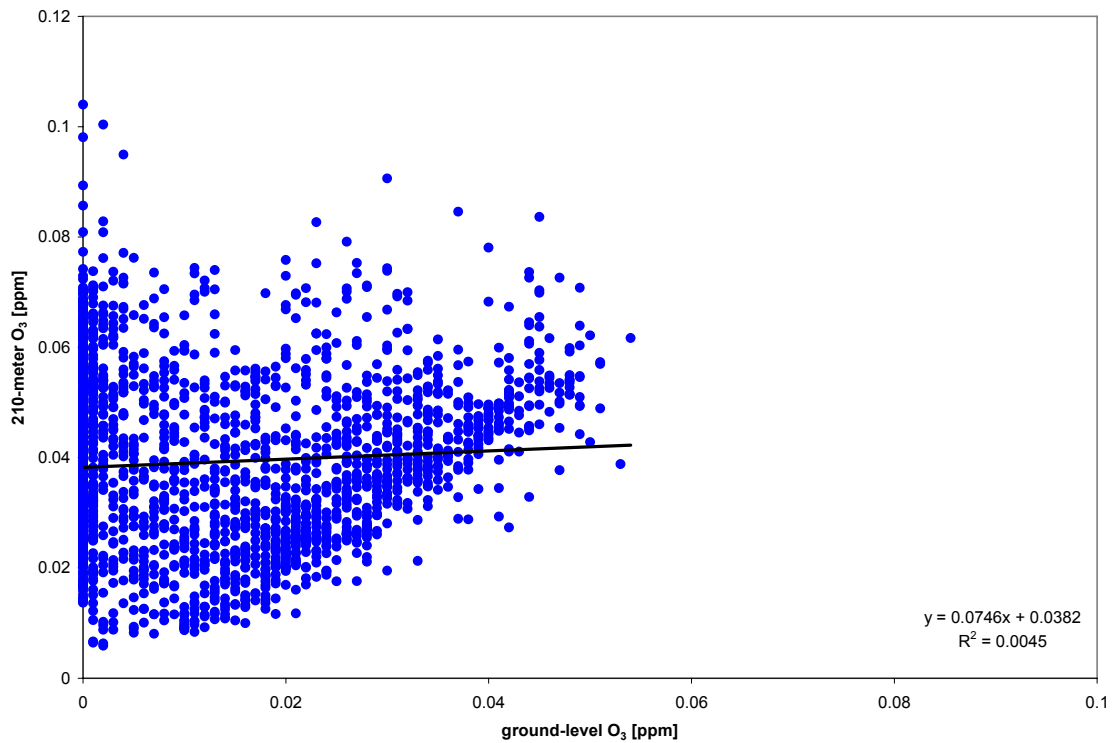


FIGURE 9.6: Correlation between nighttime 210-meter and ground-level O₃ concentrations (20:00 CST – 08:00 CST), 01 June 2005 – 30 November 2005

9.1.2. Dry-Bulb Temperature

With an R^2 value equal to 0.3333, the correlation between ground-level ozone and ground-level dry-bulb (air) temperature (measured at Tulsa International Airport) was weak. However, a noticeable relationship existed between high ozone concentrations and corresponding high dry-bulb temperatures. At low ground level O_3 concentrations, there was a random distribution within the 0-35°C dry-bulb temperature range (Figure 9.7).

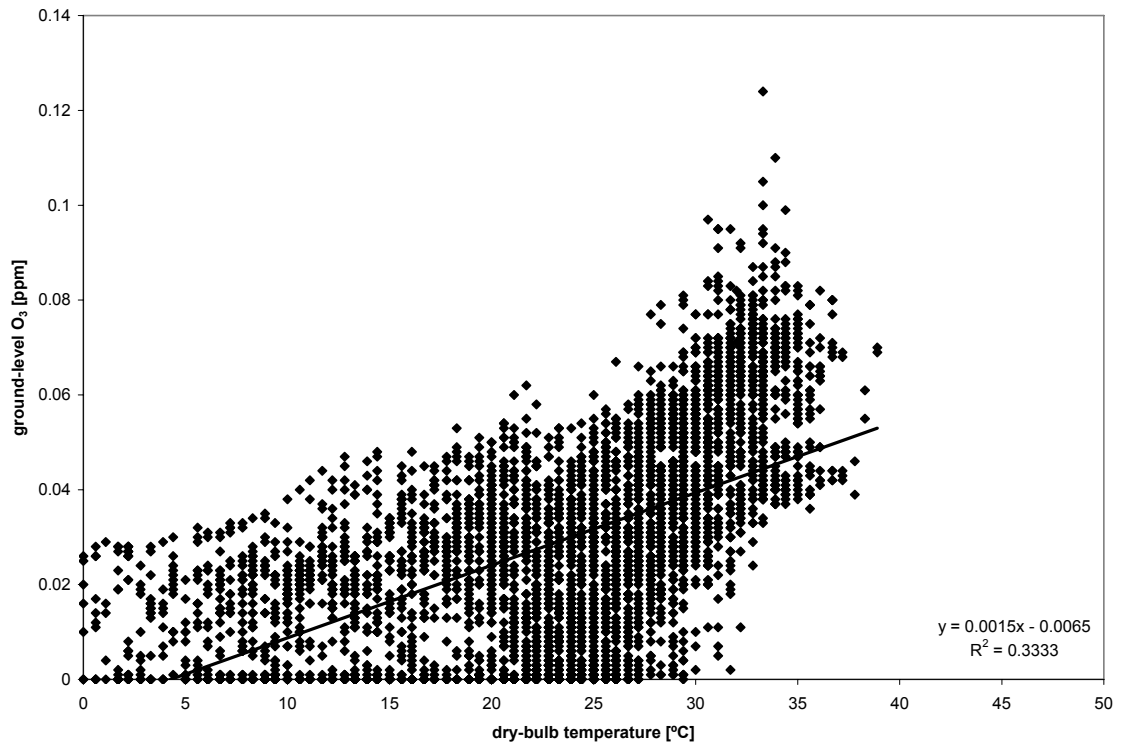


FIGURE 9.7: Correlation between ground-level O_3 and dry-bulb temperature, 01 June 2005 – 30 November 2005

In fact, only 44% of O₃ concentrations equal to or exceeding 0.03 ppm occurred at a dry-bulb temperature of 30°C or higher. At 0.05 ppm, however, this percentage improved to 74%. When high ground-level ozone concentrations were measured, a strong positive correlation was observed in conjunction with high ground-level air temperatures. All occurrences of 0.07 ppm or higher O₃ were coupled with a dry-bulb temperature of at least 27°C, and all exceedances of the 0.09 ppm ground-level O₃ concentration threshold took place when the dry-bulb temperature was at least 30°C. The relationship between ground-level O₃ and dry-bulb temperature is summarized in Table 9.1.

TABLE 9.1: Percentages of O₃ exceedances at selected dry-bulb temperatures

O ₃ (ppm) ≥	n	% ≥ 25°C	% ≥ 27°C	% ≥ 30°C
0.01	3183	57	45	28
0.02	2624	63	52	34
0.03	1892	74	64	44
0.04	1254	85	76	57
0.05	730	96	92	74
0.06	437	99	99	91
0.07	201	100	100	97
0.08	57	100	100	96
0.09	17	100	100	100
0.10	4	100	100	100

A contraction of the research data interval from 6 months to 4 months, including the period generally considered as the ozone season (01 June 2005 – 30 September 2005), resulted in the exclusion of many of the low O₃ concentrations observed in the 6-month analysis, leaving a linear distribution of higher ground-level ozone concentrations (Figure

9.8). As a result, the correlation between ground-level O₃ and ground-level dry-bulb temperature improved ($R^2 = 0.4897$).

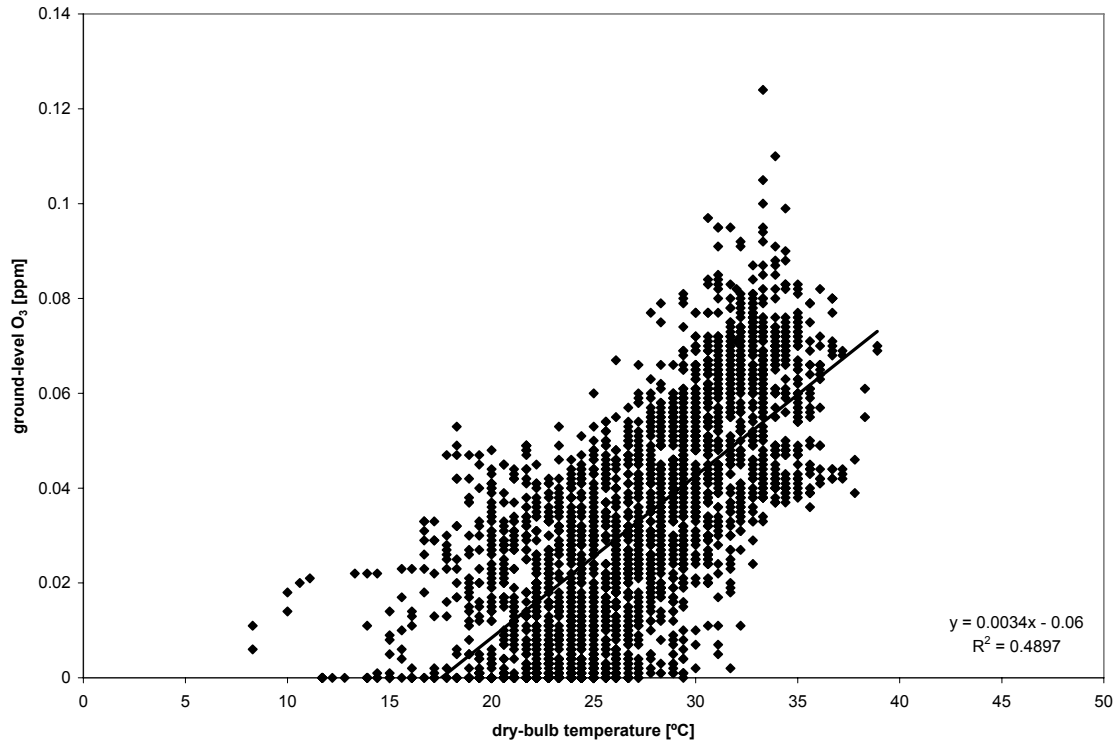


FIGURE 9.8: Correlation between ground-level O₃ and dry-bulb temperature, 01 June 2005 – 30 September 2005

Ozone concentrations at 210 meters were less responsive to surface meteorological processes, as indicated by the weaker correlation with dry-bulb temperature at this level than at ground level (Figure 9.9). When the six-month research data period was considered, R^2 equaled 0.2592, suggestive of a more random distribution than was observed with ground-level O₃, particularly at high dry-bulb temperatures. Decreasing the research data interval to four months resulted in a sharp decrease in correlation ($R^2 = 0.1023$).

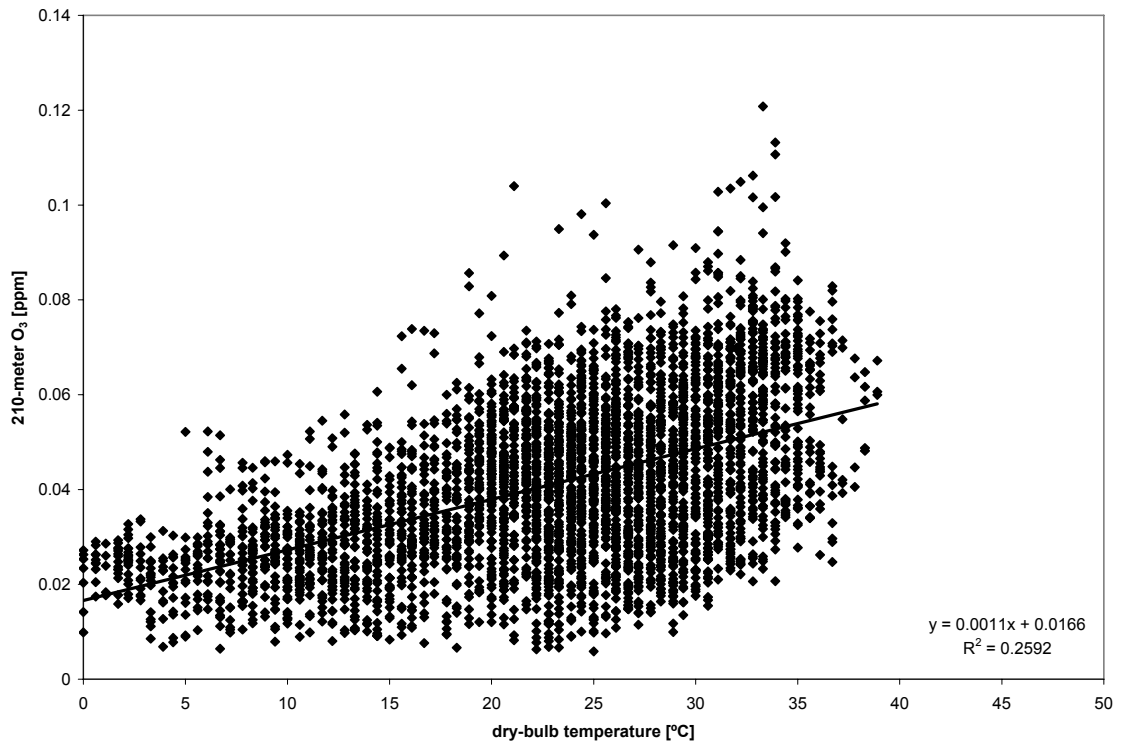


FIGURE 9.9: Correlation between 210-meter O₃ and dry-bulb temperature, 01 June 2005 – 30 November 2005

9.1.3. Water Vapor

Water vapor in the lower atmosphere can be expressed in several ways, including relative humidity (RH%), wet-bulb temperature, and dew-point temperature, as discussed in Section 4.2. All water vapor variables were measured at Tulsa International Airport.

Wet-bulb temperatures did not provide a good fit with the ground-level or 210-meter ozone concentrations. When ground-level ozone was considered, substantial interference was present at low concentrations over the six-month research period. Correlation was poor, as R^2 equaled 0.1233 (Figure 9.10).

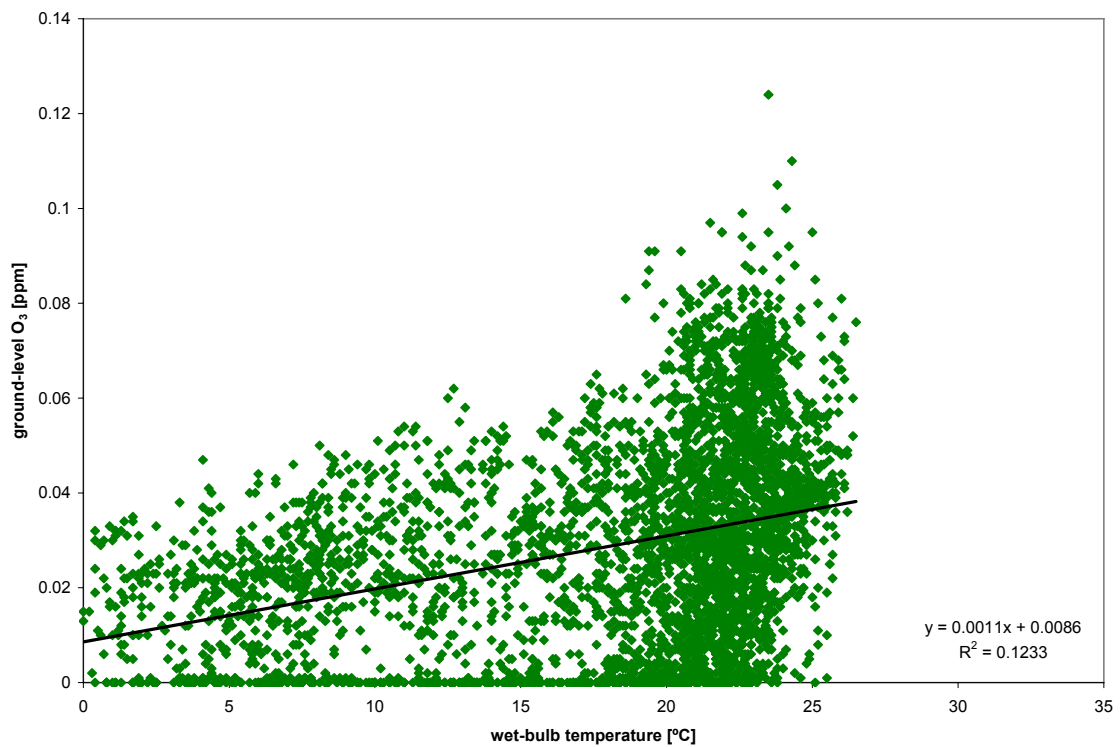


FIGURE 9.10: Correlation between ground-level O₃ and wet-bulb temperature, 01 June 2005 – 30 November 2005

Reduction of the research data interval to four months eliminated much of the random scatter present at low O₃ concentration levels. However, better correlation was not achieved, as R² actually decreased slightly to 0.1185.

At 210 meters, the correlation between ozone and wet-bulb temperature was higher than the ground-level correlation over the six-month research period (R² = 0.1727), although still weak. The data tended to separate into two distinct groups – one at very low O₃ concentrations, and another, more pronounced region at very high O₃ concentrations (Figure 9.11).

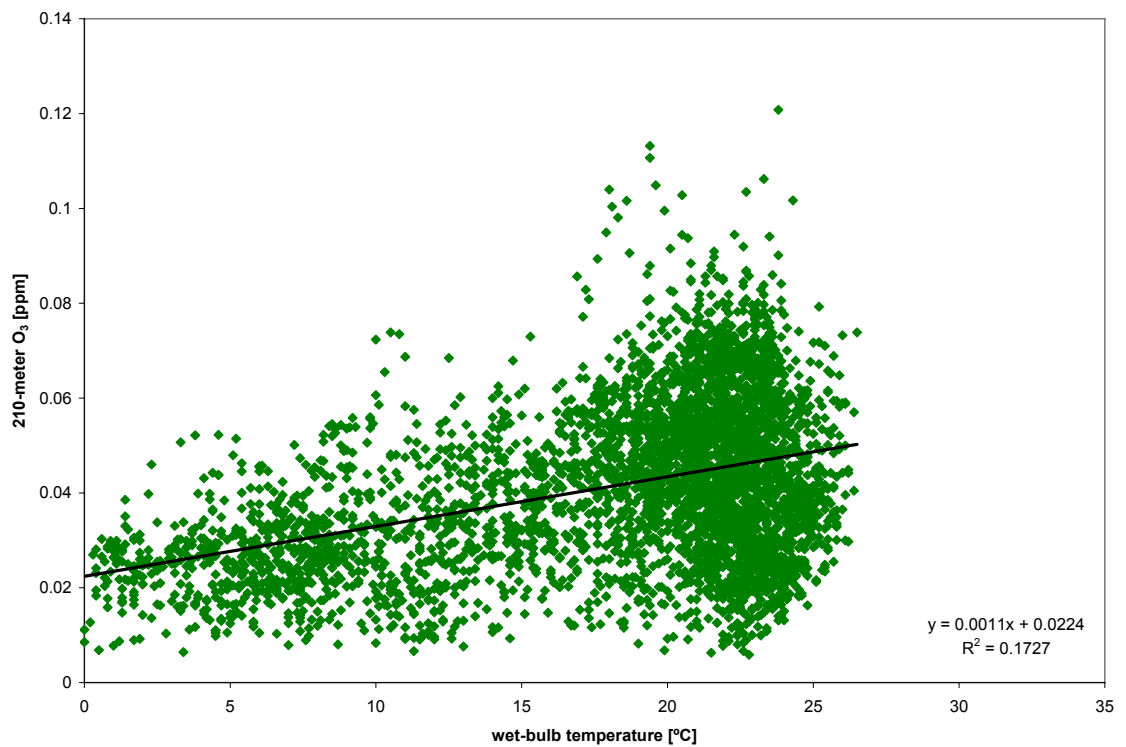


FIGURE 9.11: Correlation between 210-meter O₃ and wet-bulb temperature, 01 June 2005 – 30 November 2005

As with the ground-level ozone data, the 210-meter ozone time interval under consideration was reduced to four months in order to remove the low O₃ concentrations that occurred late in the year, thus attempting to achieve a higher correlation between O₃ and wet-bulb temperatures. Instead, the opposite occurred as the correlation decreased to virtually zero ($R^2 = 0.0023$).

Dew-point temperature correlation to ground-level and 210-meter O₃ was very similar to the wet-bulb correlation, since both measures of water vapor content are proportional with regard to one another. Therefore, the scatter plots correlating O₃ and dew-point temperature were identical to the wet-bulb correlation graphs, with the lone exception of a slight shift in temperature for each O₃ datum, as dew-point temperatures are always lower than wet-bulb temperatures unless the air is completely saturated.

The best correlations between O₃ and water vapor were achieved by considering relative humidity. Unlike wet-bulb and dew-point temperatures, relative humidity is a function of temperature and pressure instead of temperature alone.

When the six-month research data interval was considered, the correlation between ground-level O₃ and RH% was not particularly high ($R^2 = 0.3356$), but a distinct negative relationship between the two clearly existed (Figure 9.12), as higher RH% values corresponded to lower O₃ concentrations.

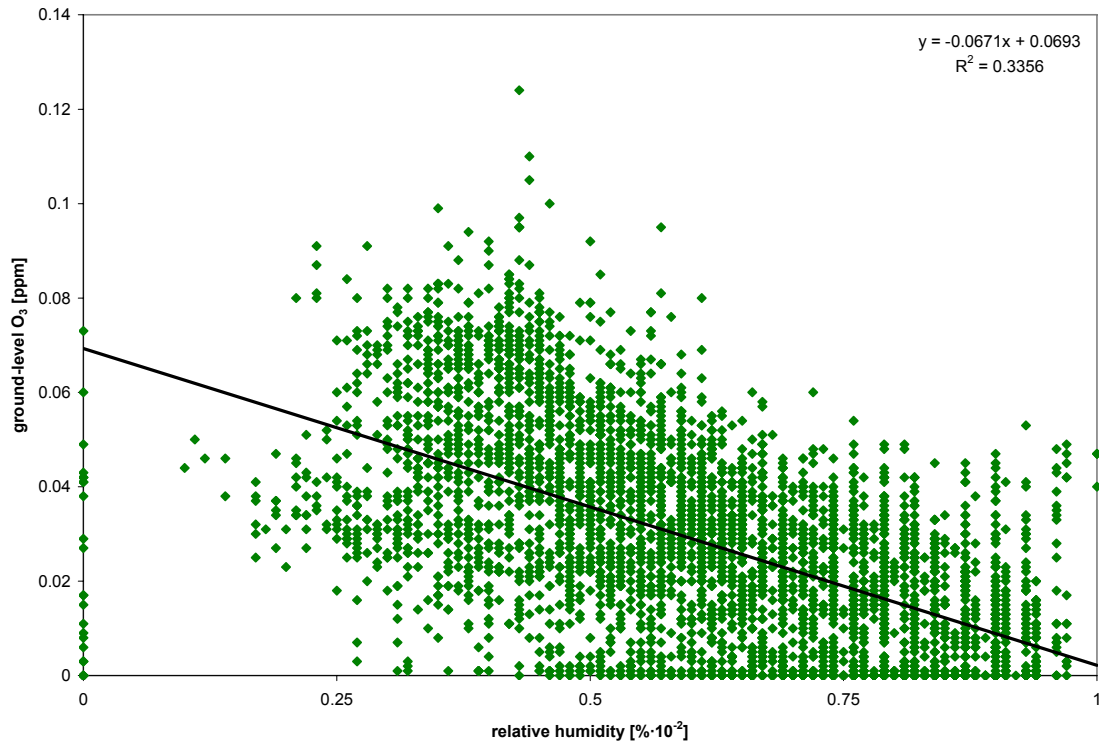


FIGURE 9.12: Correlation between ground-level O₃ and relative humidity, 01 June 2005 – 30 November 2005

Refinement of the data interval to the four-month ozone season improved the correlation between ground-level O₃ and RH%, as R^2 increased significantly to 0.5286. Most of the interference at lower ozone concentrations was eliminated, resulting in a linear distribution with a negative slope (Figure 9.13)

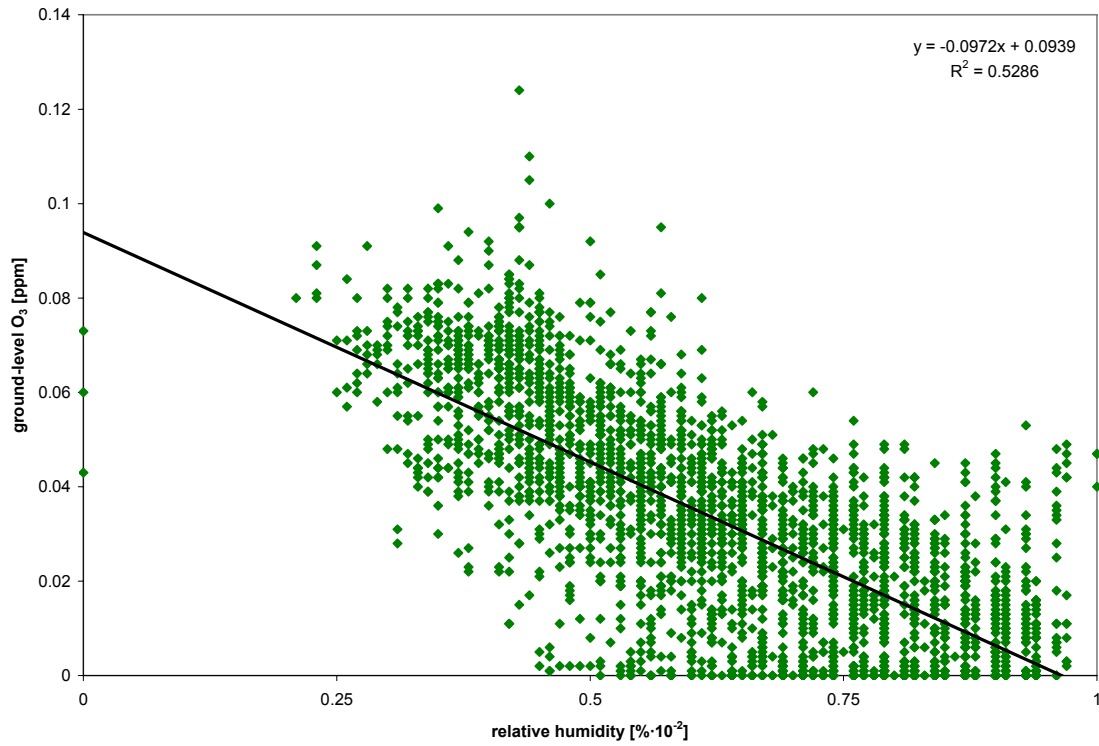


FIGURE 9.13: Correlation between ground-level O₃ and relative humidity, 01 June 2005 – 30 September 2005

Ozone from the 210-meter level was also plotted against RH%, but over the course of the six-month research data interval, no correlation was established ($R^2 = 0.0558$) (Figure 9.14).

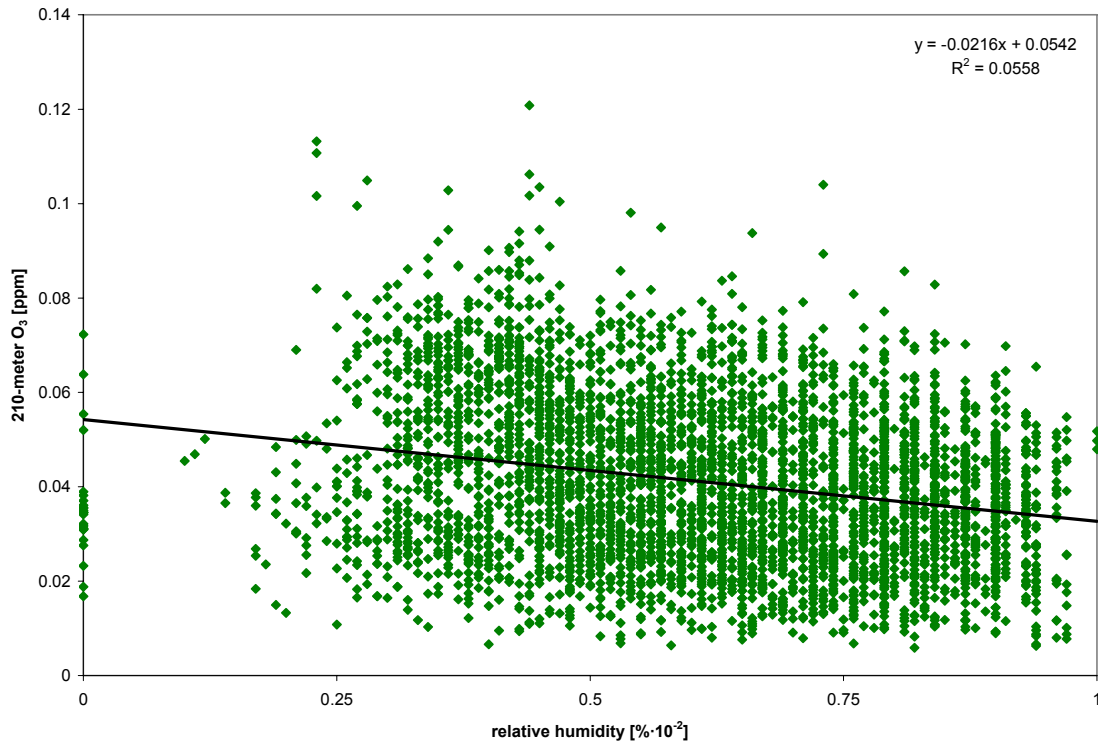


FIGURE 9.14: Six-month correlation between 210-meter O₃ concentration and relative humidity, 01 June 2005 – 30 November 2005

However, this result improved with the four-month data interval, as R^2 equaled 0.1763. The increased correlation between the two parameters likely reflected more vigorous mixing during the late summer months, which in turn transported water vapor more effectively through the depth of the boundary layer. Nonetheless, the correlation remained poor, signifying that ground-level ozone was more responsive to water vapor in the lower atmosphere than ozone measured at 210 meters.

9.1.4. Air Pressure

Although a discernable correlation was found between ground-level ozone and air pressure (measured at Tulsa International Airport) when considered as a component of relative humidity, no appreciable relationship existed between ground-level O₃ and air pressure alone, measured in hecto-Pascals (hPa). Most O₃ concentrations fell within a range of 980 hPa to 1000 hPa. The coefficient of determination for the six-month research interval was 0.0273 (Figure 9.15).

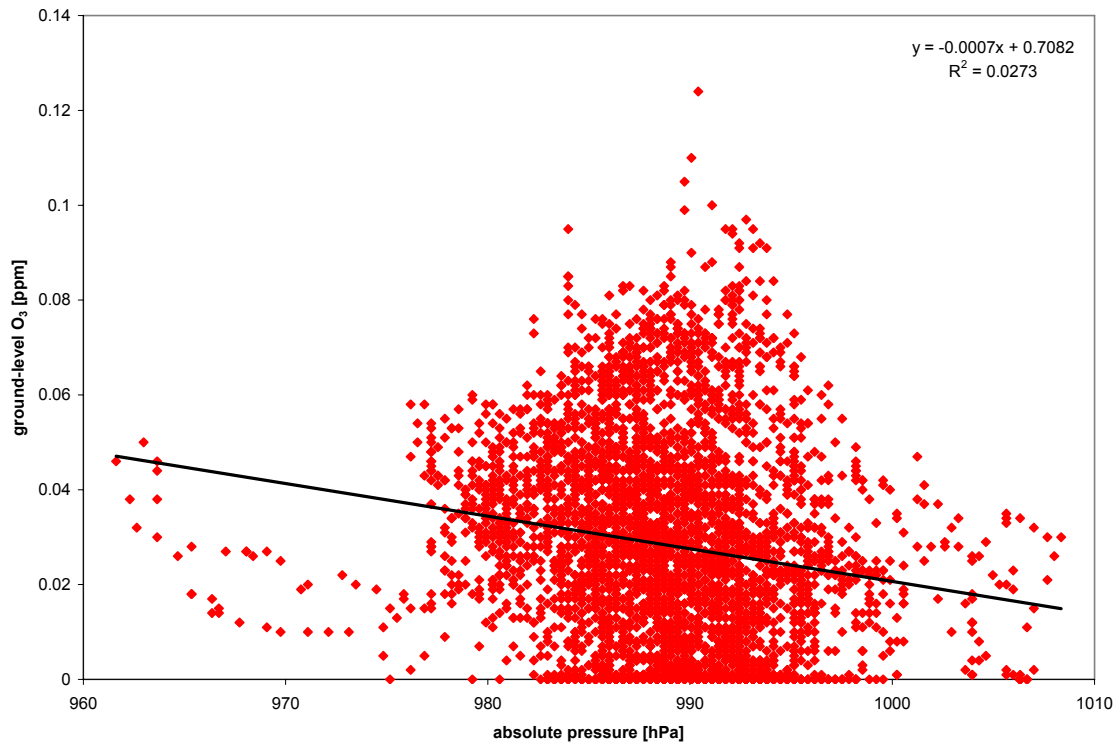


FIGURE 9.15: Correlation between ground-level O₃ and air pressure, 01 June 2005 – 30 November 2005

Consideration of O₃ concentrations from the four-month ozone season did not result in an improvement of R², which decreased to 0.0122.

Likewise, no correlation existed between ozone measured at 210 meters and ground-level air pressure. Although air pressure measurements were made at ground level, adherence to the hydrostatic equation requires that air pressure at 210 meters would be proportionally lower (see Section 4.1). When analyzed, R² equaled 0.006 for the six-month data interval (Figure 9.16).

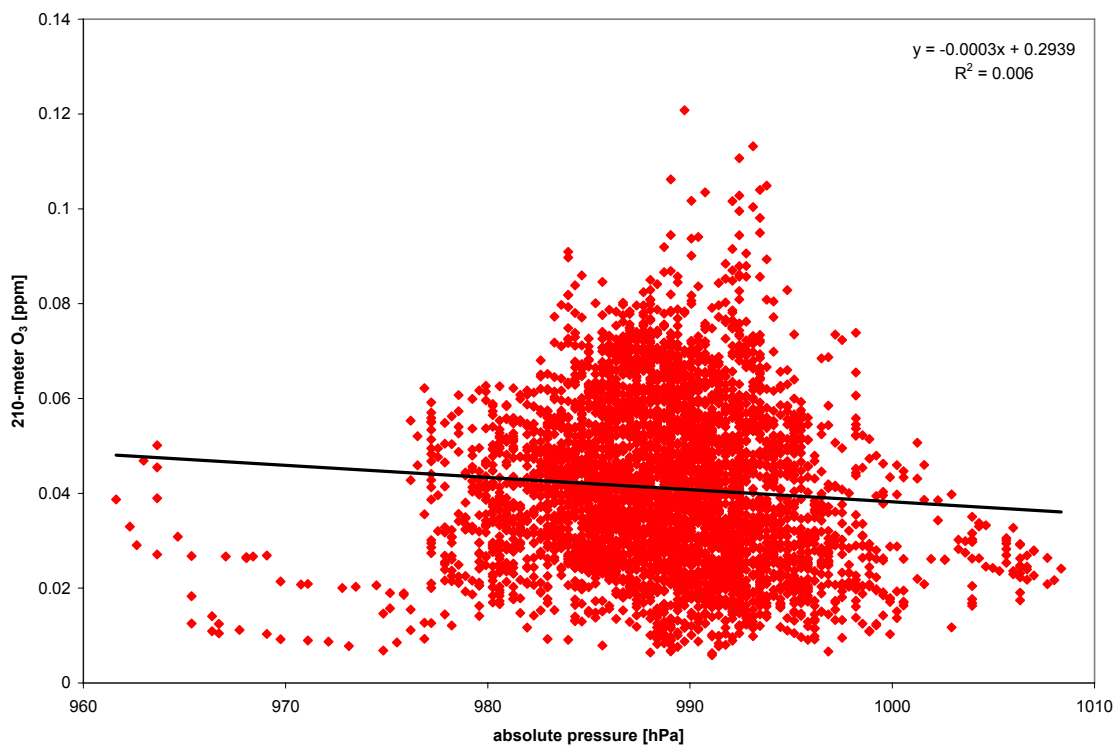


FIGURE 9.16: Correlation between 210-meter O₃ and ground-level air pressure, 01 June 2005 – 30 November 2005

Outlying data points were eliminated when the research interval was reduced to four months, but the correlation between 210-meter ozone concentrations and ground-level air pressure did not improve. With an R^2 value of 0.0068, no correlation was found to exist between the two.

9.1.5. Wind Speed and Direction

Wind speeds and directions were measured at ground level (Tulsa International Airport) and at 210 meters (the roof of the Bank of Oklahoma Tower). When ground-level ozone was paired with ground-level wind speed, a very weak correlation was found, as the coefficient of determination equaled 0.1121 (Figure 9.17). Distribution at low to moderate wind speeds was random. However, a noticeable threshold existed between high O_3 concentrations and wind speeds at ground level, as all concentrations equal to or greater than 0.08 ppm occurred at wind speeds lower than $5 \text{ m}\cdot\text{s}^{-1}$. While Figure 9.17 suggests a positive correlation between ground-level wind speed and ground-level ozone, this effect results from the randomness of the data at low concentrations, as the correlation is negative at O_3 concentrations ≥ 0.01 ppm.

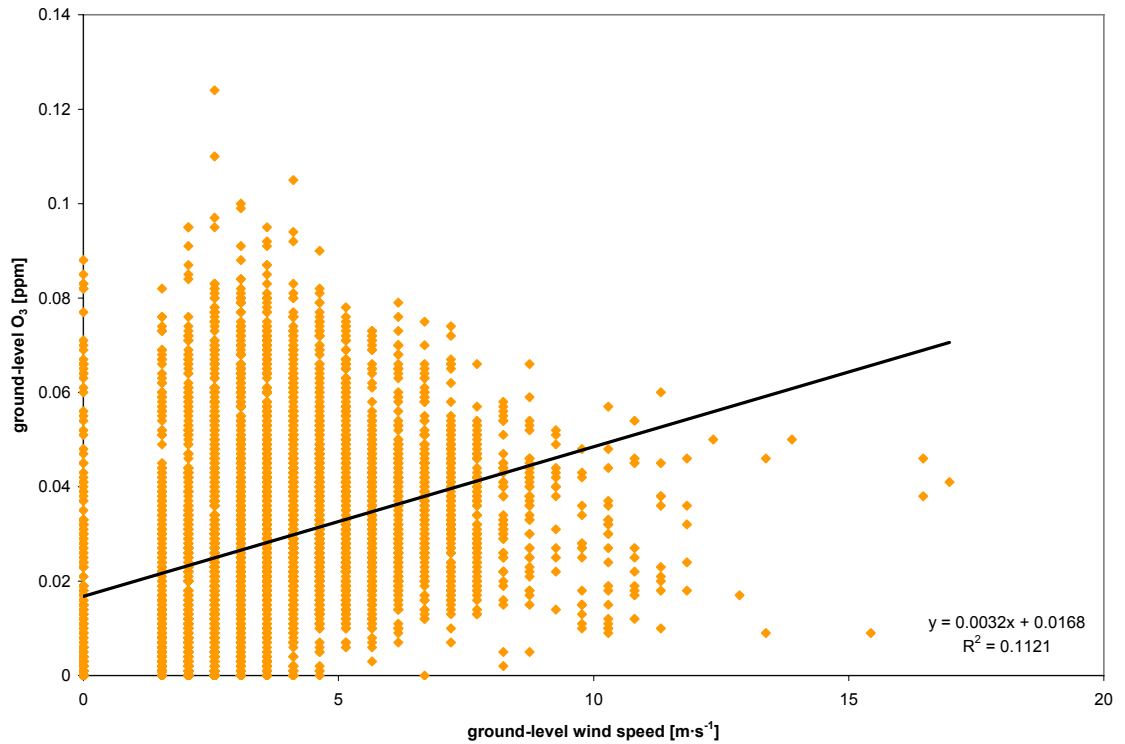


FIGURE 9.17: Correlation between ground-level O₃ and ground-level wind speed, 01 June 2005 – 30 November 2005

Comparison of ground-level ozone concentrations with wind speeds measured at 210 meters resulted in no correlation, as R^2 equaled 0.0005 (Figure 9.18). However, it should be noted that high ozone concentrations ($O_3 \geq 0.08$ ppm) only occurred when the 210-meter wind speed was less than $4 \text{ m}\cdot\text{s}^{-1}$, a trend similar to that observed with ground-level ozone and wind speeds. As with ground-level wind speed, a negatively-sloped regression trend line is occurs when 210-meter wind speed is paired with ground-level O₃ values ≥ 0.01 ppm.

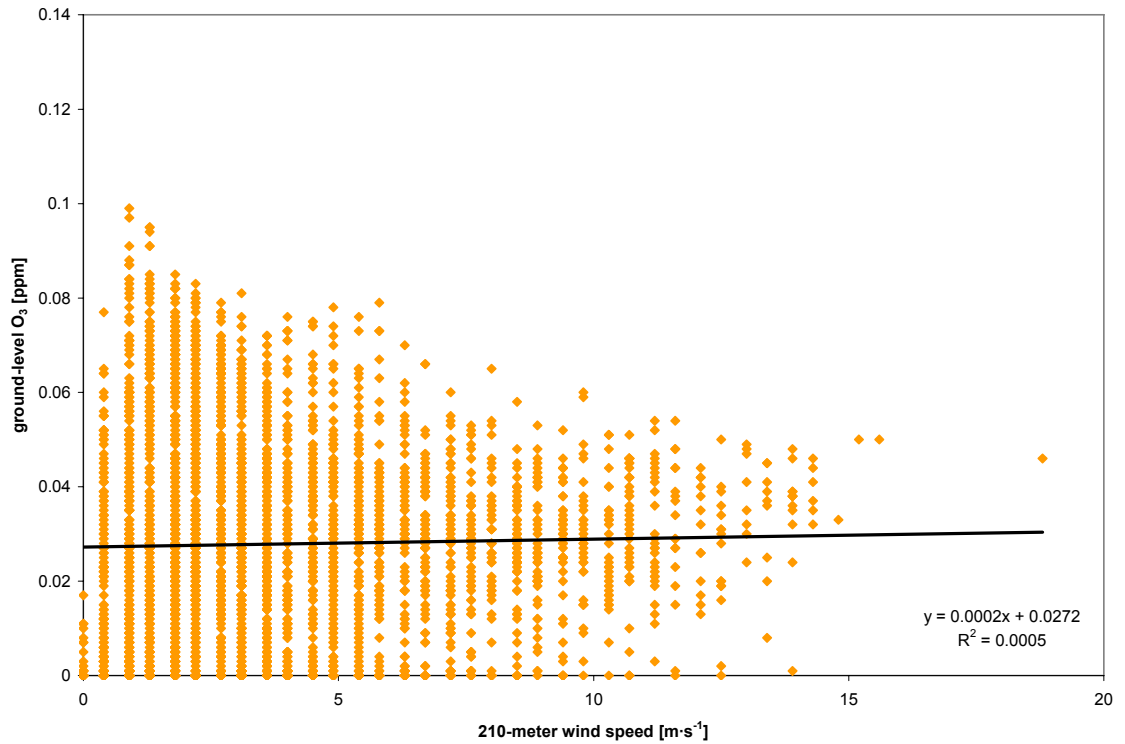


FIGURE 9.18: Correlation between ground-level O₃ and 210-meter wind speed, 01 June 2005 – 30 November 2005

Ozone concentrations measured at 210 meters showed no dependence on wind speeds at ground level or aloft. When 210-meter O₃ concentrations were plotted against ground-level wind speed, the coefficient of determination was negligible at a value of 0.0191 (Figure 9.19). Again, a noticeable trend was evident at higher O₃ concentrations, as the exceedance of the 0.08 ppm 210-meter ozone threshold required ground-level wind speeds below 6 m·s⁻¹.

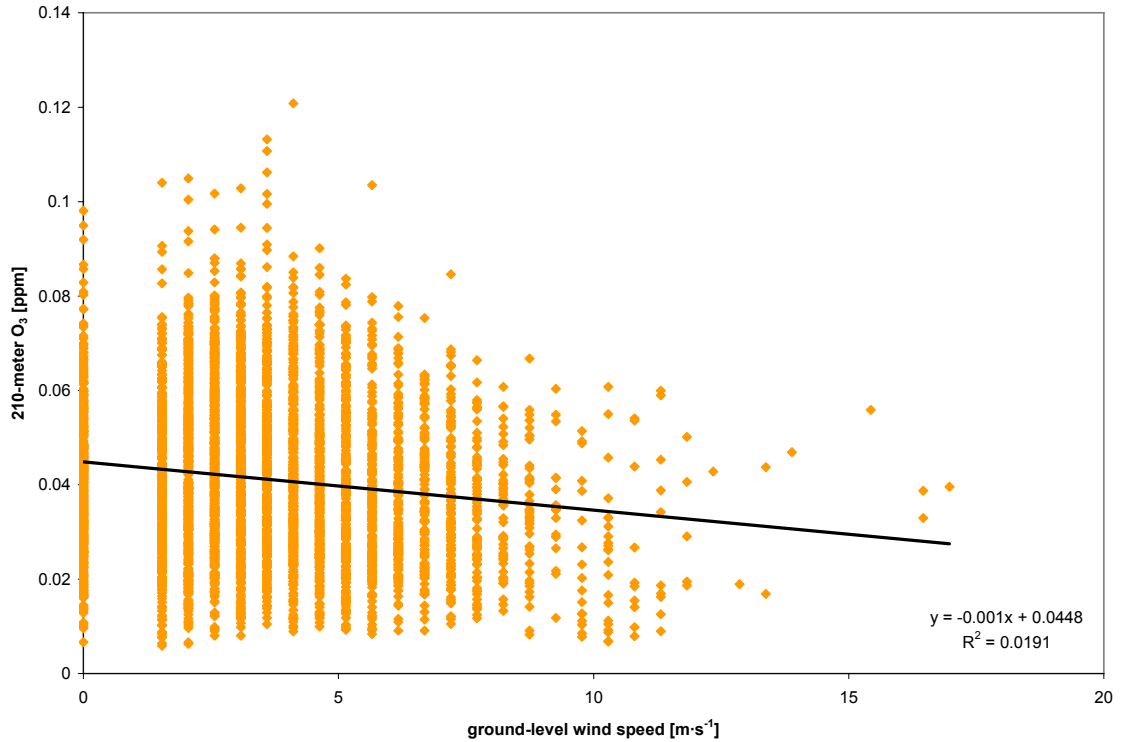


FIGURE 9.19: Correlation between 210-meter O₃ and ground-level wind speed, 01 June 2005 – 30 November 2005

Likewise, consideration of 210-meter wind speeds did not yield any correlation with 210-meter ozone concentrations. In fact, R^2 was again negligible at a value of 0.003 (Figure 9.20). In accordance with the other comparisons between wind speeds and ozone concentrations at both levels, however, high O₃ concentrations ($O_3 \geq 0.08$ ppm) at 210 meters also exhibited a relationship with low wind speeds at the same height. With the exception of two outliers, all wind speeds fell below $4 \text{ m}\cdot\text{s}^{-1}$ above the 0.08 ppm concentration threshold.

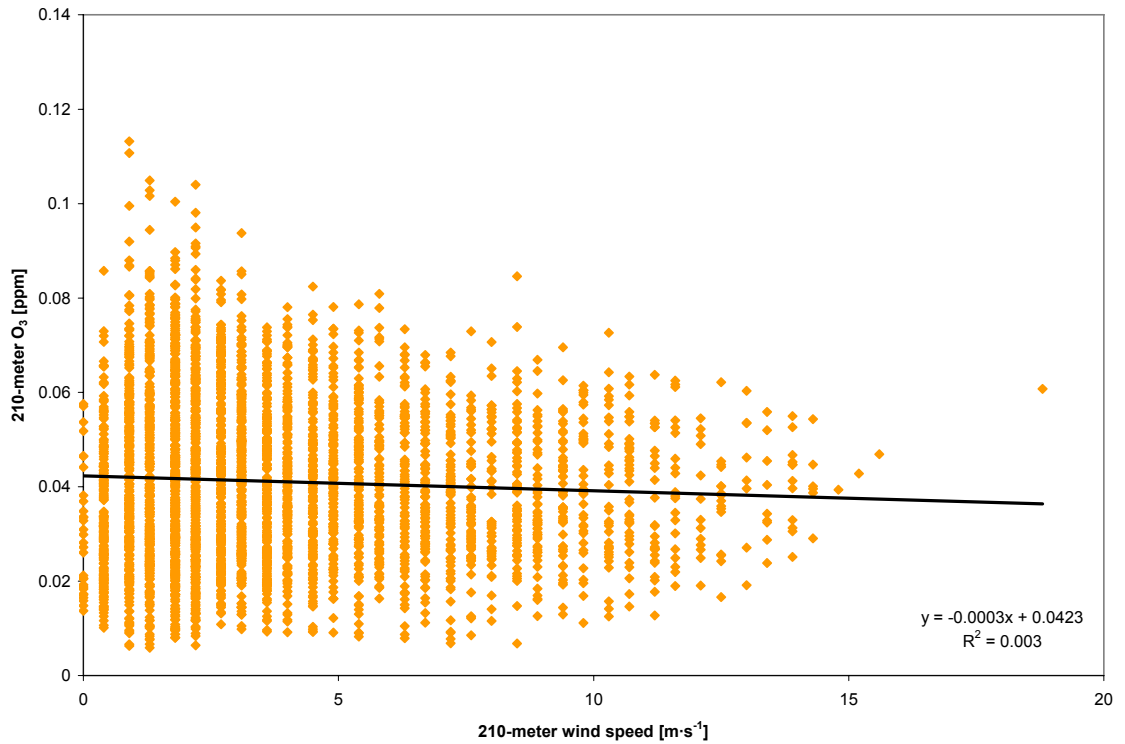


FIGURE 9.20: Correlation between 210-meter O₃ and 210-meter wind speed, 01 June 2005 – 30 November 2005

During the course of the research project, winds at ground level originated from the south (180°) more than any other direction, accounting for the direction of flow 25% of the time. In fact, winds at ground level originated from 180° ± 45° over 50% of the time. Therefore, southerly winds were the dominant wind direction during the months in which ozone posed a significant health threat (Figure 9.21).

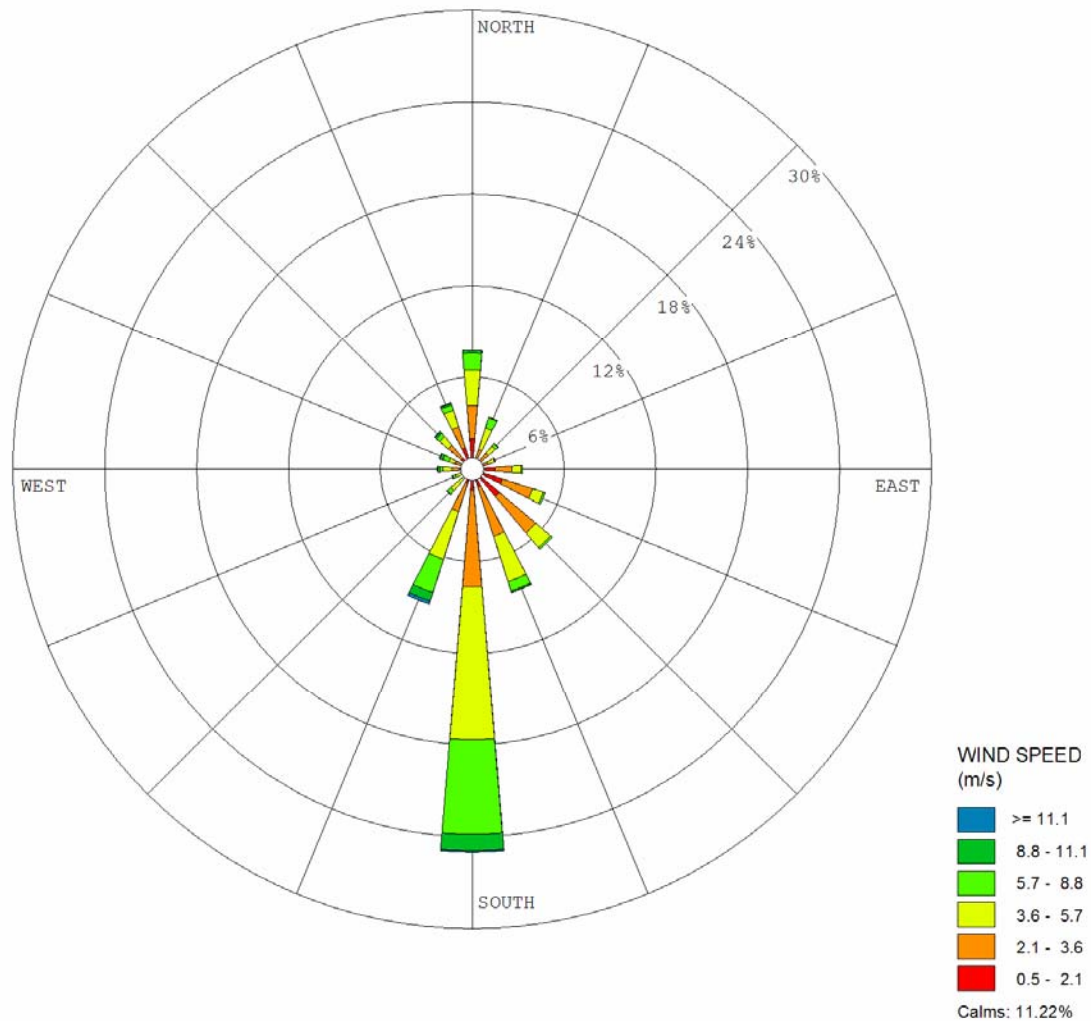


FIGURE 9.21: Ground-level wind frequency plot, 01 June 2005 – 30 November 2005

High ground-level O₃ concentrations, defined in this paper as ≥ 0.08 ppm, tended to coincide with winds originating from the east-southeast. Almost 30% of these ozone concentrations originated from $120^\circ \pm 20^\circ$. Over 50% of high O₃ concentrations occurred when the wind direction was $150^\circ \pm 50^\circ$, particularly significant when considering that 21% of the wind direction data associated with O₃ concentrations ≥ 0.08 ppm were missing and were therefore not included in the calculation. Based on this information, only 26% of the observed high O₃ concentrations did not correspond to wind directions

between 100° and 200°. Of the remaining high concentration values, nearly 11% occurred during calm winds, which have no associated component of direction (Table 9.2).

TABLE 9.2: Frequencies of ground-level wind direction with ground-level ozone ≥ 0.08 parts per million

Wind Dir (°)	n	% Total
100	2	3.5
110	3	5.3
120	4	7.0
130	3	5.3
140	5	8.8
150	1	1.8
160	2	3.5
170	2	3.5
180	2	3.5
190	2	3.5
200	2	3.5
other	11	19.3
calm	6	10.5
missing	12	21.1

Wind directions measured on the roof of the Bank of Oklahoma tower were in a slightly different format than those measured at Tulsa International Airport, as the ground-level anemometer recorded direction in increments of 10°, while the 210-meter anemometer measured direction in increments of 22.5°. When the 210-meter wind direction was considered instead of ground-level wind parameters, the results were surprising. Nearly 50% of the time, ground-level O₃ concentrations equal to or in excess of 0.08 ppm were associated with winds originating from the south-southwest (202.5°). While the

frequency of southerly winds in conjunction with high ground-level ozone concentrations were similar, the differences included: a) the 210-meter wind direction associated with high ground-level ozone concentrations was confined to a much narrower directional interval; and b) the most favored ground-level wind direction for high ground-level O₃ was southeast (140°), which had a frequency of 8.77%, whereas the most frequently occurring 210-meter wind direction associated with high ground-level O₃ was south-southwest (202.5°) (Table 9.3).

TABLE 9.3: Frequencies of 210-meter wind direction with ground-level ozone ≥ 0.08 parts per million

Wind Dir (°)	n	% Total
112.5	0	0.0
135.0	0	0.0
157.5	0	0.0
180.0	2	3.5
202.5	28	49.1
225.0	2	3.5
other	8	14.0
calm	0	0.0
missing	17	29.8

At 210 meters, the dominant wind direction deviates slightly from ground-level, as winds at height tend to approach geostrophic balance with the decreasing effects of surface friction. Thus, winds at this level originated from the south-southwest (202.5°) more than any other direction, with a frequency of 35%. Winds originated from $202.5^\circ \pm 22.5^\circ$ more than 60% of the time at this height (Figure 9.22).

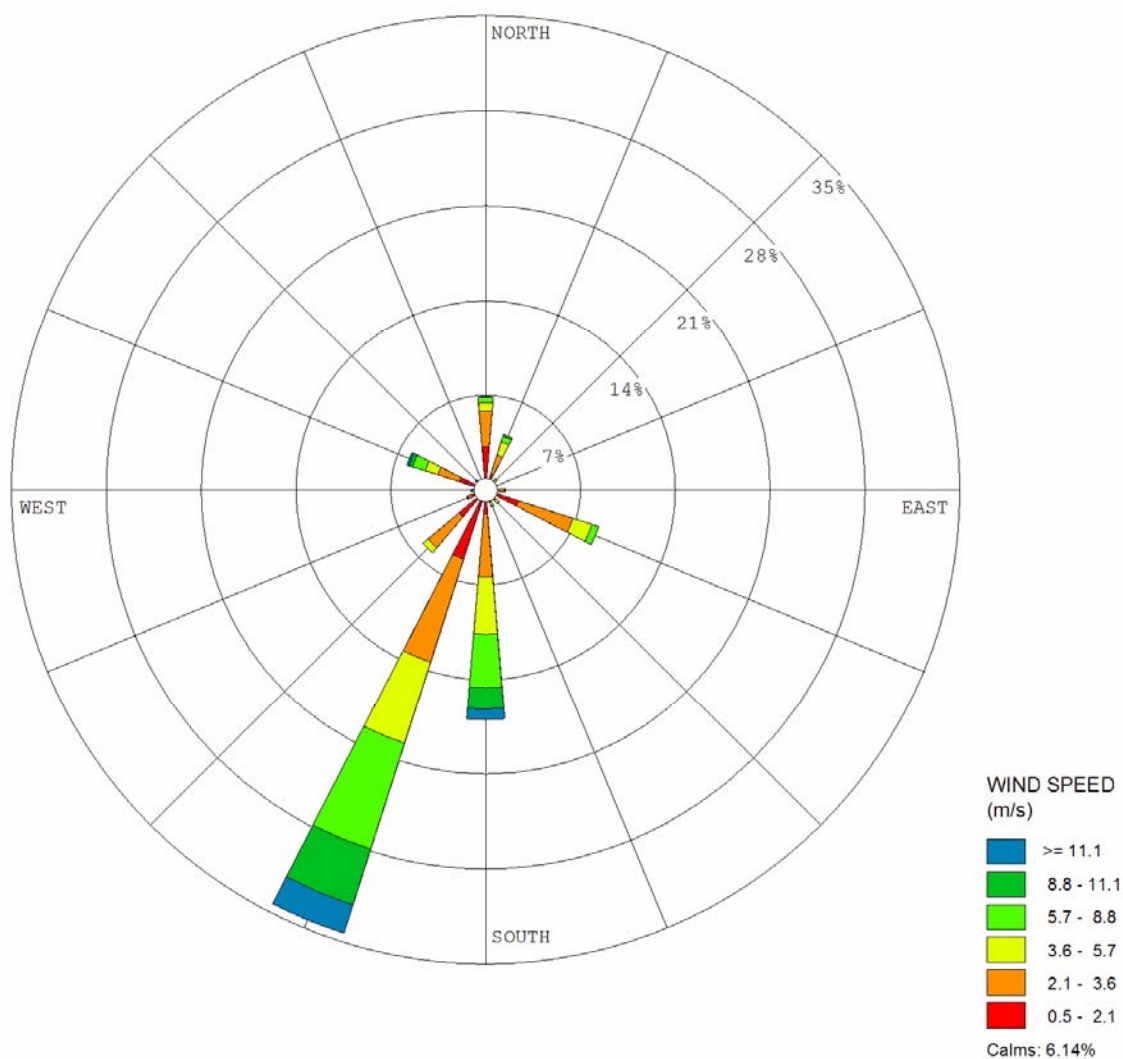


FIGURE 9.22: 210-meter wind frequency plot, 01 June 2005 – 30 November 2005

By comparison, 210-meter ozone concentrations were more uniformly distributed among possible wind directions than were O_3 concentrations at ground level. Although less than 10% of the sample had missing wind direction data, the $150^\circ \pm 50^\circ$ interval accounted for approximately 6% fewer high O_3 concentrations at this level (Table 9.4).

TABLE 9.4: Frequencies of ground-level wind direction with 210-meter ozone ≥ 0.08 parts per million

Wind Dir (°)	n	% Total
100	3	4.8
110	5	7.9
120	4	6.4
130	2	3.2
140	4	6.4
150	3	4.8
160	1	1.6
170	1	1.6
180	2	3.2
190	3	4.8
200	2	3.2
other	18	28.6
calm	9	14.3
missing	6	9.5

As with the relationship between ground-level ozone and wind directions measured at 210 meters, the comparison between 210-meter O₃ and wind directions measured at the same level yielded insightful results. South-southwesterly winds (202.5°) remained the most prominent wind direction for high ozone concentrations, but at a frequency of 36.51%, the spread was more uniformly distributed among wind directions with a southerly component. It should be noted, however, that 67% of the distribution fell within the interval $157.5^\circ \pm 45^\circ$, with 14.29% of the remaining data classified as missing. Thus, high 210-meter O₃ concentrations overwhelmingly occurred in the presence of winds with a southerly component (Table 9.5).

TABLE 9.5: Frequencies of 210-meter wind direction with 210-meter ozone ≥ 0.08 parts per million

Wind Dir (°)	n	% Total
112.5	8	12.7
135.0	1	1.6
157.5	2	3.2
180.0	6	9.5
202.5	23	36.5
225.0	2	3.2
other	12	19.1
calm	0	0.0
missing	9	14.3

9.1.6. Ultraviolet Radiation

Ultraviolet (UV) radiation was measured at an Oklahoma Mesonet site in the nearby town of Skiatook, approximately 17 km northwest of the ground level ozone monitoring site and 20 km north of the Bank of Oklahoma, the 210-meter ozone monitoring site, respectively.

Comparison of UV radiation with ground-level ozone concentrations produced a positive correlation, although not exceedingly strong ($R^2 = 0.4483$). This degree of correlation was partially due to the lag between maximum incoming solar radiation and maximum O₃ concentration, typically on the order of 1-3 hours (Figure 9.23).

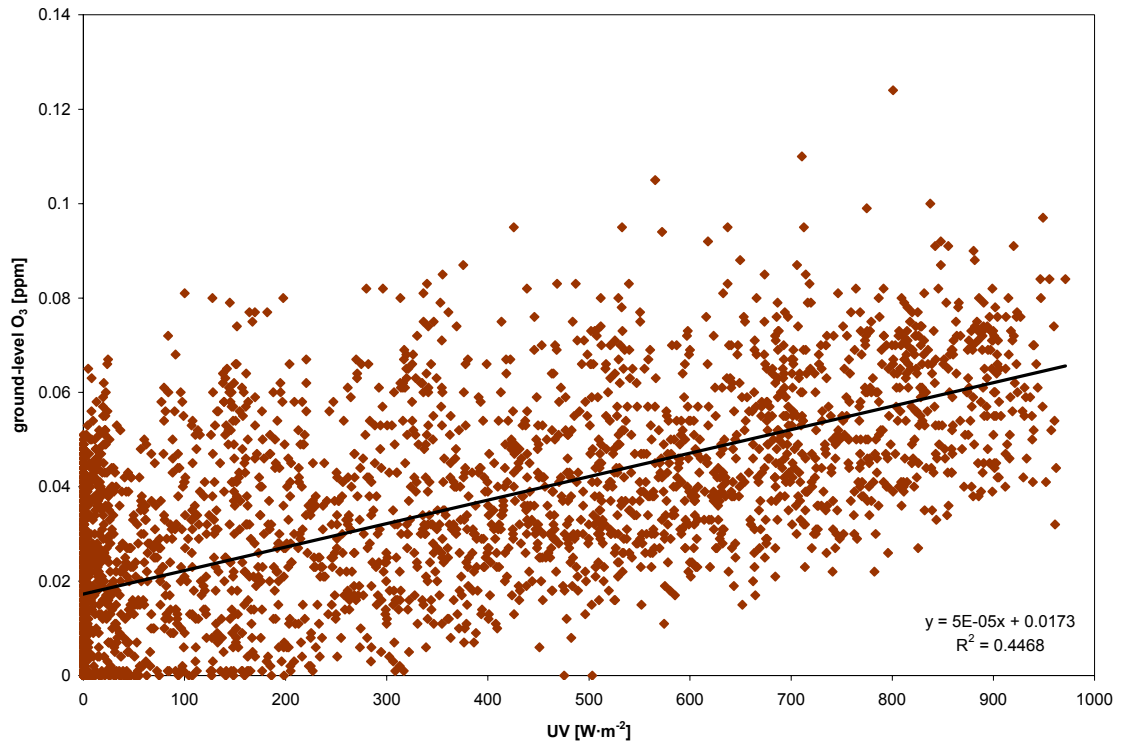


FIGURE 9.23: Correlation between ground-level O₃ and solar radiation, 01 June 2005 – 30 November 2005

When the data were offset so that ground-level O₃ lagged incoming UV by 2 hours, the best correlation ($R^2 = 0.6065$) was achieved (Figure 9.24). The correlation for a 1-hour offset was similar ($R^2 = 0.5759$), while the correlation for the 3-hour lag was weaker, as the coefficient of determination had decreased to 0.5316.

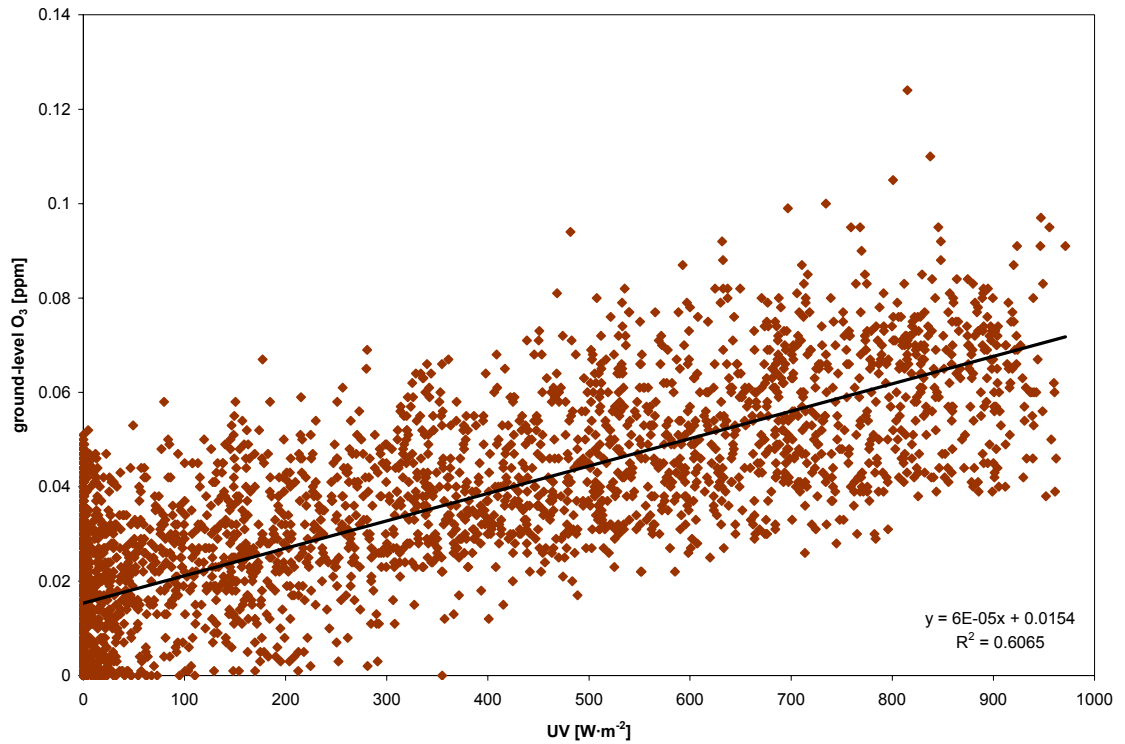


FIGURE 9.24: Maximum correlation between ground-level O₃ and solar radiation (2-hour offset), 01 June 2005 – 30 November 2005

The observed lag between 210-meter ozone and incoming solar radiation was larger than the offset between UV and ground level ozone, partially due to a lag in the time required for mixing between ground level and 210 meters. When no offset was instituted, no correlation existed (Figure 9.25) ($R^2 = 0.0257$).

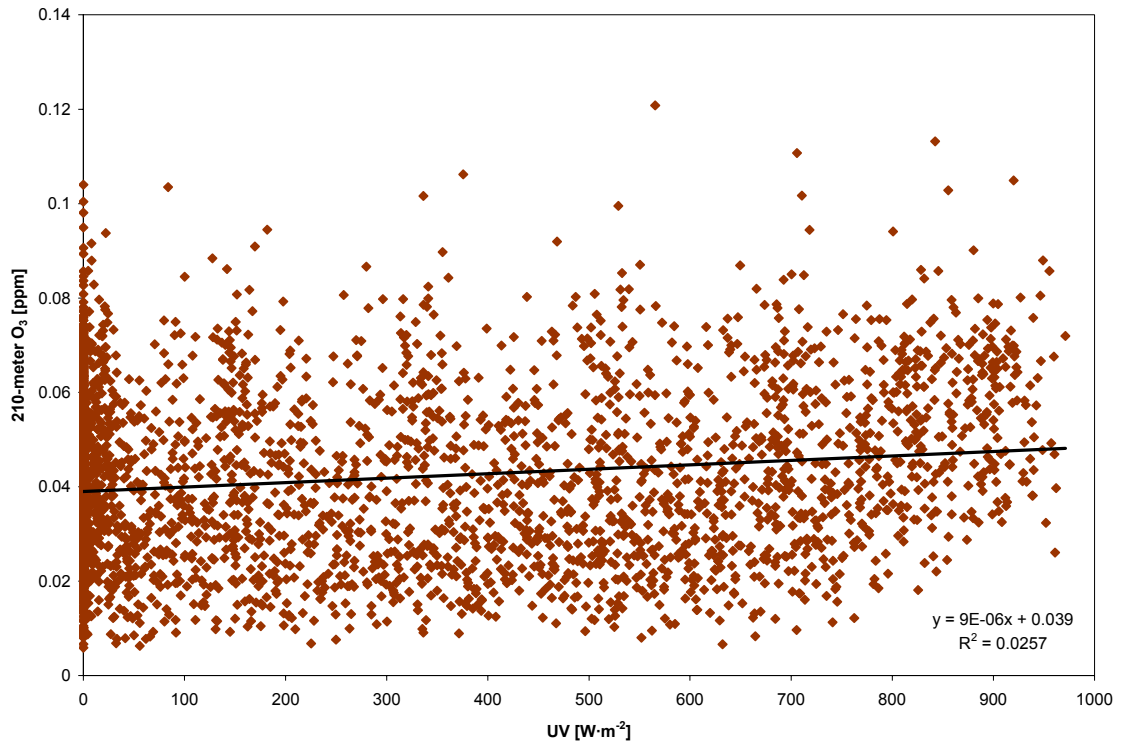


FIGURE 9.25: Correlation between 210-meter O₃ and solar radiation, 01 June 2005 – 30 November 2005

Correlation gradually improved to a maximum R² of 0.2246 with a solar radiation offset of 4 hours (Figure 9.26). This value remained virtually unchanged with a 5-hour offset. With an offset of six hours, the correlation decreased, as R² equaled 0.1982. The coefficient of determination thereafter continued to decrease as the lag time increased.

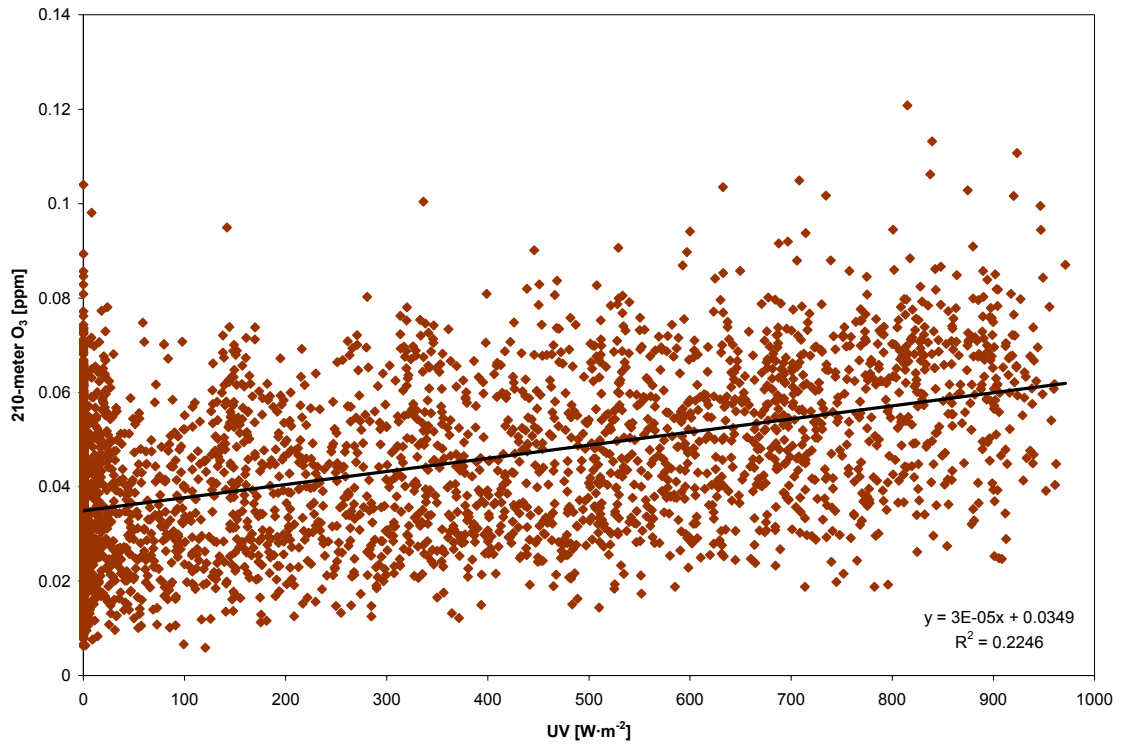


FIGURE 9.26: Maximum correlation between 210-meter O₃ and solar radiation (4-hour offset), 01 June 2005 – 30 November 2005

9.2. Ozonesonde Measurements of Background O₃

Background ozone concentrations are especially important when assessing the origin and magnitude of transported ozone. One of the most important findings in this research study concerns the behavior of the background (residual) ozone concentration, which was measured both as the nocturnal O₃ concentration minimum at 210 meters and as the residual O₃ concentration in the troposphere by vertically profiling the atmosphere with ozone soundings, or “ozonesondes.”

As has been previously discussed, ozone measured at 210 meters was well mixed with ground-level ozone during the day, but decoupled during the overnight hours, thus behaving as an independent system. Objective analysis suggests that the background concentration ozone, measured as the nocturnal difference in ozone concentrations between ground level and 210 meters, ranged between 0.01 and 0.06 parts per million in the Tulsa metropolitan area, although the range was typically a much smaller 0.03-0.05 ppm interval. These values are consistent with background concentrations measured in previous research studies (Plaza et al., 1997; Zhang et al., 1998; Baumann et al., 2000; Mudway and Kelly, 2000; Gangoiti et al., 2001; Liu et al., 2004).

Nocturnal wind speeds at 210 meters were rarely negligible during the course of the research study, even during the overnight hours when winds tended to be calm at ground level. Subsequently, a transport vector was always present at this elevation. Appreciable

wind speeds aloft therefore signified that the background ozone concentration at 210 meters was transient and therefore not of local origin.

The existence of an appreciable background ozone concentration above the 210-meter level, while documented in previous literature, was nonetheless verified by profiling the vertical extent of tropospheric ozone with the launch of an ozonesonde on 08 October 2005 in the Tulsa metropolitan area. The resulting profile indicated that O_3 concentrations above the surface were generally uniform with height through the lower and mid-troposphere, where residual ozone concentrations on the order of 0.01 parts per million were measured (Figure 9.27).

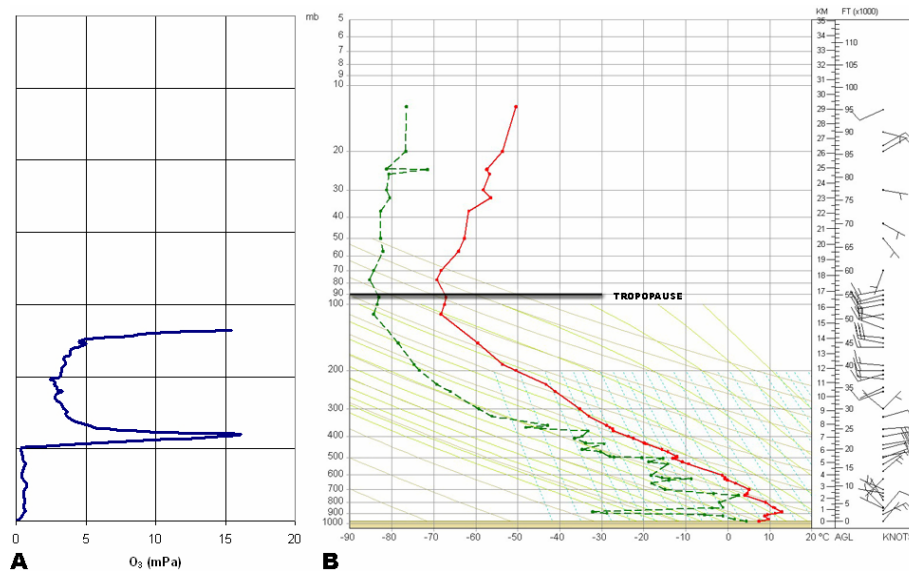


FIGURE 9.27: A) Vertical ozone concentrations measured at 8:00 CST on 08 October 2005 at Tulsa, Oklahoma, and B) Corresponding 6:00 CST atmospheric sounding from Norman, Oklahoma

However, a noticeable ozone maximum occurred at approximately 400 hPa, or approximately 7 km above ground level. The abrupt increase in free tropospheric ozone occurred well below the height of the local troposphere, indicated on the 6:00 CST Norman, Oklahoma atmospheric sounding at an elevation of 17 km. Geopotential height analysis at the 300 hPa level on the morning of 08 October indicated a bifurcated polar jet stream with an embedded upper-level “shortwave” trough over Oklahoma (Figure 9.28). It appears that the intrusion of high O₃ concentrations at 400 hPa may be attributable to the passage of the trough, as a narrow zone of tropopause folding likely occurred as well.

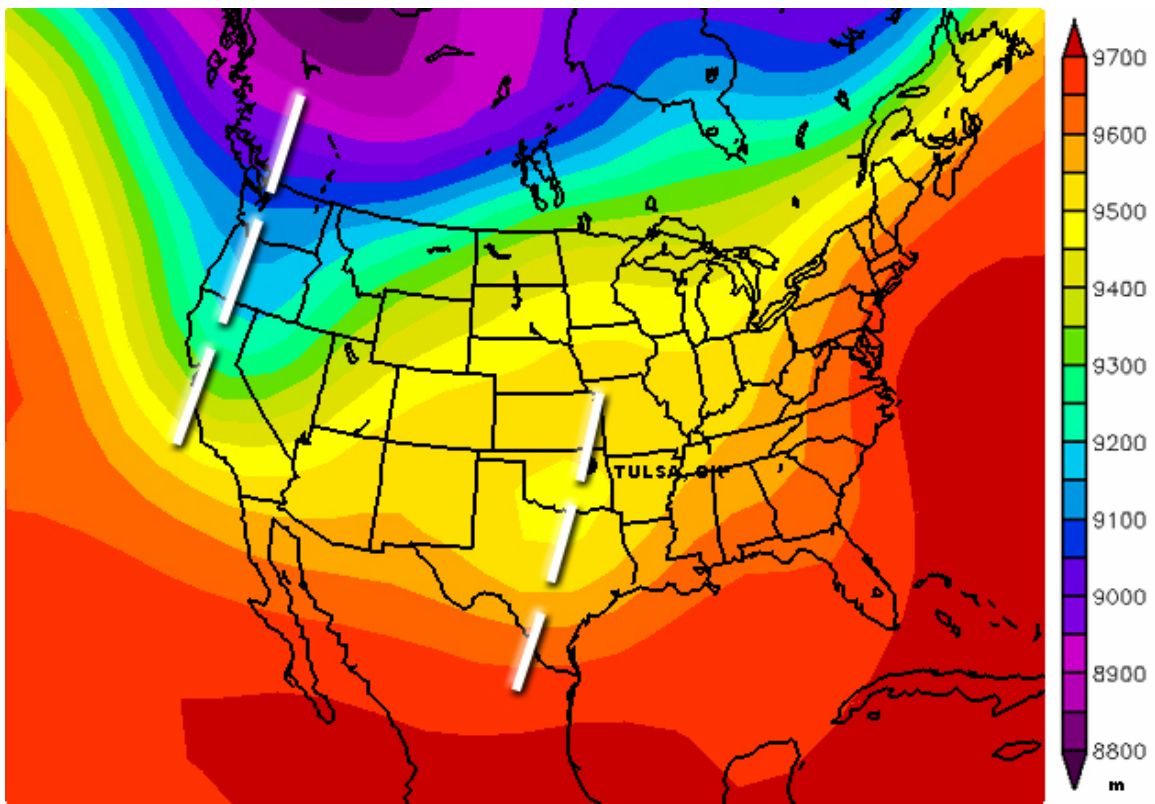


FIGURE 9.28: 300 hPa geopotential height analysis, 6:00 CST, 08 October 2005 (NOAA, 2006)

Aside from the ozone maximum at 400 hPa, background ozone concentrations in the troposphere were relatively low at the time of the local ozonesonde launch when compared with values reported in previous research. The lack of ozone in the lower troposphere was likely due to the passage of the polar front in conjunction with the aforementioned upper-level trough (Figure 9.29). Unlike boundary-layer fronts, the polar front marks the equator-ward extent of the permanent polar air mass, and it is characterized by a vertical discontinuity through the troposphere. The polar front is always associated with the polar jet stream, although it can meander several hundred kilometers from the jet core.

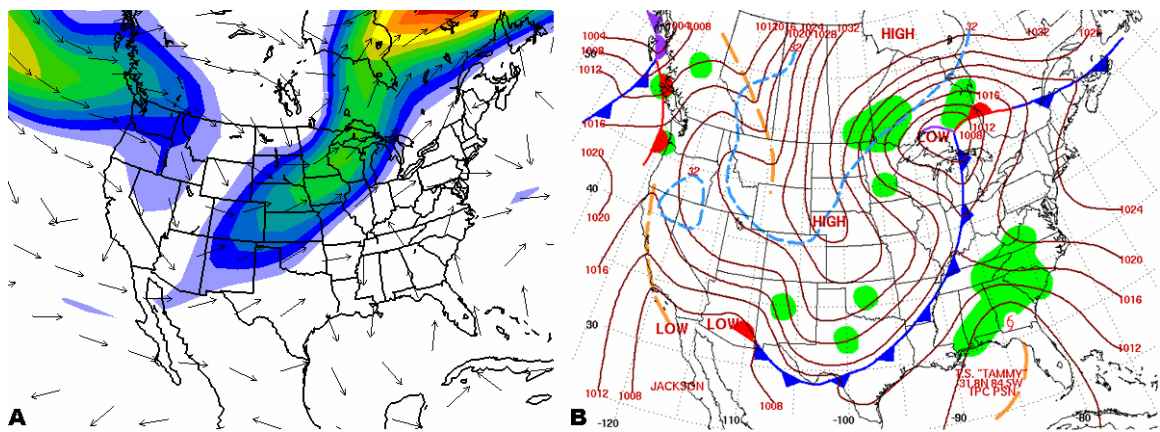


FIGURE 9.29: A) Polar jet stream; and B) the passage of the polar front, 06 October 2005 (NOAA, 2006)

Although vertical ozone profiling of the entire troposphere was limited to a single ozonesonde in the context of this research study, previous measurements from ozone soundings were taken on a weekly basis at Huntsville, Alabama (35.2°N, 86.6°W) as part of a joint long-term research project between the University of Alabama-Huntsville, NOAA, and NASA. Ozonesondes in the Huntsville study were launched during the

period beginning on 20 April 1999 and ending on 20 August 2005 (UAH, 2006). Since Huntsville is a mid-sized metropolitan area in the same geographical region as Tulsa with similar climatology, conclusions pertaining to the vertical characteristics of ozone can be drawn and subsequently applied to the Tulsa study.

Residual ozone concentrations in the troposphere above Huntsville were found to be on the order of 0.05-0.07 ppm during the course of the 2005 ozone season (prior to the final ozonesonde launch at this location on 20 August) (UAH, 2006). In fact, little variation was observed in the vertical ozone column from June through August. When the scope of ozone sounding analysis was broadened to include the entire Huntsville data set, a clear trend emerged: significant variation in tropospheric ozone coincided with the passages of mid-latitude cyclones and attendant upper-level pressure troughs, similar to the pattern observed in the 08 October 2005 Tulsa ozonesonde. At least thirteen intrusions of stratospheric ozone into the troposphere are discernable in the 6-year Huntsville ozonesonde record (UAH, 2006). Each is characterized by high ozone concentrations in the troposphere (> 0.3 ppm), and the origin of these reservoirs was presumably the descent of stratospheric ozone into the mid-troposphere as a result of tropopause folding in the vicinity of the polar jet stream and associated cyclones.

Does stratospheric ozone directly contribute to boundary layer ozone concentrations, or is it instead supplying the tropospheric ozone reservoir, which requires longer transport time to the surface? Of the thirteen identified stratospheric ozone intrusions in the Huntsville ozonesonde record, only one mission was coupled with an additional flight on

the following day, yielding insight to this question. At 12:00 CST on 08 April 2000, an ozone maximum in excess of 0.3 parts per million was observed at an altitude of 9 km, well below the 17 km height of the tropopause (Figure 9.30) (UAH, 2006). The lower boundary of the mid-troposphere ozone maximum approached 5 km. Meanwhile, ozone concentrations in the lowest 3 km of the atmosphere were on the order of 0.025-0.030 ppm (UAH, 2006).

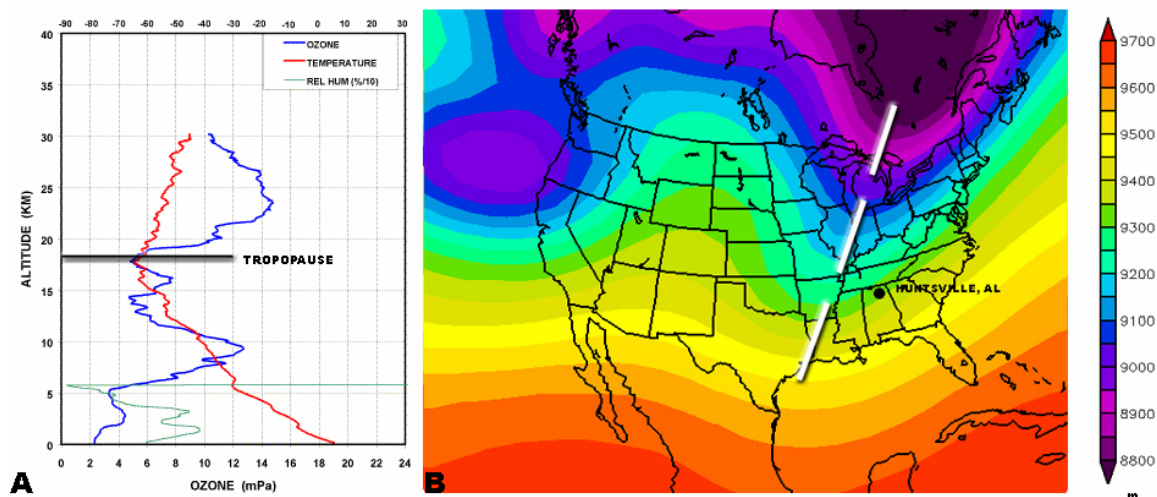


FIGURE 9.30: A) Ozone maximum in the mid-troposphere at Huntsville, Alabama corresponding to the B) approach of an upper-level trough (300 hPa heights expressed as meters) at 12:00 CST on 08 April 2000 (UAH, 2006; NOAA, 2006)

Twelve hours later, at 00:00 CST on 09 April, a subsequent ozone sounding indicated that ozone concentrations in the mid-troposphere (5-10 km) had decreased considerably, as no maximum was observed at this altitude (Figure 9.31) (UAH, 2006). Instead, ozone concentrations increased in the lowest 3 km of the atmosphere, and were measured in the 0.05-0.06 ppm range (UAH, 2006).

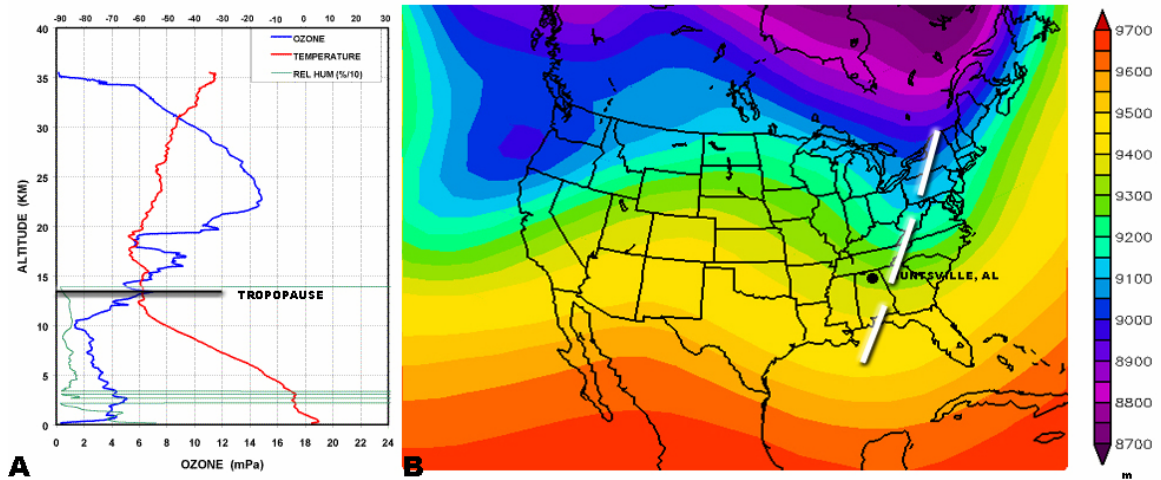


FIGURE 9.31: A) Ozone maximum in the lower troposphere at Huntsville, Alabama corresponding to the B) departure of an upper-level trough (300 hPa heights expressed as meters) at 00:00 CST on 09 April 2000 (UAH, 2006, NOAA, 2006)

Thus, while the stratospheric intrusion of ozone into the troposphere most assuredly contributes to the overall reservoir of residual ozone in the free troposphere, it can also influence boundary layer ozone concentrations on short time scales following the passage of a mid-latitude cyclone and upper-level trough within the global atmospheric circulation.

It has been established that background ozone concentrations are highly dynamic in response to the characteristics of the synoptic upper-level meteorological regime, implying an appreciable component of ozone transport. Thus, if ozone isn't solely locally produced, then what is its origin? Attention must be turned to two processes: vertical transport through the troposphere, and horizontal transport in boundary-layer winds, including the nocturnal low-level jet.

9.3. Vertical Transport and the Global Atmospheric Circulation

Analysis of the 210-meter data indicated that the long-term ozone signal was sinusoidal. Under the influence of strong anti-cyclonic subsidence, background values in the range of 0.05-0.06 ppm were commonly observed. Although these high residual concentrations were most frequent during the mid- to late-summer months when the influence of subtropical ridging was at its peak, background concentrations exceeding 0.04 ppm were observed during the fall months with the passage of weaker anti-cyclones.

Relatively low residual ozone concentrations coincided with the passages of upper-level cyclones. Background concentrations in the range of 0.01-0.02 ppm commonly accompanied the cyclonic flow of atmospheric short-wave and long-wave disturbances, regardless of season. Low background concentrations were more frequent during the fall months, however, as a result of the increased presence of atmospheric disturbances in progressive upper-level flow associated with the polar jet stream.

Long-term ozone data collected during the study were characterized by a series of concentration maxima and minima corresponding to the passages of pressure ridges and troughs embedded within the polar jet stream (Figure 9.32). Boundary-layer ozone concentrations increased with the intensification of high pressure systems and associated pressure ridges. Conversely, boundary-layer ozone concentrations decreased with the approach and passage of upper-level pressure troughs. As winter approached, the polar jet stream shifted toward the equator. Ozone concentration variability subsequently

increased in response to an increase in the amplitude and frequency of atmospheric disturbances, and boundary-layer ozone concentrations trended downward.

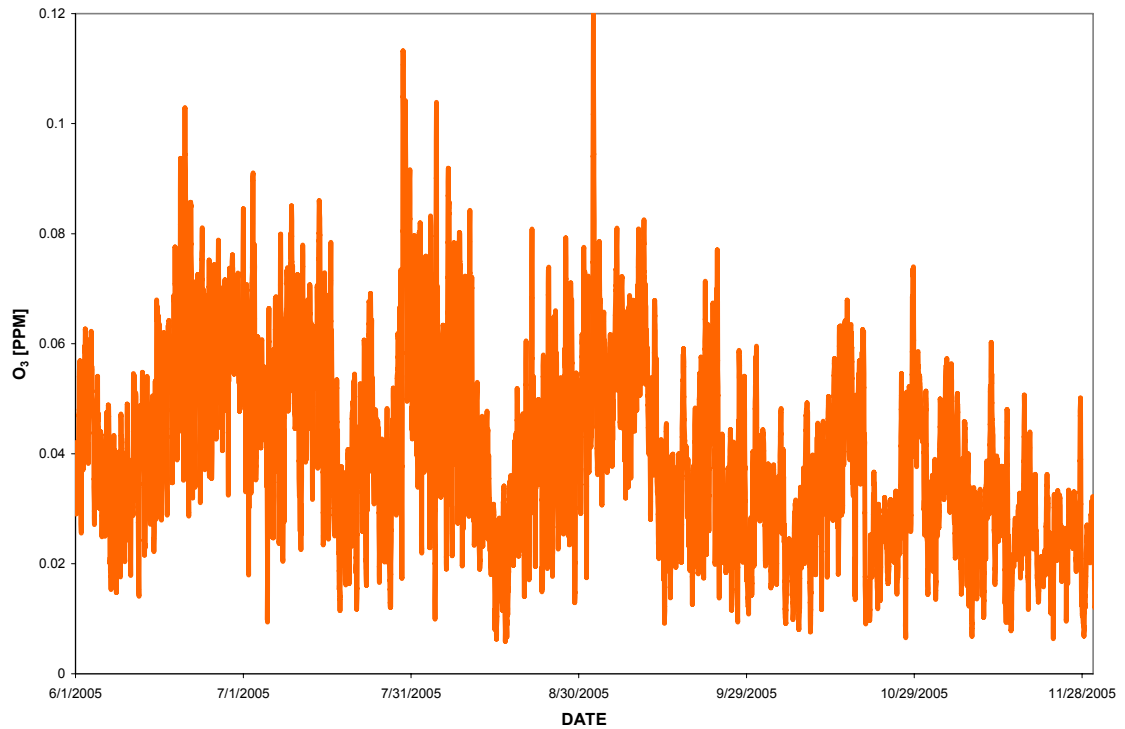


FIGURE 9.32: 210-meter ozone concentrations measured in Tulsa, Oklahoma during the 2005 ozone season

Quantification of the impacts that upper-level pressure ridge and trough passages have on the ozone budget of the lower atmosphere was achieved by considering the geopotential heights of the 300 hPa constant pressure surface. Specifically, this surface, representative of the height of the jet stream in the mid-latitudes, was used as an estimate of the amplitude and frequency of atmospheric disturbances within the polar jet (Reiter, 1963). Since the polar jet stream varies longitudinally as the troposphere thermally expands and

contracts with the yearly seasonal cycle, three upper-air sounding sites – Brownsville, Texas, Norman, Oklahoma, and Aberdeen, South Dakota – were selected for analysis (Figure 9.33). Each site is separated by approximately 10° of latitude.



FIGURE 9.33: Upper-air sounding locations in relation to Tulsa, Oklahoma

While atmospheric disturbances were hardly noticeable at Brownsville, Texas during the summer and fall months with the dominance of subtropical upper-level high pressure, relative geopotential height increases and decreases were pronounced at Aberdeen, South Dakota, a site in much closer proximity to the polar jet stream (Figure 9.34).

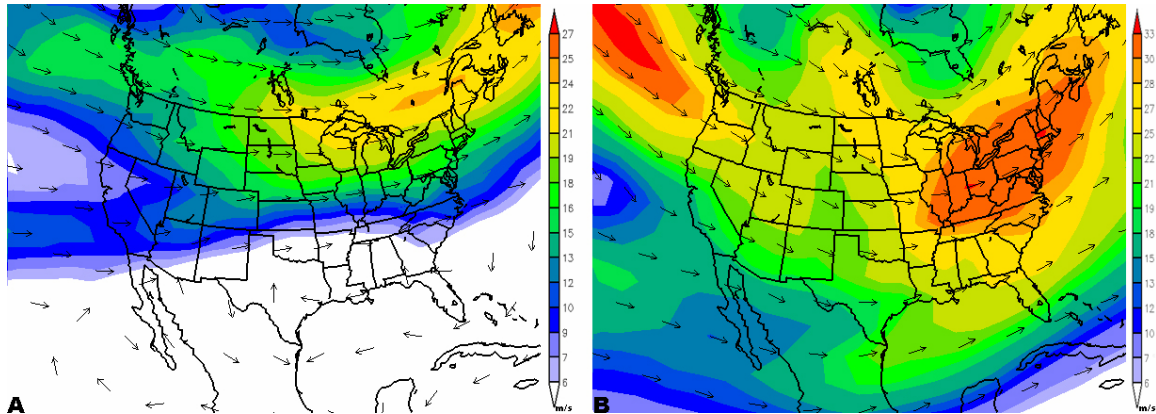


FIGURE 9.34: A) Mean 300 hPa polar jet stream, July 2005, and B) mean 300 hPa polar jet stream, November 2005 (NOAA, 2006)

It is clear from the upper-level height measurements obtained at Brownsville, Norman, and Aberdeen that the amplitude between upper-level pressure ridges and troughs varies with longitude (Figure 9.35). The seasonal maximum geopotential heights at all three locations, occurring during early July, represented the peak of thermal expansion of the troposphere. Afterwards, the troposphere began to cool with a decrease in solar radiation, resulting in a trend of lower geopotential heights.

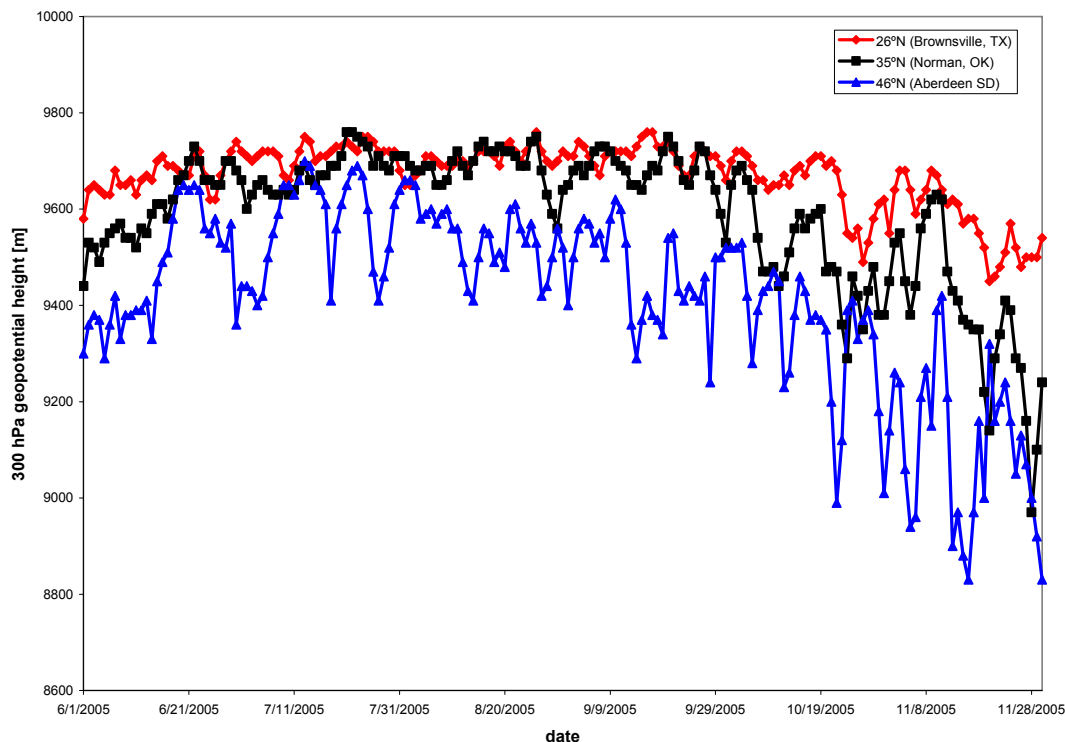


FIGURE 9.35: 300 hPa geopotential heights observed at 26°N (Brownsville, Texas), 35°N (Norman, Oklahoma), and 46°N (Aberdeen, South Dakota) during the 2005 six-month ozone season

Correlation between the 24-hour (daily) ozone average measured at 210 meters in Tulsa, Oklahoma and the 300 hPa geopotential height measured in Brownsville, Texas was weak ($R^2 = 0.14$), primarily due to the subtle nature of upper-level height responses to atmospheric disturbance at a significant distance equator-ward from the polar jet stream (Figure 9.36). Brownsville, Texas is located at a latitude of 26°N, only 3°N of the Tropic of Cancer. This region is in the descending limb of the equatorial Hadley Cell circulation, resulting in a strong subtropical anti-cyclonic influence. The polar jet stream

and accompanying atmospheric disturbances are therefore usually located well to the north during the summer months.

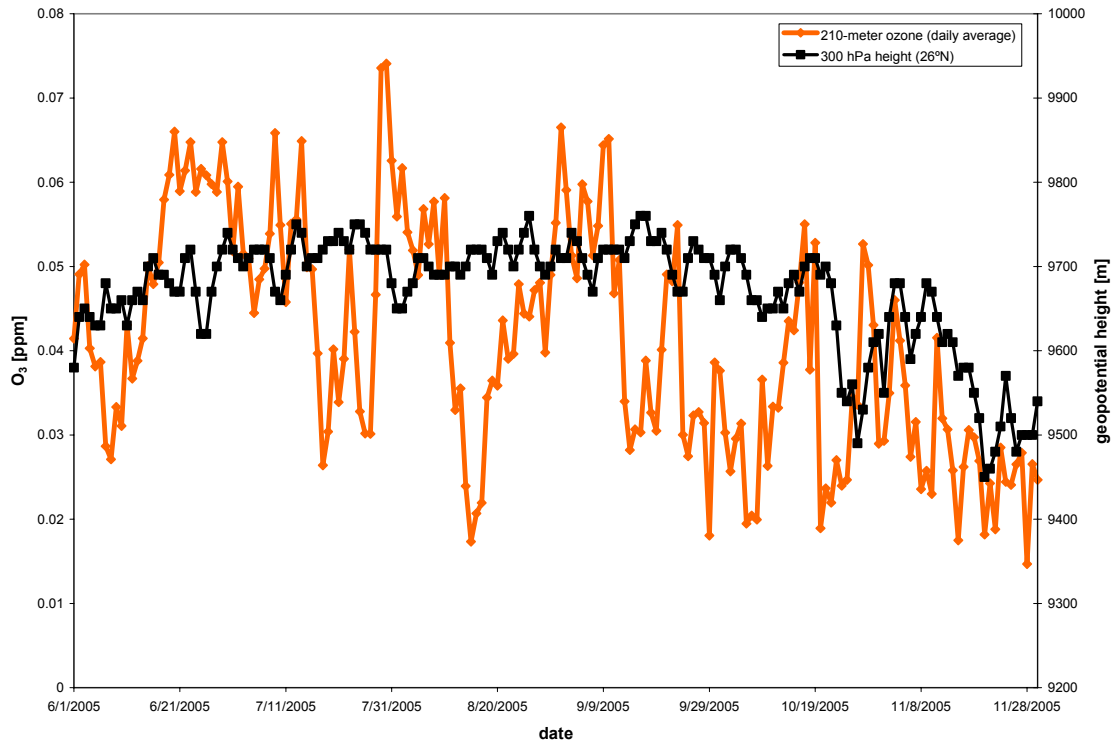


FIGURE 9.36: 210-meter ozone concentrations measured in Tulsa, Oklahoma (36°N) compared with 300 hPa geopotential heights measured in Brownsville, Texas (26°N)

Boundary-layer ozone concentrations measured at Tulsa, Oklahoma were compared with 300 hPa geopotential heights measured at nearby Norman, Oklahoma, the nearest source of upper-level meteorological sounding data (Figure 9.37). Correlation was weak ($R^2 = 0.22$), due in part to the spatial and temporal variations between the polar jet stream and the ozone study location, as the mean position of the polar jet stream during the 6-month study was 50°N.

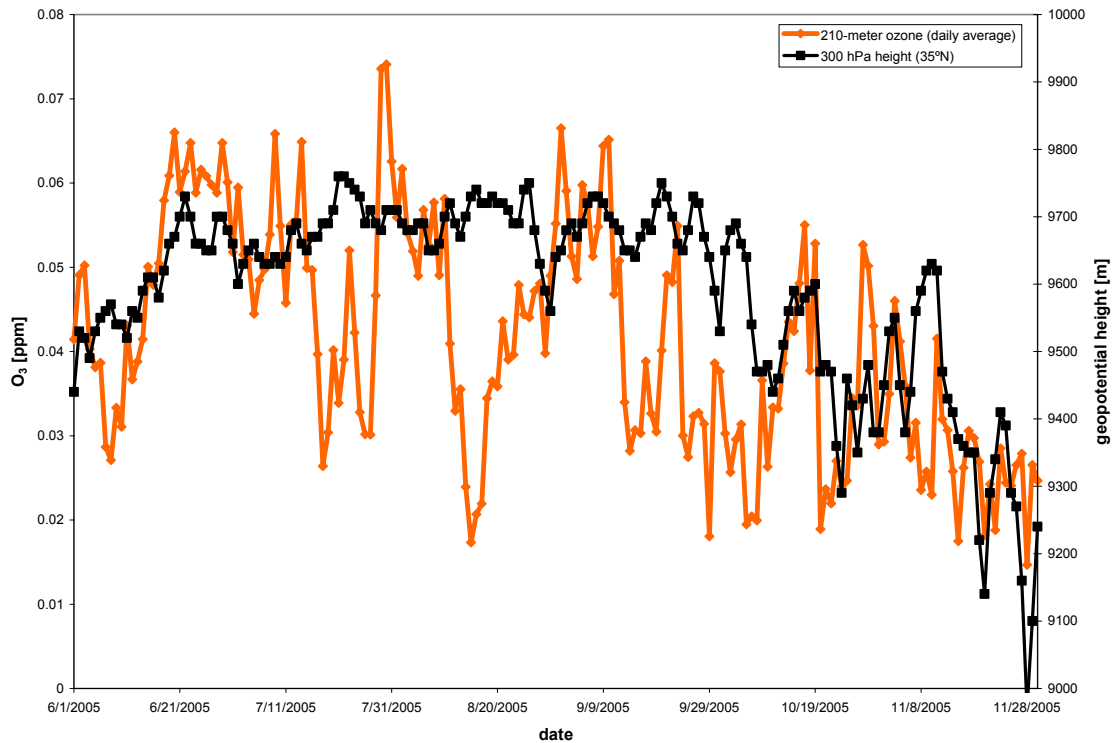


FIGURE 9.37: 210-meter ozone concentrations measured in Tulsa, Oklahoma (36°N) compared with 300 hPa geopotential heights measured in Norman, Oklahoma (35°N)

Geopotential heights representative of the 300 hPa constant pressure surface measured at Aberdeen, South Dakota were also compared with the 210-meter ozone concentrations measured at Tulsa, Oklahoma, as the sounding location was in close proximity to the mean position of the polar jet stream (Figure 9.38). As a result, the correlation increased appreciably ($R^2 = 0.36$). Furthermore, better agreement of the graphed data was achieved when the 210-meter ozone trace was plotted against the Aberdeen, South Dakota 300 hPa geopotential height data than with the Norman, Oklahoma or Brownsville, Texas 300 hPa geopotential heights – again a possible reflection of the proximity between Aberdeen, South Dakota (46°N) and the mean position of the polar jet stream (50°N).

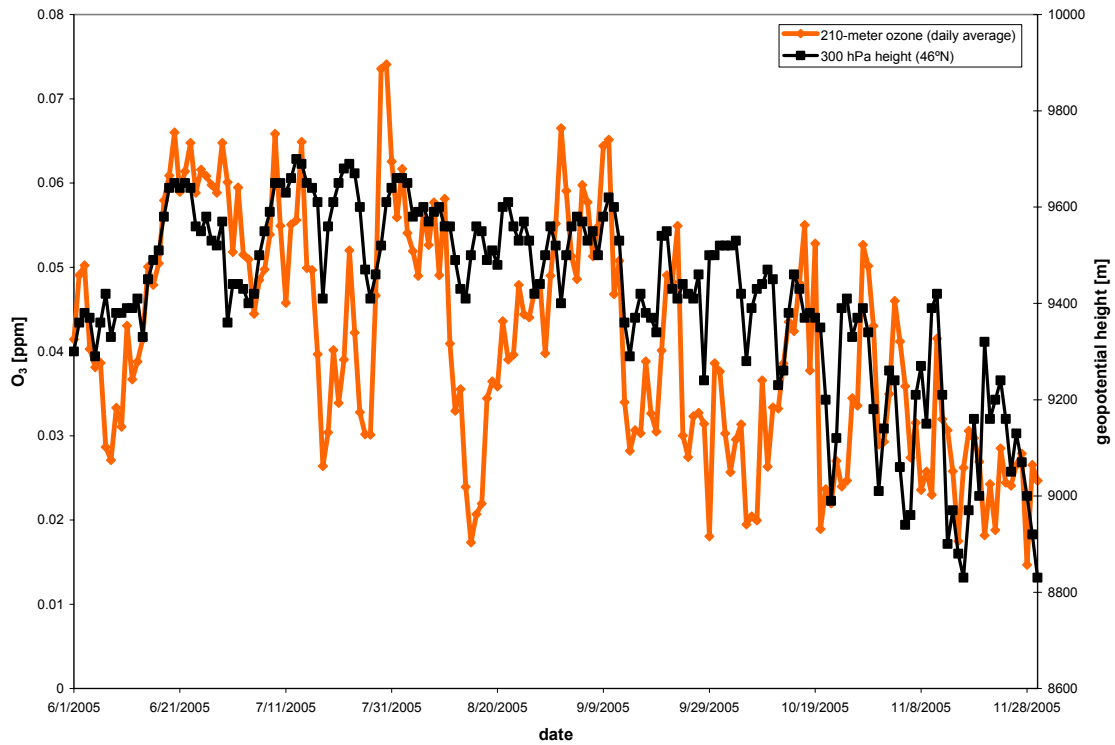


FIGURE 9.38: Boundary-layer ozone concentrations measured in Tulsa, Oklahoma (36°N) compared with 300 hPa geopotential heights measured in Aberdeen, South Dakota (46°N)

The best correlation between 210-meter ozone and 300 hPa geopotential heights measured at 46°N was achieved when a lag time was introduced between the two. The highest coefficient of determination ($R^2 = 0.38$) occurred with a lag of 18 hours, consistent with the vertical tilt of atmospheric waves and the subsequent offset of upper-level troughs and ridges with respect to their lower tropospheric counterparts (Figure 9.39). This indicated that maximum ozone concentrations were associated with 300 hPa ridges centered to the west of Tulsa.

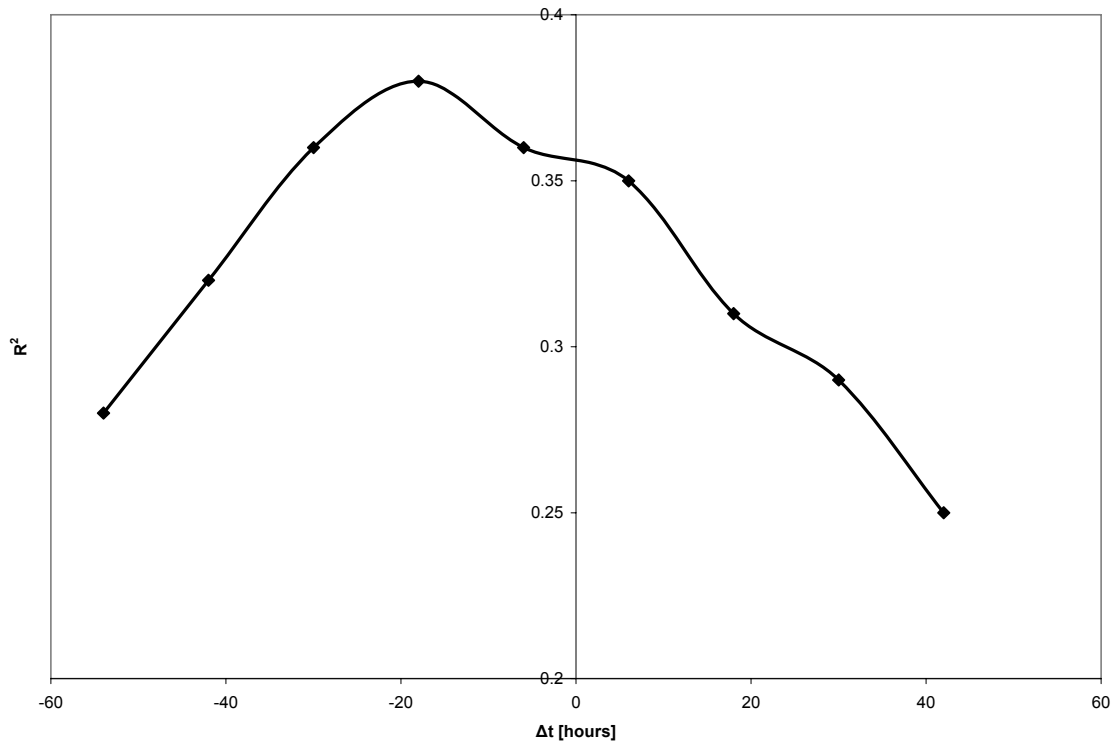


FIGURE 9.39: Correlation (as R^2) based on time shift between 210-meter ozone concentrations measured in Tulsa, Oklahoma and 300 hPa geopotential heights measured in close proximity to the polar jet stream at Aberdeen, South Dakota; Positive shifts correspond to height values that have been advanced in time with respect to ozone, while negative shifts correspond to ozone concentrations that have been advanced in time with respect to geopotential heights

Vertical tilt of upper-level ridges and troughs could have accounted for the lag observed between 210-meter ozone and 300 hPa geopotential heights. With the approach of upper-level ridges, mass convergence in the downstream entrance into an adjacent upper-level trough resulted in large-scale subsidence through the vertical extent of the troposphere, and background ozone concentrations in the boundary layer increased to values as high as

0.06 parts per million. This synoptic meteorological regime favored not only an increase in the background ozone concentration, but also an increase in local photochemical production, as high temperatures, low relative humidity, and low wind speeds often accompany large-scale subsidence. When these conditions persisted for periods exceeding one week with the onset of Rossby wave ridging, the combination of very high background concentrations and ideal photochemical production in the boundary layer resulted in the most severe ozone pollution episodes observed during the research study.

As upper-level troughs progressed toward the study location, a marked decrease in background ozone concentrations was observed. Specifically, large-scale mass divergence downstream from the axes of approaching troughs resulted in a broad region of tropospheric ascent, leading to a decrease in the background ozone concentration measured at 210 meters. Under this synoptic meteorological regime, minimum (background) ozone concentrations measured at 210 meters were recorded. The lift associated with large-scale mass divergence in the upper troposphere promoted increasing wind speed, moisture advection, and cloud formation. Thus, local photochemical production was limited, and in conjunction with the relatively low background concentrations that were observed, total boundary-layer ozone concentrations remained low during upper-level trough passages.

Although the highest degree of correlation between 210-meter ozone and 300 hPa geopotential heights was observed with a small lag, the coefficient of determination did not exceed 0.40. Interference resulting from the imperfect fit between static upper-level

meteorological sounding data and a dynamic polar jet stream likely limited the degree of correlation, as no continuous, direct measure of jet stream heights is available. Nonetheless, the statistical correlation between 210-meter ozone and 300 hPa geopotential heights clearly improved with 300 hPa constant pressure surface heights in close proximity to the mean position of the polar jet stream. Visual inspection of the preceding figures (particularly Figure 9.38) indicates that 210-meter ozone maxima corresponded to 300 hPa height maxima, and likewise, 210-meter ozone minima corresponded to 300 hPa height minima. Furthermore, the amplitudes of both the 210-meter concentrations and the 300 hPa geopotential heights increased with the influence of the proximal polar jet stream toward the end of the research study. Therefore, the selection of data from the Aberdeen, South Dakota upper-air sounding site proved to be advantageous, as it was close enough to the mean position of the polar jet stream to improve the correlation between 210-meter ozone and 300 hPa geopotential heights when compared with sites closer to the equator.

An illustration of the dynamic relationship between residual ozone concentrations at 210 meters and the global atmospheric circulation is evident in the research data spanning the two-week period beginning on 18 July 2005 and ending on 27 July 2005. During this interval, a peak in background ozone concentrations and 300 hPa heights that occurred on 25 July was bound by relative background O₃ and 300 hPa geopotential height minimums indicative of trough passages on 18 July and 27 July, respectively (Figure 9.40).

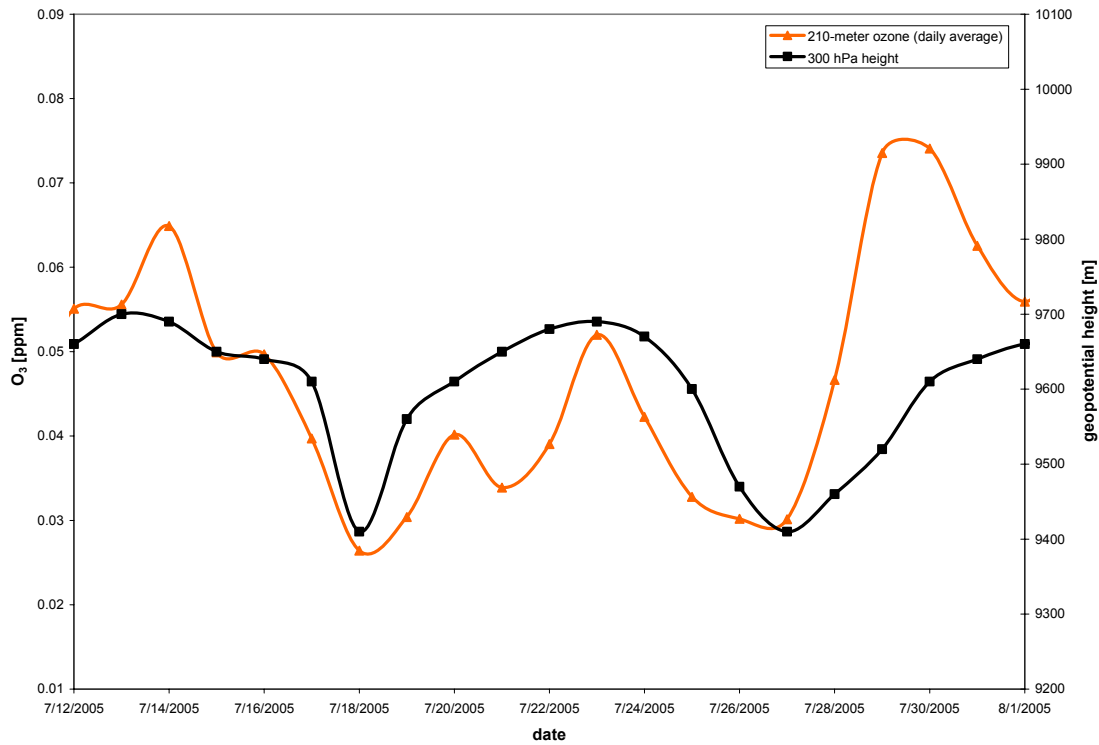


FIGURE 9.40: Boundary-layer ozone concentrations measured in Tulsa, Oklahoma (36°N) compared with 300 hPa geopotential heights measured in Aberdeen, South Dakota (46°N) for the period beginning on 18 July 2005 and ending on 27 July 2005

Inspection of Northern Hemisphere 300 hPa constant pressure analyses indicates that the observed 210-meter residual O₃ minimum on 18 July coincided with the passage of an upper-level trough through central portions of North America, thereby dampening the influence of a subtropical anti-cyclone centered at 30°N (Figure 9.41).

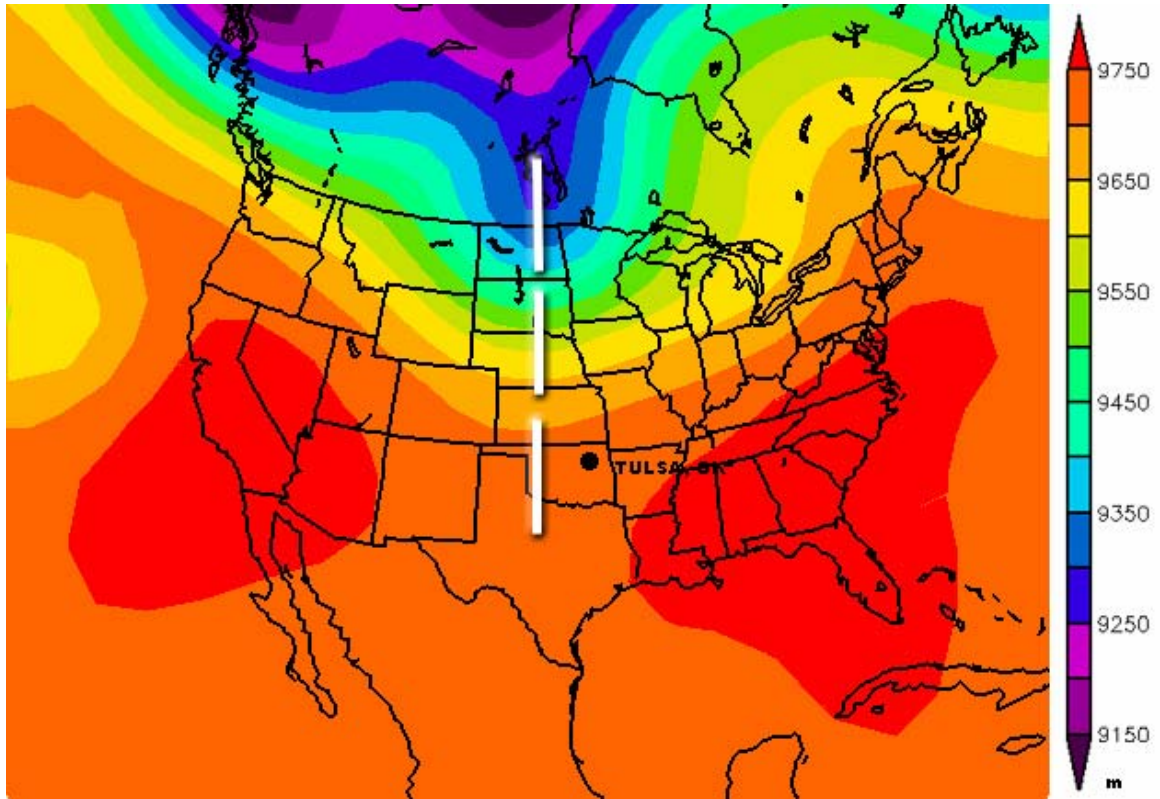


FIGURE 9.41: 300 hPa geopotential height analysis, 18 July 2005 (NOAA, 2006)

Once the upper-level trough shifted into eastern Canada by 23 July, the polar jet stream again migrated northward, and the 30°N subtropical anti-cyclone expanded across the interior U.S., with the 300 hPa 9690-meter geopotential height contour surging as far north as 46°N (Figure 9.42). Background ozone concentrations subsequently peaked in response to the onset of tropospheric subsidence.

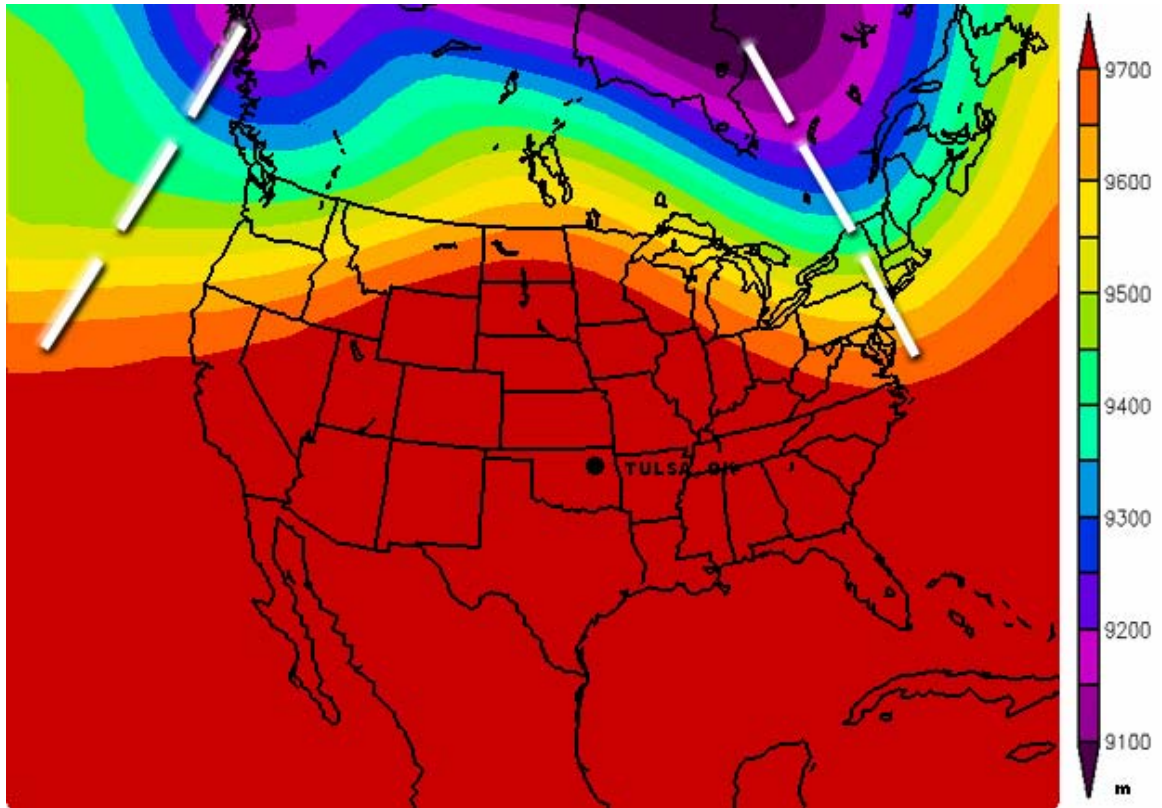


FIGURE 9.42: 300 hPa geopotential height analysis, 23 July 2005 (NOAA, 2006)

By 27 July, another upper-level trough propagated eastward across North America, again muting the strength and aerial coverage of the 30°N subtropical anti-cyclone. The polar jet stream shifted southward, with the 300 hPa 9600-meter geopotential height contour extending into northern Kansas (Figure 9.43). As expected, background ozone concentrations minimized with the passage of the atmospheric disturbance.

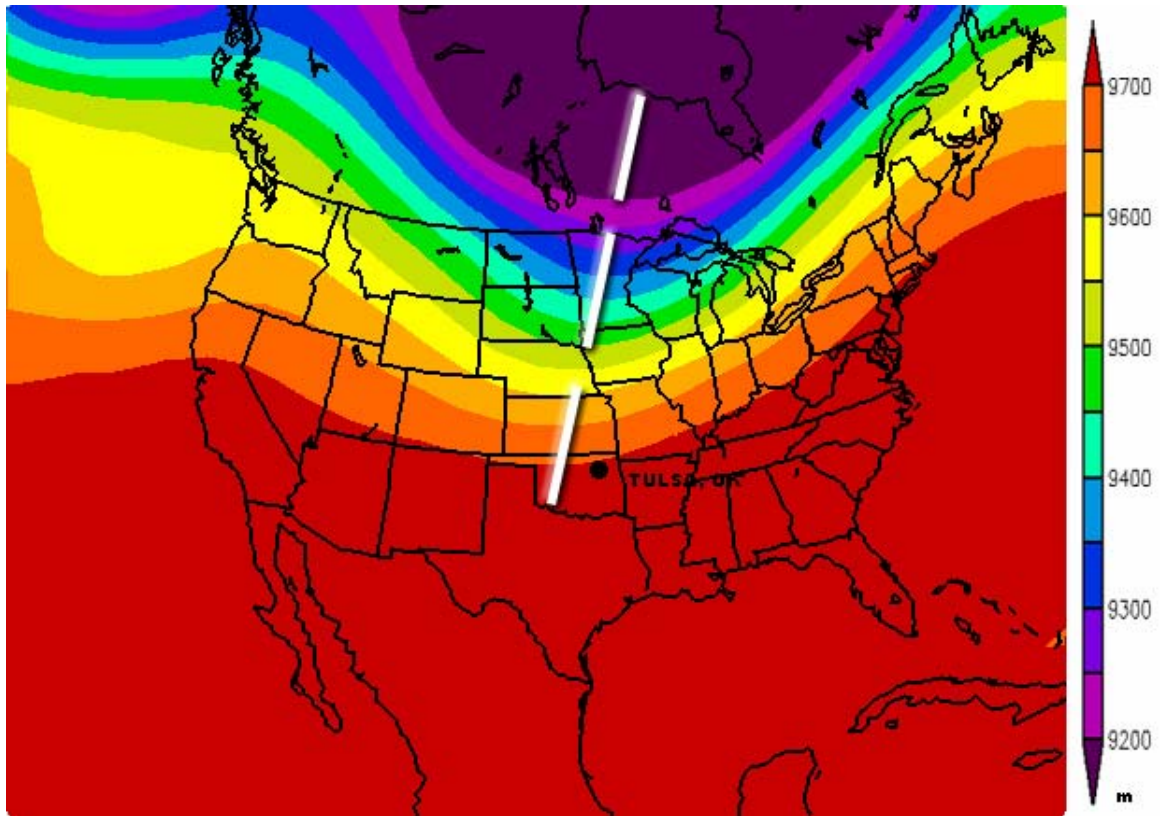


FIGURE 9.43: 300 hPa geopotential height analysis, 27 July 2005 (NOAA, 2006)

Although 18 July 2005 – 27 July 2005 exemplifies the relationship between background ozone concentrations and 300 hPa geopotential heights, many paired fluctuations between 300 hPa geopotential heights and the 210-meter O₃ concentration were present in the 2005 research data record, particularly during the fall months with the seasonal shift of the polar jet stream toward the equator.

9.4. Horizontal Transport

Two modes of possible horizontal ozone transport must be considered: the lateral movement of local ozone plumes as a result of ground-level winds, and the transfer of local ozone in the nocturnal low-level jet.

9.4.1. Local Surface Winds

Assessment of the magnitude and spatial extent of ground-level horizontal ozone transport in the region of the research study was achieved by comparing 1-hour ozone concentrations in the Dallas – Fort Worth, Texas metropolitan area with corresponding ozone concentrations in southern Oklahoma. Specifically, two monitoring sites in the greater Dallas – Fort Worth area, Denton and Midlothian, were considered, as well as the Burneyville site in southern Oklahoma (Figure 9.44). Denton and Midlothian were advantageous site selections due to their locations on the north and south sides of the Dallas-Fort Worth metropolitan area, respectively. Burneyville, located approximately 80 km north of Denton and 130 km north of Dallas – Fort Worth, is close enough to experience same day ozone transport from the metropolitan area of 5.5 million persons when southerly winds are present.

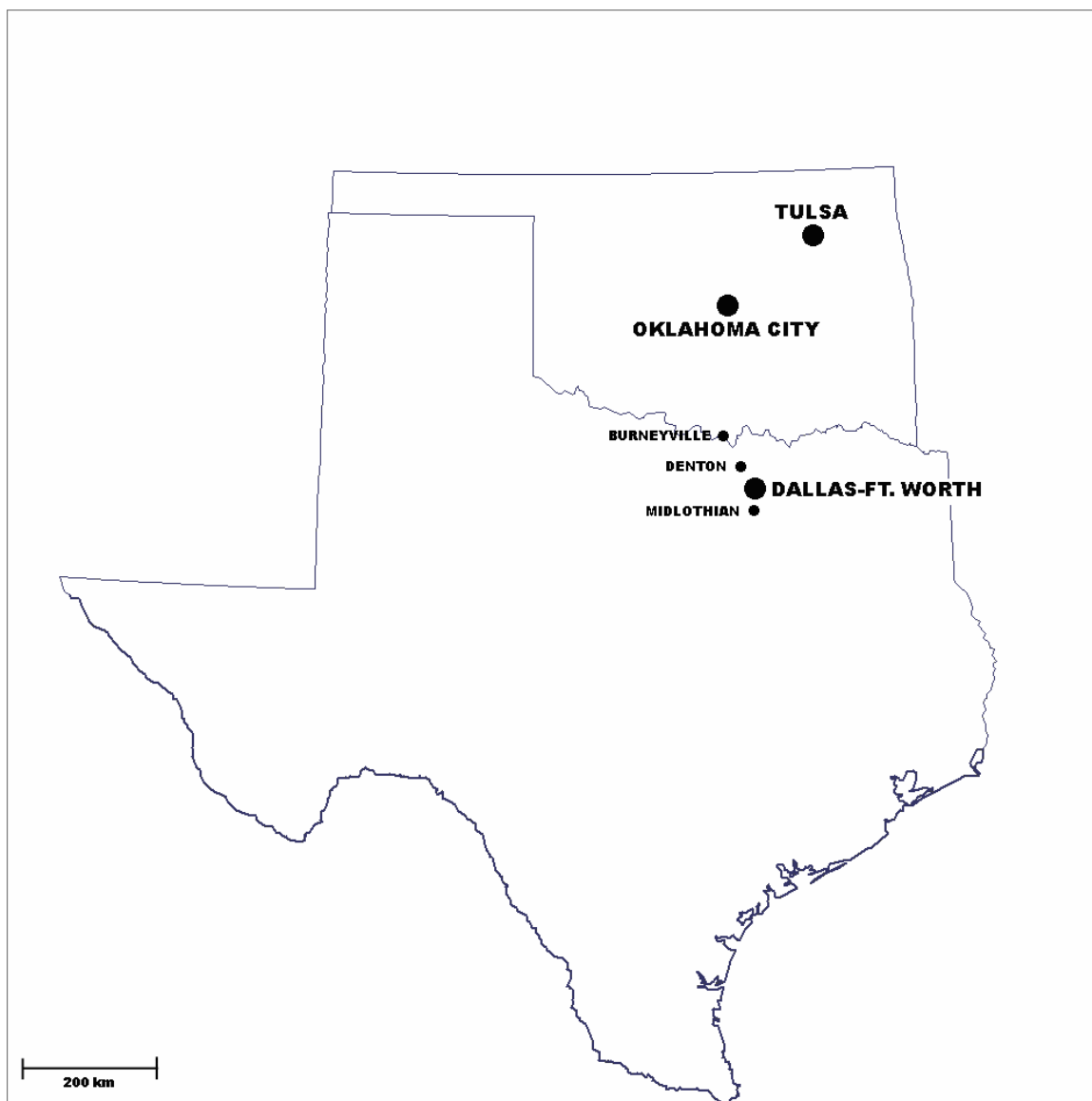


FIGURE 9.44: Location of Burneyville, Oklahoma in relation to the Dallas – Fort Worth, Texas metropolitan area

Monitoring was operational at Burneyville during the 1999 and 2000 ozone seasons, and days on which the following criteria were met were included in the analysis: 1) Burneyville must have a 1-hour O_3 concentration ≥ 0.075 ppm; 2) Denton must have a 1-hour O_3 concentration ≥ 0.075 ppm; and 3) the average daily surface wind direction at

Burneyville must contain a southerly component. As a result, 22 days met the established criteria in 1999, and 35 days qualified in 2000. Statistically, the selected days accounted for 55% of the total days that O₃ concentrations of 0.075 ppm were reached or exceeded in Burneyville in 1999, and 81% of the total days that O₃ concentrations reached or exceeded 0.075 ppm in Burneyville in 2000. Midlothian equaled or exceeded O₃ concentrations of 0.075 ppm on 12 of the selected days in 1999 and 23 of the selected days in 2000.

Burneyville recorded O₃ concentrations \geq 0.075 ppm with the presence of southerly average daily wind directions on 25 days in 1999. Denton recorded O₃ concentrations \geq 0.075 ppm with the presence of southerly average daily wind directions on 22 days in 1999, or 88% of the time that Burneyville did. Midlothian only recorded O₃ concentrations \geq 0.075 ppm with the presence of southerly average daily wind directions on 12 days in 1999, 48% of the time that Burneyville did. In 2000, Burneyville recorded O₃ concentrations \geq 0.075 ppm with the presence of southerly average daily wind directions on 37 days. Denton recorded O₃ concentrations \geq 0.075 ppm with the presence of southerly average daily wind directions on 35 days, 95% of the time that Burneyville did. Again, Midlothian recorded fewer O₃ concentrations \geq 0.075 ppm than the other sites in the presence of southerly average daily wind directions on 23 days, 62% of the time that Burneyville did. Regression analysis for the 1999 and 2000 ozone seasons shows a strong correlation between ground-level O₃ concentrations in Denton and Burneyville (Figure 9.45).

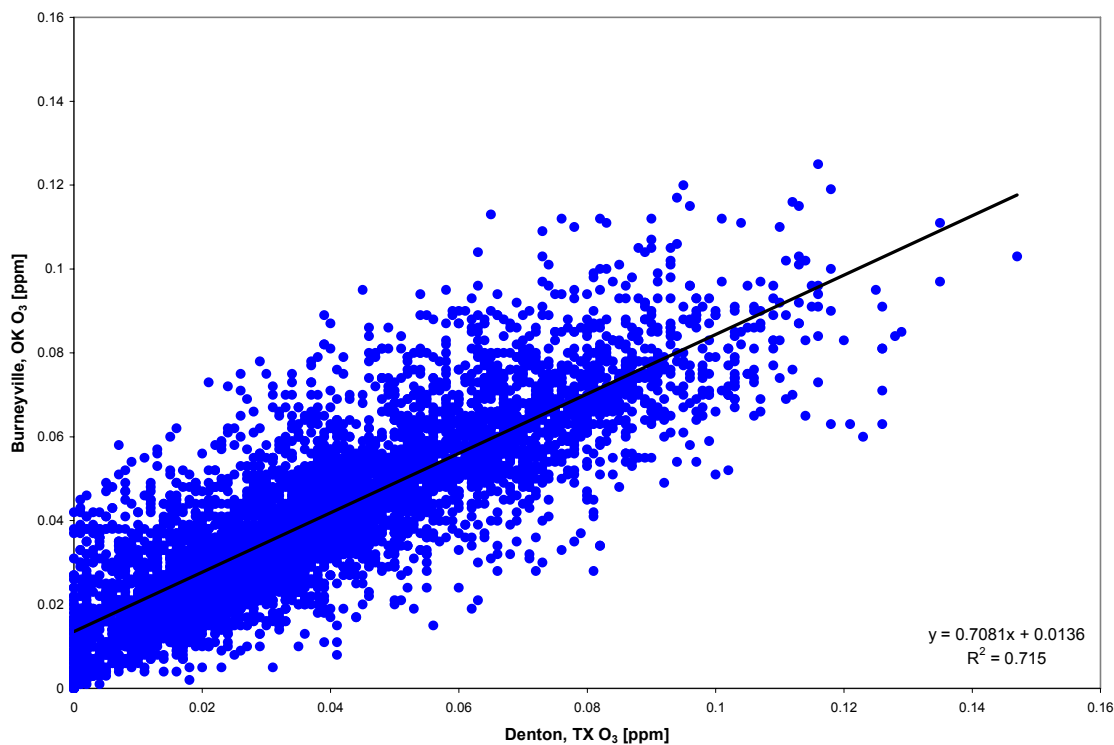


FIGURE 9.45: Correlation between ozone concentrations at Burneyville, Oklahoma and Denton, Texas during the 1999 and 2000 O₃ seasons

A gauge of transport is the time characteristic of peak ozone concentration in Burneyville. Normally, locally generated ground-level ozone peaks in the early to mid-afternoon, when solar radiation is most intense (Solomon et al., 2000). However, O₃ tended to peak at the Burneyville monitoring station late in the day, indicative of surface transport. Accordingly, a seasonal “latency” histogram has been developed to analyze the average daily ozone concentrations at Burneyville and Denton. This technique plots the frequency of ozone levels ≥ 0.075 ppm as a function of the 1-hour intervals in which ozone was recorded. Furthermore, only days in which the aforementioned analysis criteria (southerly winds, O₃ ≥ 0.075 ppm at Burneyville and Denton) were considered.

Data from 1999 and 2000 clearly demonstrate that latency exists between O₃ concentrations in Denton and Burneyville. The 1999 latency histogram comparing Burneyville and Denton indicates that the entire O₃ production process occurs earlier in the day at Denton than at Denton than at Burneyville (Figure 9.46). At Denton, ozone, on average, peaked during the early to mid-afternoon, with the 14:00 CST one-hour interval occurring most frequently. Conversely, the most frequent one-hour interval for peak ozone concentrations at Burneyville was 17:00 CST.

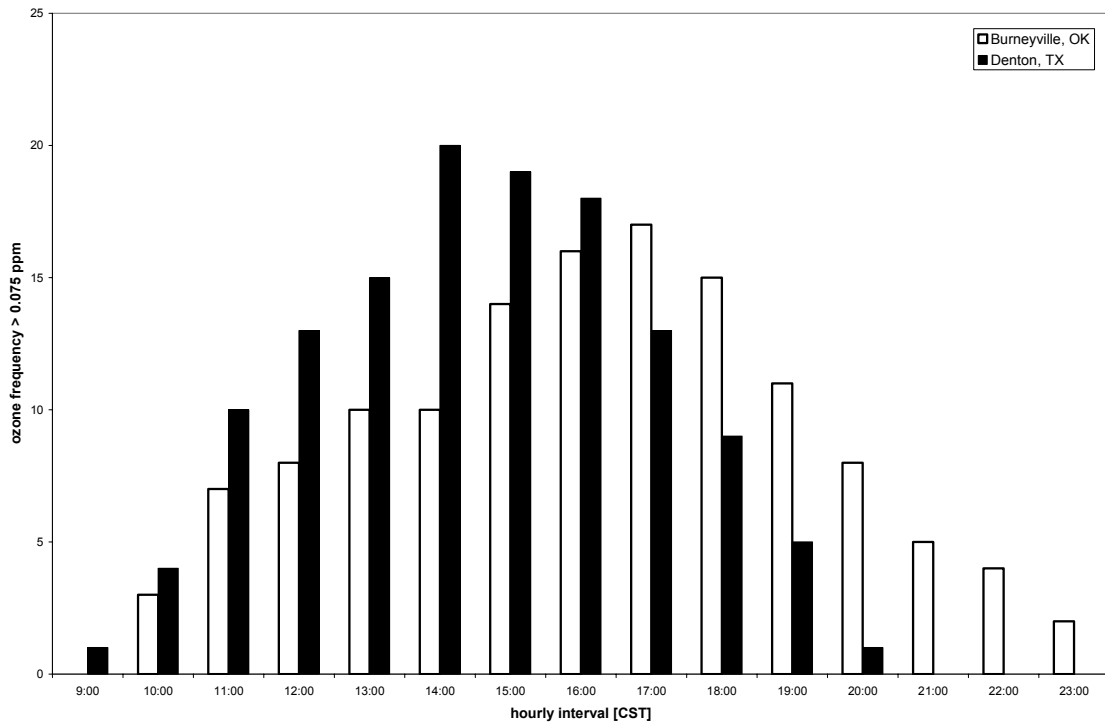


FIGURE 9.46: Latency between peak ozone concentrations at Burneyville, Oklahoma and Denton, Texas during the 1999 O₃ season

The latency histogram comparing Burneyville and Denton during the 2000 ozone season also indicates that the O₃ production process occurs earlier in day at Denton than at

Burneyville (Figure 9.47). At Denton, ozone, on average, peaked during the early to mid-afternoon, with the 14:00 CST – 16:00 CST interval occurring most frequently. The most frequent one-hour interval at Burneyville was 18:00 CST.

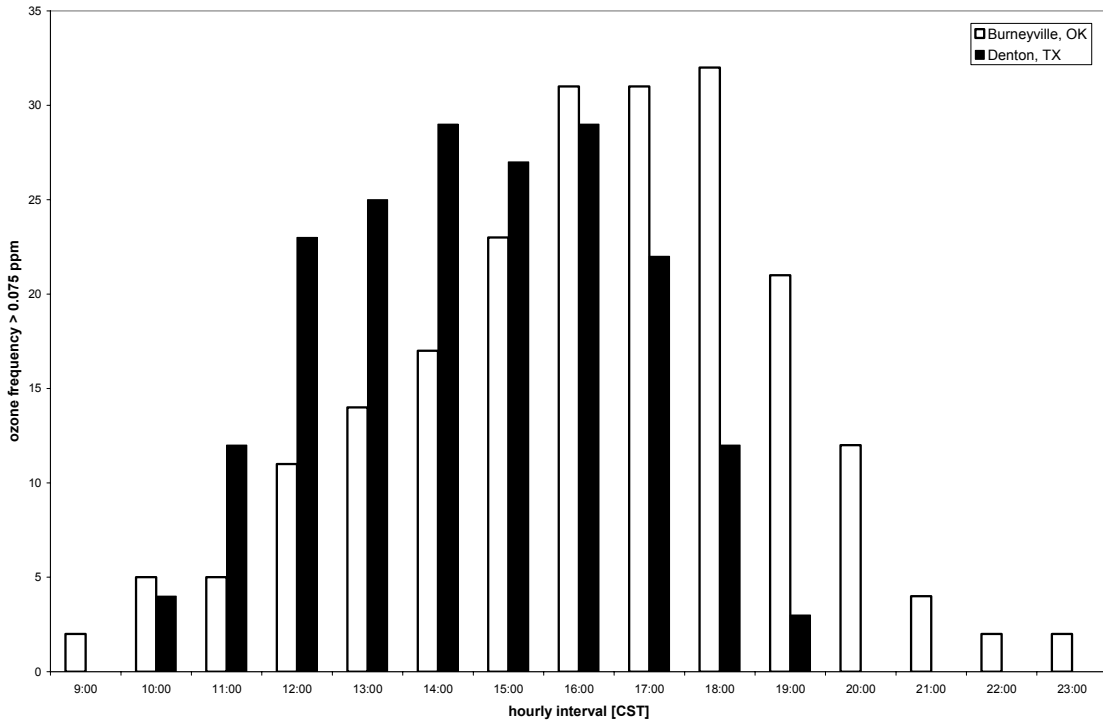


FIGURE 9.47: Latency between peak ozone concentrations at Burneyville, Oklahoma and Denton, Texas during the 2000 O₃ season

In addition to the lag time in O₃ peaks at Denton and Burneyville during the 1999 and 2000 ozone seasons, the latency histograms indicate that ozone concentrations peak at Denton earlier in the day than at Burneyville. O₃ concentrations peak at Denton following the morning rush hour, typical of local production. At Burneyville, however, O₃ peaks four hours later as southerly surface winds transport ozone and precursor

compounds northward. Late evening peaks, 21:00 CST to 00:00 CST, never occurred at Denton, but were observed several times at Burneyville.

While ozone transported in ground-level winds from Dallas – Fort Worth clearly impacts sites in southern Oklahoma on the order of 100 km to the north, does it significantly impact ozone concentrations in Tulsa? Ground-level wind vectors cannot account for 12-hour transport of ozone on a scale of 400 km, as sustained winds of $10 \text{ m}\cdot\text{s}^{-1}$ for long periods of time were not realized during the 1999-2000 research study, nor were they realized during the 2005 research study. Since ozone and precursor compounds are affected by surface depositional processes, the nocturnal low-level jet appears to be the most promising mechanism for transport occurring over a horizontal distance of 400 km.

9.4.2. Nocturnal Low-Level Jet

The impacts that the nocturnal low-level jet have on the residual ozone concentration at 210 meters were analyzed by determining the frequency of low-level jet occurrence and by assessing the strength of the low-level jet during the days on which its presence was detectable at the study location. Evidence of the nocturnal low-level jet was gathered from the Haskell, Oklahoma NOAA wind profiler site, where ultrasonically-derived wind speeds and directions are measured and recorded in one-hour averages. Overall, a nocturnal low-level jet was observed on 78 of 183 days included in the research study. The mean nocturnal low-level jet direction of origin was $198.96^\circ \pm 30.62^\circ$, and the mean wind speed was $18.21 \text{ m}\cdot\text{s}^{-1} \pm 5.14 \text{ m}\cdot\text{s}^{-1}$. From this information, magnitudes of the

nocturnal low-level jet were quantified according to the conditions set forth in Section 4.2, with Bonner's type 1, 2, and 3 classes hereafter defined as "weak," "moderate," and "strong" nocturnal low-level jets, respectively.

Weak nocturnal low-level jets constituted 32 of the 78 instances of the low-level jet during the study period, or 41.03% of the total. The mean direction of origin was $190.56^\circ \pm 38.07^\circ$, and the mean height above ground-level was $750 \text{ m} \pm 81.72 \text{ m}$, with an average low-level jet height of 500 meters occurring 61.11% of the time.

Moderate and strong nocturnal low-level jets were also an appreciable component of the total, as they were observed on 23 of the 78 known low-level jet episodes during the study. The mean direction of the moderate low-level jet was $199.61^\circ \pm 24.92^\circ$, while the mean direction of the strong low-level jet was $210.00^\circ \pm 19.71^\circ$. The mean height of the moderate nocturnal low-level jet was $597.82 \text{ m} \pm 235.24 \text{ m}$, and the jet core was observed at an elevation of 500 meters above ground-level 78.26% of the time. Strong nocturnal low-level jets tended to occur at slightly higher elevations, with a mean of $869.57 \text{ m} \pm 327.43 \text{ m}$. Statistics for weak, moderate, and strong nocturnal low-level jets are summarized in Table 9.6.

TABLE 9.6: Nocturnal low-level jet statistics, Haskell, Oklahoma, 01 Jun 2005 – 30 Nov 2005

Type	Interval (m·s ⁻¹)	n	Mean Dir. (°)	σ (°)	Mean Ht. (m)	σ (m)
1	12 ≤ x < 16	32	190.6	38.1	750.0	81.7
2	16 ≤ x < 20	23	199.6	24.9	597.8	235.2
3	20 ≤ x	23	210.0	19.7	869.6	327.4

Although nocturnal low-level jets were present on nearly 50% of the days included in the research study, they were less likely to occur during the months in which average ozone concentrations reach peak levels. Instead, low-level jets were more frequent in early June and again in October and November, coinciding with the approach of the upper-level polar jet stream (Table 9.7). When the polar jet and attendant atmospheric disturbances traverse the middle latitudes of the North American continent, geostrophic balance in the general atmospheric circulation is maintained by a decrease in tropospheric pressure along the lee side of the Rocky Mountains as the polar jet sinks and deflects to the right. This process, known as lee cyclogenesis, enhances the strength of the nocturnal low-level jet. Thus, the frequency of the nocturnal low-level jet decreased at the study location during the summer months as the polar jet stream shifted toward the north.

TABLE 9.7: Comparison of nocturnal low-level jet frequency and magnitude at Haskell, Oklahoma between July 2005 and November 2005

	n	Class 1 (%)	Class 2 (%)	Class 3 (%)
July	10	70	10	20
November	16	6	13	81

Therefore, it appears that the nocturnal low-level jet is not a major factor in the seasonally high O₃ concentrations at the study location, as the low-level jet is infrequent when consistently high ozone concentrations are most prevalent. It is known from observation, however, that winds with a southerly component are common at the study location, even if the definition of a low-level jet is not met. Since winds originated from 202.5° ± 22.5° more than 60% of the time at 210 meters, it is reasonable to assume that the residual ozone at this height constituting the background ozone concentration possibly originated from the same direction.

The most significant source that falls within 202.5° ± 22.5° of the study location is the Dallas – Fort Worth metropolitan area. Previous research found a strong correlation between ozone concentrations in Dallas – Fort Worth and Oklahoma City (Kastner-Klein et al., 2002). At a distance of approximately 350 km from the study location, ozone transport could occur within 12 hours if wind speeds were maintained at 10 m·s⁻¹.

Calculations from a simple Gaussian dispersion model indicate that at a distance of approximately 400 km, representative of the transport vector between Tulsa and Dallas – Fort Worth, the centerline concentration of O₃ would be negligible. This approach requires many assumptions, including the classification of ozone as a steady-state, non-reactive pollutant, but even so, the result suggests that a metropolitan source area at considerable distance cannot account for the observed background ozone concentration.

$$C = \frac{Q}{2\pi u \sigma_y \sigma_z} \exp\left(-\frac{1}{2} \frac{y^2}{\sigma_y^2}\right) \left\{ \left[-\frac{1}{2} \frac{(z-H)^2}{\sigma_z^2} \right] + \exp\left[-\frac{1}{2} \frac{(z+H)^2}{\sigma_z^2} \right] \right\} \quad (9.1)$$

Concentration (C) in the Gaussian dispersion equation is calculated as $\mu\text{g}\cdot\text{m}^{-3}$. Additional components of the equation include the horizontal and vertical dispersion parameters, σ_y and σ_z , which are functions of boundary-layer stability and distance from the source, the emissions rate Q (expressed as $\mu\text{g}\cdot\text{s}^{-1}$), the effective stack height H (210 meters), the average wind speed (u) at H (in $\text{m}\cdot\text{s}^{-1}$), and the horizontal and vertical deviations from the centerline, y and z (also expressed in meters). This calculation was performed with NOAA HYSPLIT, a Lagrangian trajectory model that ingests actual meteorological data and computes Gaussian dispersion downwind from the source (NOAA, 2007). When plume concentrations were calculated using the NOAA HYSPLIT dispersion model, even the worst-case O_3 pollution scenarios resulted in a minimal contribution of ozone in Tulsa from the Dallas – Fort Worth metropolitan area. In fact, concentrations were orders of magnitudes lower at the end point than they were at the source.

The NOAA HYSPLIT model was run over a continuous period of 24 hours. Actual meteorological data were input over the duration of the model simulation – 18:00 CST on 02 November 2005 through 18:00 CST on 03 November 2005. This date was selected because it offered a representative sample of a strong nocturnal low-level jet (Figure 9.48).

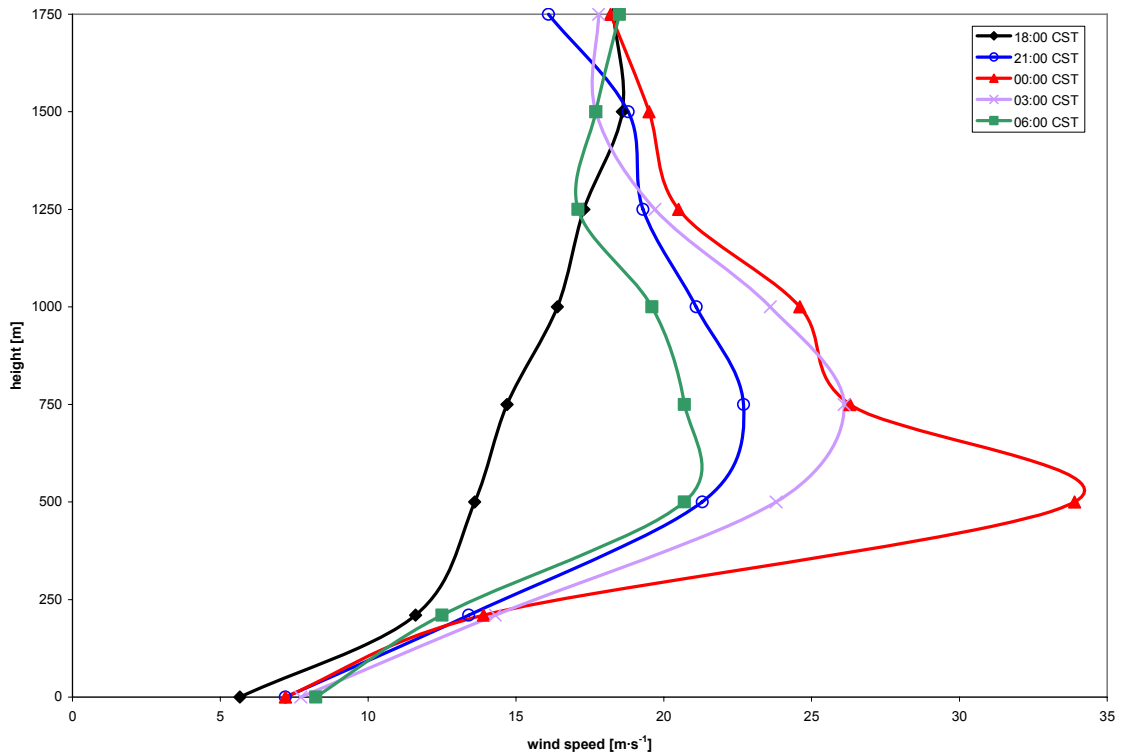


FIGURE 9.48: Evolution of the nocturnal low-level jet in the Tulsa metropolitan area, 18:00 CST, 02 November 2005 – 06:00 CST, 03 November 2005

Emission rates were set at $20 \times 10^{12} \mu\text{g}\cdot\text{hr}^{-1}$, equivalent to a 10 km x 10 km x 0.2 km box with an average, steady-state O_3 concentration of $250 \mu\text{g}\cdot\text{m}^{-3}$, or roughly 0.12 ppm. While the dimensions of the box are smaller than the aerial footprint of Dallas – Fort Worth, several model runs were attempted in order to fit expected concentrations close to the source. When a larger mass flow rate was used, unrealistic concentrations were observed downwind, and smaller mass flow rates also resulted in unrealistic downwind conditions.

Modeled plumes at the continuous $20 \times 10^{12} \mu\text{g}\cdot\text{hr}^{-1}$ emission rate in the Dallas – Fort Worth metropolitan area yielded O_3 concentrations varying between $60 \mu\text{g}\cdot\text{m}^{-3}$ (0.028 ppm) and $550 \mu\text{g}\cdot\text{m}^{-3}$ (0.256 ppm) immediately downwind from the source. However, transported O_3 concentrations of no larger than $10 \mu\text{g}\cdot\text{m}^{-3}$ (0.005 ppm) were calculated at a distance of 400 km to the north in the Tulsa metropolitan area (Figure 9.49).

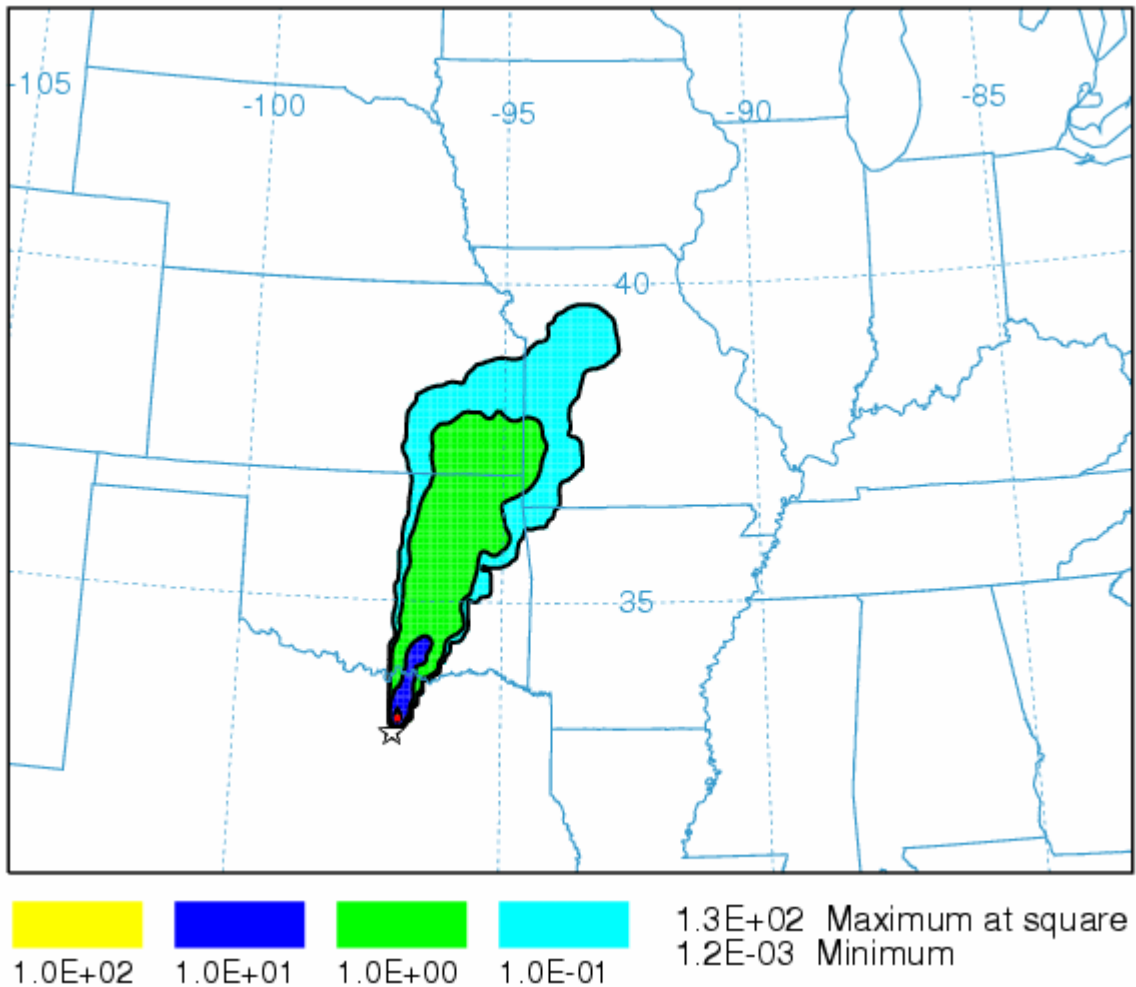


FIGURE 9.49: 12-hour NOAA HYSPLIT steady-state O_3 plume simulation with NCEP GDAS meteorological data at 06:00 CST on 03 November 2005 (concentrations reported in $\mu\text{g}\cdot\text{m}^{-3}$)

Again, emphasis must be placed on the assumptions made in the NOAA HYSPLIT model simulation. No depositional processes or reactions were considered, effectively classifying the transported O₃ as steady state. While ozone behaves in a steady-state manner above ground level where it is largely free from depositional processes and reactions, some deposition will nonetheless occur, resulting in a lower concentration at the terminus. Also, the difficulty in constructing a three-dimensional domain on a metropolitan scale was highlighted by the necessity for a surface footprint (100 km²) much smaller than the actual footprint of Dallas – Fort Worth (~ 2500 km²). Otherwise, the modeled O₃ concentrations in close proximity to the source were unrealistic. Even with the pronounced limitations of using this type of modeling scheme to predict the long-range transport of ozone, it can still be inferred that O₃ concentrations transported at a distance of 400 km are orders of magnitude lower than at the source. Furthermore, meso-scale meteorological conditions supporting the transport of O₃ over long distances are the exception, not the rule. Thus, the availability of locally-produced ozone for distant transport is limited from any single source.

10. SUMMARY AND CONCLUSIONS

Tulsa, Oklahoma and similarly-sized cities in the mid-latitudes have long been plagued by episodes of ozone air pollution. Beginning in the 1970s, when the United States Environmental Protection Agency established a one-hour O₃ concentration standard, ozone has been at the forefront of local, state and federal air quality regulations, continuing with the current transition to a new, stricter eight-hour standard. Health and economic implications arising from “non-attainment” are profound, and this study therefore sought to investigate local ozone concentrations during the summer and fall months of 2005 with the intent of determining the relative contributions of locally photochemically produced and distantly transported ozone, respectively, which could then be compared with meteorological processes of varying scale in an effort to improve air pollution forecasting.

10.1. Background Ozone in the Troposphere

In order to assess the impact that transport had on local ozone concentrations, it was necessary to measure O₃ in a vertical configuration within the atmospheric boundary layer so that locally produced ozone could effectively be filtered from the data set. Thus, ozone concentrations were recorded on the roof of the Bank of Oklahoma Tower in downtown Tulsa at an elevation of 210 meters and compared with data from a ground-

level control site operated by the Oklahoma Department of Environmental Quality located nearby. Selection of the 210-meter level for ozone measurement proved to be advantageous for several reasons. Not only did the 210-meter data provide a basis for establishment of the background ozone concentration at the study location, but it also provided significant insight into the dynamic behavior of residual ozone while allowing for a comparison between meteorological processes in the troposphere and ozone concentrations in the boundary layer.

This 6-month study indicated that ozone concentrations in the atmospheric boundary layer are influenced by large-scale subsidence in the troposphere. Nocturnal concentrations at 210 meters effectively constituted the background, or residual level of ozone, indicative of transient O₃ reservoirs within the troposphere. Thus, ozone at ground level is not solely a product of local photochemistry, but instead is a combination of local sources and large-scale vertical transport. The background ozone concentration was clearly observed in the 210-meter data, as the nocturnal minimum ranged between 0.02 and 0.06 parts per million over the course of the study. Conversely, ozone concentrations at ground level were strongly diurnal, approaching 0 parts per million during the overnight hours.

What can be gained by establishing the background ozone concentration in Tulsa? By understanding the relationship between locally produced ozone and transported ozone, mitigation strategies can be focused. Local production only appears to account for 25-50% of the total local ozone concentration, with the highest concentrations observed

during meteorological conditions that favor optimal photochemical production. Control strategies therefore must also account for episodes that cause increases in the background ozone concentration, as these episodes were commonly observed in conjunction with high ground-level readings.

When considered over the course of the six-month study, background concentrations exhibited a sinusoidal pattern characterized by a series of large-scale maxima and minima with varying frequency and amplitude. If the residual concentration were solely a function of incoming solar radiation, then it should peak in conjunction with the summer solstice and decrease thereafter, coinciding with the axial tilt of the Earth. As the data indicated, however, this was not the case.

Instead, two aspects of the 210-meter ozone measurements contradict the notion that concentrations in the troposphere behave according to the amount of solar radiation received in the troposphere. First, the highest ozone concentrations recorded at the Tulsa study location occurred during August and September, two months after the summer solstice. Thus, an appreciable lag existed between the two. Explanation of the underlying processes responsible for this discrepancy lies in the second signal observed in the 210-meter data set – the aforementioned sinusoidal behavior of O₃ during the study. Specifically, the passage of atmospheric waves dictated the favorability, or lack thereof, of meteorological conditions in the troposphere for increased background concentrations. Variation in the six-month trace of 210-meter ozone concentrations mirrored the passages of atmospheric waves, with residual O₃ maxima aligning with

pressure ridge axes and O₃ minima aligning with pressure trough axes, respectively. Inspection revealed that pressure trough passages were usually of short duration, characteristic of baroclinic “short” waves progressing along the polar jet stream, while influences from pressure ridges were generally of longer duration, as the general circulation of the troposphere at the study location was characterized by baroclinic waves and by large-scale, slow-moving Rossby waves over the course of the experiment.

With the approach of baroclinic and Rossby wave ridges, not only did large-scale subsidence lead to an increase in O₃ concentrations in the atmospheric boundary layer, but an enhancement of local photochemistry occurred as well, as low wind speeds, low relative humidity, and increased solar radiation and air temperature – all characteristics of anti-cyclonic flow regimes – contributed to high ozone concentrations at ground level. Therefore, anti-cyclones provide an optimal scenario for high boundary-layer ozone concentrations, particularly during the summer months. Not only was ozone transported downward in subsiding flow, but photochemical production was maximized as well. This combination of factors explains why high background and locally photochemically produced O₃ concentrations typically coincide with one another, resulting in severe air pollution episodes. The effects that anti-cyclones and related weather patterns have on boundary-layer ozone concentrations were observed during the fall months as well, although muted. Not only did a seasonal shift in Earth’s axial tilt result in less incoming solar radiation when compared with the summer months, but Rossby wave ridging was less pronounced during the fall, and large-scale subsidence was confined to the rapid passages of baroclinic wave ridges.

Even though background ozone concentrations were measured at 210 meters, they nonetheless constituted an important indicator of the actual ground-level concentration (Figure 10.1). While ozone is clearly more diurnal at ground level than at 210 meters, the two levels vigorously mix in the presence of sunlight and the subsequent onset of convective eddies, thus transforming the boundary layer into a uniform reservoir. As a result, background O₃ concentrations are an important component of the daily maximum measured at ground level. However, local meteorological conditions are also important in assessing the potential for air pollution episodes in the boundary layer.

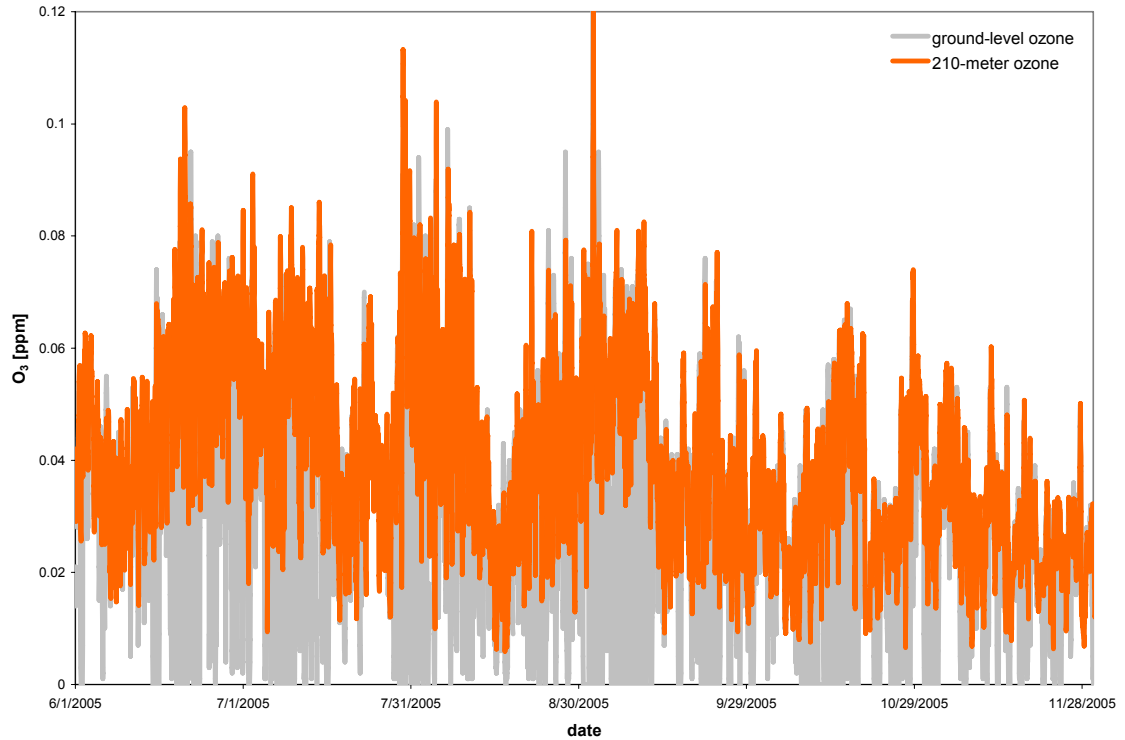


FIGURE 10.1: 210-meter ozone concentrations superimposed on ground-level ozone concentrations, indicating the homogeneity of the boundary layer during the daytime, when maximum concentrations at the two levels are nearly identical; non-overlapping minimum concentrations are indicative of nocturnal measurements when the boundary layer decouples.

10.2. Local Meteorological Variables

Attention was paid to several boundary-layer meteorological variables measured at ground level and at 210 meters. Upon analysis, it was determined that three parameters – ground-level dry-bulb (air) temperature, relative humidity, and wind speed – were by far the most important when predicting the likelihood of high ground-level ozone

concentrations. In fact, a relatively strong correlation existed between ozone and each of these variables. When an arbitrary 1-hour ground level O₃ concentration of 0.08 parts per million was compared with corresponding dry-bulb temperatures, a lower threshold of 27°C was noted as the minimum ambient temperature required for this concentration level. Both relative humidity and ground-level (10-meter) wind speed were negatively correlated with ground level concentrations, as the 0.08 parts per million O₃ level required an upper bound of 50% RH and 5 m·s⁻¹ wind speed, respectively. Furthermore, all three boundary-layer meteorological conditions together were necessary over the course of several consecutive hours in order for the O₃ concentration threshold to be met. Otherwise, ground-level ozone concentrations remained relatively low.

TABLE 10.1: Maximum correlations (as R²) observed between ozone (ground-level, 210 meters) and ground-level meteorological variables

	Dry-Bulb Temp.	RH	Solar Rad.	Wind Spd.
Ground-Level O ₃	0.4897	0.5286	0.6065	0.1121
210-Meter O ₃	0.2592	0.1763	0.2246	0.0191

What does the dependence of local photochemical production on ground-level dry-bulb temperature, relative humidity, and wind speed suggest about the ozone generation process? Several conclusions can be drawn, with each providing a predictive tool in the forecasting of the local concentration potential.

- **Air Temperature**

The necessity of high dry-bulb temperatures ($> 27^{\circ}\text{C}$) for ground-level ozone concentrations in excess of 0.08 parts per million is indicative of a high degree of incoming solar radiation, as strong surface heating results from the uninhibited transfer of energy. In addition, intermediate thermally-driven chemical reactions also benefit from warm temperatures in the lower atmosphere. Finally, strong surface heating also drives vigorous boundary-layer convection, which acts as a positive feedback loop not only by promoting photochemical production, but also by transferring the background ozone concentrations of the free troposphere to ground level.

- **Relative Humidity**

Since relative humidity serves as a proxy for the hydroxyl (OH) radical, the availability of H_2O , observed as an increase in relative humidity, results in an increase in boundary-layer OH. Primary conversion of NO_2 to O_3 sink species is driven through reactions with OH, where HNO_3 is the end product. Therefore, increasing relative humidity limits the potential for high ozone concentrations.

- **Wind Speed**

As with relative humidity, a negative correlation was also observed between ground-level ozone and wind speed. In general, ozone concentrations exceeding the 0.08 parts per million threshold required wind speeds lower than $5 \text{ m}\cdot\text{s}^{-1}$. Why? At higher wind speeds, increased dispersion limited the potential for high ground-level concentrations. In other words, ozone can accumulate in the absence of strong winds, thus maximizing local concentrations. When winds speeds exceed $5 \text{ m}\cdot\text{s}^{-1}$, local reservoirs of high ozone concentrations mix with ozone-deficient air from other regions, lowering the overall concentration.

- **Solar Radiation**

Strong correlation was observed between ground-level ozone and ultraviolet radiation, provided that a sufficient lag existed between the two. The best fit occurred with a lag of 2 hours between the two, accounting for the time between the initial photochemical reactions of precursor compounds and the highest observed concentration of ground-level ozone. Even with a lag, the correlation was poor between 210-meter ozone and solar radiation, again indicating that the background ozone is of an aged, transported origin, thus remaining relatively unaffected by local photochemistry.

Other local meteorological variables, including air pressure, wet-bulb temperature, and dew-point temperature, were of decreased importance to local ozone concentrations when compared with ground-level temperature, wind speed, and relative humidity. At 210 meters, ground-level variables showed poor or no correlation to ozone, regardless of whether it was measured at that elevation or at ground level. Thus, the background ozone concentration appears to be largely unaffected by local, short-term meteorology.

10.3. Horizontal Transport

Based on ground-level data from the Dallas – Fort Worth metropolitan area and an adjacent monitoring station along the Red River in southern Oklahoma, same-day surface transport of ozone was clearly observed during an interval of two consecutive years. Southerly winds were required for transport, and as a result of the 80 km distance between the northern suburbs of Dallas – Fort Worth and the Oklahoma – Texas border, a lag of 3 to 4 hours in the daily maximum ground-level O₃ concentrations was observed between the two points.

While transport was appreciable over a distance of 80 km, no significant transport was calculated over a span of 400 km, roughly the distance between the Dallas – Fort Worth metropolitan area and the Tulsa metropolitan area. If transport were to occur over this distance in a timely manner, the nocturnal low-level jet appeared to be the most likely mechanism. However, the generation of an ozone plume in a modified Gaussian dispersion calculation revealed that even with high ozone concentrations originating in

Dallas – Fort Worth and subsequent northward transport in a strong low-level jet, only minimal contributions (< 0.005 ppm) could be expected in Tulsa. Therefore, horizontal ozone transport appears to be largely confined to distances of much less than 400 km, as dispersion and deposition dominate over long pathways.

10.4. Implications Resulting from Climate Change

What implications does a changing global climate hold for the long-term trends in ground-level ozone concentrations in the middle latitudes? Massive amounts of climate-altering “greenhouse” gases have been directly and indirectly released into Earth’s atmosphere since the dawn of the Industrial Revolution. In particular, atmospheric carbon dioxide (CO₂) concentrations have increased by nearly 100 ppm to a current level of 379 ppm, higher than any concentrations preserved in ice core records from the past 650,000 years (IPCC, 2007). Current predictions call for a global mean temperature increase of 2.0-4.5°C over the next century, and this estimate has recently been reaffirmed by the Intergovernmental Panel on Climate Change (IPCC, 2007). Much attention has been given to the threat that sea-level rise poses to coastal cities, but the potential for a major shift in global weather patterns will exist as well.

Specifically, an increase in global mean temperature threatens the hemispheric balance between polar and subtropical air masses, marked by the polar jet stream and accompanying polar front. If the loss of the polar ice cap is realized, then the Arctic mean temperature will increase more significantly than the global mean, perhaps by as

much as a factor of ten. In the event that drastic Arctic warming occurs, a possible outcome is a northward progression of the polar jet stream in an effort to maintain temperature equilibrium. Thus, the mean track of atmospheric waves in the Northern Hemisphere could shift poleward as well, resulting in a more permanent regime of subtropical anti-cyclones in the mid-latitudes. A recent report by Fu et al. (2006) noted that a poleward shift of the polar jet stream has been observed in the Northern Hemisphere. When tropospheric re-analyses of the mean position of the polar jet were constructed for the period spanning from 1979 through 1997, a poleward shift of 1° latitude was discovered (Fu et al., 2006). Since high ozone concentrations are favored in regions of broad-scale anti-cyclonic circulation, ozone pollution episodes of increased magnitude and duration must be considered as a consequence of climate change.

Not only are the large urban centers of Mexico City, Dallas-Ft. Worth, Houston, and Los Angeles major sources of ozone precursor compounds, but they are also located within the belt of semi-permanent subtropical high-pressure systems in the Northern Hemisphere, and it is therefore no coincidence that these mega-cities regularly experience severe ozone pollution episodes. If subtropical high pressure systems migrate poleward in response to a northward shift of the polar jet stream, large metropolitan areas in more northern latitudes may experience decreasing air quality as well. After all, many of the major cities in the United States, including New York and Chicago, are located near the 40th parallel, and most of Europe's population centers are north of the subtropics.

In the event that the mean positions of subtropical anti-cyclones shift poleward, profound climate consequences will arise even if the encroachment is only a few degrees of latitude. The combination of favorable meteorological conditions for high background and local photochemical concentrations combined with the presence of a high human population density in the mid-latitudes (including most major U.S. cities) will result in a long-term increase in tropospheric ozone pollution. As a greenhouse gas, ozone in the troposphere has a relatively high radiative forcing range of $0.25\text{-}0.65 \text{ W}\cdot\text{m}^{-2}$, which directly corresponds to a net temperature increase in the lower atmosphere (Figure 10.2) (IPCC, 2007). While these values are lower than the radiative forcing imparted by CO_2 emissions ($1.49\text{-}1.83 \text{ W}\cdot\text{m}^{-2}$), they nevertheless highlight the contributory effect that increasing concentrations of background ozone in the troposphere will have on climate change.

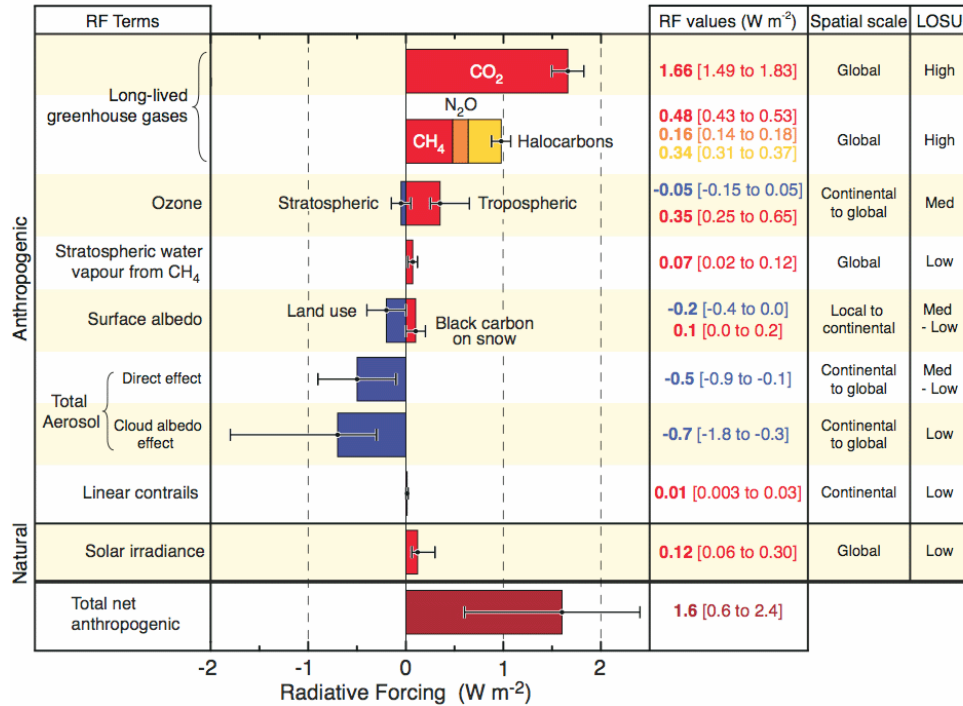


FIGURE 10.2: Positive and negative radiative forcing of greenhouse gases that contribute to a net warming and cooling of the atmosphere, respectively. “LOSU” refers to the level of scientific understanding (IPCC, 2007).

What are the specific air quality implications of climate change in Tulsa, Oklahoma, and other similarly-sized metropolitan areas in the mid-latitudes? As with mega-cities, mid-sized urban centers struggle with ozone pollution episodes as well. Although large cities have a greater local production potential, the impact that background concentrations have in both settings largely dictates the severity of ozone pollution, and high background concentrations imply that only modest levels of local photochemical production are necessary for dangerous pollution episodes, and in some cases, violation of local, state, and federal air quality regulations. Thus, any upward shift in the background ozone concentration, such as the more permanent presence of subtropical anti-cyclones, will

compromise ozone air quality in the mid-sized cities of the middle latitudes. Furthermore, local ozone production will be enhanced as well, as the sunny, stagnant conditions associated with anti-cyclones are optimal for photochemical reactions.

10.5. Recommendations for Implementation and Future Study

A desired outcome of this study is the integration of the research findings into the current ozone forecasting techniques that facilitate the air quality issuances prepared on a daily basis by the Oklahoma Department of Environmental Quality. In determining which day or, more likely, period of days are favorable for high ozone concentrations, i.e. nearing the 8-hour EPA NAAQS of 0.085 parts per million, it is important to consider the behavior of the background concentration. Since it may not be feasible to directly measure the residual value of ozone on a regular basis, attention must be paid to the location and migration of the polar jet stream, and Rossby waves in particular, which are readily characterized by the positions of ridges and troughs relative to the polar jet stream on the 300 hPa constant pressure charts, in turn an excellent indicator of atmospheric wave progression. As was shown in the research, atmospheric Rossby waves are not discernable at ground level, and pressure at this level could not be correlated with ozone concentrations. Cognizance of Rossby wave behavior in the troposphere is important not only because ground-level ozone concentrations are so strongly influenced by them, but also because their eastward progression through the middle latitudes of the Northern Hemisphere is sufficiently slow that ozone pollution episodes as well as periods of relatively low levels of O₃ can be expected over a duration of several days. While

subsidence from smaller-scale baroclinic waves can also result in marked increases in the background ozone concentration, Rossby waves were shown to coincide with persistent ozone pollution episodes.

Therefore, attention to forecasts generated by numerical weather prediction is especially important. Several forecast models are available, but for extended periods during which Rossby waves in the troposphere can be tracked, the most appropriate is the Global Forecast System, or GFS. Developed and maintained by the National Centers for Environmental Prediction (NCEP), the GFS has a horizontal resolution of 0.5° longitude x 0.5° latitude. It is ideally suited for the analysis and prediction of tropospheric Rossby waves and the concomitant positions of large-scale pressure ridge and trough axes, as it provides numerical (and graphical) forecasts through 384 hours, or 16 days from the time of initialization.

Other forecast models, including the North American Mesoscale Weather Research and Forecasting model (NAM-WRF) and the Rapid Update Cycle (RUC) model, are not suited for extended prognostication of tropospheric pressure characteristics, as they are only available for a period of 84 hours and 12 hours from initialization, respectively. However, each is at a much higher resolution than the GFS (20 km), with forecasts of even higher resolution (12 km) also available, thus providing a more detailed short-term forecast of the dynamic motion of the troposphere, including the relatively rapid progression of baroclinic waves. Additionally, forecasted values of air temperature, relative humidity, and wind speed – all important when considering local photochemical

production of ozone – can also be gained from these short-term, high-resolution meteorological models.

Therefore, the following forecast strategy is recommended:

1. Based on daily 00 UTC (18:00 CST) GFS model runs, identify days with potentially high background O₃ concentrations based on 300 hPa pressure ridge axes and encroachment of subtropical anti-cyclones (including baroclinic and Rossby waves), allowing extended forecasting of ozone through 384 hours, or 16 days.
2. Refine short-term ozone forecasting by integrating ground-level meteorological parameters, namely air temperature, relative humidity, wind speed, and solar radiation, based on the NAM-WRF model. This will allow high-resolution forecasting incorporating both the characteristics of the troposphere (particularly baroclinic waves) as well as expected conditions in the boundary layer, but will be limited to 84 hours, or 3.5 days. Since the NAM-WRF updates on a 12-hour cycle, higher resolution forecasts can be generated on this cycle as well.
3. Implement ozone “now-casting” based on the RUC and on products issued by the local National Weather Service (NWS) office. In addition to the high, short-term resolution that the RUC offers, point forecast matrices are available from the NWS, providing guidance on a 3-hour basis for a variety of ground-level

meteorological parameters, again including air temperature, relative humidity, and wind speed. Since high ozone concentrations occur when each variable is present along with one another over a duration of several consecutive hours, the point forecast matrix is an instantaneous and easy-to-use decision-making tool that is available for same-day forecasting.

In fact, the point forecast matrix available daily from the NWS is exceptionally well-suited for short term “now-casting” because it blends data from a variety of meteorological models with forecaster experience. Identification of likely time periods for high ozone concentration can be made from successive lines of forecast data, where air temperature, relative humidity, and wind speed are all listed in three hour intervals (Figure 10.3).

```

POINT FORECAST MATRICES
NATIONAL WEATHER SERVICE TULSA OK
409 AM CDT WED JUN 7 2006

OKZD60-080015-
TULSA-TULSA OK
36.2DN 95.90W
409 AM CDT WED JUN 7 2006

DATE                WED 06/07/06          THU 06/08/06          FRI 06/09/06
UTC 3HRLY           08 11 14 17 20 23 02 05 08 11 14 17 20 23 02 05 08 11 14 17 20 23
CDT 3HRLY           03 06 09 12 15 18 21 00 03 06 09 12 15 18 21 00 03 06 09 12 15 18

MAX/MIN
TEMP                67 75 85 91 91 79 72 67 64 73 85 92 92 83 76 73 70 79 90 97 97
DEWPT               64 67 65 62 60 61 63 64 64 64 63 61 62 63 63 63 64 65 66 65 65
RH                  90 76 51 38 36 54 73 90100 73 48 36 37 51 64 71 81 62 45 35 35
WIND DIR             NE  N  N  NE NE  E  E  E  E  S  S  S  S  S  S  S  S  S  S  SW  S
WIND SPD             1  1  5  9  8  4  2  1  1  3  5  8  9  9  8  6  6  9 14 16 17
CLOUDS               FW  FW  FW  FW  FW  FW  FW  FW  FW  FW  FW  FW  FW  FW  FW  FW  FW  FW  FW  FW
POP 12HR              5  0  0  0  0  0  0  0  0  0  0  0  0  0  0  0  0  0  0  5
QPF 12HR              0  0  0  0  0  0  0  0  0  0  0  0  0  0  0  0  0  0  0  0
OBVIS                PF

```

FIGURE 10.3: Point forecast matrix issued by the NWS forecast office in Tulsa, Oklahoma on June 7, 2006 (NWS Tulsa, 2006)

As an example of the utility that a point forecast matrix offers to short-term ozone forecasting, consider the daily product that was issued by the NWS forecast office in Tulsa on 07 June 2006. During the three-day period, only two 3-hour blocks met the three criteria necessary for high ground-level ozone concentrations: 14:00 – 17:00 CST (20:00 – 23:00 UTC) on Wednesday, 07 June, and again between 14:00 – 17:00 CST (20:00 – 23:00 UTC) on Thursday, 08 June. Although the air temperature and relative humidity met high ozone criteria again on Friday, June 10, wind speeds did not, as they were forecast to exceed $5 \text{ m}\cdot\text{s}^{-1}$ ($10 \text{ mi}\cdot\text{hr}^{-1}$). One-hour ozone concentrations did not surpass 0.08 ppm during the three-day interval, indicating that while surface conditions briefly supported high ground-level ozone on 07 and 08 June, the background concentration was likely insufficient for excessive total concentrations.

Aside from the operational recommendations regarding the findings of this study, additional research is necessary, particularly with regard to the dynamic behavior of the background ozone concentration. Is the background ozone concentration behaving similarly in other mid-latitude locations? How much fluctuation occurs vertically, even at those elevations confined to the boundary layer, which is the extent of the tallest man-made structures? In order to gain a more complete understanding of how the background ozone concentration behaves, these questions must be answered.

It is possible that the signature observed between background ozone and the propagation of atmospheric waves would be more readily evident at a different elevation. The selection of 210 meters in this study was one of necessity – it represented the height of

the tallest building in Tulsa, where access and pre-existing utilities allowed for easy maintenance and data acquisition. Studies on the order of days and weeks have been carried out on various transmission towers, as they can be equipped with temporary power and data recording devices. When designing a tower study that lasts for several months or even years, however, the installation must be more permanent, which would inevitably incur high operational and maintenance costs. Nonetheless, a long-term study of the vertical profile of boundary-layer ozone would be advantageous in furthering the understanding of its relationship with the global circulation, particularly if ozone were sampled at an interval of 250-500 meters.

Likewise, a horizontal network of elevated boundary-layer ozone monitors would also contribute to the knowledge of background ozone behavior in relation to the polar jet stream and attendant atmospheric waves. While the background ozone data acquired in Tulsa undoubtedly revealed a distinct pattern mimicking the propagation of atmospheric waves across the mid-latitudes, correlation between the two presumably could be improved if background concentrations closer to the position of the polar jet were available. If boundary-layer ozone analyzers were paired with upper-air meteorological sounding sites, more conclusions regarding the background concentration in relation to geopotential heights could be drawn.

Another topic for future exploration is the role that stratospheric-tropospheric exchange plays in the ozone budget of the troposphere. Recent research suggests that appreciable transport of stratospheric ozone into the troposphere occurs in the vicinity of the polar jet

stream, where the tropopause folds underneath the core of the polar jet and subsequently descends toward the surface. The magnitude and rate of ozone exchanged through this process is unclear, but given the relatively high ozone concentrations in the stratosphere coupled with observational ozonesonde evidence of stratospheric ozone in the troposphere (Section 9.2), stratospheric-tropospheric exchange is a mechanism that offers a plausible explanation of high background ozone concentrations in the free troposphere. Even at very slow rates of vertical descent through the troposphere, a mean travel time from the 300 hPa level to the boundary layer would be no more than 3-4 days, well within the duration of a Rossby wave. Since tropospheric folding along the polar jet stream in the vicinity of atmospheric wave troughs is followed by an onset of anti-cyclonic, subsiding circulation, increasing background ozone concentrations are likely influenced by the 1-2 combination of stratospheric-tropospheric exchange and subsequent large-scale subsidence. An intensive effort to measure ozone concentrations in the vicinity of Rossby wave troughs and elsewhere along the polar jet stream will undoubtedly improve the overall knowledge of stratospheric ozone exchange, resulting in a better understanding of tropospheric background ozone concentrations and their connection to ozone in the atmospheric boundary layer.

Finally, a more complete understanding of the connection between tropospheric ozone and mid-latitude climate is necessary for long-term ozone prediction. What are the air quality implications arising from climate change? Will an increase in the global mean temperature force the polar jet stream toward the pole? Are subtropical highs poised to advance poleward in response, thus becoming permanently entrenched in the mid-

latitudes? These questions must be answered as a gauge for future ozone concentrations in the context of the nation's air quality, as the behavior of the polar jet stream and atmospheric wave propagation have been shown to significantly influence background ozone, which in turn largely dictate concentration potential at ground level. In Section 10.3, it was speculated that an increase in the global mean temperature could result in a poleward shift of the jet stream, promoting favorable conditions for high ground-level ozone concentrations on a more permanent basis. This scenario suggests that not only will large-scale subsidence yield increasing concentrations of background O₃, but high air temperatures, low relative humidity, and light winds – all indicative of broad anti-cyclonic circulation – will occur more frequently within the mid-latitudes, including many of the major metropolitan areas within the borders of the United States. With time, a more robust data set will clarify the long-term expectations of climate change in the mid-latitudes, including the dynamic behavior of the atmosphere. Ozone prediction and mitigation efforts can subsequently be focused on our changing world.

10.6. Concluding Remarks

In summary, ozone forecasting can be improved through the consideration of the meteorological variables that have been shown to impact local ozone concentrations, namely ground-level dry-bulb (air) temperature, relative humidity, and wind speed. Each of these parameters plays an important role in local photochemical production, and careful analysis of weather regimes favorable for the combined availability of ground level air temperatures greater than 27°C, relative humidity less than 50%, and ground

level wind speeds of less than $5 \text{ m}\cdot\text{s}^{-1}$ will signal the possibility of significant local photochemical production, as they have been associated with high ground-level ozone concentrations in the context of this research study. Long-range ozone forecasts can be generated from synoptic-scale meteorological modeling, and migration of atmospheric waves in particular. Fluctuations in the background ozone concentration mirror the passages of perturbations within the polar jet stream, and very high background concentrations, equaling or exceeding 0.06 parts per million, are possible during pronounced upper-tropospheric ridging and extended periods of anti-cyclonic circulation. Thus, long range numerical weather forecasts can be used in conjunction with the knowledge of how ozone concentrations are influenced, both in terms of local photochemical production as well as the dynamic behavior of the background ozone concentration. Finally, the long term prospects of ozone pollution – not on the order of one or two weeks, or every one or two years, but instead at an interval of several decades – can be assessed based on current predictions of climate change. If the global mean temperatures do appreciably rise, changing weather patterns in the middle latitudes may increase the magnitude and duration of ozone pollution episodes, even at modest temperature increases.

Ozone has been a constituent of the tropospheric atmosphere for millions of years, both as a consequence of stratospheric transport and as a product of the high-temperature conversion of gases in contact with lightning. Plants and trees have even contributed to ground-level ozone concentrations, as the emission of biogenic volatile organic compounds, including isoprene, inevitably incorporate into the ozone cycle. Thus, the

presence of ozone is nothing new to the lower atmosphere, predating mankind itself by eons.

What is new, however, is the emergence of a host of anthropogenic compounds that have entered the ozone cycle since the onset of the Industrial Revolution a century and a half ago, resulting in a continually increasing background concentration of tropospheric ozone. While pre-industrial ozone concentrations at ground level were a by-product of the natural system, recent increases cannot be considered as anything other than air pollution. Combustive emissions of NO_x have driven ozone concentrations to levels that have never previously been experienced in the history of civilization. Even though the most direct mechanism for ground-level ozone production is the photochemical conversion of NO_2 , a variety of other compounds also contribute to net ozone increases through indirect reactions. As long as combustion is a major industrial activity, ground-level ozone will pose a threat to air quality.

In closing, more attention must be paid to the meteorological processes that affect ozone concentrations, as chemistry alone cannot explain the occurrences of ozone episodes, particularly in relation to the tropospheric background concentration. When Cornelius Fox compiled his introductory work on the relationship between ozone and local meteorological variables in 1873, he set forth three goals that he wished to accomplish:

1. *To give a digest of the most important facts concerned with Ozone;*
2. *To point out the circumstances and the manner in which, the localities were, and the reason why, Ozone is observed in the atmosphere; and,*
3. *To give the results of my own investigations concerning these bodies.*

Fox did not have the benefit of later research by Chapman, Leighton, and others that demonstrated the dependence of ozone production on photochemical reactions. Likewise, he would never know of the meteorological relationships to ozone proposed by Wulf and Rossby in a later era when large-scale atmospheric measurements became possible. Still, his idea holds true today – meteorology is particularly important when describing the distribution and behavior of ozone – and this research study embraced his objective of detailing what is known about ozone, where it is distributed, and most importantly, what drives the distribution.

Ozone is both a friend and a foe to mankind. We rely on its protective characteristics in the stratosphere, shielding us from harmful solar rays, and yet, we are intolerant to it in the troposphere at modest concentrations, where it adversely affects respiratory function. As Fox noted over 130 years ago, meteorology is the key to understanding ozone formation and transport, and it was with this knowledge that this research study was conducted, subsequently revealing the unmistakable relationship between the background ozone concentration of the troposphere and the large-scale, dynamic circulation of the

atmosphere. Clearly, ozone isn't confined to the local or regional scope, but instead is a widespread pollutant that transcends political boundaries. Thus, it is a burden we all must share.

BIBLIOGRAPHY

- Abram, J.P., Creasey, D.J., Heard, D.E., Lee, J.D., and Pilling, M.J. (2000). Hydroxyl radical and ozone measurements in England during the solar eclipse of 11 August 1999. *Geophys. Res. Ltrs.*, **27(21)**: 3437-3440.
- Andreae, M.O. and Crutzen, P.J. (1997). Atmospheric aerosols: biogeochemical sources and role in atmospheric chemistry. *Science*, **276(5315)**:1052-1058.
- Aneja, V.P., Arya, S.P., Li, Y., Murray, G.C., and Manuszak, T.L. (2000). Climatology of diurnal trends and vertical distribution of ozone in the atmospheric boundary layer in urban North Carolina. *J. Air & Waste Manage. Assoc.*, **50(1)**: 54-64.
- Angevine, W.M., Senff, C.J., White, A.B., Williams, E.J., Koerner, J., Miller, S.T.K., Talbot, R., Johnston, P.E., McKeen, S.A., and Downs, T. (2004). Coastal boundary layer influence on pollutant transport in New England. *J. Appl. Meteorol.*, **43(10)**:1425-1437.
- Arya, S.P. (1999). *Air Pollution Meteorology and Dispersion*. Oxford, United Kingdom: Oxford University Press.
- Arya, S.P. (2001). *Introduction to Micrometeorology*. London: Academic Press.
- Atkinson, R. (2000). Atmospheric chemistry of VOCs and NO_x. *Atmos. Environ.*, **34(12-14)**:2063-2101.
- Banta, R.M., Pichugina, Y.L., and Newsom, R.K. (2003). Relationship between low-level jet properties and turbulence kinetic energy in the nocturnal stable boundary layer. *J. Atmos. Sci.*, **60(20)**:2549-2555.
- Banta, R.M., Senff, C.J., Nielsen-Gammon, J., Darby, L.S., Ryerson, T.B., Alvarez, R.J., Sandberg, S.P., Williams, E.J., and Trainer, M. (2005). A bad air day in Houston. *Bull. Amer. Meteor. Soc.*, **86(5)**:657-669.
- Baumann, K., Williams, E.J., Angevine, W.M., Roberts, J.M., Norton, R.B., Frost, G.J., Fehsenfeld, F.C., Springston, S.R., Bertman, S.B., and Hartsell, B. (2000). Ozone production and transport near Nashville, Tennessee: results from the 1994 study at New Hendersonville. *J. Geophys. Res.*, **105(D7)**:9137-9153.

- Becker, K.H., Brockmann, K.J., and Bechara, J. (1990). Production of hydrogen peroxide in forest air by reaction of ozone with terpenes. *Nature*, **346(6281)**:256-258.
- Beirle, S., Platt, U., Wenig, M., and Wagner, T. (2004). NO_x production by lightning estimated with GOME. *Adv. Space Res.*, **34(4)**:793-797.
- Berman, S., Ku, J.Y., and Rao, S.T. (1999). Spatial and temporal variation in the mixing depth over the northeastern United States during the summer of 1995. *J. Appl. Meteorol.*, **38(12)**:1661-1673.
- Bithell, M., Vaughan, G., and Gray, L.J. (2000). Persistence of stratospheric ozone layers in the troposphere. *Atmos. Environ.*, **34(16)**:2563-2570.
- Blackadar, A.K. (1957). Boundary layer wind maxima and their significance for the growth of nocturnal inversions. *Bull. Amer. Meteor. Soc.*, **38(5)**:283-290.
- Bonner, W.D. (1968). Climatology of the low level jet. *Mon. Wea. Rev.*, **96(12)**:833-850.
- Boucouvala, D., and Bornstein, R. (2003). Analysis of transport patterns during an SCOS97-NARSTO episode. *Atmos. Environ.*, **37(S2)**:73-94.
- Brasseur, G.P., Orlando, J.J., and Tyndall, G.S. (Eds.) (1999). *Atmospheric Chemistry and Global Change*. Oxford: Oxford University Press.
- Brimblecombe, P. (1996). *Air Composition and Chemistry*. Cambridge, U.K.: Cambridge University Press.
- Brock, F.V., Crawford, K.C., Elliott, R.L., Cuperus, G.W., Stadler, S.J., Johnson, H.J., and Eilts, M.D. (1995). The Oklahoma Mesonet: a technical overview. *J. Atmos. Ocean Technol.*, **12(1)**:5-19.
- Brown, S.S., Dibb, J.E., Stark, H., Aldener, M., Vozella, M., Whitlow, S., Williams, E.J., Lerner, B.M., Jakoubek, R., Middlebrook, A.M., DeGouw, J.A., Warneke, C., Goldan, P.D., Kuster, W.C., Angevine, W.M., Sueper, D.T., Quinn, P.K., Bates, T.S., Meagher, J.F., Fehsenfeld, F.C., and Ravishankara, A.R. (2004). Nighttime removal of NO_x in the summer marine boundary layer. *Geophys. Res. Ltrs.*, **31(7)**:L07108.
- Burrows, J.P., Behmann, T., Crowley, J.N., Maric, D., Lastätter-Weißemayer, A., Moortgat, G.K., Perner, D., and Weißemayer, M. (1997). Laboratory and field measurement studies of the tropospheric chemistry of nitrate and peroxy radicals. In G. Le Bras (Ed.), *Chemical Processes in Atmospheric Oxidation* (pp. 91-99). Berlin: Springer-Verlag.

- Carlson, J.D., Whalon, M.E., Landis, D.A., and Gage, S.H. (1992). Springtime weather patterns coincident with long-distance migration of potato leafhopper into Michigan. *Agric. For. Meteorol.*, **59(3-4)**:183-206.
- Carlson, T.N. (1998). *Mid-Latitude Weather Systems*. Boston: American Meteorological Society.
- Chan, L.Y., Chan, C.Y., and Qin, Y. (1998). Surface ozone pattern in Hong Kong. *J. Appl. Meteorol.*, **37(10)**:1153-1165.
- Cooray, V., and Rahman, M. (2005). Efficiencies for production of NO_x and O₃ by streamer discharges in air at atmospheric pressure. *J. Electrostat.*, **63(6-10)**:977-983.
- Cox, R.A. (1988). Atmospheric chemistry of NO_x and hydrocarbons influencing tropospheric ozone. In I.S.A. Isaksen (Ed.), *Tropospheric ozone: Regional and global scale interactions*. (pp. 263-292). Dordrecht, Netherlands: D. Reidel Publishing Co.
- Crowley, J.N. and Carl, S.A. (1997). OH formation in the photoexcitation of NO₂ beyond the dissociation threshold in the presence of water vapor. *J. Phys. Chem. A*, **101(23)**:4178-4184.
- Crutzen, P.J. (1988). Tropospheric ozone: an overview. In I.S.A. Isaksen (Ed.), *Tropospheric ozone: Regional and global scale interactions*. (pp. 3-32). Dordrecht, Netherlands: D. Reidel Publishing Co.
- Desqueyroux, H., Pujet, J.C., Prosper, M., Squinazi, F., and Momas, I. (2002). Short-term effects of low-level air pollution on respiratory health of adults suffering from moderate to severe asthma. *Environ. Res.*, **89(1)**:29-37.
- Dessler, A. (2000). *The Chemistry and Physics of Stratospheric Ozone*. London: Academic Press.
- Djurić, D. (1994). *Weather Analysis*. New Jersey: Prentice-Hall.
- Doswell, C.A., Anderson, L.C., and Imy, D.A. (1991). *Basic Convection I – A Review of Atmospheric Thermodynamics*. Norman, Oklahoma: National Oceanic and Atmospheric Administration.
- Dufour, A., Amodei, M., Ancellet, G., and Peuch, V.H. (2005). Observed and modeled “chemical weather” during ESCOMPTE. *Atmos. Res.*, **74(1-4)**:161-189.
- Egorova, T., Zubov, V., Jagovkina, S., and Rozanov, E. (1999). Lightning production of NO_x and ozone. *Phys. Chem. Earth (C)*, **24(5)**:473-479.

- Evett, J.B. and Liu, C. (1987). *Fundamentals of Fluid Mechanics*. New York: McGraw-Hill.
- Fast, J.D., and McCorcle, M.D. (1990). A two-dimensional numerical sensitivity study of the Great Plains low-level jet. *Mon. Weather Rev.*, 118(1):151-163.
- Fenger, J. (1999). Urban air quality. *Atmos. Environ.*, **33(29)**:4877-4900.
- Finlayson-Pitts, B.J., and Pitts, J.N. (1997). Tropospheric air pollution: ozone, airborne toxics, polycyclic aromatic hydrocarbons, and particles. *Science*, **276(5315)**:1045-1052.
- Finlayson-Pitts, B.J., and Pitts, J.N. (2000). *Chemistry of the Upper and Lower Atmosphere: Theory, Experiments, and Applications*. New York: Academic Press, Inc.
- Fleagle, R.G., and Businger, J.A. (1980). *An Introduction to Atmospheric Physics*. New York: Academic Press, Inc.
- Folkens, I. and Chatfield, R. (2000). Impact of acetone on ozone production and OH in the upper troposphere at high NO_x. *J. Geophys. Res.*, **105(D9)**:11585-11599.
- Fox, C.B. (1873). *Ozone and Antozone: Their History and Nature*. London: J. & A. Churchill.
- Fu, Q., Johanson, C.M., Wallace, J.M., and Reichler, T. (2006). Enhanced mid-latitude tropospheric warming in satellite measurements. *Science*, **312(5777)**:1179.
- Gangoiti, G., Millán, M.M., Salvador, R., and Mantilla, E. (2001). Long-range transport and re-circulation of pollutants in the western Mediterranean during the project Regional Cycles of Air Pollution in west-central Mediterranean area. *Atmos. Environ.*, **35(36)**: 6267-6276.
- Garratt, J.R. (1994). *The Atmospheric Boundary Layer*. Cambridge, United Kingdom: Cambridge University Press.
- Gaza, R.S. (1998). Mesoscale meteorology and high ozone in the northeast United States. *J. Appl. Meteorol.*, **37(9)**:961-977.
- Ghim, Y.S., Oh, H.S., and Chang, Y.S. (2001). Meteorological effects on the evolution of high ozone episodes in the greater Seoul area. *J. Air & Waste Manage. Assoc.*, **51(2)**:185-202.
- Glickman, T.S. (Ed.) (2000). *Glossary of Meteorology*. Boston, Massachusetts: American Meteorological Society.

- Graedel, T.E. and Crutzen, P.J. (1993). *Atmospheric Change: An Earth System Perspective*. New York: W.H. Freeman and Co.
- Grewe, V., Brunner, D., Dameris, M., Grenfell, J.L., Hein, R., Shindell, D., and Staehelin, J. (2001). Origin and variability of upper tropospheric nitrogen oxides and ozone at northern mid-latitudes. *Atmos. Environ.*, **35(20)**:3421-3433.
- Grewe, V., Reithmeier, C., and Shindell, D.T. (2002). Dynamic-chemical coupling of the upper troposphere and lower stratosphere region. *Chemosphere*, **47(8)**:851-861.
- Grewe, V., Shindell, V.T., and Eyring, V. (2004). The impact of horizontal transport on the chemical composition in the tropopause region: lightning NO_x and streamers. *Adv. Space Res.*, **33(7)**:1058-1061.
- Gould, R.F. (Ed.) (1972). *Photochemical Smog and Ozone Reactions*. Washington, D.C.: American Chemical Society.
- Heidam, N.Z., Christensen, J., Wählin, P., and Skov, H. (2004). Arctic atmospheric contaminants in NE Greenland: levels, variations, origins, transport, transformations and trends, 1990-2001. *Sci Total Environ.*, **331(1-3)**:5-28.
- Hess, S.L. (1979). *Introduction to Theoretical Meteorology*. Malabar, Florida: Krieger Publishing Co.
- Hidy, G.M. (2000). Ozone process insights from field experiments – Part I: overview. *Atmos. Environ.*, **34(12-14)**:2001-2022.
- Hjorth, J., Jensen, N.R., Skov, H., Capellani, F., and Restelli, G. (1997). Gas-Phase reactions of interest in night-time tropospheric chemistry. In G. Le Bras (Ed.), *Chemical Processes in Atmospheric Oxidation* (pp. 113-119). Berlin: Springer-Verlag.
- Holton, J.R. (1992). *An Introduction to Dynamic Meteorology*. New York: Academic Press.
- Indian Nations Council of Governments [INCOG]. (2002). *Tulsa metropolitan area 8-hour ozone early action*. Tulsa, Oklahoma.
- Indian Nations Council of Governments [INCOG]. (2006). Ozone alert. Retrieved 03/2006 from <http://www.ozonealert.com/>
- Inter-Governmental Panel on Climate Change [IPCC]. (2007). *Climate Change 2007: The Physical Science Basis*. Contribution of Working Group I to the Fourth Assessment Report of the Intergovernmental Panel on Climate Change. Geneva, Switzerland.

- Jacob, D.J. (1998). The oxidizing power of the atmosphere. In T. Potter and B. Colman (Eds.), *Handbook of Weather, Climate and Water*. New York: McGraw-Hill.
- Jacob, D.J. (2000). Heterogeneous chemistry and tropospheric ozone. *Atmos. Environ.*, **34(12-14)**:2131-2159.
- Jaffe, D.H., Singer, M.E., and Rimm, A.A. (2003). Air pollution and emergency department visits for asthma among Ohio Medicaid recipients, 1991-1996. *Environ. Res.*, **91(1)**:21-28.
- Kang, D., Aneja, V.P., Mathur, R., and Ray, J.D. (2004). Observed and modeled VOC chemistry under high VOC/NO_x conditions in the southeast United States national parks. *Atmos. Environ.*, **38(29)**:4969-4974.
- Kastner-Klein, P.M., Williams, D., and Hall, F. (2002). Impact of long-range transport on ozone pollution in the Oklahoma City metro area. *American Meteorological Society 12th Joint Conference on the Applications of Air Pollution Meteorology with the Air and Waste Management Association*, Norfolk, Virginia, 20-24 May 2002.
- Kim, Y.K., Lee, H.W., Park, J.K., and Moon, Y.S. (2002). The stratosphere-troposphere exchange of ozone and aerosols over Korea. *Atmos. Environ.*, **36(3)**:449-463.
- Le Bras, G., Poulet, G., Butkovskaya, N., Daële, V., Johnstone, D., Lançar, I.T., Laverdet, G., Mellouki, A., Ray, A., Téton, S., and Vassali, I. (1997). Laboratory studies of NO₃ and OH reactions of tropospheric relevance. In G. Le Bras (Ed.), *Chemical Processes in Atmospheric Oxidation* (pp. 135-142). Berlin: Springer-Verlag.
- Leighton, P.A. (1961). *Photochemistry of Air Pollution*. New York: Academic Press.
- Lelieveld, J., Peters, W., Dentener, F.J., and Krol, M.C. (2002). Stability of tropospheric hydroxyl chemistry. *J. Geophys. Res.*, **107(D23)**:4715.
- Lesclaux, R., Boyd, A.A., Bridier, I., Caralp, F., Catoire, V., Fenter, F.F., Lightfoot, P.D., Nozière, B., Rowley, D.M., Veyret, B., and Villenave, E. (1997). Peroxy radical reactions of tropospheric interest. In G. Le Bras (Ed.), *Chemical Processes in Atmospheric Oxidation* (pp. 143-150). Berlin: Springer-Verlag.
- Levy, H. (1984). Tropospheric ozone: transport or chemistry? In *Atmospheric Ozone. Proceedings of the Quadrennial Ozone Symposium* (pp. 730-734). Dordrecht, Netherlands: Kluwer Academic Publishers.
- Lin, C.H., Wu, Y.L., Lai, C.H., Lin, P.H., Lai, H.C., and Lin, P.L. (2004). Experimental investigation of ozone accumulation overnight during a wintertime ozone episode in south Taiwan. *Atmos. Environ.*, **38(26)**:4267-4278.

- Lin, C.Y.C., Jacob, D.J., Munger, J.W., and Fiore, A.M. (2000). Increasing background ozone in surface air over the United States. *Geophys. Res. Ltrs.*, **27(21)**: 3465-3468.
- Lu, W.Z., and Wang, X.K. (2004). Interaction patterns of major air pollutants in Hong Kong territory. *Sci. Total Environ.*, **324(1-3)**:247-259.
- McConnell, R., Berhane, K., Gilliland, F., London, S.J., Islam, T., Gauderman, W.J., Avol, E., Margolis, H.G., and Peters, J.M. (2002). Asthma in exercising children exposed to ozone: a cohort study. *Lancet*, **359(9304)**:386-391.
- McDonnell, W.F., Horstman, D.H., Hazucha, M.J., Seal, E., Haak, E.D., Salaam, S.A., and House, D.E. (1983). Pulmonary response during exposure to low concentrations of ozone. In S.T. Lee, M.G. Mustafa, and M.A. Mehlman (Eds.). *International Symposium on the Biomedical Effects of Ozone and Related Photochemical Oxidants* (pp. 139-144). Princeton, N.J.: Princeton Scientific Publishers.
- McPherson, R.A., Fiebrich, C.A., Crawford, K.C., Elliott, R.L., Kilby, J.R., Grimsley, D.L., Martinez, J.E., Basara, J.B., Illston, B.G., Morris, D.A., Kloesel, K.A., Stadler, S.J., Melvin, A.D., Sutherland, A.J., Shrivastava, H., Carlson, J.D., Wolfenbarger, J.M., Bostic, J.P., and Demko, D.B. (2007). Statewide monitoring of the mesoscale environment: a technical update on the Oklahoma Mesonet. *J. Atmos. Ocean Technol.*, **24(3)**:301-321.
- Mentel, T.F., Sohn, M., and Wahner, A. (1999). Nitrate effect in the heterogeneous hydrolysis of dinitrogen pentoxide on aqueous aerosols. *Phys. Chem. Chem. Phys.*, **1(24)**:5451-5457.
- Michelson, I. (1970). *The Science of Fluids*. New York: Van Nostrand Reinhold.
- Millán, M.M., Sanz, M.J., Salvador, R., and Mantilla, E. (2002). Atmospheric dynamics and ozone cycles related to nitrogen deposition in the western Mediterranean. *Environ. Pollut.*, **118(2)**:167-186.
- Monks, P.S. (2000). A review of the observations and origins of the spring ozone maximum. *Atmos. Environ.*, **34(21)**:3545-3561.
- Mudway, I.S., and Kelly, F.J. (2000). Ozone and the lung: a sensitive issue. *Mol. Aspects Med.*, **21(1-2)**:1-48.
- National Aeronautics and Space Administration [NASA]. (2000). *Studying Earth's Environment from Space*. Retrieved 12/2006 from <http://www.ccpo.odu.edu/SEES/index.html>

- National Oceanic and Atmospheric Administration [NOAA]. (1998). *Automated surface observing system: user's guide*. Retrieved 04/2007 from <http://www.nws.noaa.gov/asos/>
- National Oceanic and Atmospheric Administration [NOAA]. (2006). Earth System Research Laboratory upper-air database. Retrieved 10/2006 from <http://www.esrl.noaa.gov/>
- National Oceanic and Atmospheric Administration [NWS Norman]. (2006). Forecast products, National Weather Service, Norman, Oklahoma. Retrieved 03/2006 from <http://www.srh.noaa.gov/oun/>
- National Oceanic and Atmospheric Administration [NWS Tulsa]. (2006). Forecast products, National Weather Service, Tulsa, Oklahoma. Retrieved 06/2006 from <http://www.srh.noaa.gov/tsa/>
- National Research Council [NRC]. (1977). *Ozone and other photochemical oxidants*. Washington, D.C.: National Academy of Sciences.
- National Research Council [NRC]. (1991). *Rethinking the ozone problem in urban and regional air pollution*. Washington, D.C.: National Academy Press.
- O'Neill, M.S., Loomis, D., and Borja-Aburto, V.H. (2004). Ozone, area social conditions, and mortality in Mexico City. *Environ. Res.*, **94(3)**:234-242.
- Oklahoma Department of Environmental Quality [ODEQ]. (2004). *Revisions to the state implementation plan for the control of ozone air pollution: Tulsa metropolitan area 8-hour ozone early action compact*. Oklahoma City, Oklahoma: ODEQ Air Quality Division.
- Oklahoma Department of Environmental Quality [ODEQ]. (2005). *Tulsa early action compact: December 31, 2005 progress report*. Oklahoma City, Oklahoma: ODEQ Air Quality Division.
- Palmén, E., and Newton, C.W. (1969). *Atmospheric Circulation Systems: Their Structure and Physical Interpretation*. New York: Academic Press.
- Pasqualini, V., Robles, C., Garzino, S., Greff, S., Bousquet-Melou, A., and Bonin, G. (2003). Phenolic compounds content in *Pinus halepensis* Mill. needles: a bioindicator of air pollution. *Chemosphere*, **52(1)**:239-248.
- Pefley, R.K. and Murray, R.I. (1966). *Thermofluid Mechanics*. New York: McGraw-Hill.
- Pison, I., and Menut, L. (2004). Quantification of the impact of aircraft traffic emissions on tropospheric ozone over Paris area. *Atmos. Environ.*, **38(7)**:971-983.

- Plaza, J., Pujadas, M., and Artíñano, B. (1997). Formation and transport of the Madrid ozone plume. *J. Air & Waste Manage. Assoc.*, **47(7)**: 766-774.
- Pochanart, P., Kato, S., Katsuno, T., and Akimoto, H. (2004). Eurasian continental background and regionally polluted levels of ozone and CO observed in northeast Asia. *Atmos. Environ.*, **38(9)**:1325-1336.
- Pont, V., and Fontan, J. (2001). Comparison between weekend and weekday ozone concentration in large cities in France. *Atmos. Environ.*, **35(8)**:1527-1535.
- Prandtl, L. and Tietjens, O.G. (1957). *Fundamentals of Hydro- and Aeromechanics*. New York: Dover.
- Rao, T.N., Arvelius, J., Kirkwood, S., and von der Gathen, P. (2004). Climatology of ozone in the troposphere and lower stratosphere over the European Arctic. *Adv. Space Res.*, **34(4)**:754-758.
- Rappenglück, B., Forster, C., Jakobi, G., and Pesch, M. (2004). Unusually high levels of PAN and ozone over Berlin, Germany, during nighttime on August 7, 1998. *Atmos. Environ.*, **38(36)**:6125-6134.
- Reiter, E.R. (1963). *Jet-Stream Meteorology*. Chicago: University of Chicago Press.
- Reiter, E.R. (1978). Impact of stratospheric ozone on tropospheric concentrations. In A.L. Morris and R.C. Barras (Eds.), *Air Quality Meteorology and Atmospheric Ozone* (pp.506-519). Baltimore, MD: American Society for Testing and Materials.
- Ridley, B., Atlas, E., Selkirk, H., Pfister, L., Montzka, D., Walega, J., Donnelly, S., Stroud, V., Richard, E., Kelly, K., Tuck, A., Thompson, T., Reeves, J., Baumgardner, D., Rawlins, W.T., Mahoney, M., Herman, R., Friedl, R., Moore, F., Ray, E., and Elkins, J. (2004). Convective transport of reactive constituents to the tropical and mid-latitude tropopause region: I. Observations. *Atmos. Environ.*, **38(9)**:1259-1274.
- Rodríguez, S., Torres, C., Guerra, J.C., and Cuevas, E. (2004). Transport pathways of ozone to marine and free-troposphere sites in Tenerife, Canary Islands. *Atmos. Environ.*, **38(28)**:4733-4747.
- Rohli, R.V., Russo, M.M., Vega, A.J., and Cole, J.B. (2004). Tropospheric ozone in Louisiana and synoptic circulation. *J. Appl. Meteorol.*, **43(10)**:1438-1451.
- Rosenthal, J.S., Helvey, R.A., Battalino, T.E., Fisk, C., and Greiman, P.W. (2003). Ozone transport by mesoscale and diurnal wind circulations across southern California. *Atmos. Environ.*, **37(S2)**:51-71.

- Seaman, N.L. (2000). Meteorological modeling for air-quality assessments. *Atmos. Environ.*, **34(12-14)**:2231-2259.
- Seinfeld, J.H. (1975). *Air Pollution: Physical and Chemical Fundamentals*. New York: McGraw-Hill, Inc.
- Seinfeld, J.H. (1986). *Atmospheric Chemistry and Physics of Air Pollution*. New York: John Wiley & Sons, Inc.
- Selwyn, B.J., Hardy, R.J., and Stock, T.H. (1983). Effect of exposure to air pollution on the respiratory function of healthy runners: methods and preliminary findings. In S.T. Lee, M.G. Mustafa, and M.A. Mehlman (Eds.). *International Symposium on the Biomedical Effects of Ozone and Related Photochemical Oxidants* (pp. 487-497). Princeton, N.J.: Princeton Scientific Publishers.
- Shaw, W.J., Doran, J.C., and Coulter, R.L. (2004). Boundary-layer evolution over Phoenix, Arizona and the premature mixing of pollutants in the early morning. *Atmos. Environ.*, **39(4)**:773-786.
- Simpson, D. (2005). Editorial cartoon. *Tulsa World*, specific date unknown.
- So, K.L., and Wang, T. (2003). On the local and regional influence on ground-level ozone concentrations in Hong Kong. *Environ. Pollut.*, **123(2)**:307-317.
- Solomon, P., Cowling, E., Hidy, G., and Furiness, C. (2000). Comparison of scientific findings from major ozone field studies in North America and Europe. *Atmos. Environ.*, **34(12-14)**:1885-1920.
- Stedman, J.R. (2004). The predicted number of air pollution related deaths in the UK during the August 2003 heatwave. *Atmos. Environ.*, **38(8)**:1087-1090.
- Steinbacher, M., Henne, S., Dommen, J., Wiesen, P., and Prevot, A.S.H. (2004). Nocturnal trans-alpine transport of ozone and its effects on air quality on the Swiss Plateau. *Atmos. Environ.*, **38(27)**:4539-4550.
- Stuckey, H.T., and Sattler, M.L. (2003). Air quality in the 21st century: community outreach in north central Texas. *Environ. Int.*, **29(2-3)**:341-346.
- Stull, R.B. (1988). *An Introduction to Boundary Layer Meteorology*. Dordrecht, Netherlands: Kluwer Academic Publishers.
- Stull, R.B. (2000). *Meteorology for Scientists and Engineers*. Pacific Grove, CA: Brooks/Cole.
- Sutton, O.G. (1953). *Micrometeorology*. New York: McGraw-Hill Book Co., Inc.

- Trainer, M., Parrish, D.D., Goldan, P.D., Roberts, J., and Fehsenfeld, F.C. (2000). Review of observation-based analysis of the regional factors influencing ozone concentrations. *Atmos. Environ.*, **34(12-14)**:2045-2061.
- Tulet, P., Suhre, K., Mari, C., Solmon, F., and Rosset, R. (2002). Mixing of boundary layer and upper tropospheric ozone during a deep convective event over Western Europe. *Atmos. Environ.*, **36(28)**:4491-4501.
- United States Environmental Protection Agency [EPA]. (2004). 8-hour ozone national ambient air quality standards, final rules. *Federal Register* (30 April 2004) 69(84):23858-23951.
- United States Environmental Protection Agency [EPA]. (2005). *Plan for review of the national ambient air quality standards for ozone*. Research Triangle Park, North Carolina: EPA Office of Air Quality Planning and Standards.
- United States Environmental Protection Agency [EPA]. (2006). National primary and secondary ambient air quality standards; Requirement for preparation, adoption, and submittal of implementation plans. *Code of Federal Regulations* Title 40, Pts. 50-51.
- United States Environmental Protection Agency [EPA Review]. (2006). *Review of the national ambient air quality standards for ozone: policy assessment of scientific and technical information* (EPA-452/D-05-002). Research Triangle Park, North Carolina: EPA Office of Air Quality Planning and Standards.
- University of Alabama-Huntsville [UAH]. (2006). *1999-2005 Ozone Data*. Retrieved 11/2006 from <http://vortex.nsstc.uah.edu/atmchem/ozonesonde/>
- Wang, T., Lam, K.S., Lee, A.S.Y., Pang, S.W., and Tsui, W.S. (1998). Meteorological and chemical characteristics of the photochemical ozone episodes observed at Cape D'Aguilar in Hong Kong. *J. Appl. Meteorol.*, **37(10)**:1167-1178.
- Wark, K., Warner, C.F., and Davis, W.T. (1998). *Air Pollution: Its Origin and Control*. Menlo Park, California: Addison-Wesley.
- Warneck, P. (2000). *Chemistry of the Natural Atmosphere*. New York: Academic Press.
- Wells, A.F. (1986). *Structural Inorganic Chemistry*. Oxford: Oxford University Press.
- Whiteman, C.D., Bian, X., and Zhong, S. (1997). Low-level jet climatology from enhanced rawinsonde observations at a site in the southern Great Plains. *J. Appl. Meteor.*, **36(10)**:1363-1376.

- Williams, D.J. (2001). *An investigation of the meteorological impact on ozone and precursor compound transport in the south central United States*. Unpublished master's thesis, University of Oklahoma, Norman, OK.
- Wilson, A.M., Wake, C.P., Kelly, T., and Salloway, J.C. (2005). Air pollution, weather, and respiratory emergency room visits in two northern New England cities: an ecological time-series study. *Environ. Res.*, **97(3)**:312-321.
- Yang, J., McBride, J., Zhou, J., and Sun, Z. (2005). The urban forest in Beijing and its role in air pollution reduction. *Urban Forestry & Urban Greening*, **3(2)**:65-78.
- Zhang, J., Rao, S.T., and Daggupati, S.M. (1998). Meteorological processes and ozone exceedances in the northeastern United States during the 12-16 July 1995 episode. *J. Appl. Meteorol.*, **37(8)**:776-789.
- Zhang, J., and Rao, S.T. (1999). The role of vertical mixing in the temporal evolution of ground-level ozone concentrations. *J. Appl. Meteorol.*, **38(12)**:1674-1691.

SELECTED REFERENCES

- Akimoto, H. (2003). Global air quality and pollution. *Science*, **302(5651)**:1716-1719.
- Aloyan, A.E., Arutyunyan, V., Haymet, A.D., He, J.W., Kuznetsov, Y., and Lubertino, G. (2003). Air quality modeling for Houston-Galveston-Brazoria area. *Environ. Int.*, **29(2-3)**:377-383.
- Appenzeller, C. and Davies, H.C. (1992). Structure of stratospheric intrusions into the troposphere. *Nature*, **358(6387)**:570-572.
- Attri, A.K., Kumar, U., and Jain, V.K. (2001). Formation of ozone by fireworks. *Nature*, **411(6841)**:1015-1015.
- Baker, J., Walker, H., and Cai, X. (2004). A study of the dispersion and transport of reactive pollutants in and above street canyons – a large eddy simulation. *Atmos. Environ.*, **38(39)**:6883-6892.
- Baldasano, J.M., Valera, E., and Jiménez, P. (2002). Air quality data from large cities. *Sci. Total Environ.*, **307(1-3)**:141-165.
- Baldwin, M.P., Thompson, D.W.J., Shuckburgh, E.F., Norton, W.A., and Gillett, N.P. (2003). Weather from the stratosphere? *Science*, **301(5631)**:317-319.
- Baldwin, M.P., and Dunkerton, T.J. (2005). The solar cycle and stratosphere-troposphere dynamical coupling. *J. Atmos. Solar Terr. Phys.*, **67(1-2)**:71-82.
- Balsley, B.B., Frehlich, R.G., Jensen, M.L., Meillier, Y., and Muschinski, A. (2003). Extreme gradients in the nocturnal boundary layer: structure, evolution, and potential causes. *J. Atmos. Sci.*, **60(20)**:2496-2508.
- Barnard, W.F., Saxena, V.K., Wenny, B.N., and DeLuisi, J.J. (2003). Daily surface UV exposure and its relationship to surface pollutant measurements. *J. Air & Waste Manage. Assoc.*, **53(2)**:237-245.
- Barrero, M.A., Grimalt, J.O., and Cantón, L. (2006). Prediction of daily ozone concentration maxima in the urban atmosphere. *Chemom. Intell. Lab. Syst.*, **80(1)**:67-76.

- Bassow, H. (1976). *Air Pollution Chemistry: An Experimenter's Sourcebook*. Rochelle Park, New Jersey: Hayden Book Co., Inc.
- Baumgardner, R.E., and Edgerton, E.S. (1998). Rural ozone across the eastern United States: analysis of CASTNet data, 1988-1995. *J. Air & Waste Manage. Assoc.*, **48(8)**:674-688.
- Beaney, G., and Gough, W.A. (2002). The influence of tropospheric ozone on the air temperature of the city of Toronto, Ontario, Canada. *Atmos. Environ.*, **36(14)**:2319-2325.
- Beck, J.P., Asimakopoulos, N., Bazhanov, V., Bock, H.J., Chronopoulos, G., De Muer, D., Ebel, A., Flatøy, F., Hass, H., van Haver, P., Hov, Ø., Jakobs, H.J., Kirchner, E.J.J., Kunz, H., Memmesheimer, M., van Pul, W.A.J., Speth, P., Trickl, T., and Varotsos, C. (1997). Exchange of ozone between the atmospheric boundary layer and free troposphere. In Ø Hov (Ed.), *Tropospheric Ozone Research: Tropospheric Ozone in the Regional and Sub-Regional Context* (pp. 111-130). Berlin: Springer-Verlag.
- Beekmann, M., Ancellet, G., Blonsky, S., De Muer, D., Ebel, A., Elbern, H., Hendricks, J., Kowol, J., Mancier, C., Sladkovic, R., Smit, H.G.J., Speth, P., Trickl, T., and van Haver, P. (1997). Stratosphere-troposphere exchange: regional and global tropopause folding occurrence. In Ø Hov (Ed.), *Tropospheric Ozone Research: Tropospheric Ozone in the Regional and Sub-Regional Context* (pp. 131-149). Berlin: Springer-Verlag.
- Beevers, S.D., and Carslaw, D.C. (2005). The impact of congestion charging on vehicle emissions in London. *Atmos. Environ.*, **39(1)**:1-5.
- Berkowitz, C.M., Zaveri, R.A., Bian, X., Zhong, S., Disselkamp, R.S., Laulainen, N.S., and Chapman, E.G. (2001). Aircraft observations of aerosols, O₃, and NO_y in a nighttime urban plume. *Atmos. Environ.*, **35(13)**:2395-2404.
- Bernstein, J.A., Alexis, N., Barnes, C., Bernstein, I.L., Nel, A., Peden, D., Diaz-Sanchez, D., Tarlo, S.M., and Williams, P.B. (2004). Health effects of air pollution. *J. Allergy Clin. Immunol.*, **114(5)**:1116-1123.
- Betts, A.K., Gatti, L.V., Cordova, A.M., Silva Dias, M.A.F., and Fuentes, J.D. (2002). Transport of ozone to the surface by convective downdrafts at night. *J. Geophys. Res.*, **107(D20)**:8046.
- Blanchard, C.L., Lurmann, F.W., Roth, P.M., Jeffries, H.E., and Korc, M. (1999). The use of ambient data to corroborate analyses of ozone control strategies. *Atmos. Environ.*, **33(3)**:369-381.

- Blanchard, C.L. (2000). Ozone process insights from field experiments – Part III: extent of reaction and ozone formation. *Atmos. Environ.*, **34(12-14)**:2035-2043.
- Blanchard, C.L., and Stoeckenius, T. (2001). Ozone response to precursor controls: comparison of data analysis methods with the predictions of photochemical air quality simulation models. *Atmos. Environ.*, **35(7)**:1203-1215.
- Blanchard, C.L., and Fairley, D. (2001). Spatial mapping of VOC and NO_x-limitation of ozone formation in central California. *Atmos. Environ.*, **35(22)**:3861-3873.
- Bloomfield, P., Royle, J.A., Steinberg, L.J., and Yang, Q. (1996). Accounting for meteorological effects in measuring urban ozone levels and trends. *Atmos. Environ.*, **30(17)**:3067-3077.
- Bojkov, R.D. and Fabian, P. (Eds.) (1989). *Proceedings of the Quadrennial Ozone symposium 1988 and Tropospheric Ozone Workshop: Ozone in the Atmosphere*. (pp. 477-480). Hampton, Virginia: A. Deepak Publishing Co.
- Brankov, E., Henry, R.F., Civerolo, K.L., Hao, W., Rao, S.T., Misra, P.K., Bloxam, R., and Reid, N. (2003). Assessing the effects of transboundary ozone pollution between Ontario, Canada and New York, USA. *Environ. Pollut.*, **123(3)**:403-411.
- Bruntz, S.M., Cleveland, W.S., Graedel, T.E., Kleiner, B., and Warner, J.L. (1974). Ozone concentrations in New Jersey and New York: statistical association with related variables. *Science*, **186(4160)**:257-259.
- Cadle, R.D., and Allen, E.R. (1970). Atmospheric photochemistry. *Science*, **167(3916)**:243-249.
- Chang, T.Y., Chock, D.P., Nance, B.I., and Winkler, S.L. (1997). A photochemical extent parameter to aid ozone air quality management. *Atmos. Environ.*, **31(17)**:2787-2794.
- Chen, K.S., Ho, Y.T., Lai, C.H., Tsai, Y.A., and Chen, S.J. (2004). Trends in concentration of ground-level ozone and meteorological conditions during high ozone episodes in the Kao-Ping Airshed, Taiwan. *J. Air & Waste Manage. Assoc.*, **54(1)**:36-48.
- Cleveland, W.S., and Graedel, T.E. (1979). Photochemical air pollution in the northeast United States. *Science*, **204(4399)**:1273-1278.
- Cobourn, W.G., and Lin, Y. (2004). Trends in meteorologically adjusted ozone concentrations in six Kentucky metro areas, 1998-2002. *J. Air & Waste Manage. Assoc.*, **54(11)**:1383-1393.

- Colville, R.N., Hutchinson, E.J., Mindell, J.S., and Warren, R.F. (2001). The transport sector as a source of air pollution. *Atmos. Environ.*, **35(9)**:1537-1565.
- Cooper, C.D., and Alley, F.C. (1994). *Air Pollution Control: A Design Approach*. Prospect Heights, Illinois: Waveland Press.
- Cooper, O., Forster, C., Parrish, D., Dunlea, E., Hübler, G., Fehsenfeld, F., Holloway, J., Oltmans, S., Johnson, B., Wimmers, A., and Horowitz, L. (2004). On the life cycle of a stratospheric intrusion and its dispersion into polluted warm conveyor belts. *J. Geophys. Res.*, **109(D23)**:D23S09.
- Crutzen, P. and Lawrence, M. (1997). Ozone clouds over the Atlantic. *Nature*, **388(6643)**:625-626.
- Dawson, G.A. (1980). Nitrogen fixation by lightning. *J. Atmos. Sci.*, **37(1)**:174-178.
- Dayan, U. and Levy, I. (2002). Relationship between synoptic-scale atmospheric circulation and ozone concentrations over Israel. *J. Geophys. Res.*, **107(D24)**, 4813.
- de Leeuw, F.A.A.M. (2002). A set of emission indicators for long-range transboundary air pollution. *Environ. Sci. & Policy*, **5(2)**:135-145.
- Dickerson, R.R., Huffman, G.J., Luke, W.T., Nunnermacher, L.J., Pickering, K.E., Leslie, A.C.D., Lindsey, C.G., Slinn, W.G.N., Kelly, T.J., Daum, P.H., Delany, A.C., Greenberg, J.P., Zimmerman, P.R., Boatman, J.F., Ray, J.D., and Stedman, D.H. (1987). Thunderstorms: an important mechanism in the transport of air pollutants. *Science*, **235(4787)**:460-465.
- Dickerson, R.R., Gockel, B.S., Luke, W.T., McNamara, D.P., Nunnermacher, L.J., Pickering, K.E., Greenberg, J.P., and Zimmerman, P.R. (1989). Profiles of photochemically active trace gases in the troposphere. In R.D. Bojkov and P. Fabian (Eds.), *Proceedings of the Quadrennial Ozone symposium 1988 and Tropospheric Ozone Workshop: Ozone in the Atmosphere*. (pp. 463-466). Hampton, Virginia: A. Deepak Publishing Co.
- Ding, A. and Wang, T. (2006). Influence of stratosphere-to-troposphere exchange on the seasonal cycle of surface ozone at Mount Waliguan in western China. *Geophys. Res. Ltrs.*, **33(3)**:L03803.
- Dommen, J., Neftel, A., Sigg, A., and Jacob, D.J. (1995). Ozone and hydrogen peroxide during summer smog episodes over the Swiss Plateau: measurements and model simulations. *J. Geophys. Res.*, **100(D5)**:8953-8966.
- Draxler, R.R. (2000). Meteorological factors of ozone predictability at Houston, Texas. *J. Air & Waste Manage. Assoc.*, **50(2)**:259-271.

- Duardo, J.A. (1967). *Study to develop a technique for measurement of high altitude ozone parameters* (EOS Report 7087-IR-1). Cambridge, Massachusetts: National Aeronautics and Space Administration.
- E. Roberts Alley and Associates, Inc. [Roberts] (1998). *Air Quality Control Handbook*. New York: McGraw-Hill.
- Elminir, H.K. (2005). Dependence of urban air pollutants on meteorology. *Sci. Total Environ.*, **350(1-3)**:225-237.
- Fast, J.D., and Berkowitz, C.M. (1997). Evaluation of back trajectories associated with ozone transport during the 1993 North Atlantic Regional Experiment. *Atmos. Environ.*, **31(6)**:825-837.
- Fatogoma, O., and Jacko, R.B. (2002). A model to estimate mixing height and its effects on ozone modeling. *Atmos. Environ.*, **36(22)**:3699-3708.
- Finlayson, B.J., and Pitts, J.N. (1976). Photochemistry of the polluted troposphere. *Science*, **192(4235)**:111-119.
- Fritz, S. and Stevens, G.C. (1950). Atmospheric ozone at Washington, D.C. *Mon. Weather Rev.*, **78(8)**:135-147.
- Führer, J., and Booker, F. (2003). Ecological issues related to ozone: agricultural issues. *Environ. Int.*, **29(2-3)**:141-154.
- Götz, F.W.P. (1951). Ozone in the atmosphere. In T.F. Malone (Ed.), *Compendium of Meteorology* (pp. 275-291). Boston: American Meteorological Society.
- Grewe, V. (2005). The origin of ozone. *Atmos. Chem. Phys. Discuss.*, **5(5)**:9641-9668.
- Grooß, J.U., Brühl, C., and Peter, T. (1998). Impact of aircraft emissions on tropospheric and stratospheric ozone. Part I: chemistry and 2-D model results. *Atmos. Environ.*, **32(18)**:3173-3184.
- Grøntoft, T., Henriksen, J.F., and Seip, H.M. (2004). The humidity dependence on ozone deposition onto a variety of building surfaces. *Atmos. Environ.*, **38(1)**:59-68.
- Guarnieri, F.L., Echer, E., Pinheiro, D.K., and Schuch, N.J. (2004). Vertical ozone and temperature distributions above Maria, Brazil (1996-1998). *Adv. Space Res.*, **34(4)**:759-763.
- Haugen, D.A. (Ed.). (1973). *Workshop on Micrometeorology*. Boston, Massachusetts: American Meteorological Society.

- Heuss, J.M., Kahlbaum, D.F., and Wolff, G.T. (2003). Weekday/weekend ozone differences: what can we learn from them? *J. Air & Waste Manage. Assoc.*, **53(7)**:772-788.
- Hill, R.D., Rinker, R.G., and Wilson, H.D. (1980). Atmospheric nitrogen fixation by lightning. *J. Atmos. Sci.*, **37(1)**:179-192.
- Holton, J.R., Haynes, P.H., McIntyre, M.E., Douglass, A.R., Rood, R.B., and Pfister, L. (1995). Stratosphere-troposphere exchange. *Rev. Geophys.*, **33(4)**:403-439.
- Huser, A., Nilsen, P.J., and Skåtun, H. (1997). Application of k-ε model to the stable ABL: pollution in complex terrain. *J. Wind Eng. Ind. Aerodyn.*, **67-68**:425-436.
- Isaksen, I.S.A. (Ed.) (1988). *Tropospheric Ozone: Regional and Global Scale Interactions*. Proceedings of the NATO Advanced Workshop on Regional and Global Ozone Interaction and its Environmental Consequences. Dordrecht, Netherlands: D. Reidel Publishing Co.
- Isaksen, I.S.A., Zerefos, C., Kourtidis, K., Meleti, C., Dalsøren, S.B., Sundet, J.K., Grini, A., Zanis, P., and Balis, D. (2005). Tropospheric ozone changes at unpolluted and semipolluted regions induced by stratospheric ozone changes. *J. Geophys. Res.*, **110(D2)**:D02302.
- Jiang, G., and Fast, J.D. (2004). Modeling the effects of VOC and NO_x emission sources on ozone formation in Houston during the TexAQS 2000 field campaign. *Atmos. Environ.*, **38(30)**:5071-5085.
- Jo, W.K. and Nam, C.W. (1999). Characteristics of urban ground-level ozone in Korea. *J. Air & Waste Manage. Assoc.*, **49(12)**:1425-1433.
- Johnston, H. (1972). Newly recognized vital nitrogen cycle. *Proc. Nat. Acad. Sci. USA*, **69(9)**:2369-2372.
- Karoly, D.J. (2003). Ozone and climate change. *Science*, **302(5643)**:236-237.
- Kastner-Klein, P., and Plate, E.J. (1999). Wind-tunnel study of concentration fields in street canyons. *Atmos. Environ.*, **33(24-25)**:3973-3979.
- Kato, S., Kajii, Y., Itokazu, R., Hirokawa, J., Koda, S., and Kinjo, Y. (2004). Transport of atmospheric carbon monoxide, ozone, and hydrocarbons from Chinese coast to Okinawa Island in the western Pacific during winter. *Atmos. Environ.*, **38(19)**:2975-2981.
- Katzenstein, A.S., Doezema, L.A., Simpson, I.J., Blake, D.R., and Rowland, F.S. (2003). Extensive regional atmospheric hydrocarbon pollution in the southwestern United States. *Proc. Nat. Acad. Sci. USA*, **100(21)**:11975-11979.

- Khrgian, A.K. (1975). *The Physics of Atmospheric Ozone*. Jerusalem: Keter Publishing House.
- Kim, G.D., Davis, W.T., and Miller, T.L. (2004). Prediction of the vertical profile of ozone based on ground-level ozone observations and cloud cover. *J. Air & Waste Manage. Assoc.*, **54(4)**:483-494.
- Kleinman, L.I. (2000). Ozone process insights from field experiments – Part II: observation-based analysis for ozone production. *Atmos. Environ.*, **34(12-14)**:2023-2033.
- Kley, D. (1997). Tropospheric chemistry and transport. *Science*, **276(5315)**:1043-1045.
- Kroening, J.L. (1965). Stratosphere and troposphere: transport of material between them. *Science*, **147(3660)**:862-864.
- Lagzi, I., Mészáros, R., Horváth, L., Tomlin, A., Weidinger, T., Turányi, T., Ács, F., and Haszpra, L. (2004). Modelling ozone fluxes over Hungary. *Atmos. Environ.*, **38(36)**:6211-6222.
- Laskin, D. (2006). The great London smog. *Weatherwise*, **59(6)**:42-45.
- Lechón, Y., Cabal, H., Gómez, M., Sánchez, E., and Sáez, R. (2002). Environmental externalities caused by SO₂ and ozone pollution in the metropolitan area of Madrid. *Environ. Sci. & Policy*, **5(5)**:385-395.
- Lee, J.T., Kim, H., Hong, Y.C., Kwon, H.J., Schwartz, J., and Christiani, D.C. (2000). Air pollution and daily mortality in seven major cities of Korea, 1991-1997. *Environ. Res.*, **84(3)**:247-254.
- Lee, K., Parkhurst, W.J., Xue, J., Özkaynak, H., Neuberger, D., and Spengler, J.D. (2004). Outdoor/indoor/personal ozone exposures of children in Nashville, Tennessee. *J. Air and Waste Manage. Assoc.*, **54(3)**:352-359.
- Lee, S.T., Mustafa, M.G., and Mehlman, M.A. (Eds.) (1983). *International Symposium on the Biomedical Effects of Ozone and Related Photochemical Oxidants*. Princeton, N.J.: Princeton Scientific Publishers.
- Lelieveld, J., and Crutzen, P.J. (1994). Role of deep cloud convection in the ozone budget of the troposphere. *Science*, **264(5166)**:1759-1761.
- Li, Q., Jacob, D.J., Logan, J.A., Bey, I., Yantosca, R.M., Liu, H., Martin, R.V., Fiore, A.M., Field, B.D., and Duncan, B.N. (2001). A tropospheric ozone maximum over the Middle East. *Geophys. Res. Ltrs.*, **28(17)**:3235-3238.

- Li, Q., Jacob, D.J., Park, R., Wang, Y., Heald, C.L., Hudman, R., Yantosca, R.M., Martin, R.V., and Evans, M. (2005). North American pollution outflow and the trapping of convectively lifted pollution by upper-level anticyclone. *J. Geophys. Res.*, **110(D10)**:D10301.
- Lin, C.Y.C., Jacob, D.J., and Fiore, A.M. (2001). Trends in exceedances of the ozone air quality standard in the continental United States, 1980-1998. *Atmos. Environ.*, **35(19)**:3217-3228.
- Luttinger, D., and Wilson, L. (2003). A study of air pollutants and acute asthma exacerbations in urban areas: status report. *Environ. Pollut.*, **123(3)**:399-402.
- Mahlman, J.D. (1997). Dynamics of transport processes in the upper troposphere. *Science*, **276(5315)**:1079-1083.
- Mao, H. and Talbot, R. (2004). Relationship of surface O₃ to large-scale circulation patterns during two recent winters. *Geophys. Res. Ltrs.*, **31(6)**:L06108.
- Mao, H. and Talbot, R. (2004). Role of meteorological processes in two New England ozone episodes during summer 2001. *J. Geophys. Res.*, **109**, D20305, doi:10.1029/2004JD004850.
- Milanchus, M.L., Rao, S.T., and Zurbenko, I.G. (1998). Evaluating the effectiveness of ozone management efforts in the presence of meteorological variability. *J. Air & Waste Manage. Assoc.*, **48(3)**: 201-215.
- Miller, D.F., Alkezweeny, A.J., Hales, J.M., and Lee, R.N. (1978). Ozone formation related to power plant emissions. *Science*, **202(4373)**:1186-1188.
- Miller, P.R., Stolte, K.W., Duriscoe, D.M., and Pronos, J. (1996). *Evaluating Ozone Air Pollution Effects on Pines in the Western United States* (General Technical Report PSW-GTR-155). Berkeley, California: U.S. Department of Agriculture, Pacific Southwest Research Station.
- Miyazaki, K., Iwasaki, T., Shibata, K., and Deushi, M. (2005). Roles of transport in the seasonal variation of the total ozone environment. *J. Geophys. Res.*, **110(D18)**:D18309.
- Moody, J.L., Oltmans, S.J., Levy, H., and Merrill, J.T. (1995). Transport climatology of tropospheric ozone: Bermuda, 1988-1991. *J. Geophys. Res.*, **100(D4)**:7179-7194.
- Morris, A.L., and Barras, R.C. (Eds.) (1978). *Air Quality Meteorology and Atmospheric Ozone*. Baltimore, MD: American Society for Testing and Materials.

- Nappo, C.J. and Herwehe, J.A. (1989). Observations of ozone profiles in the developing convective boundary layer. In R.D. Bojkov and P. Fabian (Eds.), *Proceedings of the Quadrennial Ozone symposium 1988 and Tropospheric Ozone Workshop: Ozone in the Atmosphere*. (pp. 477-480). Hampton, Virginia: A. Deepak Publishing Co.
- Narasimhan, R., Keller, J., Subramaniam, G., Raasch, E., Croley, B., Duncan, K., and Potter, W.T. (2000). Ozone modeling using neural networks. *J. Appl. Meteorol.*, **39(3)**:291-296.
- Nelson, S.E., Howieson, E., and Amburn, S. (2002). Experiences with a grid-based forecasting approach using IFPS at the Tulsa WFO. *American Meteorological Society Interactive Symposium on AWIPS*, Orlando, Florida, 12-17 January 2002.
- Ostro, B.D., Tran, H., and Levy, J.I. (2006). The health benefits of reduced tropospheric ozone in California. *J. Air & Waste Manage. Assoc.*, **56(7)**:1007-1021.
- Parrish, D.D., Holloway, J.S., Trainer, M., Murphy, P.C., Forbes, G.L., and Fehsenfeld, F.C. (1993). Export of North American ozone pollution to the North Atlantic Ocean. *Science*, **259(5100)**:1436-1439.
- Placet, M. Mann, C.O., Gilbert, R.O., and Niefer, M.J. (2000). Emissions of ozone precursors from stationary sources: a critical review. *Atmos. Environ.*, **34(12-14)**:2183-2204.
- Porter, P.S., Rao, S.T., Zurbenko, I.G., Dunker, A.M., and Wolff, G.T. (2001). Ozone air quality over North America: Part II – an analysis of trend detection and attribution techniques. *J. Air & Waste Manage. Assoc.*, **51(2)**:283-306.
- Prados, A.I., Dickerson, R.R., Doddridge, B.G., Milne, P.A., Moody, J.L., and Merrill, J.T. (1999). Transport of ozone and pollutants from North America to the North Atlantic Ocean during the 1996 Atmosphere/Ocean Chemistry Experiment (AEROCE) intensive. *J. Geophys. Res.*, **104(D21)**:26219-26233.
- Pun, B.K., Seigneur, C., and White, W. (2003). Day-of-week behavior of atmospheric ozone in three U.S. cities. *J. Air & Waste Manage. Assoc.*, **53(7)**: 789-801.
- Randel, W.J., Stolarski, R.S., Cunnold, D.M., Logan, J.A., Newchurch, M.J., and Zawodny, J.M. (1999). Trends in the vertical distribution of ozone. *Science*, **285(5434)**:1689-1692.
- Rao, S.T., Zurbenko, I.G., Neagu, R., Porter, P.S., Ku, J.Y., and Henry, R.F. (1997). Space and time scales in ambient ozone data. *Bull. Am. Meteorol. Soc.*, **78(10)**:2153-2166.

- Rappenglück, B., and Fabian, P. (1999). An analysis of simultaneous online GC measurements of BTEX aromatics at three selected sites in the greater Munich area. *J. Appl. Meteorol.*, **38(10)**:1448-1462.
- Rappenglück, B., Oyola, P., Olaeta, I., and Fabian, P. (2000). The evolution of photochemical smog in the metropolitan area of Santiago de Chile. *J. Appl. Meteorol.*, **39(3)**:275-290.
- Rasool, S.I. (Ed.). (1973). *Chemistry of the Lower Atmosphere*. New York: Plenum Press.
- Ravishankara, A.R., Hancock, G., Kawasaki, M., and Matsumi, Y. (1998). Photochemistry of ozone: surprises and recent lessons. *Science*, **280(5360)**:60-61.
- Ren, X., Harder, H., Martinez, M., Leshner, R.L., Oligier, A., Simpao, J.B., Brune, W.H., Schwab, J.J., Demerjian, K.L., He, Y., Zhou, X., and Gao, H. (2003). OH and HO₂ chemistry in the urban atmosphere of New York City. *Atmos. Environ.*, **37(26)**:3639-3651.
- Riveros, H.G., Arriaga, J.L., Tejeda, J., Julián-Sánchez, A., and Riveros-Rosas, H. (1998). Ozone and its precursors in the atmosphere of Mexico City. *J. Air & Waste Manage. Assoc.*, **48(9)**:866-871.
- Rohrer, F. and Berresheim, H. (2006). Strong correlation between levels of tropospheric hydroxyl radicals and solar ultraviolet radiation. *Nature*, **442(7099)**:184-187.
- Rondanelli, R., Gallardo, L., and Garreaud, R.D. (2002). Rapid changes in ozone mixing ratios at Cerro Tololo (30°10'S, 70°48'W, 2200 m) in connection with cutoff lows and deep troughs. *J. Geophys. Res.*, **107(D23)**, 4677, doi:10.1029/2001JD001334.
- Rossby, C.G. (1942). Boundary-layer problems in the atmosphere and ocean. *Ann. NY Acad. Sci.*, **44(1)**:3-12.
- Russell, A., and Dennis, R. (2000). NARSTO critical review of photochemical models and modeling. *Atmos. Environ.*, **34(12-14)**:2283-2324.
- Ryan, W.F., Doddridge, B.G., Dickerson, R.R., Morales, R.M., Hallock, K.A., Roberts, P.T., Blumenthal, D.L., Anderson, J.A., and Civerolo, K.L. (1998). Pollutant transport during a regional O₃ episode in the Mid-Atlantic states. *J. Air & Waste Manage. Assoc.*, **48(9)**:786-797.
- Ryerson, T.B., Trainer, M., Holloway, J.S., Parrish, D.D., Huey, L.G., Sueper, D.T., Frost, G.J., Donnelly, S.G., Schauffler, S., Atlas, E.L., Kuster, W.C., Goldan, P.D., Hübler, G., Meagher, J.F., and Fehsenfeld, F.C. (2001). Observations of ozone formation in power plant plumes and implications for ozone control strategies. *Science*, **292(5517)**:719-723.

- Sánchez, M.L., Rodríguez, R., and López, A. (1997). Ozone dry deposition in a semi-arid steppe and in a coniferous forest in southern Europe. *J. Air & Waste Manage. Assoc.*, **47(7)**:792-799.
- Schultz, D.M., and Doswell, C.A. (2000). Analyzing and forecasting Rocky Mountain lee cyclogenesis often associated with strong winds. *Wea. Forecasting*, **15(2)**:152-173.
- Seinfeld, J.H. (1989). Urban air pollution: state of the science. *Science*, **243(4892)**:745-752.
- Seinfeld, J.H. and Pandis, S.N. (1998). *Atmospheric Chemistry and Physics*. New York: John Wiley & Sons, Inc.
- Sistla, G., Zalewsky, E., and Henry, R. (2002). An examination of the 6:00 a.m. – 9:00 a.m. measurements of ozone precursors in the New York City metropolitan area. *J. Air & Waste Manage. Assoc.*, **52(2)**: 181-188.
- Solomon, B.D. and Gorman, H.S. (1998). State-level air emissions trading: the Michigan and Illinois models. *J. Air & Waste Manage. Assoc.*, **48(12)**:1156-1165.
- Spedding, D.J. (1974). *Air Pollution*. Oxford, United Kingdom: Oxford University Press.
- Stehr, J.W., Ball, W.P., Dickerson, R.R., Doddridge, B.G., Piety, C.A., and Johnson, J.E. (2002). Latitudinal gradients in O₃ and CO during INDOEX 1999. *J. Geophys. Res.* **107(D19)**:8015.
- Stephenson, D.B. (2000). Use of the “odds ratio” for diagnosing forecast skill. *Wea. Forecasting*, **15(2)**:221-232.
- Suhre, K., Cammas, J.P., Nédelec, P., Rosset, R., Marenco, A., and Smit, H.G.J. (1997). Ozone-rich transients in the upper equatorial Atlantic troposphere. *Nature*, **388(6643)**:661-663.
- Suppan, P., and Schädler, G. (2004). The impact of highway emissions on ozone and nitrogen oxide levels during specific meteorological conditions. *Sci. Total Environ.*, **334-335**:215-222.
- Taha, H., Konopacki, S., and Akbari, H. (1998). Impacts of lowered urban air temperatures on precursor emission and ozone air quality. *J. Air & Waste Manage. Assoc.*, **48(9)**: 860-865.
- Thompson, M.L., Reynolds, J., Cox, L.H., Guttorp, P., and Sampson, P.D. (1999). A review of statistical methods for the meteorological adjustment of tropospheric ozone (NRCSE-TRS No. 26). Seattle: National Research Center for Statistics and the Environment.

- Unger, N., Shindell, D.T., Koch, D.M., and Streets, D.G. (2006). Cross influences of ozone and sulfate precursor emissions changes on air quality and climate. *Proc. Nat. Acad. Sci. USA*, **103**(12):4377-4380.
- United States Environmental Protection Agency [EPA]. (1997). National ambient air quality standards for ozone, final rule. *Federal Register* (18 July 1997) 62(138):38855-38896.
- Varandas, A.J.C., and Zhang, L. (2005). Vibrational relaxation of highly excited HO₂ in collisions with O₂. *Chem. Phys. Lett.*, **402**(1-3):399-407.
- Vaughan, G., and Price, J.D. (1989). Ozone transport into the troposphere in a cut-off low event. In R.D. Bojkov and P. Fabian (Eds.), *Proceedings of the Quadrennial Ozone symposium 1988 and Tropospheric Ozone Workshop: Ozone in the Atmosphere*. (pp. 415-418). Hampton, Virginia: A. Deepak Publishing Co.
- Vautard, R., Szopa, S., Beekmann, M., Menut, L., Hauglustaine, D.A., Rouil, L., and Roemer, M. (2006). Are decadal anthropogenic emission reductions in Europe consistent with surface ozone observations? *Geophys. Res. Lett.*, **33**, L13810, doi:10.1029/2006GL026080.
- Vingarzan, R. and Thomson, B. (2004). Temporal variation in daily concentrations of ozone and acid-related substances at Saturna Island, British Columbia. *J. Air & Waste Manage. Assoc.*, **54**(4):459-472.
- Volk, C.M., Elkins, J.W., Fahey, D.W., Salawitch, R.J., Dutton, G.S., Gilligan, J.M., Proffitt, M.H., Loewenstein, M., Podolske, J.R., Minschwaner, K., Margitan, J.J., and Chan, K.R. (1996). Quantifying transport between the tropical and mid-latitude lower stratosphere. *Science*, **272**(5269):1763-1768.
- Volz, A., Mihelcic, D., Müsgen, P., Pätz, H.W., Pilwat, G., Geiss, H., and Kley, D. (1988). Ozone production in the Black Forest: direct measurements of RO₂, NO_x, and other relevant parameters. In I.S.A. Isaksen (Ed.), *Tropospheric ozone: Regional and global scale interactions*. (pp. 293-302). Dordrecht, Netherlands: D. Reidel Publishing Co.
- Vukovich, F.M., Wayland, R., and Sherwell, J. (1999). Characteristics of ozone in the Baltimore-Washington area as established from one-hour average concentrations. *J. Air & Waste Manage. Assoc.*, **49**(7):794-803.
- Wang, G., and Ostoja-Starzewski, M. (2004). A numerical study of plume dispersion motivated by a mesoscale atmospheric flow over a complex terrain. *Appl. Math. Model.*, **28**(11):957-981.
- Wegman, L., and Sasser, E. (2005). The path toward clean air: implementing new standards for ozone and fine particles. *Environ. Manager*, **April 2005**:8-15.

- Wennberg, P.O. (2006). Radicals follow the sun. *Nature*, **442(7099)**:145-146.
- Wesely, M.L. and Hicks, B.B. (2000). A review of the current status of knowledge on dry deposition. *Atmos. Environ.*, **34(12-14)**:2261-2282.
- Weston, K.J., Kay, P.J.A., Fowler, D., Martin, A., and Bower, J.S. (1989). On the extent of photochemical ozone production over the U.K. In R.D. Bojkov and P. Fabian (Eds.), *Proceedings of the Quadrennial Ozone symposium 1988 and Tropospheric Ozone Workshop: Ozone in the Atmosphere*. (pp. 455-458). Hampton, Virginia: A. Deepak Publishing Co.
- White, W.H., Anderson, J.A., Blumenthal, D.L., Husar, R.B., Gillani, N.V., Husar, J.D., and Wilson, W.E. (1976). Formation and transport of secondary air pollutants: ozone and aerosols in the St. Louis urban plume. *Science*, **194(4261)**:187-189.
- Wilkening, K.E., Barrie, L.A., and Engle, M. (2000). Trans-Pacific air pollution. *Science*, **290(5489)**:65-67.
- Williams, M. (2004). Air pollution and policy—1952-2002. *Sci. Total Environ.*, **334-335(1)**:15-20.
- Wilson, A.M., Salloway, J.C., Wake, C.P., and Kelly, T. (2004). Air pollution and the demand for hospital services: a review. *Environ. Int.*, **30(8)**:1109-1118.
- Wilson, F.W. (2002). Additional measures of skill for probabilistic forecasts. *American Meteorological Society 16th Conference on Probability and Statistics in the Atmospheric Sciences*, Orlando, Florida, 12-17 January 2002.
- Wolff, G.T., Kelly, N.A., and Ferman, M.A. (1981). On the sources of summertime haze in the eastern United States. *Science*, **211(4483)**:703-705.
- Wolff, G.T., Dunker, A.M., Rao, S.T., Porter, P.S., and Zurbenko, I.G. (2001). Ozone air quality over North America: Part I – a review of reported trends. *J. Air & Waste Manage. Assoc.*, **51(2)**:273-282.
- World Meteorological Organization [WMO]. (1998). *Scientific assessment of ozone depletion: executive summary* (Report No. 44). Geneva: Global Ozone Research and Monitoring Project.
- Wulf, O.R. (1935). Light absorption in the atmosphere and its photochemistry. *J. Opt. Soc. Am.*, **25**:231-236.
- Wulf, O.R. and Deming, L.S. (1937). The distribution of atmospheric ozone in equilibrium with solar radiation and the rate of maintenance of the distribution. *Terr. Mag.*, **42(2)**:195-202.

- Wulf, O.R. (1942). The distribution of atmospheric ozone. *Proc. 8th Am. Sci. Congr.*, **7**:439-446.
- Xiangdong, Z., Xiuji, Z., Jie, T., Yu, Q., and Chuenyu, C. (2004). A meteorological analysis on a low tropospheric ozone event over Xining, north western China on 26-27 July 1996. *Atmos. Environ.*, **38(2)**:261-271.
- Xie, S., Yu, T., Zhang, Y., Zeng, L., Qi, L., and Tang, X. (2004). Characteristics of PM₁₀, SO₂, NO_x and O₃ in ambient air during the dust storm period in Beijing. *Sci. Total. Environ.*, **345(1-3)**:153-164.
- Xu, J., Zhu, Y., and Li, J. (1997). Seasonal cycles of surface ozone and NO_x in Shanghai. *J. Appl. Meteorol.*, **36(10)**:1424-1429.
- You, C.F., Li, G.H., Qi, H.Y., and Xu, X.C. (2004). Motion of micro-particles in channel flow. *Atmos. Environ.*, **38(11)**:1559-1565.
- Zbinden, R.M., Cammas, J.P., Thouret, V., Nédélec, P., Karchner, F., and Simon, P. (2005). Mid-latitude tropospheric ozone columns from the MOZAIC program: climatology and interannual variability. *Atmos. Chem. Phys.*, **6(4)**:1053-1073.
- Zerefos, C.S., and Ghazi, A. (Eds.) (1984). *Atmospheric Ozone*. Proceedings of the Quadrennial Ozone Symposium. Dordrecht, Netherlands: Kluwer Academic Publishers.
- Zhang, R., Lei, W., Tie, X., and Hess, P. (2004). Industrial emissions cause extreme urban ozone diurnal variability. *Proc. Nat. Acad. Sci. USA*, **101(17)**:6346-6350.

APPENDIX I: METEOROLOGICAL TRENDS

GROUND-LEVEL DRY-BULB TEMPERATURE, 01 JUNE - 30 NOV 2005

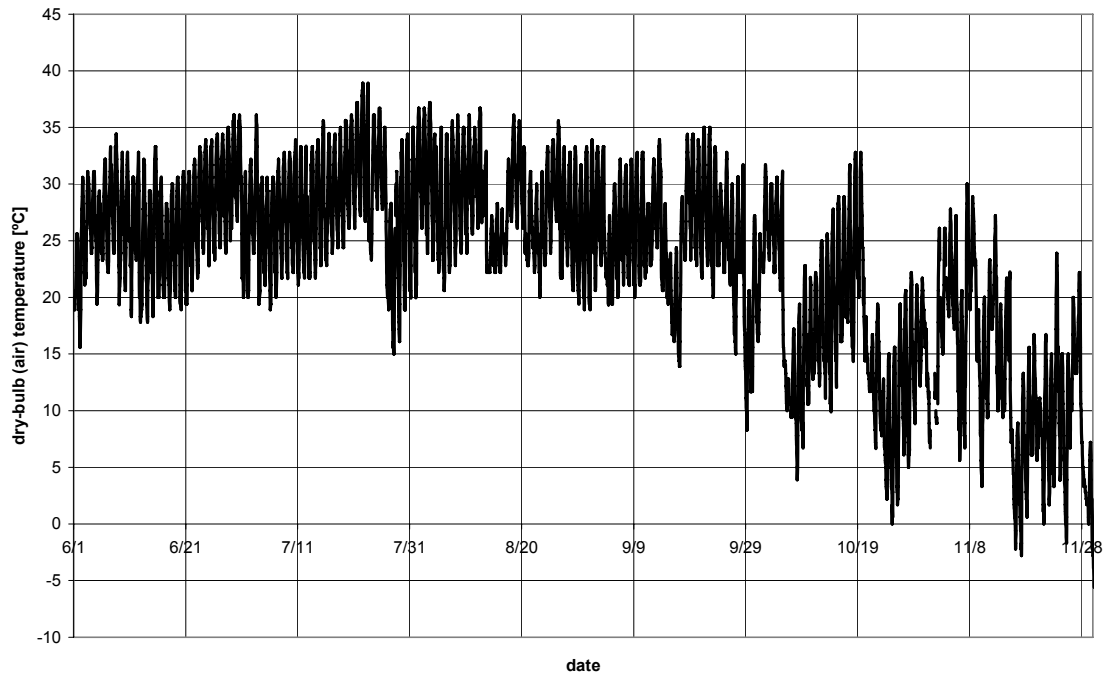


FIGURE A.1: 6-month plot of hourly ground-level dry-bulb temperature, Tulsa International Airport (01 June 2005 – 30 November 2005)

GROUND-LEVEL DEW-POINT TEMPERATURE, 01 JUNE - 30 NOVEMBER 2005

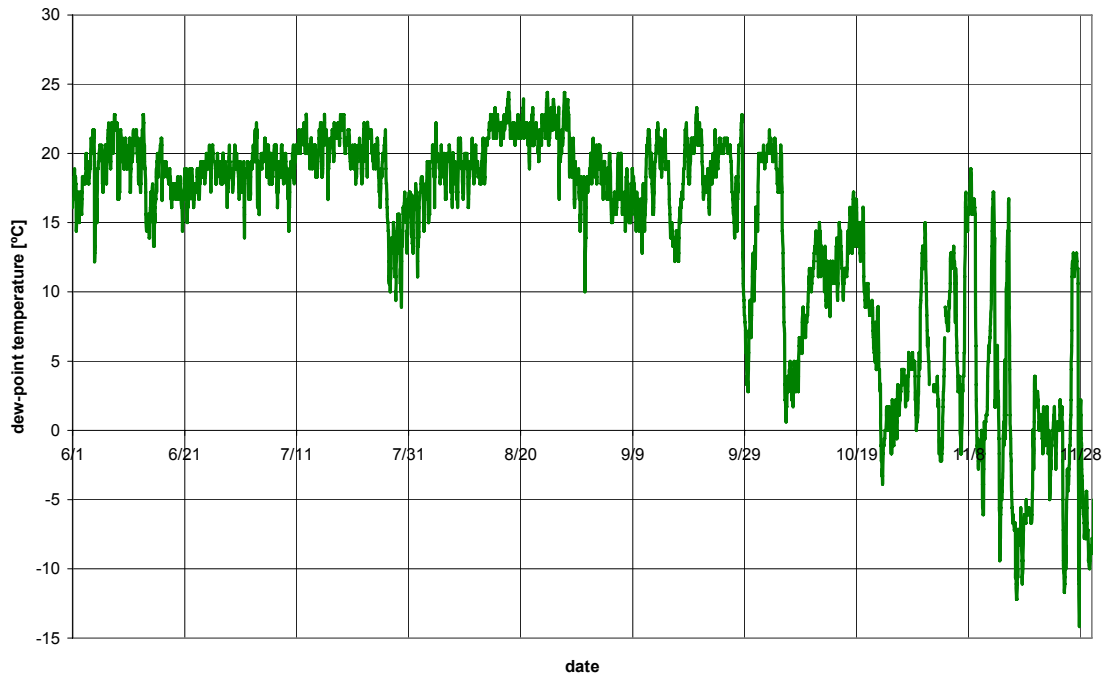


FIGURE A.2: 6-month plot of hourly ground-level dew-point temperature, Tulsa International Airport (01 June 2005 – 30 November 2005)

GROUND-LEVEL AIR PRESSURE, 01 JUNE - 30 NOVEMBER 2005

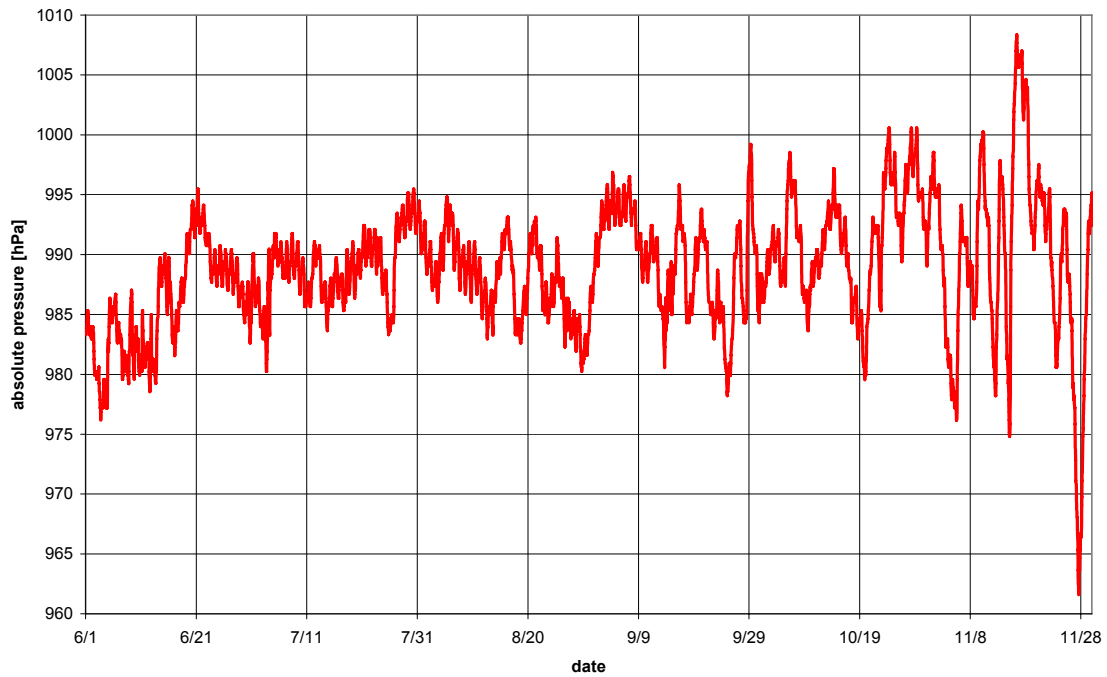


FIGURE A.3: 6-month plot of hourly ground-level air pressure, Tulsa International Airport (01 June 2005 – 30 November 2005)

GROUND-LEVEL WIND SPEED, 01 JUNE - 30 NOVEMBER 2005

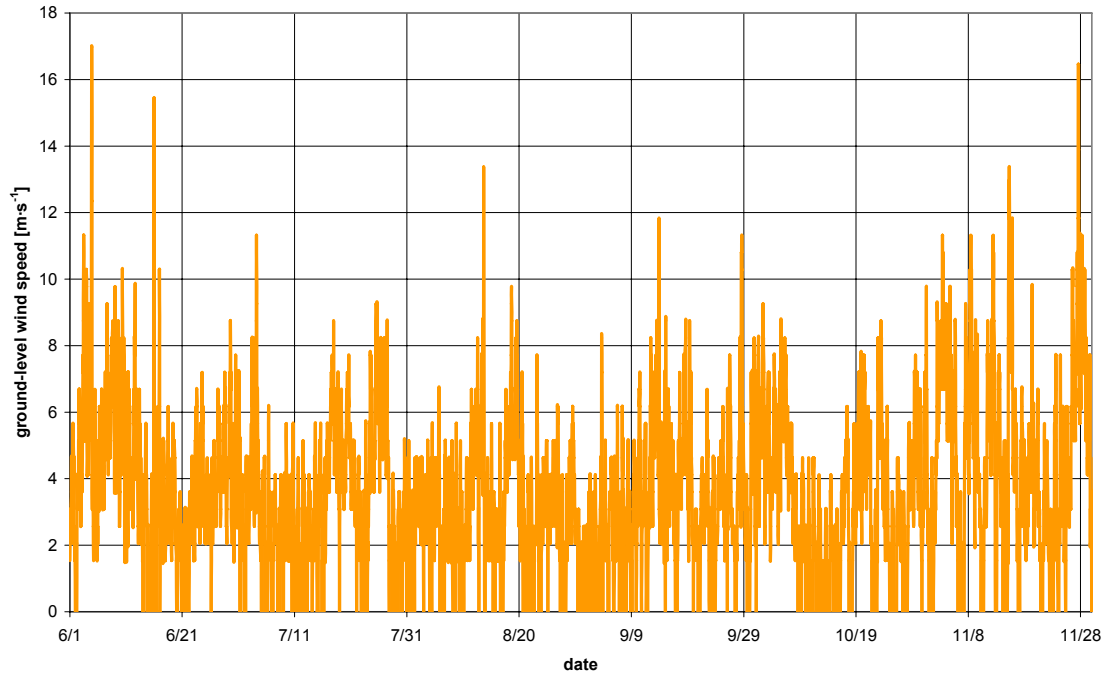


FIGURE A.4: 6-month plot of hourly ground-level wind speed, Tulsa International Airport (01 June 2005 – 30 November 2005)

210-METER WIND SPEED, 01 JUNE - 30 NOVEMBER 2005

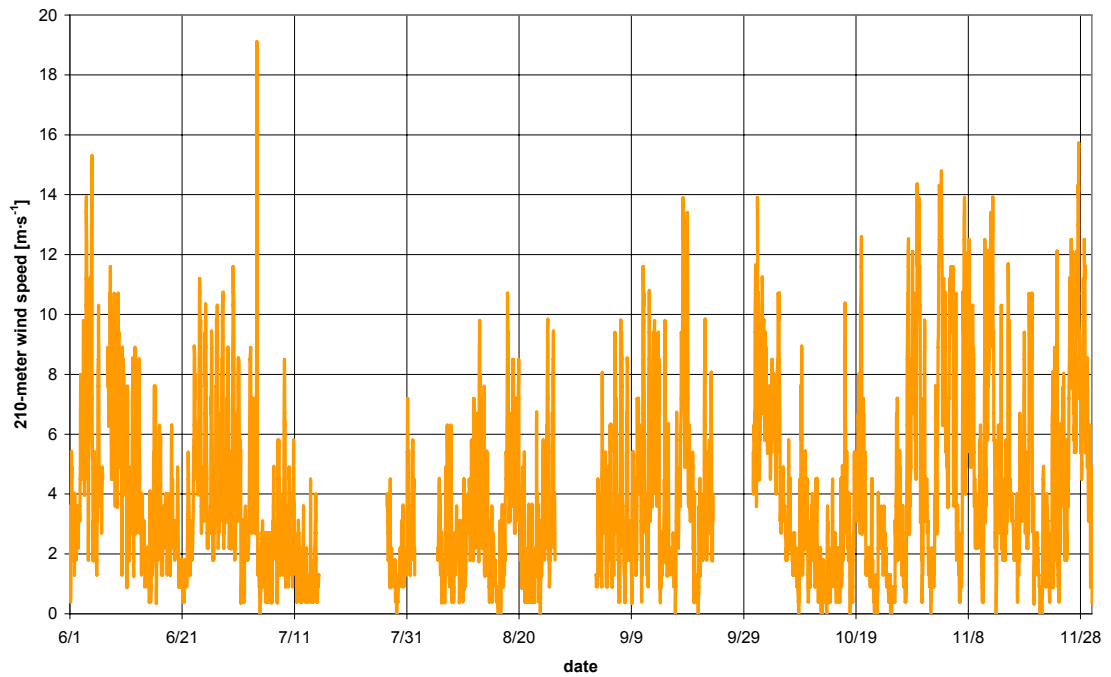


FIGURE A.5: 6-month plot of hourly 210-meter wind speed, Bank of Oklahoma Tower (01 June 2005 – 30 November 2005)

APPENDIX II: OPERATIONAL PHOTOGRAPHS



FIGURE A.6: Downtown Tulsa, Oklahoma (including the Bank of Oklahoma Tower, in foreground); 210-meter data collection occurred at the City of Tulsa Communications Facility, an enclosed structure on the roof of the Bank of Oklahoma Tower.



FIGURE A.7: Roof of the City of Tulsa Communications Facility, Bank of Oklahoma Tower; 210-meter ozone analyzer inlet was mounted on an adjacent pole on this structure.



FIGURE A.8: Ozone analyzer inlet, Bank of Oklahoma Tower; inlet was protected from water intrusion by a downward-placed funnel (blue object in photograph to the left of the access ladder).



FIGURE A.9: Thermo Electron Corp. Model 49C O₃ Analyzer (front), Bank of Oklahoma Tower; easy access was provided as a result of placement on a communications rack.



FIGURE A.10: Thermo Electron Corp. Model 49C O₃ Analyzer (back), Bank of Oklahoma Tower; the inlet stream was protected with a particulate matter filter that required replacement every two weeks (orange object).



FIGURE A.11: 2B Technologies Model 202 O₃ payload, 08 October 2005 ozonesonde launch; the analyzer and accompanying circuit board were assembled in a padded box for landing protection.



FIGURE A.12: Ozonesonde launch, 08 October 2005; the balloon launch carried the ozone analyzer, two transmitters (for tracking), a camera, and a landing chute.

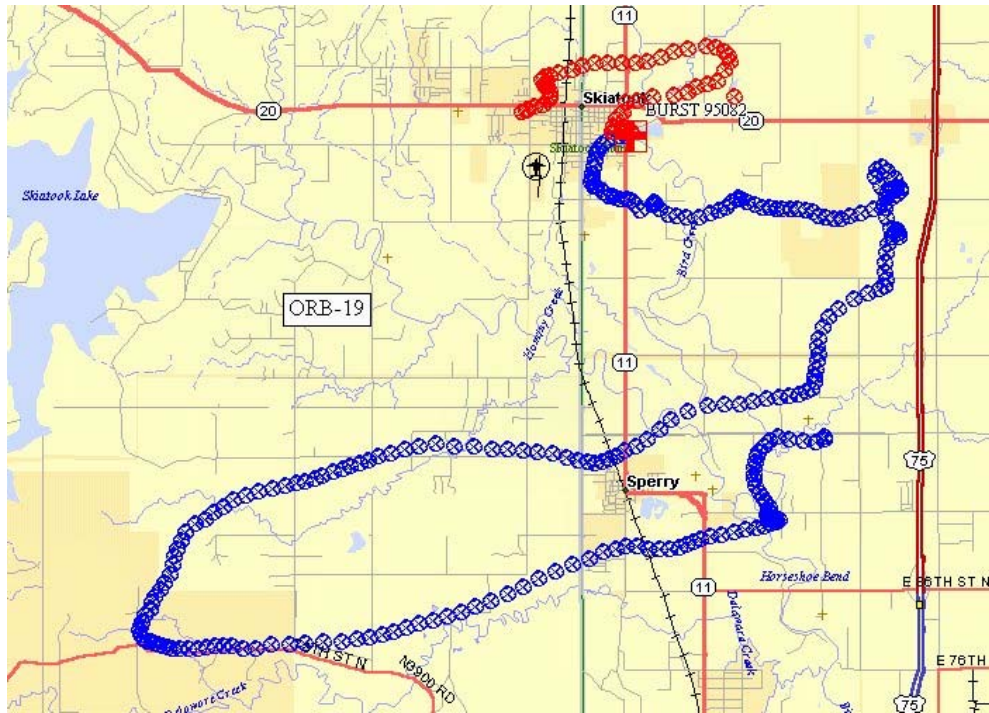


FIGURE A.13: Ozonesonde flight path, 08 October 2005 (ascent represented as a blue track; descent represented as a red track); the balloon, while rising vertically into the stratosphere, did not stray far from the launch point as a result of relatively weak wind speeds.



FIGURE A.14: Image captured by onboard camera as the ozonesonde was at an altitude of 25,300 meters over the City of Tulsa on 08 October 2005.

APPENDIX III: NEWS ARTICLES



Research for a Better Tulsa

OSU graduate students combine rigorous academic research with practical application to real-world issues. Civil Engineering Ph.D. student David Williams' research on Tulsa's ozone levels is just one example of how OSU-Tulsa works for a better community and beyond.

OSU-Tulsa checks David Williams, on top of the BOC Tower in downtown Tulsa, checks weathering instrument for his research on the city's ozone.

Center for Health Sciences Okmulgee **Tulsa** Stillwater

THE STATE'S UNIVERSITY



FIGURE A.15: Oklahoma State University promotional advertisement appearing in the *Tulsa World*, February 10, 2006.

The purpose of the research is to measure how much ozone is produced locally during an entire ozone season, which typically begins in May and ends in October.

Getting in the **Zone**

With summertime ozone alerts a distant memory and winter weather upon us, one Oklahoma State University-Tulsa student's research on the ozone is heating up.

David Williams, a civil engineering doctoral student at OSU-Tulsa, has been collecting data on Tulsa's ozone since May. Now Williams will begin to analyze that data and study the effects of the ozone on Tulsa's air quality. Williams was awarded a fellowship of \$37,000 by the Environmental Protection Agency (EPA) to complete the study.

"OSU is committed to research efforts that will make beneficial impacts in our community and nationally," said OSU-Tulsa President Gary Trennepohl. "David Williams' research is a great example of combining rigorous academic research with practical application to real-world issues."

The EPA's Greater Research Opportunities (GRO) Graduate Fellowship Program will fund Williams' research for a period of three years. The GRO program sponsors master's and doctoral level students in environmentally related fields of study. More than 1,300 applicants compete each year for approximately 100 fellowships through a rigorous merit review process.

Williams said he is honored to receive a prestigious fellowship for his research that could benefit state and national environmental agencies.

"When choosing a Ph.D. project, I wanted to focus on an issue that was relevant to the local area," Williams said. "I think it is important for state universities to research topics that affect the local population."

Williams said the purpose of his research is to get a measurement of how much ozone is locally produced during an entire ozone season, which typically begins in May and ends in October.

"In this project, I'll be trying to determine if the ozone is solely locally generated or if transported ozone is significantly affecting the air quality in Tulsa," Williams said. "Tulsa's amount of ground-level ozone is one of the pollutants that determine the EPA's designation of our city."

According to the EPA, a city or area may be designated as "attainment" or "nonattainment" based on the number of violations of the national 8-hour ozone standard over a three-year period.

"The outcome of this research could ultimately impact Tulsa's status on attainment," Williams said. "It could certainly assist the Oklahoma Department of Environmental Quality (ODEQ) when it considers and implements strategies on tackling ozone problems."

ODEQ donated two analyzing instruments to OSU for the purpose of this study. Williams said the units, which are the

same instruments used to measure data to determine "ozone alerts," were placed on the roof of the Bank of Oklahoma Tower in downtown Tulsa in May to collect data. The City of Tulsa provided the space and power for the instrumentation.

Williams also launched an ozone analyzer-equipped research balloon, known as an "ozonesonde," for additional data collection. He plans to present his research at the EPA's national conference in September 2006.

"While at OSU-Tulsa, I've had the opportunity to study with world-class faculty," Williams said. "I'm excited about applying that knowledge as emphasis continues to be placed on protection of the environment."

Trish McBeath



Photo: Gary Lindber

OSU-Tulsa researcher David Williams checks ozone analyzing instruments atop the BOK Tower in downtown Tulsa.

VANGUARD

22 Research at Oklahoma State University • www.pr.okstate.edu

FIGURE A.16: Article appearing in the 2006 issue of *Vanguard*, the research magazine of Oklahoma State University.

Cherokee Heritage Center receives financial support

TAHLEQUAH, Okla. – The Cherokee Heritage Center and the Cherokee Nation reached an agreement recently that will allow the CHC to concentrate on programming.

Melanie Knight, CN executive officer, said finances have been a challenge for the CHC for several years.

"We wanted to provide a level of financial stability so they can focus on fundraising and programming activities and other things they would like to do without worrying about how they are going to make payroll," Knight said.

The CN will provide more financial support and allow the CHC to take advantage of other tribal services.

"Many of the operational employees have become employees of the (Cherokee) Nation in order to get them a consistent employment package with fringe benefits, insurance, a 401(k) – access to things they didn't have," Knight said. "They also have access to our internal systems like IS (Information Systems), getting a Web page

and getting support for that. They are also getting support from facilities. We are doing some facilities repair over there and getting them into our capital improvement planning for the next five to 10 years."

The CHC will also have access to CN central systems such as human resources and accounting.

"We were doing some cultural programming and they were doing some cultural programming and many times it was similar kinds of work that could really get the benefit of some synergy if we worked together on them," Knight said. "Another objective was the work and coordinating – what they are doing with what we are doing with the Cultural Resource Center."

Cherokee Nation Enterprises is also involved.

"The part of the agreement that involved CNE has to do with the retail operations," Knight said. "CNE's being able to provide support there in regard to marketing, in regard to point of sales systems and the technology they will use in the gift shop."

Cherokee awarded EPA Fellowship to research ozone, air quality

TULSA, Okla. – With summertime ozone alerts a distant memory, one Oklahoma State University-Tulsa student's research heated up during the winter.

Cherokee citizen David Williams, a civil engineering doctoral student at OSU-Tulsa, has been collecting data on Tulsa's ozone since May 2005. Now Williams is analyzing that data and studying the effects of the ozone on Tulsa's air quality. Williams was awarded a fellowship of \$37,000 by the Environmental Protection Agency to complete the study.

"OSU is committed to research efforts that will make beneficial impacts in our community and nationally," said OSU-Tulsa President Gary Trennepohl. "David Williams' research is a great example of combining rigorous academic research with practical application to real-world issues."

The EPA's Greater Research Opportunities Graduate Fellowship Program will fund Williams' research for three years. The GRO program sponsors master's degree- and doctoral-level students in environmentally related fields of study. More than 1,300 applicants compete each year for approximately 100 fellowships.

Williams said he is honored to receive a fellowship for his research that could benefit state and national environmental agencies.

"When choosing a Ph.D. project, I wanted to focus on an issue that was relevant to the local area," Williams said. "I think it is important for state universities to research topics that affect the local population."

Williams said the purpose of his research is to get a measurement of how much ozone is locally produced during an entire ozone season, which typically begins in May and ends in October.

"I'll be trying to determine if the ozone is solely locally generated or if transported ozone is significantly affecting the air quality in Tulsa," Williams said. "Tulsa's amount of ground-level ozone is one of the pollutants that determine the EPA's designation of our city."



David Williams

According to the EPA, a city or area may be designated as "attainment" or "nonattainment" based on the number of violations of the national eight-hour ozone standard over a three-year period.

"The outcome of this research could ultimately impact Tulsa's status on attainment," Williams said. "It could certainly assist the Oklahoma Department of Environmental Quality when it considers and implements strategies on tackling ozone problems."

ODEQ donated two analyzing instruments to OSU for the purpose of this study. Williams said the units, which are the same instruments used to measure data to determine "ozone alerts," were placed on the roof of the Bank of Oklahoma Tower in Tulsa in May to collect data. The City of Tulsa provided the space and power for the instrumentation.

Williams also launched an ozone analyzer-equipped research balloon, known as an "ozoneosonde," for additional data collection. He plans to present his research at the EPA's national conference in September 2006.

"While at OSU-Tulsa, I've had the opportunity to study with world-class faculty," Williams said. "I'm excited about applying that knowledge as emphasis continues to be placed on protection of the environment."

Williams is the son of Thomas and Nedra Williams, and the grandson of the late Hubert and Ruth (Cochran) Williams and Irene and the late Alvie McMillan, all of Catoosa.

Cherokee Language

GWY JEBUQ

Great for Children!



\$19.95 each
plus S&H

Share the Cherokee language with your children with these delightful CDs. Each one has a booklet with all the phrases in both English and Cherokee.



\$19.95 each
plus S&H

Share the Cherokee language with your children with these delightful CDs. Each one has a booklet with all the phrases in both English and Cherokee.

Also available:
Cherokee Glossary - The most complete glossary to date! Over 9500 words - explained! Edited and verified by Cherokee speakers - by Cherokees - for Cherokees! **\$49.95** plus S&H
The Lord's Prayer in Cherokee.
 Anthony Martin brings this beautiful CD to you with reverence and respect. Also original flute music and the "Legend of Choosing a Chief."
\$15.95 plus S&H

Call us today! 1-800-776-0842

Various Indian Peoples Publishing Co
 (918) 457-5834 Tahlequah, OK www.nativelanguages.com

Practice Cherokee - Animals		
Y C <i>Gi - til</i> Dog	TØL <i>I - na - da</i> Snake	DUH P <i>A - wo - ha - ð</i> Eagle
Ø H <i>W - ra</i> Cat	V α <i>Da - yab</i> Beaver	† Ø P <i>So - gwi - li</i> Horse

FIGURE A.17: Press release appearing in the April 2006 issue of the Cherokee Phoenix.

APPENDIX IV: ORIGINAL PUBLICATIONS

- Williams, D.J. (2006). Thermodynamics and weather balloons. *Weather*, **61(10)**:286-287.
- Williams, D.J. (**in press**). APRS and High-Altitude Research Balloons. *QST*, Accepted 02 December 2005.

Thermodynamics and weather balloons

Weather – October 2006, Vol. 61, No. 10

David Joe Williams
Oklahoma State University

Every day, hundreds of meteorological balloons are launched at various sites worldwide, providing atmospheric data that constitutes the backbone of weather forecasting. Weather balloons routinely burst at altitudes in excess of 25 000 m. In a recent experiment, an ozone sounding, or 'ozonesonde', was launched from a rural site near Tulsa, Oklahoma. Launch occurred at 1400 UTC on 8 October 2005 (Fig. 1). The balloon, weighing 600 g and constructed of latex, was designed for meteorological purposes. While standard meteorological data was not collected by the ozonesonde, corresponding data was available from the 1200 UTC atmospheric sounding launched at nearby Norman, Oklahoma (WMO 72357). Ozonesonde altitude data, recorded by an on-board GPS receiver, indicated a maximum (burst) altitude of 28 981 m. While the altitude achieved by the ozonesonde balloon is not remarkable, the fact that the balloon was visible during the entire flight with the naked eye is extraordinary. Although weak winds and clear skies contributed to the exceptional visibility of the balloon by ground observers, a simple thermodynamic relationship was responsible for the physical behaviour of the balloon itself.

Thermodynamic properties of the atmosphere that impact all meteorological balloons aided in the physical expansion of the ozonesonde balloon, thus contributing to its visibility at high altitudes. Compressible fluid properties – namely volume (V), pressure (p), and temperature (T) – are related through a combination of Charles' Law and Boyle's Law known as the ideal gas law (Eq. (1)). Application of this relationship can be used to determine the instantaneous volume (and subsequently the diameter) of an ozonesonde balloon that was launched on 8 October 2005 in an effort to construct a vertical ozone profile.

$$pV = nRT \quad (1)$$

The number of moles of helium (n) and the specific gas constant of helium (R) remain constant within the enclosed volume of the balloon through the atmospheric column, so the ideal gas law can be restated in terms of p , V , and T :

Thus,

$$V_F = \frac{p_0 V_0 T_F}{p_F T_0} \quad (2)$$

Assuming that the balloon is a perfect sphere,

$$V_0 = \frac{4}{3} \pi r_0^3 \quad (3)$$

Manufacturer specifications indicate an inflated balloon diameter of 1.77 m at standard temperature and pressure (25 °C, 1015 mbar). With this assumption, that the initial diameter was approximately 1.77 m, the initial balloon volume was calculated as 2.95 m³.

The 1200 UTC Norman, Oklahoma upper-

air sounding on 8 October 2005 (Fig. 2) indicated that the dry bulb temperature at 29 494 m above sea-level was -50.5 °C, and the corresponding pressure was 12.5 mbar. The maximum achieved balloon altitude was slightly less than this altitude (28 981 m), so the extrapolated temperature and pressure at maximum altitude are -51 °C and 13 mbar, respectively.

The uncorrected ground level pressure at the time of launch was 975 mbar, and the ground level temperature was 11 °C at nearby Tulsa, Oklahoma International Airport. Based on this data, the launch diameter and volume were calculated as 1.78 m and 2.93 m³, respectively.

When the corrected initial inflated balloon volume of 2.93 m³ was applied to Eq. (2) with corresponding sounding data, the final (burst) balloon volume was calculated as 171.78 m³.

At 28 981 m, the balloon diameter was 6.90 m, an increase of 388% over the ground level balloon diameter of 1.78 m. Figure 3,



Fig. 1 Preparation of the ozonesonde balloon for launch, 8 October 2005 (© 2005 Scott Mayes)

286



FIGURE A.18: Thermodynamics and Weather Balloons, part 1 (*Weather*, 61(10):286-287)

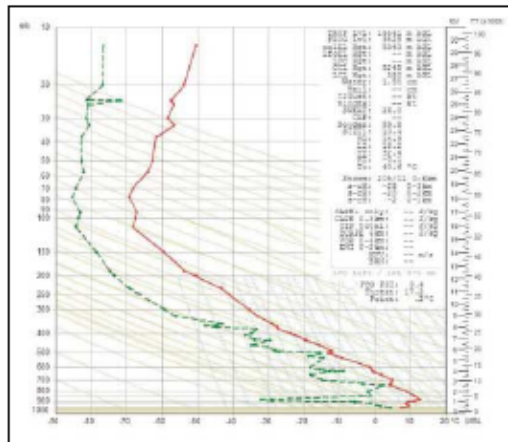


Fig. 2 1200 UTC Norman, Oklahoma sounding, 8 October 2005

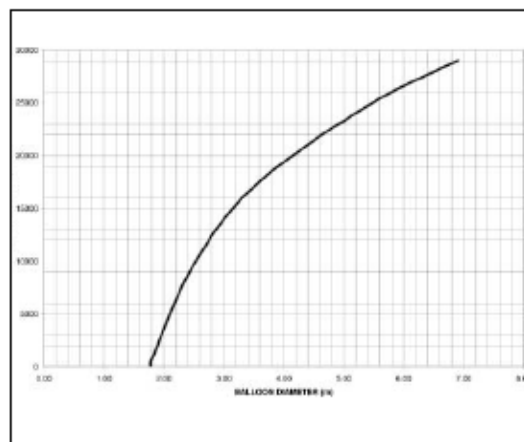


Fig. 3 Balloon diameter as a function of height

prepared with temperature and pressure data from the 1200 UTC atmospheric sounding, indicates a rapid increase in balloon diameter per unit altitude above 15 000 m.

The change in the rate of volumetric expansion is a consequence of the increase of pressure change as altitude increases. Above the troposphere, atmospheric pressures decrease rapidly as the bulk of the atmosphere is concentrated near the surface.

The ozonesonde balloon that was launched on 8 October 2005 was visible at

all altitudes, including the burst altitude of 28 981 m. In fact, it was more clearly visible at this altitude than it was at 5000–10 000 m, glistening in the overhead sky much like a neighbouring planet at dawn or dusk. Why was the ozonesonde balloon visible at such a high altitude? The balloon was volumetrically much larger at high altitude than it was when it was launched. Even though it was at a greater distance from the ground observer, it also had a diameter nearly 400% larger than it had prior to launch. The increase in balloon volume coupled with the balloon

colour (white) in stark contrast to the blackness of space in the thin atmosphere of the stratosphere allowed visible ground tracking of the ozonesonde balloon for the duration of the 2.5 hour flight.

Even though most people take them for granted, meteorological balloons are invaluable data gathering tools that allow short, medium, and long-term weather forecasting to be something more substantial than educated guesses. The construction of a weather balloon – specifically the ability to accommodate large volumetric expansion – is a critical issue in the attainment of data at high altitudes. Without this practical application of the works of Robert Boyle and Jacques Charles, meteorology would not be the same.

Acknowledgements

Data contained in this article were obtained as part of an ozone research project funded in part by Sigma Xi and the United States Environmental Protection Agency. Special thanks to William Potter, PhD, Associate Professor of Chemistry, the University of Tulsa and to Harry Mueller, Oklahoma Research Balloons.

Correspondence to: Mr David Joe Williams,
School of Civil and Environmental
Engineering, Oklahoma State University
e-mail: david.williams@okstate.edu
doi: 10.1256/wea.251.05

© Royal Meteorological Society, 2006



Fig. 4 Photo taken from ozonesonde balloon over Tulsa, Oklahoma, 25 300 m, 8 October 2005; the body of water in the photograph, Robert S. Kerr Reservoir, was at a ground distance of 175 km from the balloon (© 2005 Harry Mueller/Oklahoma Research Balloons)

APPENDIX V: OZONE ANALYZER SPECIFICATIONS

- 2B Technologies Model 202 (<http://www.twobtech.com/>)

OZONE MONITOR SPECIFICATIONS

Power Requirements 11-14 V DC, nominally 300 mA at 12 V, 3.6 watt

Dimensions 3.5" x 8.3" x 11.6"

Weight 4.7 lbs (2.1 kg)

Weight with case removed 1.6 lb (0.7 kg)

Precision higher of 1.5 ppbv or 2%

Accuracy higher of 1.5 ppbv or 2%

- Thermo Electron Corp., Model 49C (<http://www.thermo.com/>)

SPECIFICATIONS

Preset ranges	0-0.05, 0.1, 0.2, 0.5, 1, 2, 5, 10, 20, 50, 100, 200 ppm 0-0.1, 0.2, 0.4, 1, 2, 4, 10, 20, 40, 100, 200, 400 mg/m ³
Custom ranges	0-0.05 to 200 ppm 0-0.1 to 400 mg/m ³
Zero noise	0.5 ppb RMS
Lower detectable limit	1.0 ppb
Zero drift	<1 ppb/24 hour <2 ppb/7 day
Span drift	less than 1% per month (including drift of transducers)
Response time	20 seconds (10 seconds lag time)
Precision	1 ppb
Linearity	± 1% Fullscale
Sample flow rate	1-3 liters/min
Operating temperature	20 - 30°C (may be safely operated over the range of 0 - 45°C)*
Power requirements	90-110 VAC @ 50/60 Hz 105-125 VAC @ 50/60 Hz 210-250 VAC @ 50/60 Hz 150 Watts
Physical dimensions	16.75" (W) X 8.62" (H) X 23"(D)
Weight	35 lbs.
Outputs	selectable voltage 4-20 mA, RS-232, RS-485

* In non-condensing environments

CURRICULUM VITAE

David Joe Williams

Candidate for the Degree of

Doctor of Philosophy

Thesis: OZONE IN THE ATMOSPHERIC BOUNDARY LAYER: TRANSPORT MECHANISMS AND PREDICTIVE INDICATORS AT 36°N

Major Field: Civil Engineering

Biographical:

Personal Data: Born in Claremore, Oklahoma, on 26 October 1977; the son of Thomas and Nedra (McMillan) Williams. Tribal Citizen, Cherokee Nation.

Education: Graduated from Catoosa High School, Catoosa, Oklahoma in May 1996; received a Bachelor of Arts (Geology) from the University of Tulsa, Tulsa, Oklahoma in December 1999; received a Master of Environmental Science from the University of Oklahoma, Norman, Oklahoma in December 2001; received a Master of Science in Environmental Engineering from Oklahoma State University, Stillwater, Oklahoma in December 2004. Completed the requirements for the Doctor of Philosophy degree with a major in Civil Engineering at Oklahoma State University in May 2007.

Honors and Awards: Tau Beta Pi; Chi Epsilon; Sigma Gamma Epsilon; Sigma Xi; Order of the Engineer; United States Environmental Protection Agency GRO Doctoral Research Fellow; Sigma Xi Grant in Aid of Research, 2005; American Meteorological 2006 Summer Policy Colloquium (NSF Paleoclimate Division Grant); Valedictorian, Catoosa High School, 1996; Oklahoma Academic All-State, 1996; Oklahoma State Regents' Academic Scholar, 1996-2001; American Radio Relay League Scholarship, 1996; American Meteorological Society Scholar, 1996-1997; EPA Tribal Lands Scholar, 1999-2000, 2001-2003; AISES AT Anderson Scholar, 2003-2004; Cherokee Nation Graduate Scholar, 2003-2004; 2005-2007; Air and Waste Management Association Scholar, Oklahoma Chapter, 2005-2006

Professional Experience and Organizations: Student Intern, Cherokee Nation Office of Environmental Services, 1998; Grading Assistant, University of Tulsa Physics Department, 1997-1998; Student Employee, ODEQ Air Quality Division, 2002; Graduate Research and Teaching Assistant, OSU Department of Civil and Environmental Engineering, 2002-2007; OSU Instructor (Fluid Mechanics) 2007; Expert Witness (Air Pollution), 2005; EPA Doctoral Research Fellow, 2005-2007; Board of Directors, Oklahoma Chapter of the Air and Waste Management Association; Student Member, American Society of Civil Engineers; Student Member, American Meteorological Society, Student Member, Air and Waste Management Association; Student Member, New York Academy of Sciences, Student Member, Royal Meteorological Society; Associate Member, Sigma Xi; Student Member, American Indian Science and Engineering Society; Student Member, National Ground Water Association.

Name: David Joe Williams

Date of Degree: May 2007

Institution: Oklahoma State University

Location: Stillwater, Oklahoma

Title of Study: OZONE IN THE ATMOSPHERIC BOUNDARY LAYER:
TRANSPORT MECHANISMS AND PREDICTIVE INDICATORS AT 36°N

Pages in Study: 253

Candidate for Degree of Doctor of Philosophy

Major Field: Civil Engineering

Scope and Method of Study: The objectives of this study were the estimation of the background ozone concentration specific to the study location, correlation between the background concentration and ground-level ozone, evaluation of the relationship between meteorological parameters and ozone (measured as the background concentration and at ground level), and identification of transport pathways for the component of local ozone concentrations not explained by local photochemistry. Ozone was measured in 1-hour averages at an elevation of 210 meters above ground level, with a companion set of control data measured in 1-hour averages at ground level. Data collection occurred in Tulsa, Oklahoma, a mid-sized city located at a latitude of 36°N, over the period beginning on 01 June 2005 and ending on 30 November 2005. Additionally, meteorological data were collected at the 210-meter ozone installation and were retrieved from National Oceanic and Atmospheric Administration sites that measure and record ground-level conditions, upper-air soundings, and vertical wind profiles. Solar radiation data was retrieved from the Oklahoma Mesonet.

Findings and Conclusions: Local meteorological conditions were found to be more important to local photochemical generation of ozone than to the behavior of the 210-meter concentration, representative of background ozone in the troposphere. Specifically, a negative correlation with an R^2 of 0.5286 was achieved between ground-level ozone and relative humidity, while a positive correlation with an R^2 of 0.4897 was achieved between ground-level ozone and dry-bulb temperature. All ground-level ozone concentrations ≥ 0.08 ppm occurred at dry-bulb temperatures $\geq 27^\circ\text{C}$ and relative humidity $\leq 50\%$. Solar radiation was of marked importance to ground-level concentrations as well, as R^2 equaled 0.6065. Wind speed had a lower correlation with ground-level ozone ($R^2 = 0.1121$), but all occurrences of ground-level ozone ≥ 0.08 ppm during the study were accompanied by ground-level wind speeds $< 5 \text{ m}\cdot\text{s}^{-1}$. When compared with 210-meter ozone, local meteorological conditions showed poor or no correlation. Instead, the 210-meter concentration was found to be correlated with geopotential heights at 300 hPa, representative of the height of the polar jet stream. This correlation improved as heights in close proximity to the mean position of the polar jet were considered, with a maximum R^2 of 0.38 when 210-meter ozone was compared with 300 hPa geopotential heights at 46°N. Furthermore, the best correlation was achieved with an 18-hour lag between 210-meter ozone and 300 hPa geopotential heights, accounting for the vertically-tilted structure of atmospheric waves. From the correlation between 210-meter ozone and 300 hPa geopotential heights, it can be concluded that atmospheric disturbances, both as Rossby and baroclinic waves, strongly influence the tropospheric background ozone concentration, as high concentrations were favored during large-scale anti-cyclonic subsidence, while low concentrations were favored during large-scale cyclonic lift. These processes ultimately affected ground-level ozone, as a strong correlation was shown with 210-meter ozone ($R^2 = 0.8781$) during the afternoon hours. Horizontal ozone transport was shown to be appreciable at a distance of 80 km, but based on dispersion modeling, transport at a horizontal distance of 400 km did not appear to contribute significantly to ground-level concentrations.

Advisor Approval: _____

Dee Ann Sanders, Ph.D.